UNIVERSITAT DE BARCELONA

Control strategies and gene expression dynamics of the plant pathogen *Ralstonia solanacearum*

Estratègies de control i dinàmica d'expressió gènica en el fitopatogen *Ralstonia solanacearum*

Marina Puigvert Sànchez

Facultat de Biologia

Departament de Genètica, Microbiologia i Estadística

Programa de Doctorat: Genètica

"Control strategies and gene expression dynamics of the plant pathogen *Ralstonia solanacearum*"

(Estratègies de control i dinàmica d'expressió gènica en el fitopatogen *Ralstonia solanacearum*)

Memòria presentada per Marina Puigvert Sànchez per tal d'optar al títol de Doctora expedit per la Universitat de Barcelona. Tesi doctoral realitzada sota la direcció del Dr. Marc Valls Matheu al Departament de Genètica, Microbiologia i Estadística de la Facultat de Biologia (UB) i al Centre de Recerca en Agrigenòmica (CRAG).

Signatura del Director i Tutor,

Signatura de la Doctoranda,

Dr. Marc Valls i Matheu

Marina Puigvert Sànchez

Barcelona, Abril 2018

Control strategies and gene expression dynamics of the plant pathogen *Ralstonia solanacearum*

Marina Puigvert

Marina Puigvert

Control strategies and gene expression dynamics
of the plant pathogen *Ralstonia solanacearum*

PhD thesis, April 2018

University of Barcelona | Centre for Research in Agricultural Genomics

Cover design: Francesc Puigvert Mas

Dedicat a la meva família

Acknowledgements/Agraïments

Una tesi no és feina d'una sola persona. Per sort, he estat molt afortunada d'anar a parar a un grup on he pogut comptar amb el recolzament de tothom, i a un centre on he pogut conèixer gent meravellosa. Aquests agraïments van a tothom que, d'una manera o altra, m'han ajudat en el meu dia a dia, i que gràcies a ells la meva vida ha sigut una mica més fàcil i divertida durant aquesta etapa que ara tanco.

MARC VALLS

Naturalment, els meus primers i més profunds agraïments van per a tu, que des del primer dia en què em va convidar al seu grup, sempre m'has donat la oportunitat de créixer tant a nivell personal com a nivell professional. Moltes gràcies per ser el meu mentor tot aquest temps. He pogut explotar i aprendre d'aquest doctorat com no ho podria haver fet en cap altre grup. Gràcies per tot el que m'has ensenyat i per la teva paciència i optimisme en moments de crisi! Gràcies per confiar més en mi que gairebé jo mateixa.

NÚRIA SÁNCHEZ-COLL

També vull donar les gràcies a la Núria, per donar-me sempre la teva opinió més sincera en tot moment i per la confiança que vas dipositar en mi des del principi. Gràcies per tota l'ajuda que m'has brindat aquests anys, i sobretot moltes gràcies per donar-me l'empenta necessària per llançar-me a la piscina com ara amb l'EPSR. He pogut aprendre moltíssim gràcies a tu!

BIOBACT

A tots els membres del grup Biobact que m'han fet més divertida i enriquidora aquesta experiència: **Marc**, ja no recordo el laboratori sense tu! Moltes gràcies per ajudar-me amb la feina sempre que t'ho he demanat, i per estar allà per donar-li canya a tothom amb les responsabilitats! Molta sort amb la tesi, encara que sé que no la necessites! **Saúl**, el meu company de tesi, hem passat per totes les fases junts i, t'ho dic de debò, ha sigut un alleujament poder compartir les preocupacions de cada etapa amb tu! Gràcies per ser el hacker del lab i per ajudar-me mil i una vegades amb els meus problemes tècnics. **Alexino**, todavía espero la historia de los conejos asesinos. Estoy segura que habría merecido muchísimo la pena si sólo me hubiese hecho reír la mitad de lo que me he llegado a reír contigo! Gracias por echarme una mano cuando te lo he pedido y por todas las horas de confesiones en el P2! Muchos ánimos con la tesis, que ya casi lo tienes! **Pau**...ai Pau! Me'n recordaré sempre del dia que vas venir al CRAG a informar-te sobre el grup, tot motivat, i també de les teves liades varies mesos després d'aquell dia! Bromes a part, estic molt contenta d'haver coincidit amb tu i de que siguis tu qui porti la continuació del projecte. Ets una gran persona i sé que seràs molt bon científic. Molts ànims aquests anys que queden de tesi! **Eugenia**, we've been confidents one from the other during this last year. I'm very happy of having met you and having shared our experiences and thoughts and concerns. Thank you for your joy and for always having a smile for everyone. Good luck with the PhD, I'm sure you'll nail it! **Liang**, thank you for helping me when I needed it, especially with the PCRs when they were never working! I wish you all the best for the rest of your PhD. **Anurag**, thank you for always be willing to give me a hand when I needed extra hands. Good luck and enjoy your PhD in Barcelona! **Brian** and **Jose**, it's a pity we couldn't share many experiences together, but I wish you all the best in and outside science! Hopefully, we will hang out togethermany times! Y, finalmente **Agnese**, espero que disfrutes de la etapa Biobact con nosotros!

EX-BIOBACTS

La **Paola**, por haber creído en mí desde el principio, por haberme guiado en la ciencia y en parte también en la vida. Gracias por tus consejos, por nuestras escapadas chéveres, por todas las risas y por los ratos jugando al Set!

La **Crina**, perquè has estat un referent a seguir i per tot el que m'has ensenyat. Sense oblidar totes les estones de tes en què ens hem sincerat i marujeat una mica!

La **Montse**, perquè tenir-te com a postdoc va ser de les millors coses que ens podia passar al grup! Gràcies pel teu bon rotllo i també per posar-nos ordre al P2, sense tu ha sigut una mica desastre!

A l'**Ivan Erill**, per ensenyar-me trucs útils de l'excel i d'organització de dades. Va ser un plaer compartir el projecte del metiloma junts i poder aprendre de tu.

Roger, gràcies per la dedicació en tot moment, per voler aprendre i deixar-me ensenyar-te. Gràcies per ser tan responsable i tan entregat. Potser inclús et vas passar algunes vegades de massa dedicat, que arribaves a hores encara més intempestives que jo!

Pedro! Kiwi! PedoR! Quantes hores ens devem haver passat parlant de la vida i rient amb totes les nostres anècdotes? Encara em pixo de riure el dia que vaig venir sigilosament a ajudar-te, o amb les pistes que em vas deixar durant el Secret Santa del CRAG. Gràcies per entendre'm, per deixar-me adoptar-te com a estudiant i per fer-me els dies al CRAG divertits fins a plorar de riure!

A tota la resta d'antics membres de Biobact: **Melis, Cristina, Guillem, Jonathan, Vanesa, Rachid, Patrycja, Irma, Sergio** and **Haibin**; thank you all for the wonderful moments we shared!

POL REY

Pol, tu també ets, de fet, un exmembre de Biobact, però per sobre d'això ets el meu amic. Fa anys que ens coneixem i hem passat per moltes etapes. Confio molt en tu i tenir-te al CRAG, tant quan les Arabidopsis feien broma com quan fèiem cata de maduixes, ha sigut fantàstic. És meravellós pujar a berenar i que se te'n vagi de les mans, o anar a la teva oficina en qualsevol moment només per posar-nos al dia. Gràcies per ser-hi sempre!

RAQUEL SALVADOR

Crec que t'ho he dit més d'una vegada, però ho repetiré: gràcies per ser la meva millor amiga del CRAG! Gràcies per ser tan semblant a mi, per entendre'ns inclús amb una mirada, per deixar-me confessar i per confessar-te amb mi. Has estat un pilar fonamental durant aquest anys de tesi i sé que ho seguiràs sent després, sense importar on estigui cadascuna!

EQUIP EPSR

Raquel, Jorge, habéis sido los mejores compañeros para la aventura del EPSR que nadie pueda pedir. Gracias por todo el apoyo, por involucraros tanto, por no odiarme por todo lo que os pedía y por estar ahí incluso cuando perdía los nervios. Pero sobretodo, gracias por haber hecho que algo que era sólo una idea se convirtiera en realidad. Me alegro mucho de haber compartido esta experiencia con vosotros. Gracies també a tothom que va participar en aquesta aventura de diverses maneres, des de direcció i l'administració del CRAG fins als estudiants de doctorat que també van contribuir a fer realitat aquest projecte.

EQUIP CASA RURAL

Gràcies a tots amb els que hem compartit alguns caps de setmanes de casa rural, on sempre ens ho hem passat de conya! Pels jocs fins les mil de la nit, per les paelles valencianes i les excursions per la muntanya. Espero que en el futur encara n'hi pugui haver moltes més!

FIRST FLOOR & MANOLO'S LAB

Bàsicament a tothom de la primera planta; però sobretot al lab rosa i al virlab, als que hi sou i ja no hi sou, per haver-me adoptat en més d'una ocasió i tenir-me allà incordiant cada 2x3! Thanks to the Monte's for the great moments spent together and your help at any time! Vicky, por tu apoyo en todo momento y por hacer que la vida de los doctorandos del CRAG sea un poco mejor. Y a Miguel, por ser tan alegre y contagiarnos a todos con ese buen humor!

LIPM & LBI

Thanks to all the members of the LIPM that I met during my stay in Toulouse, specially to Fabien, Keke, Gaofei and Antony. You guys made my stay unforgetable! Thanks for the dinners and the beers shared! Also to the people in LBI in Sao Paulo, thanks for taking care of me! For all the food you made me try (and the Kilos I gained!) and for teaching me Bioinformatics in Portuguese. ***Belesa*** together!

LA COLLA I LA FAMILIA DE VIC

Gràcies a tots i cadascún dels membres de la colla i de la família Rovira-Freixa, per haver-me acceptat amb els braços oberts, i per totes les estones que hem compartit, de divertides, de tristes, de boges, de bromes i de tendres. Gràcies per ser tan únics, especials, i sobretot, bona gent. Aquests anys de tesi no haguessin estat el mateix sense vosaltres. Gràcies pels ànims i per les estones de riure fins a plorar durant aquest temps en què ho he necessitat tant!

ALS MEUS

A vosaltres: **Alba**, **Raúl**, **Jeli**, **David**, **Adrià** i **Albert**, perquè cadascú a la seva manera és una part indispensable de la meva vida. Gràcies per les estones al 64, pels cafès i cerveses i hores de converses sobre llibres i la vida, per les classes de dansa del ventre, room escapes i les hores de jocs varis. Gràcies per ser-hi sempre, en els moments importants i quotidians, els bons i no tan bons, per buscar qualsevol excusa per veure'ns i per fer-me feliç. Gràcies per la paciència que heu tingut amb mi aquests anys i pel costat que m'heu fet! A la **Teresa**, per haver compartit les nostres tesis malgrat la distància (sort de l'Skype i les trucades de Whatsapp!). Thank you **Lu** and **Minmin**, for being next to me despite of being physically in the other side of the world! Und natürlich danke ich der **Domingueren**, die schönstige Gruppe der Welt! Danke für unsere tausende Anekdoten!

LA MEVA FAMÍLIA

Gràcies per l'ajuda, la paciència i el recolzament moral. Gràcies per donar-me forces quan m'he sentit més dèbil. Per animar-me sempre en qualsevol aventura/repte en què m'he llançat. Per fer-me el dia a dia més fàcil. Aquesta tesi és gairebé tan meva com vostra! Gràcies mare, pare, Roser i Pedro. I gràcies també a la meva àvia, que veurà aquest somni fet realitat des del cel.

Finalment, gràcies al meu company de vida, de ciència, de viatges i de swing. Per creure en mi i fer-me sempre costat. Gràcies Arnau.

Table of Contents

Index

chapter 1

INTRODUCTION

1.1 MOLECULAR MECHANISMS OF BACTERIAL PHYTOPATHOGENS

Biology of plant pathogenic bacteria

A plethora of bacterial species are beneficial, not only for the proper maintenance of the nutrient cycle, but also through symbiotic relationships with plants and animals. However, there are some species that cause diseases and have been – or are still – a threat to humans, either by directly affecting health or food production. Bacterial phytopathogens as a whole are responsible for a great proportion of food supply damages at a global level, resulting in important economic losses and nutritional limitations in many countries (Oerke and Dehne 2004). According to the Food and Agriculture Organization of the United Nations (FAO), the world's most important staple crops are affected by severe diseases caused by various bacterial pathogen species, such as *Erwinia stewartii* (maize), *Xanthomonas oryzae* (rice), *Xanthomonas translucens* pv *undulosa* (wheat), *Ralstonia solanacearum* (potato) and *X. axonopodis* pv *manihotis* (cassava) (Strange and Scott 2005). Recently, a list of the 10 most devastating bacterial plant pathogens included *Pseudomonas syringae*, *Ralstonia solanacearum*, *Erwinia amylovora* and several *Xanthomonas* spp (Mansfield et al. 2012) (Table 1, Figure 1).

These distinct bacterial genera have evolved different strategies to successfully colonize and multiply in such a broad-range of plant species and tissues. Bacteria can enter into the plant through natural openings –stomata or hydathodes- or wounds, and must be able to survive and proliferate in the plant to become pathogenic. Therefore, some pathogens have developed the ability to colonise the apoplast- or intercellular spaces-, which is a nutrient-rich environment. On the other hand, some other species possess the ability to multiply within the xylem vessels, which is assumed to be nutrient-limited. There are also bacterial species that have become epiphytes, and survive on plant surfaces, such as the rhizosphere or the phyllosphere, while others are saprophyte and survive from dead matter in the soil.

In addition to the capacity of colonizing different plant tissues, pathogens can exploit the plant's nutrients according to the following lifestyles: biotrophy – the pathogen extracts nutrients from living cells-, necrotrophy – nutrients are acquired by killing host cells-, or hemibiotrophy –the pathogen maintains the host cells alive until it switches to a necrotrophic stage. However, this terminology was traditionally used to classify pathogenic fungi according to certain histological features during the infection process (Lo Presti et al. 2015). With very few exceptions, fungal pathogens that stay within extracellular compartments and, thus, do not affect host cell viability, are considered biotrophs. On the contrary, necrotrophic pathogens penetrate inside the host cells and kill them. Conversely, bacterial phytopathogens remain extracellular in all cases and during all stages of the infection process. With the exception of *Agrobacterium tumefaciens*, which is considered a clear biotroph, difficulties in assigning one or the other lifestyle to the different bacterial plant pathogens resulted in a massive classification of bacterial phytopathogens as

hemibiotrophs (Kraepiel and Barny 2016). Especially striking is the case of *R. solanacearum*, which has been equally classified as biotroph and necrotroph in the literature (Ahn et al. 2011; Jacobs et al. 2013). New classification systems taking into account other features, such as the virulence mechanisms deployed, might be more suitable to better group bacterial phytopathogens according to their lifestyle.

Table 1. Most devastative plant pathogenic bacterial species*.

Rank	Pathogen	(Main) Affected crops
1	*Pseudomonas syringae* pathovars	Tomato, bean, olive tree, oats,
2	*Ralstonia solanacearum*	Most solanaceous: Potato, tomato, eggplant,
3	*Agrobacterium tumefaciens*	Grapevines, nut trees, stone fruits
4	*Xanthomonas oryzae* pv. *oryzae*	Rice
5	*Xanthomonas campestris pathovars*	Pepper, tomato and all cultivated brassicas
6	*Xanthomonas axonopodis* pv. *manihotis*	Cassava
7	*Erwinia amylovora*	Most rosaceous: apple, pear, raspberry…
8	*Xylella fastidiosa*	Grapevines, coffee, *Prunus* spp, *Citrus* spp
9	*Dickeya dadantii* and *solani*	Potato
10	*Pectobacterium carotovorum and atrosepticum*	Potato

*Adapted from (Mansfield et al. 2012).

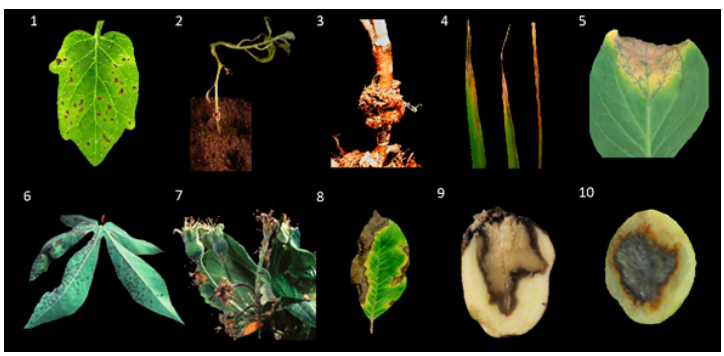

Figure 1. Major bacterial plant diseases affecting crops.

1) *Pseudomonas syringae*–tomato leaf, 2) *Ralstonia solanacearum*–tomato plant, 3) *Agrobacterium tumefaciens* – blueberry plant, 4) *Xanthomonas oryzae* pv. *oryzae* – rice leaves. 5) *X. campestris* – cabbage leaf, 6) *X. axonopodis* pv. *manihotis* – cassava leaf, 7) *Erwinia amylovora* – apple leaves and flowers, 8) *Xylella fastidiosa* – plum leaf, 9) *Dickeya dadantii* – potato tuber, 10) *Pectobacterium carotovorum* – potato tuber. Picture 1 is from K. Loeffler and A. Collmer, picture 2 is original from this work, picture 3 (Kado 2002), picture 4 (Sun et al. 2016), pictures 5, 6, 7 and 9 are adapted (Mansfield et al. 2012), picture 8 (Alves and Setter 2004) and picture 10 (Huang et al. 2012).

General virulence determinants

Bacteria need to activate and deploy a wide array of virulence mechanisms to overcome the plant cell's protection layers. These pathogenic factors help bacteria to invade the host, to evade its defenses and to cause disease (Mole et al. 2007; Wu et al. 2008). A battery of virulence mechanisms are shared among animal and plant bacterial pathogens and include: adhesion and biofilm formation, secretion systems, toxin production and modulation of plant hormone homeostasis. Besides, many bacterial phytopathogens also make use of cell wall degrading enzymes to degrade the plant cell wall, which is missing in animal cells (Wu et al. 2008; Melotto and Kunkel 2013).

Bacterial adhesion to host cells is an essential step for further colonization. Hence bacteria have evolved adherence mechanisms, such as adhesins or lectins, which are highly specific carbohydrate-binding proteins and confer host cell recognition and binding (Romantschuk 1992). The XadM and LecM from *Xanthomonas oryzae* pv. *oryzae* and *R. solanacearum*, respectively, have been reported to play a role in attachment, biofilm formation and virulence (Pradhan et al. 2012; Meng 2013). In addition to lectins, bacterial also bear pili and fimbriae, which are filamentous appendages that protrude outside bacterial cells. For instance, type IV pili mediate attachment, biofilm formation and virulence in a great number of bacterial plant pathogens, such as *Xanthomonas citri*, *Acidovorax avenae*, *Ralstonia solanacearum*, *Xylella fastidiosa* and *Pseudomonas syringae* (Bahar et al. 2009; Nguyen et al. 2012; Wairuri et al. 2012; Petrocelli et al. 2016; Shi and Lin 2018).

Biofilm formation is, in fact, one of the most beneficial adaptations for pathogenic bacteria. Biofilms are cellular aggregates on surfaces that give bacteria several advantages: tolerance to high concentrations of antimicrobial compounds, unrecognition of bacterial infection by host cells and activation of bacterial quorum sensing pathways (Caserta et al. 2010; Bjarnsholt 2013). Biofilms contribute to bacterial epiphytic survival and attachment to host cells in the intercellular spaces or to the xylem vessels (Buttner and Bonas 2010). Usually, attachment and aggregation on the host surface is the first step to colonization (Danhorn and Fuqua 2007). Biofilm formation depends on the secretion of exopolysaccharide (EPS) and lectins, which act as a bond between EPS and the bacterial surface (Flemming and Wingender 2010). Furthermore, in some bacterial phytopathogens such as *R. solanacearum* and *X. campestris*, the EPS is a major virulence factor, as its accumulation leads to the plant vasculature collapse (Buttner and Bonas 2010).

Pathogenic bacteria also hijack plant hormone homeostasis and signaling pathways, either to suppress plant stress responses or to manipulate plant growth for nutrient acquisition (Ma and Ma 2016). For instance, *Agrobacterium tumefaciens* expresses cytokinins (Akiyoshi et al. 1984) and *Pseudomonas syringae* pv *savastanoi* synthesizes auxins (Smidt and Kosuge 1978) to induce plant overgrowth and increase gall size. Furthermore, some bacterial species produce

phytotoxins that interfere with different hormone pathways. This is the case of *P. syringae*, which synthesizes several well-studied toxins in different pathovars (Bender et al. 1999). Some of them are: coronatine, an analogue of Jasmonic Acid, which induces re-opening of stomata and enhances bacterial entrance (Melotto et al. 2006) and syringolin A, which generates Salicylic Acid-insensitive cells at the infection site and surrounding tissues to avoid plant stress responses (Misas-Villamil et al. 2013).

To introduce toxins, enzymes, other effector proteins or DNA into the host cell, bacteria use six different secretion systems (TSS). A summary of their main features is presented in Table 2. Interestingly, most of them have been reported to play a role in pathogenesis in different species, placing them as one of the main virulence factors in pathogenic bacteria (Tseng et al. 2009).

Table 2. Secretion systems in Gram-negative phytopathogenic bacteria.

System type	Mechanism	Molecules secreted	Bacterial phytopathogens
T1SS	ABC transporters	Toxins, enzymes	*P. carotovorum, D. dadantii*
T2SS	Sec-mediated	Toxins, enzymes	*P. carotovorum, D. dadantii*
T3SS	Injectisome	Effector proteins	Most pathogenic species
T4SS	Injectisome	DNA, proteins	*A. tumefaciens*
T5SS	Tat-mediated	Adhesins, toxins, enzymes	*R. solanacearum, D. dadantii*
T6SS	Injectisome	Effector proteins	*R. solanacearum, P. atrosepticum*

Type I and type II secretion systems (T1SS and T2SS) are mainly involved in secretion of toxins and extracellular enzymes, such as proteases, pectinases, cellulases and glycanases. These enzymes are commonly known as plant cell-wall degrading enzymes (CWDE) and, although their role is important in many bacterial pathogens, they are mostly relevant in rot producing pathogens like *Pectobacterium carotovorum* and *Dickeya dadantii* (Collmer and Keen 1986).

The type III secretion system (T3SS) is by far the main virulence determinant in bacterial pathogens. It consists of a highly conserved injectisome-like apparatus that delivers effector proteins directly into the host cell cytoplasm to modulate its normal functioning and physiology, including the inhibition and alteration of the plant cell defense responses (Cornelis and Van Gijsegem 2000). The T3SS and its effectors have been extensively studied in a number of species within the genera *Pseudomonas*, *Xanthomonas* and *Ralstonia*, among others (Alfano and Collmer 2004).

Structurally similar to the T3SS, the type IV secretion system (T4SS) is composed of a pilus-like structure that translocates not only proteins but also nucleic acids within the host cell cytoplasm.

A. tumefaciens has been the model species to study the transference of T-DNA and virulence proteins to alter growth of plant cells (Shirasu and Kado 1993; Christie et al. 2005). However, the T4SS has been shown to be involved in other processes, such as natural transformation in *R. solanacearum* (Kang et al. 2002) or bacteriolytic activity in competing bacteria such as *X. citri* (Souza et al. 2015).

The type V secretion system (T5SS) machinery resembles to that of the T2SS, as both are dependent on universal secretion pathways known as Tat (two-arginine) and Sec (general secretion), respectively. T5SS mainly secretes adhesins, proteases and toxins, and has been described to be involved in bacterial attachment to leaf surfaces in *D. dadantii* (Rojas et al. 2002) and in *R. solanacearum* virulence (Gonzalez et al. 2007).

Finally, the type VI secretion system (T6SS) is the most recently discovered secretion system. It is considered an analogue of the T3SS and T4SS-injectisome structures and has a role in virulence in phytopathogenic bacteria. It has been studied in *A. tumefaciens* (Wu et al. 2008), *P. atrosepticum* (Liu et al. 2008) and more recently in *R. solanacearum* (Zhang et al. 2012).

The proper and coordinate expression of these pathogenic determinants is essential for disease establishment and progression. Different disease stages may require the activation of specific molecular machineries. Therefore, unravelling novel virulence factors, understanding their function and defining their genetic expression profile is crucial for the development of new tools to combat bacterial plant diseases.

Pathogen recognition and plant defense mechanisms

Plants are constantly threatened by pathogens with very dissimilar colonization abilities and virulence machineries, and yet disease is not a common event. In fact, disease has been traditionally described as a combination of three factors: the pathogen –virulence and abundance-, the host – susceptibility and growth stage-, and the environment – temperature and moisture (Agrios 2005). Altogether, these components contribute to the host predisposition of a certain biotic stress by specific environmental conditions. When the three factors are favorable, a successful plant-pathogen interaction that leads to disease takes place.

To protect themselves, plants have developed physical and chemical barriers to prevent pathogen entrance. These passive barriers include the leaf cuticle, the plant cell wall and secretion of defense enzymes or antimicrobial compounds (Göhre and Robatzek 2008).

However, many pathogens can overcome this first defense barrier, and thus, plants have evolved pathogen recognition systems to induce a set of immune responses. Two forms of active defense strategies involving different types of receptors have been described: the PAMP- or the

Effector-triggered immunity (PTI or ETI, respectively). The first type of receptors are localized at the Plasma Membrane and recognize Pathogen- (or Microbe-) Associated Molecular Patterns (PAMPs/MAMPs). These are typically structural molecules found in many microorganisms, such as flagellin and lipopolysaccharide in gram-negative bacteria, or xylanases and chitin in fungi, and are detected by plant Pattern Recognition Receptors (PRRs) (Nurnberger et al. 2004; Nicaise et al. 2009). Upon microbial recognition, a series of defense responses corresponding to the PTI is induced. Briefly, an increase of cytosolic Ca^{2+} triggers an oxidative burst and induction of PR (Pathogenesis Related) gene transcription for callose deposition and lignification (Boller and Felix 2009; Segonzac and Zipfel 2011).

According to the so-called zigzag model (Jones and Dangl 2006), evolution has pushed the acquisition of microbial effectors that are directly injected to the plant cell cytoplasm to bypass the PTI response. For instance, *P. syringae* effectors AvrRpm1 and AvrRpt2 are known to directly interact with the PAMP-signaling regulator RIN4 to inhibit PTI in *A. thaliana* (Kim et al. 2005), while XopN and XopX1 from *X. campestris* suppress the callose deposition response (Cui et al. 2009). However, plants are also endowed with (NB)-LRR receptors (Nuclotide-Binding Leucine-Rich Repeat), a second type of receptors located in the plant cell cytosol that intercept specific bacterial effector proteins (Boller and Felix 2009). Effector recognition triggers a fast and amplified immune response known as Effector-Triggered Immunity (ETI), which is associated to a systemic acquired resistance (SAR) and to the Hypersensitive Response (HR), a programmed cell death reaction confined at the site of pathogen attack to avoid pathogen growth (Huysmans et al. 2017).

Although PTI and ETI were regarded as the first and second forms of immunity respectively, recent studies suggest that there is actually no separation between PTI and ETI, but they rather happen simultaneously (Thomma et al. 2011). For instance flagellin, which is considered one of the major PAMPs in phytopathogenic bacteria, has been demonstrated to induce HR in *Arabidopsis thaliana* (Naito et al. 2007). Furthermore, a role for bacterial flagella in virulence has been reported in many species, such as *R. solanacearum* or *Pectobacterium carotovorum* (Tans-Kersten et al. 2004; Hossain et al. 2005), therefore becoming no longer a PAMP but an effector. New models that explain more accurately plant-pathogen interactions are thus being proposed. One example is Pritchard&Birch's model (Pritchard and Birch 2014), which explains how callose deposition is induced during the PTI while it reduces the rate of effector translocation, implying that PTI and ETI can be active at the same time. Still, current models only take into consideration two sides of the triangle: hosts and pathogens. The lack of models that integrate environmental factors poses a need for the development of new models to elucidate the interplay of the three elements in plant-pathogen interactions.

1.2 *RALSTONIA SOLANACEARUM* AND BACTERIAL WILT

The *R. solanacearum* species complex and its threat to crop production

Ralstonia solanacearum is a devastative plant pathogenic bacterium responsible for the bacterial wilt disease. It was initially described in 1896 by E. F. Smith as *Bacillus solanacearum* (Smith 1896), later classified as *Pseudomonas solanacearum* (Smith 1914), *Burkholderia solanacearum* (Yabuuchi et al. 1992), and, since 1995, as *Ralstonia solanacearum* (Yabuuchi et al. 1995). *R. solanacearum* is a soil-borne gram-negative β-proteobacterium capable of infecting an enormous range of plant species. From economically important crops- potato, tomato, eggplant or banana- to ornamental plants –geranium or petunia- and model plant species in research – *Arabidopsis thaliana* or tobacco-, *R. solanacearum* can affect over 200 different plant species from 50 botanical families (Hayward 1991). It is worldwide spread but is especially endemic from the tropical and subtropical regions of the globe as its optimal growth temperature is around 30ºC. *R. solanacearum* accounts for considerable yield losses varying from 0 to 91% in tomato, 33 to 90% in potato, 10 to 30% in tobacco and 80 to 100% in banana (Yuliar et al. 2015).

Due to its extreme phenotypic and genotypic diversity, *R. solanacearum* is regarded as a species complex (RSSC) which includes two related species, *R. syzygii* and the Blood Disease Bacterium (BDB) (Fegan and Prior 2005). The RSSC has been divided into different categories according to distinct phenotypic traits. The species have been classified at the subspecies level into five races defining the host range (Buddenhagen 1962; He et al. 1983), into five biovars based on their ability to metabolize specific sugars and alcohol carbohydrates (Hayward 1964; Hayward 1994), and into four phylotypes (I-IV) and 23 sequevars depending on their endoglucanase sequence comparison (Fegan and Prior 2005) (Table 3). The latter classification also correlates with the geographical origin of isolates and allows their arrangement into a phylogenetic tree (Figure 2). Briefly, phylotype I strains originated in Asia, phylotype II in America, phylotype III were original from Africa and surrounding islands in the Indic Ocean, and phylotype IV is distributed across Australia, Indonesia and Japan. Table 3 summarizes the different classification systems and their main features.

Although *R. solanacearum*'s natural environments comprise all warm regions of the globe, race 3 biovar 2 strains – now included in phylotype IIB sequevar1 (IIB-1) (Fegan and Prior 2005)- are the causative agents of potato brown rot and represent a major risk in more temperate areas since they grow optimally at cooler temperatures. This group of *R. solanacearum* strains were actually responsible for European and North American potato brown rot outbreaks in the late 80s and early 90s. The dispersal of the pathogen was most probably mediated by importation of contaminated material (Elphinstone 1996; Janse et al. 2004). At that time, the European Plant Protection Organization (EPPO) reviewed the geographical distribution of the bacterium and reported its presence in some EPPO countries (Denmark, The Netherlands and Germany)

(available at www.eppo.int/). Since 1992, *R. solanacearum* is included in the EPPO A2 quarantine pest list for Europe and serious phytosanitary measures are taken to avoid pathogen spread and maximize its eradication. With the current worldwide presence of the phytopathogen (Figure 3), phylotype IIB-1 strains are considered the major risk of bacterial wilt outbreaks in Europe (Champoiseau et al. 2009). Some of the most well studied strains belonging to phylotype IIB-1 are: IPO1609, UY031 and UW551.

Table 3. Main classification systems of the *R. solanacearum* species complex.

RACE CLASSIFICATION					
Race	**Host range**			**Geographical distribution**	
1	Wide: tobacco, tomato, potato, eggplant, and many other solanaceous crops and weeds			Tropical and subtropical Asia, America and Australia	
2	Banana, almost exclusively			Central and South America, and Southeast Asia	
3	Mostly potato and tomato; latent infections in: *S. dulcamara, S. nigrum, S. cinereum, Pelargonium hortorum, Melampodium perfoliatum*			Higher altitudes in tropical and subtropical areas (lower optimal temperature)	
4	Ginger			Philippines	
5	Mulberry			China	
BIOVAR CLASSIFICATION					
Metabolisation of	**Biovar**				
	1	**2**	**3**	**4**	**5**
Cellobiose	-	+	+	-	+
Lactose	-	+	+	-	+
Maltose	-	+	+	-	+
Dulcitol	-	-	+	+	-
Mannitol	-	-	+	+	+
Sorbitol	-	-	+	+	-
PHYLOTYPE CLASSIFICATION					
Phylotype	**Geographical origin**	**Main features**			**Strains**
I	Asia	Includes all strains belonging to biovars 3, 4, and 5			GMI1000, OE1-1
IIA	America	Includes strains from biovars 1 and 2; and exclusively race 2 strains			K60, CFBP2957
IIB	America	Includes strains from biovars 1 and 2; and exclusively race 3 strains			UW551, UY031
III	Africa	Includes strains from biovars 1 and 2			CMR15
IV	Indonesia, Japan, Australia	Includes strains from biovars 1 and 2; and related species *R. syzygii* and *R. celebensis*.			PSI07

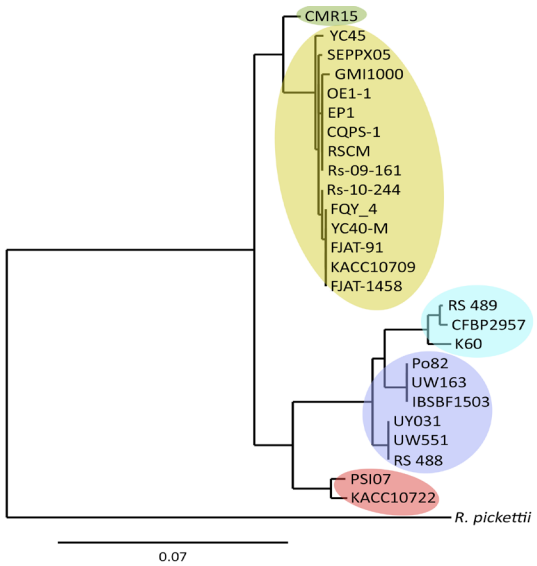

Figure 2. Phylogenetic tree of the *Ralstonia solanacearum* species complex.

The tree was constructed using the conserved *rpoA* sequence with the online tool www.phylogeny.fr applying the following pipeline: DNA sequences were aligned using MUSCLE and curated with GBlocks, and phylogeny was performed with PhyML (Dereeper et al. 2008; Dereeper et al. 2010). *R. pickettii* strain ATCC27511 was used as outgroup. Strains belonging to each of the four *egl*-based phylotypes are highlighted in colors: yellow (phylotype I), light blue (phylotype IIA), blue (phylotype IIB), green (phylotype III) and red (phylotype IV).

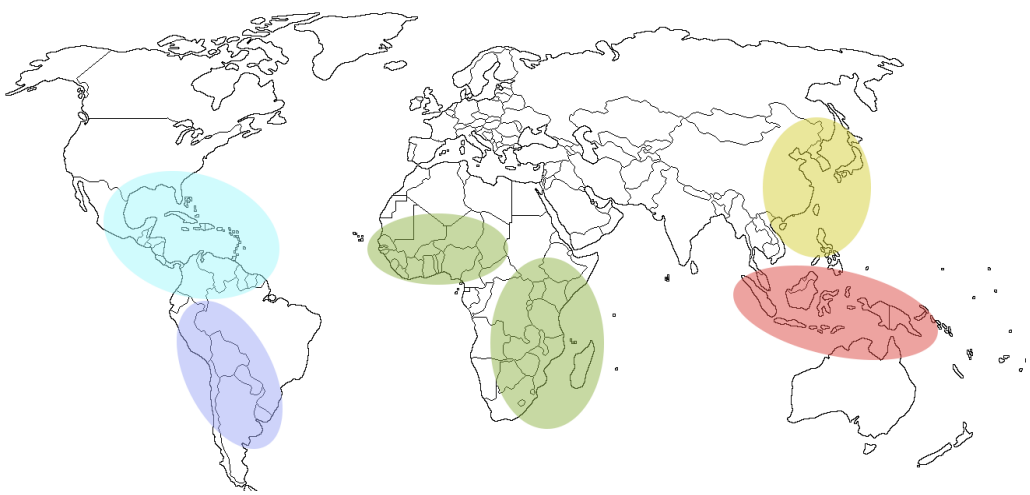

Figure 3. Geographical distribution of the *R. solanacearum* species complex.

Presence of the different *R. solanacearum* phylotypes where the pathogen is endemic. Colors indicate the prevalent phylotype in each region: yellow (phylotype I), light blue (phylotype IIA), blue (phylotype IIB), green (phylotype III) and red (phylotype IV).

R. solanacearum life cycle

R. solanacearum can survive as saprophyte in soil and waterways for long periods (van Elsas et al. 2000; Alvarez et al. 2007) by activating a survival mechanism known as the viable but nonculturable (VNC) state. The VNC state allows the bacterium to become quiescent and overcome starvation, although it is reversible and bacteria resuscitate and become pathogenic again when they encounter a plant (Grey and Steck 2001).

R. solanacearum must specifically recognize the host plants in the rhizosphere. It was proposed that the pathogen is attracted preferentially to tomato root exudates than to rice exudates, which is not a natural host for *R. solanacearum* (Yao and Allen 2006). After surface colonization, bacterial invasion starts by root penetration through the elongation zone, root wounds or secondary root emerging points (Vasse et al. 1995). Shortly after, the pathogen progresses through the cortex by invading the cortical apoplastic spaces, and very few days after infection bacteria already colonize the vascular cylinder and the xylem vessels (Digonnet et al. 2012). A role for cell wall-degrading enzymes at these colonization stages has been suggested (Tans-Kersten et al. 1998; Huang and Allen 2000). Once in the vascular system, the pathogen can massively multiply, reaching bacterial densities up to 10^{10} CFU/ml (approximately 10^{9} CFU/g tissue) (Vasse et al. 1995; Jacobs et al. 2012). At such high densities, bacteria produces enormous amounts of exopolysaccharide (EPS), which ultimately obstruct the plant vasculature and lead to plant death due to improper water flow (Figure 4). When the plant dies, bacteria can return to the soil to complete the cycle and spread around through irrigation water and waterways (Hong et al. 2008) (Figure 5).

Besides surviving in water, the pathogen can remain in soil for many years –as deep as 75 cm in soil contaminated with wilted plant debris, as well as in seed tubers (Graham et al. 1979). This is specially a problem for phylotype IIB-1 strains, which survive at lower temperatures and spread throughout Europe via contaminated potato tubers (Graham et al. 1979; Elphinstone et al. 1998; Caruso et al. 2005). Another feature associated to pathogen persistence, is the fact that *R. solanacearum* can asymptomatically colonize weeds at very high densities (Hayward 1991). Some of these reservoir weeds, such as *Solanum dulcamara*, *S. nigrum* or *Urtica dioica,* grow in river edges and become a latent source of inoculum that can contaminate rivers and spread the bacteria to nearby and distant fields (Caruso et al. 2005) (Figure 5).

Figure 4. Bacterial wilt in potato plants.
Healthy (left) or *R. solanacearum* UY031 (right) inoculated potato plants at 10 dpi.

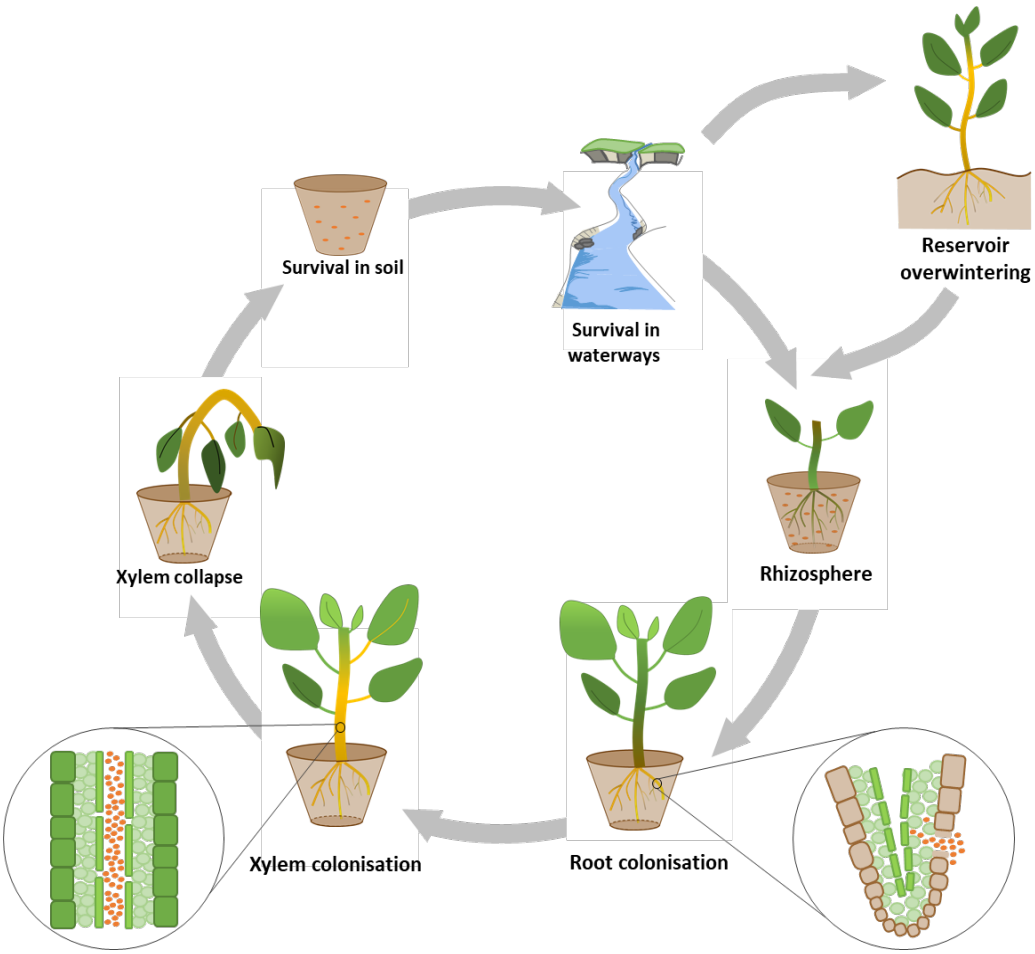

Figure 5. *R. solanacearum* life cycle.

R. solanacearum survives for long periods in soil and waterways until environmental conditions are favorable for plant infection. At this point, bacteria enter the roots through secondary root emerging points or root wounds. First, they colonize the apoplast, which is the intercellular space present between the root cortex and the parenchymatic cells. Then, bacteria reach the xylem vessels and colonize the vascular system throughout the entire plant. Within the vascular system, bacteria multiply extensively and massive production of exopolysaccharide occludes the xylem vessels. Collapse of some vessels results in the first visible wilting symptoms. Occlusion of the whole vasculature ends with complete plant wilting and death, and finally bacteria from dead plants are released back to the soil. The cycle concludes with an outer branch corresponding to latent infections. In this case, *R. solanacearum* is able to colonize the root system and, to some extent, the stem xylem vessels, without causing wilting symptoms. The exact mechanisms by which *R. solanacearum* is unable to cause disease in some weed reservoirs remains still unknown, although the pathogen might use this system to overwinter and survive to unfavorable environmental conditions.

Since these plants also provide the bacterium with shelter against unfavorable environmental conditions, it was proposed that *R. solanacearum* overwinters by using some of these reservoir species (Wenneker et al. 1999).

Virulence determinants in *R. solanacearum*

The virulent phenotype of *R. solanacearum* has been traditionally associated to the mucoid morphology of colonies grown on solid medium (Kelman 1954). However, non-mucoid hypopathogenic colonies also showed alterations not only in motility and chemotaxis (Kelman and Hruschka 1973), but also in lipopolysaccharide composition and indole-3-acetic acid synthesis (Buddenhagen and Kelman 1964; Whatley et al. 1980), revealing the interconnectivity and complexity of pathogenicity factors in *R. solanacearum*. Advances in the development of new molecular genetic tools, allowed the identification of many genes and molecular mechanisms key for bacterial virulence. The main pathogenicity factors described in *R. solanacearum* are indicated in Table 4 and described below.

Table 4. Main virulence determinants described in *R. solanacearum.**

FUNCTION	GENES / PRODUCTS	ROLE IN VIRULENCE	REFERENCES
T3SS and T3Es	*hrp* genes, T3Es and *hpa* genes	Host specificity, suppression of host defenses,	(Boucher C.A. 1985; Boucher et al. 1987)
T2SS and cell wall degrading enzymes	*gsp* genes and Egl, Pme, PglA, PehBC, CbhA	Degradation of host substrates	(Kang et al. 1994; Liu et al. 2005)
T5SS	*tat* gene cluster, Tat-secreted proteins	Mutants with reduced virulence	(Gonzalez et al. 2007)
T6SS	*tss* genes, VgrR and Hcp	Mutants with reduced virulence, motility and biofilm formation	(Zhang et al. 2012; Zhang et al. 2014)
Exopolyssacharide (EPS)	*eps* gene operon	Occlusion of the plant vascular system	(Denny and Baek 1991)
Protection enzymes	Catalases, peroxidases, superoxide dismutases	Plant phenolic compound and ROS detoxification	(Flores-Cruz and Allen 2009)
Motility and host attachment	Flagellum, type IV pili, (lectins) chemotaxis	Adherence to host cells, host selectivity	(Tans-Kersten et al. 2001)
Efflux pumps	*acrA*, *dinF*	Resistance to antimicrobials	(Brown et al. 2007)
Metabolic adaptation	Hdf, ralfuranones, *metER*, EfpR, sucrose and nitrogen assimilation	Metabolic versatility and bacterial fitness *in planta*	(Genin 2010)
Phytohormones	Ethylene, auxin, *trans*-zeatin	Unknown role ; production controlled by HrpG	(Valls et al. 2006)

*Modified from (Genin 2010)

The Type III Secretion System and its associated Effectors

The first large-scale attempt to identify virulence-related genes in *R. solanacearum* was carried out in 1985 by random mutagenesis using the Tn5-B20 transposon (Boucher C.A. 1985). A library of 8,250 insertion mutants was screened for their loss of virulence or hypersensitive response elicitation in tomato and tobacco, respectively. The screening led to the identification of the *hrp* (hypersensitive response and pathogenicity) genes, which were simultaneously reported in *Pseudomonas syringae* (Lindgren et al. 1986), and afterwards identified in many other plant pathogenic bacteria (Barny et al. 1990; Arlat et al. 1991; Bonas et al. 1991). This cluster, comprising more than 20 genes, shared homology with the virulence determinants Yop and Ipa secretion systems from *Yersinia pestis* and *Shigella flexneri* (Gough et al. 1992; Van Gijsegem et al. 1993). As deletions in any *hrp* gene render bacteria completely avirulent and unable to elicit HR (Boucher et al. 1987), the T3SS is since then considered the main virulence determinant in most pathogenic bacterial species.

Type III effector proteins, which are translocated into the host cell cytoplasm by the T3SS injectisome, are of special interest due to their wide array of functions and targets (Galan 2009; Macho and Zipfel 2015). Approximately 100 different T3Es have been already identified in *R. solanacearum* (Peeters et al. 2013) with each strain carrying a specific and distinct set of effectors. In fact, the number of T3Es present in different *R. solanacearum* strains is strikingly higher than in other plant pathogenic bacterial species (Genin and Denny 2012). Some effectors, such as RipG7 (GALA7) in *Medicago truncatula* (Angot et al. 2006), were found to be involved in host specificity, while RipAA (AvrA) and RipP2 were involved in host restriction. It was therefore tempting to speculate that the effector repertoire in a given strain could be responsible for its host range. However, in very few cases disruption of a single effector results in a delay or loss of virulence. Some of the few T3E whose deletion have been proved to affect virulence are: RipA2 (AWR2), RipD (brg8) (Cunnac et al. 2004), RipF1_1 (PopF1) (Meyer et al. 2006) and RipR (PopS) (Jacobs et al. 2013). New hypotheses suggest, though, that effectors evolved as polyvalent proteins functional in multiple hosts (Deslandes and Genin 2014). Still, most of the T3Es are poorly understood and are difficult to study due to their redundant contribution to pathogenicity, HR elicitation or toxic effects to the host (Coll and Valls 2013).

Type II Secretion System and Cell Wall Degrading Enzymes

R. solanacearum possesses a functional type II secretion system (T2SS) encoded by the *sec* and *gsp* gene clusters. A T2SS-deficient mutant strain showed a dramatic loss of virulence in tomato plants, demonstrating an important role of the T2SS in pathogenicity (Kang et al. 1994). The Gsp-dependent T2SS is responsible for the secretion of at least 36 extracellular proteins (Zuleta 2007). 6 of the total T2SS-secreted proteins function as cell wall degrading enzymes (CWDE) and each of them have been shown to contribute to pathogenicity: the polygalacturonases PglA, PehB and

PehC (Schell et al. 1988; Huang and Allen 1997; Gonzalez and Allen 2003), the Egl endoglucanase (Roberts et al. 1988), the Pme pectin methylesterase (Tans-Kersten et al. 1998) and the CbhA cellobiohydrolase (Liu et al. 2005). However, not only CWDE but other yet unknown extracellular proteins secreted via T2SS might play an important role in pathogenicity, since a pyramiding mutant lacking the 6 CWDE genes was still more virulent than the complete T2SS mutant from Kang, et al, 1994 (Liu et al. 2005).

Type V and VI Secretion Systems (T5SS and T6SS)

By screening the first genome sequence of *R. solanacearum* GMI1000 strain (Salanoubat et al. 2002), a cluster of genes corresponding to the Tat-secretory pathway (or T5SS) was identified (Gonzalez et al. 2007). Mutation of the *tatC* gene revealed that the T5SS was involved in tomato virulence. However, the Tat secretome includes genes involved in different activities, and might be the reason why the mutant showed a pleiotropic effect with reduced polygalacturonase activity, ability to metabolize nitrate in O_2-limiting conditions, *in planta* growth and increased sensitivity to detergents.

The T6SS is, compared to the rest of the described virulence factors, the newest pathogenicity determinant identified in *R. solanacearum*. An analysis attempting to find T6SS orthologue genes from known T6SS components in *V. cholerae*, *P. aeruginosa* and *B. mallei*, identified 14 conserved genes in *R. solanacearum* and other pathogenic bacterial species (Shrivastava and Mande 2008). The main T6SS-translocated effectors include the VgrG puncturing device, similar to the bacteriophage T4 tail spike, and the Hcp hexameric ring for macromolecule transport (Mougous et al. 2006; Pukatzki et al. 2007). The first validation of a functional T6SS in *R. solanacearum*, demonstrated that deletion of *tssM* affected secretion of 38 proteins (Zhang et al. 2012). Furthermore, deletion of either of the structural genes *tssM* or *tssB* rendered bacteria less pathogenic in soil-inoculated tomato plants (Zhang et al. 2012; Zhang et al. 2014). These studies also demonstrate the existence of a link between the T6SS and biofilm formation and motility, two of the main virulence factors in *R. solanacearum*.

Exopolyssacharide secretion

The exopolyssacharide (EPS) is an acidic secreted polymer composed of three major units: N-acetylgalactosamine, 2-N-acetyl-2-deoxy-galacturonic and 2-N-acetyl-4-N-(3-hydrozxybutanoyl)-2,4,6,-tri-deoxy-D-glucose (Orgambide et al. 1991). This high molecular weight compound is encoded in the *eps* operon, which contains more than 12 genes, under control of a single promoter (Huang and Schell 1995). EPS accounts for more than 90% of the total exopolysaccharides present in the mucoid colonies and its structure is conserved among the *R. solanacearum* species complex (McGarvey et al. 1999). As non-mucoid mutants were strongly affected in virulence, the presence of mucus was associated to a virulent phenotype in *R. solanacearum* in the 50s (Kelman 1954). Later studies showed, however, that mutants in the *eps*

synthesis gene operon are not completely avirulent and can develop delayed wilting symptoms in tomato plants after soil-drench or petiole-inoculation (Kao et al. 1992; Saile et al. 1997).

To better understand its biological role, EPS localization was analyzed in colonies grown on plates showing that, although a great proportion of EPS is secreted to the extracellular environment, approximately 20% remains cell-bound and is not released (McGarvey et al. 1998). This observation suggested that free extracellular EPS might cause wilting symptoms by direct obstruction of xylem vessels or by vascular cell rupture due to the high hydrostatic pressure (Denny et al. 1990; Schell 2000). In contrast, cell-bound EPS remains attached to bacterial cells forming a capsule (McGarvey et al. 1998). Although no direct evidence confirmed this hypothesis yet, it has been suggested that cell-bound EPS might mask surface structures, protecting bacterial cells from plant defenses (McGarvey et al. 1998; Schell 2000).

Motility and host attachment

Different types of motility have been described in *R. solanacearum*. The first one is dependent on polar flagella and is responsible for either bacterial swarming (coordinated collective movement on a solid surface) or swimming (individual movement in liquid or semisolid medium). Mutations in the flagellum-encoding genes *fliC* or *fliM* have shown to delay the wilting symptoms caused by *R. solanacearum* when inoculated on soil. However, a full infective capability is still retained when bacteria are directly inoculated in the petiole (Tans-Kersten et al. 2001), thus suggesting a role for flagellum-driven motility in the early stages of plant colonization and not during xylem invasion.

In a similar fashion, Yao and Allen showed that chemotaxis is also involved in the ability of *R. solanacearum* to successfully locate and colonize host plants roots (Yao and Allen 2006). These authors showed that the pathogen is chemically attracted to the roots of host plants in preference of those from non-host plants and that, similarly to flagella-deficient strains, *cheA* and *cheW* mutants are less virulent in soil-inoculated tomato plants although they retain full pathogenicity in petiole inoculation assays.

On the other hand, Type IV pili control twitching motility and bacterial attachment to host surfaces. Type IVa pili are composed of a monomeric unit encoded by *pilA*, and are regarded as a virulence factor in *R*. *solanacearum* as *pilA* mutants are severely impaired in their ability to cause disease symptoms both in soil or petiole inoculated plants (Kang et al. 2002). In addition, it was recently reported that *R. solanacearum* also possesses Type IVb pili, encoded by the *tad* gene cluster, which also contribute to pathogenicity in potato plants (Wairuri et al. 2012). Besides, at least three different types of lectins with different binding specificities have been identified in *R. solanacearum:* LecM, LecX and LecF. The latter lectin was reported to play a role in biofilm formation and virulence in *R. solanacearum* (Pradhan et al. 2012; Meng 2013). Moreover, biofilm formation has been reported as an important virulence factor specially during the colonization of intercellular spaces (Mori et al. 2016).

Protective enzymes and efflux pumps

During plant colonization, *R. solanacearum* faces a hostile environment enriched with Reactive Oxygen Species (ROS), plant-derived phenolic compounds and other antimicrobial compounds expressed during plant defense responses. To protect itself, *R. solanacearum* is endowed with a large battery of protective enzymes such as polyphenol oxidases (Hernández-Romero et al. 2005), catalases (*katE*, *katG*), peroxidases (*bcp*), superoxide dismutases (*sodBC*) and alkyl hydroperoxide reductases (Valls et al. 2006; Flores-Cruz and Allen 2009), the expression of which is controlled by the OxyR regulator (Flores-Cruz and Allen 2011). A slight virulence defect was reported due to mutations in the *bcp* peroxidase, the *dps* iron-binding oxidoreductase and the OxyR regulator, indicating their contribution to pathogenicity (Flores-Cruz and Allen 2009; Colburn-Clifford et al. 2010). Moreover, two multidrug efflux pumps, *acrAB* and *dinF*, provide *R. solanacearum* with resistance against some antibiotics, phytoalexins and detergents and their mutation render the bacteria less virulent in soil-inoculated tomato plants (Brown et al. 2007).

Metabolic adaptation and phytohormone production

R. solanacearum activates a series of alternative metabolic pathways upon plant cell contact and during plant colonization. For instance, in *Arabidopsis thaliana* cell co-culture, *R. solanacearum* preferentially induces expression of *metE* over *metH*, although both genes encode for the enzyme that catalyzes the last step of the methionine biosynthesis pathway a in a cobalamin independent or dependent manner, respectively. Bacteria deficient in *metE* also showed a stronger aggressiveness reduction compared to *metH* mutants (Plener et al. 2012). Furthermore, *R. solanacearum* virulence also depends on ralfuranone production (Kai et al. 2014), and sucrose and nitrogen assimilation especially at early infection stages (Jacobs et al. 2012; Dalsing and Allen 2014). Recently, the catabolic repressor EfpR was reported to contribute to bacterial fitness *in planta* by gaining adaptive mutations after several infective cycles, which expands the pathogen metabolic versatility (Perrier et al. 2016). In addition, infected tomato plants showed accumulation of putrescine, which plays a role in wilting symptom acceleration. Moreover, deletion of the *speC* ornithine decarboxylase gene responsible for putrescine synthesis in *R. solanacearum* caused a complete loss of virulence in tomato plants (Lowe-Power et al. 2017). Besides its ability to modulate metabolism during plant colonization, phytomormones produced by *R. solanacearum* such as ethylene also represent candidate virulence factors (Valls et al. 2006). In fact, ethylene has been involved in disease development in the pathosystem *R. solanacearum/A. thaliana* (Hirsch et al. 2002). Collectively, these studies suggest that the metabolic adaptation of *R. solanacearum* during plant infection contributes to pathogenicity.

Sources of resistance and control strategies against *R. solanacearum*

Taking together the extremely wide geographical distribution of the RSSC, the broad range of plants that the pathogen can infect, the high aggressiveness of the disease and the amount of molecular weapons that it bears, the pathogen was placed in the second position in the list of top 10 most devastating bacterial phytopathogens (Mansfield et al. 2012). For this reason, much effort is devoted to find and develop management strategies against bacterial wilt.

The preferred prevention method against the disease is the use of natural sources of resistance found in wild species or different crop cultivars. For instance, breeding strategies in potato include the use of wild potato relatives, such as *Solanum phureja* (Sequeira and Rowe 1969; French 1982) or *Solanum commersonii* (Carputo et al. 2009; Ferreira et al. 2017), as well as *Solanum aethiopicum,* known as bitter tomato, in eggplant breeding strategies (Collonnier et al. 2001). The tomato variety Hawaii7996 was also proved to be resistant against *R. solanacearum*, and it has become increasingly used as resistant rootstock in tomato grafting (Rivard and Louws 2008). Monogenic control of resistance has been reported in few cases, for instance, in *A. thaliana* Nd-1 the gene RRS1 confers resistance against *R. solanacearum* GMI1000 (Deslandes et al. 1998; Deslandes et al. 2003). However, in most cases resistance is a polygenic trait, as in *S. commersonii* (González et al. 2013), *Medicago truncatula* (Ben et al. 2013), tomato (Thoquet et al. 1996; Carmeille et al. 2006), tobacco (Qian et al. 2013) and eggplant (Lebeau et al. 2013). Therefore, transferring these loci into commercial crop varieties is extremely challenging and sometimes may imply the introduction of linked undesirable attributes (Denny 2006).

Antibiotics such as streptomycin or copper-based compounds were traditionally used to treat a number of bacterial plant diseases (Zaumeyer 1958). However, due to their negative side effects in the environment and their threat to health, attempts to develop alternative and targeted chemical and biological control strategies have been made in last years (Sundin et al. 2016). The applicability of different microorganisms as Biological Control Agents (BCA), such as endophytes, rhizobacteria or bacteriophages, has been primarily studied in controlled conditions. Some field trials resulted relatively successful, but their application is not feasible due to colonization inconsistencies, low suppression levels and constraints related to BCA production or storage (Ramesh and Phadke 2012; Yuliar et al. 2015). In addition, new chemical control methods against *R. solanacearum* include the development of plant systemic defense inducers, for instance Acibenzolar-S-Methyl or ASM (Pradhanang et al. 2005), as well as specific *R. solanacearum* antimicrobials (Hong et al. 2016; Li et al. 2016; Raza et al. 2016; Su et al. 2016). Still, *R. solanacearum* can persist in deeper soil layers or inside asymptomatic hosts, where these compounds or biological agents cannot reach the pathogen (Graham et al. 1979), making the fight against bacterial wilt extremely challenging.

To date, avoiding introduction of contaminated seed tubers is the main control strategy in countries where *R. solanacearum* is not present, while only crop rotation, control of weed reservoirs and surveillance of irrigation water can reduce bacterial wilting in endemic regions (Denny 2006; Huet 2014). Nonetheless, the pathogen's versatile lifestyle and the existence of natural reservoirs demand integrative strategies to make the disease control and eradication extremely complicated.

1.3 ADVANCES ON GENE EXPRESSION ANALYSES IN *R. SOLANACEARUM*

Genomic studies in *R. solanacearum*

R. solanacearum is a pathogen with a complex lifestyle comprising extremely dissimilar environments. Therefore, it contains multiple virulence factors whose expression must be well orchestrated. The first identification of virulence-related genes in *R. solanacearum* was carried out through generation of a random insertion mutant library and a posterior screening of virulence-defective phenotypes in plants (Boucher C.A. 1985; Boucher et al. 1987). However, genetic and molecular studies were complex until the *R. solanacearum* strain GMI1000 genomic sequence was published in 2002 (Salanoubat et al. 2002), becoming since then the reference strain from the RSSC. The availability of the genomic sequence and annotation of the tomato strain GMI1000 represented a turning point in the identification of many virulence genes and understanding of their regulation. The analysis of the first *R. solanacearum* genome revealed that it has a bipartite structure consisting on two replicons: a chromosome (~3.7Mb) and a megaplasmid (~2.1Mb). An unusual high G+C percentage is generally maintained in the whole genomic sequence, except in specific loci that were probably obtained by horizontal gene transfer.

However, slight differences among strains belonging to different phylotypes might account for the variability in host specificity, aggressiveness level or optimal temperature range. To this aim, genomes of other strains belonging to different phylotypes have also become available (Remenant et al. 2010; Li et al. 2011; Xu et al. 2011; Remenant et al. 2012; Chen et al. 2017; Hayes et al. 2017; Patil et al. 2017; Sun et al. 2017). 85 genome assemblies from different *R. solanacearum* strains are currently available in GenBank. Thanks to the diversity of accessible genomic sequences, a comparative analysis with 19 strains belonging to the four phylotypes was performed, and resulted in the identification of candidate host-specific genes, including a list of T3Es associated to some strains (Ailloud et al. 2015).

Furthermore, development of the Single Molecule Real-Time (SMRT) DNA sequencing technology has offered the possibility to detect DNA methylated profiles (Flusberg et al. 2010). In prokaryotes, DNA methylation is an epigenetic mark occurring in adenines and cytosines, and is

largely involved in Restriction-Modification systems (Wilson and Murray 1991). Nonetheless, DNA methylation was also reported to regulate several processes, such as DNA repair or replication (Casadesus and Low 2006; Low and Casadesus 2008). Interestingly, DNA methylation has been found to affect gene expression in a number of bacterial species as well as virulence in some pathogens such as *Salmonella enterica, Yersinia pseudotuberculosis* and *Vibrio cholerae* (Low et al. 2001; Sanchez-Romero et al. 2015). However, little attention has been payed to plant pathogens with the exception of some fungal species (Zhu et al. 2016) and the impact of DNA methylation in gene expression or virulence in bacterial phytopathogens remained unexplored.

With the advances on next generation sequencing platforms, cutting-edge technologies to study global gene expression, such as microarrays or RNA-sequencing, have become affordable and widely used (Van Vliet 2009). By the use of these technologies, *R. solanacearum* has become a model bacterial species to study plant-pathogen interactions and many of its regulatory networks have been elucidated (Coll and Valls 2013).

In the coming sections, the different genetic regulation networks key for *R. solanacearum* virulence and *in planta* fitness are reviewed, from the first classical approaches in artificial medium to the latest *in planta* high-throughput analyses.

Discovery of interconnected regulatory systems to control virulence gene expression

The *phc* sensing system

One of the main regulatory networks controlling expression of many virulence related genes is the *phc* system, with PhcA in the center of it. PhcA was discovered when Brumbley and coworkers were characterizing the interesting phenomenon observed by Kelman in the 50s, which they called Phenotype Conversion (PC) (Denny et al. 1990). PC consists in a spontaneous loss of virulence of *R. solanacearum* linked to a reduction in EPS and endoglucanase (Egl) production and an increase in motility, siderophore biosynthesis and endo-polygalacturonase (PglA) levels (reviewed in (Genin and Boucher 2002)). By screening a Tn5-mutant library, the mentioned authors found that PhcA, a LysR transcriptional regulator, was responsible for this phenotypic switch (Brumbley and Denny 1990; Brumbley et al. 1993). Later studies showed that the *phcB* mutant had the same phenotype as *phcA*, with the exception that EPS and exoprotein production were restored by culturing cells in culture supernatants of wild-type bacteria (Clough et al. 1994). This led to the deduction that the presence of a certain Volatile Extracellular Factor produced by *phcB* controlled activity of PhcA. Shortly after, 3-hydroxypalmitic acid methyl ester (3-OH-PAME), or methyl 3-Hydroxymyristate (3-OH-MAME) in some strains (Kai et al. 2015), was identified as the volatile compound triggering PhcA expression at high cell densities by reliving *phcA* repression from the PhcS/PhcR two-component regulatory system (Clough et al. 1997b; Flavier et al. 1997).

In parallel to this work, other studies reported the existence of other two-component systems and regulators controlling EPS expression in a coordinate way. This is the case of the VsrA/VsrD and VsrB/VsrC systems and the regulator protein XpsR, so that VsrB/VsrC system activates EPS production in conjunction with XpsR, whose transcription is controlled by both the VsrA/VsrD system and PhcA (Huang et al. 1993; Huang et al. 1995). At that time, the EpsR regulator was also reported as an EPS biosynthesis repressor (McWilliams et al. 1995). Interestingly, other studies showed that PhcA also acts as a negative regulator of motility and PglA through the PehS/PehR two-component system (Allen et al. 1997). Finally, recent reports demonstrate the existence of other secreted molecules named ralfuranones, which are induced by activation of PhcA and contribute both to virulence and to a feedback loop in the *phc* signaling cascade (Mori et al. 2016; Mori et al. 2018) A scheme of the *phc* regulatory network is represented in red in Figure 5.

In global, the *phc* system acts as a regulatory switch of virulence genes such as EPS, cell wall degrading enzymes and motility, depending on bacterial growth and confinement. When bacterial densities are below 10^7 cells/ml, 3-OH-PAME levels are low and PhcA is inactive. In this situation, EPS and Egl are not induced and bacteria become motile. In contrast, when bacterial densities are above 10^7 cells/ml, 3-OH-PAME is accumulated and PhcA is induced by PhcSR. Bacteria can then repress expression of motility genes, but promote EPS and PglA production.

The discovery of this genetic regulatory network provided the first evidence of virulence gene batteries differentially expressed at different stages of the *R. solanacearum* life cycle, suggesting a role in switching bacterial adaptation from the saprophytic phase in soil to the parasitic xylem colonization stage.

The *SolR/SolI* quorum sensing system

In addition to the *phc* system, *R. solanacearum* possesses another auto-induction cell density-dependent system named SolR/SolI. These two proteins are part of a two-component regulatory system homologue to the LuxR/LuxI involved in the regulation of quorum sensing in many bacterial species (Fuqua and Greenberg 1998). SolI is involved in the synthesis of N-hexanoyl and N-octanoyl-homoserine lactones, autoinducer molecules that lead to SolR activation upon accumulation. When bacterial densities reach 10^8 cells/ml, SolR induces transcription of *solI* and other downstream genes such as *aidA* (Flavier et al. 1997). Nonetheless, the SolR/SolI system is also induced by accumulation of 3-OH-PAME via PhcA (Flavier et al. 1997), acting as a hierarchical autoinduction cascade: firstly induced at 10^7 cells/ml by PhcRS via 3-OH-PAME, and afterwards induced at 10^8 cells/ml by SolRI via Acyl-Homoserine lactones. Interestingly, expression of *solRI* is also dependent on the alternative sigma factor RpoS, which plays a role in stationary phase and stress survival (Flavier et al. 1998) (purple cascade in Figure 5). Since *solRI* mutants were not affected in virulence and they are induced at specially high cell densities, it was suggested that they could play a role during the last stages of the disease (Schell 2000).

The T3SS regulatory cascade

Simultaneously to the characterization of the quorum sensing systems in *R. solanacearum*, many studies focused on the description of the *hrp* cluster, a common virulence feature also present in other pathogenic bacteria (Gough et al. 1992), that was found after screening a mutant library for loss of virulence (Boucher et al. 1987).

In *R. solanacearum* the *hrp* cluster comprises more than 20 genes organized in seven transcriptional units (Arlat et al. 1992; Van Gijsegem et al. 1995). The cluster includes genes involved in T3SS regulation and structure, effector proteins as well as *hpa* (HR and pathogenicity associated) genes (Salanoubat et al. 2002). *Hrp* gene expression was found to be dependent on environmental factors such as the carbon and nitrogen sources, as they were repressed in rich medium but induced in minimal medium and *in planta* (Arlat et al. 1992). To unravel the *hrp* signaling cascade and due to its simplicity, most of the gene expression studies were performed in minimal medium, an artificial medium that reproduces the plant environmental conditions (Arlat et al. 1992). However, the most upstream receptors and regulators of the cascade specifically induced in plants, could not be identified until plant cell co-cultures were introduced. Thanks to the first *A. thaliana* and tomato cell co-cultures, the plant signal receptor in *R. solanacearum* was identified as PrhA (plant regulator of *hrp* genes) (Marenda et al. 1998). The signal sensed by PrhA, which is still unknown, is ubiquitous, plant cell contact-dependent and recognized within hours (Aldon et al. 2000). Shortly after recognition, PrhA transduces the plant signal through activation of the PrhR/PrhI two-component regulatory system (Brito et al. 2002). Activation of PrhRI triggers the transcription of the PrhJ regulator, which in turn drives expression of another regulator protein called HrpG. Finally, HrpG mediates activation of HrpB, the last component of the *hrp* signaling cascade (Brito et al. 1999). Interestingly, both HrpG and HrpB share homology with other T3SS key regulators in *Xanthomonas* and *Burkholderia* species (Wengelnik and Bonas 1996; Wengelnik et al. 1996; Lipscomb and Schell 2011). In minimal medium as well as in plant cell-coculture, HrpB ultimately induces expression of genes encoded inside and outside the *hrp* cluster by binding to the hrp_{II} box present in the HrpB-regulated promoters (Genin et al. 1992; Cunnac et al. 2004). Among the HrpB-regulated genes are: T3SS structural genes encoded by other *hrp* and *hrc* genes –hrp conserved genes also present in animal pathogens (Bogdanove et al. 1996), as well as effector proteins that are translocated into the host cell (Cunnac et al. 2004) (blue and yellow cascades in Figure 5). Interestingly, recent studies have shown that T3E translocation into host cells is controlled at the post-transcriptional level by Type 3 Chaperones, encoded in the *hpa* genes within the *hrp* cluster, to ensure proper T3E folding (Lohou et al. 2014; Lonjon et al. 2016; Lonjon et al. 2017).

Additional control of the *hrp* gene expression comes from the cell growth-dependent PhcA regulator, which represses the *hrp* signaling cascade through inactivation of the *prhIR* promoter in rich medium conditions (Yoshimochi et al. 2009). Together with the fact that *prh* and *hrpG* gene

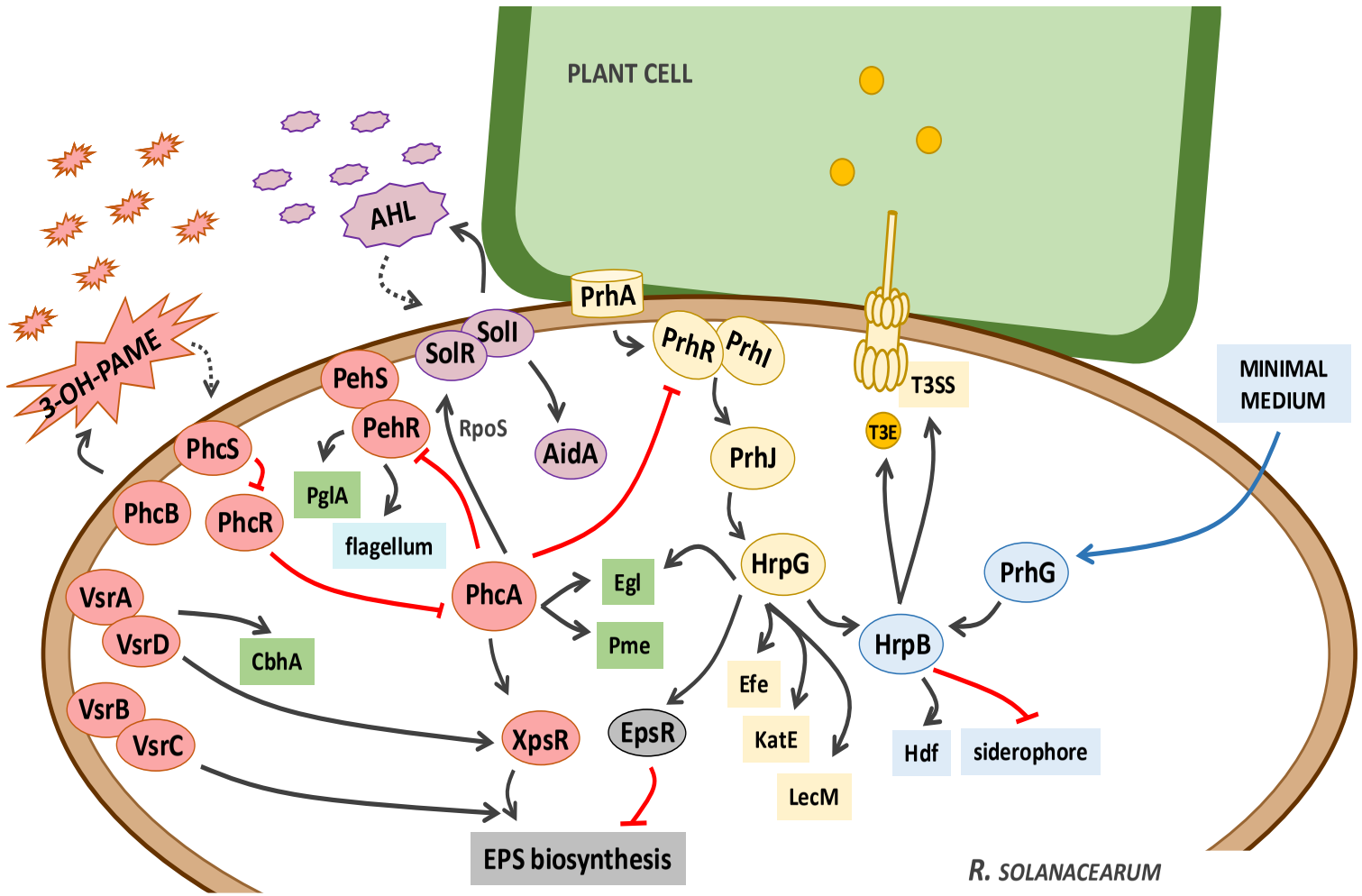
PLANT CELL
AHL
3-OH-PAME
PrhA
SolI
SolR
PrhR
PrhI
T3SS
T3E
MINIMAL MEDIUM
PehS
PehR
RpoS
AidA
PhcS
PhcB
PhcR
PglA
flagellum
PrhJ
HrpG
PrhG
VsrA
VsrD
VsrB
VsrC
CbhA
PhcA
Egl
Pme
HrpB
Efe
KatE
LecM
Hdf
siderophore
XpsR
EpsR
EPS biosynthesis
R. SOLANACEARUM

expression is restricted to plant cell contact while HrpB transcription is also induced by growth in minimal medium mediated by PrhG (Brito et al. 1999; Plener et al. 2010), this result further supports the existence of distinct signaling pathways integrated at different levels of the cascade (blue and yellow cascades in Figure 5). Besides, HrpG and HrpB defective strains have different plant infective and invasive abilities. On one hand, the *hrpG* mutant is unable to cross the root endodermis and reach the vascular system, on the other hand, a *hrpB* mutant can multiply at low densities in few xylem vessels (Vasse et al. 2000). This observation suggested that HrpG and HrpB might be necessary at different root infection stages, although both pathways are required for full pathogenicity in *R. solanacearum* as mutations in any regulator of the signaling cascade cause virulence reduction or abolition.

The Omics era: Decoding *R. solanacearum* gene expression

The introduction of high-throughput transcriptomic techniques such as microarrays or RNA-sequencing represented a breakthrough in the study of gene expression (Van Vliet 2009). The first microarray for *R. solanacearum* gene expression analysis was constructed in 2005 to identify the HrpB and HrpG regulated genes (Occhialini et al. 2005; Valls et al. 2006). In the first study, the authors detected 193 genes whose expression level was altered in a *hrpB*-deficient background when grown in minimal medium. Besides detecting known T3Es, the T3E repertoire was extended with 26 new candidate genes and, unexpectedly, it was discovered that HrpB also regulates other traits such as chemotaxis, iron uptake and metabolism of low-molecular-weight compounds (*hdf* operon). Later on, HrpG-regulated genes were also identified, and denoted that the HrpG-regulon is organized in two different pathways: one in a HrpB-dependent manner and the other independently from HrpB. The analysis of the HrpB-independent HrpG-regulated genes unraveled that HrpG also controls virulence determinants beyond the T3SS, for instance, attachment by lectins (*lecM*), phytohormone production (ethylene-*efe*), plant cell wall degradation (*egl*) and protective responses (catalse-*katE*). HrpG has been since then considered a master virulence regulator vital for host adaptation and, in line with previous studies, key for root vascular system colonization (Vasse et al. 2000) (blue and yellow cascades in Figure 5).Although still under construction (Zhang et al. 2011; Zhang et al. 2015), the use of these first transcriptomes studies allowed a more complete assembly of the *hrp* regulatory network.

Figure 5. Scheme of the *phc*, *sol* and *hrp* regulatory cascades in *R. solanacearum*.

Regulatory proteins are marked by color-coded circles depending on the signaling cascade they belong to (red-*phc* network, purple-*sol* system, yellow-plant-cell contact dependent *hrp* cascade, blue-minimal medium dependent *hrp* cascade). Rectangles indicate downstream products following the same color-code. Green boxes correspond to different cell wall degrading enzymes existing in R. solanacearum. Black arrows indicate activations while red T symbols indicate inhibitions. Abbreviations are given in the text.

Expanding knowledge on *R. solanacearum* gene expression *in planta*

Many virulence factors key for *R. solanacearum* pathogenicity could be identified and characterized using *in vitro* conditions that tried to mimic the plant environment, such as minimal medium. However, this was a limiting factor since *R. solanacearum* encounters very different environments and plant tissues along the infection process (Vasse et al. 1995). Therefore, genes involved in host adaptation or specifically needed for plant wilting could only be detected during plant colonization and not during growth in artificial media.

The first *in planta* approach to identify *R. solanacearum* genes specifically induced during growth inside the host was performed using the In Vivo Expression Technology (IVET). IVET technology consists in a library of promoter fragments cloned upstream of a promoterless copy of a gene that is required for bacterial growth within the host, and introduced in a mutant lacking this essential gene for multiplication. *R. solanacearum* IVET strains were directly introduced into tomato xylem vessels by petiole-inoculation and they were recovered at the onset of the disease (Brown and Allen 2004). Among the unique promoter fusions identified, a high proportion encoded transmembrane proteins, were related to transport and metabolic functions or were involved in stress responses. Furthermore, some of the genes detected with IVET had been previously reported to play a role in virulence, for instance, *vsrB*, *vsrD*, *rpoS*, *pehR* or *hrcC*. And, interestingly, around 60% of the selected genes for further validation were not induced in minimal medium conditions. All these data suggested that expression of these genes is regulated by specific plant signals, and that *R. solanacearum* adapts metabolically to the new environment. However, only the highest expressed genes could be detected, limiting the complete picture of *R. solanaceaum*'s behavior during plant colonization.

To solve this problem and obtain an exhaustive idea of *R. solanacearum's* gene expression changes during multiplication *in planta*, bacterial transcriptomic approaches inside the plant began to arise. For instance, Jacobs and coworkers (Jacobs et al. 2012) characterized the global gene expression in *R. solanacearum* recovered from tomato xylem vessels of early wilted plants. In line with the IVET results, the authors showed the contribution of specific bacterial metabolic pathways required for successful *in planta* colonization, such as sucrose catabolism. Interestingly, a surprisingly high concentration of sucrose was detected in tomato xylem vessels, which decreased in the presence of the pathogen. Moreover, mutants deficient in their ability to uptake and catabolize sucrose showed reduced virulence in several plant species. Nitrate assimilation and respiration genes were also induced during tomato pathogenesis, and further characterization of these pathways revealed that they contribute to stem colonization and virulence (Dalsing and Allen 2014; Dalsing et al. 2015).

To explore the bacterial gene expression responsible for host-specific adaptations, an RNA-sequencing involving multiple hosts –tomato, banana and melon- and *R. solanacearum* strains

– the banana pathogenic Moko strain, and one strain not pathogenic to banana, NPB - was carried out (Ailloud et al. 2016). In this work, the authors showed that, different bacterial strains modulate their gene expression to better adapt to a specific host. For instance, the Moko strain preferentially induced nitrate assimilation genes in banana plants, whereas the NPB strain up-regulated genes involved in denitrification. This result clearly points out that *R. solanacearum* adjusts its metabolism depending on the host that it encounters.

Besides the host factor, temperature is another variable that can affect bacterial multiplication and virulence (Bocsanczy et al. 2012). While most *R. solanacearum* strains grow optimally and are virulent at 28ºC, R3b2 strains are adapted to cool weathers and are highly aggressive at 20ºC. To understand the mechanisms to cool adaptation by R3b2 strains, the *in planta* transcriptomic responses to temperature changes were analyzed (Meng et al. 2015). Some cool virulence factors identified included LecM, AidA and AidC, three genes absent in a non-R3b2 strain and positively regulated by the quorum sensing SolI/SolR regulators. This work demonstrated that R3b2 strains deploy still unknown mechanisms to stay virulent at lower temperatures and provides a list of genes that might be key for this process.

Recently, the impact of the central regulator PhcA has also been explored by RNA-sequencing in rich and minimal medium as well as during tomato xylem colonization (Khokhani et al. 2017; Mori et al. 2018; Perrier et al. 2018). These studies demonstrate that the PhcA regulon is the largest so far described for a single regulator in *R. solanaceaum*, controlling the expression of more than 1500 genes in rich medium, almost 1000 genes in minimal medium and approximately 600 genes *in planta*. Interestingly, many genes showed a conserved PhcA-dependent expression pattern in the three conditions, such as induction of EPS, lectins and adhesins, glucanases and ralfuranone biosynthesis as well as repression of nitrate reduction and siderophore biosynthesis. Conversely, a subset of pathogenicity factors including many genes from the HrpG-HrpB regulon, was specifically induced by PhcA *in planta* and repressed in rich medium. This result contrasts with the assumption that PhcA repressed T3SS gene expression at high cell densities (Genin et al. 2005; Yoshimochi et al. 2009), and further supports previous observations of *hrp* expression *in planta* at advanced disease stages (Jacobs et al. 2012; Monteiro et al. 2012a). On the other hand, functional analyses revealed that at low cell densities, for instance during root colonization, inactive PhcA allows expression of motility and attachment mechanisms and promotes growth (Khokhani et al. 2017). These observations are in line with the fact that a *phcA* mutant strain grows faster than the WT and that it is unable to wilt plants when soil-inoculated, but still slightly infective when directly introduced in the xylem vessels (Brumbley and Denny 1990). Finally, an integrative model placed PhcA as the main regulator of a network controlling a fine tuned trade-off between growth and virulence (Peyraud et al. 2016; Peyraud et al. 2018).

Altogether, these results suggest that *R. solanacearum* deploys various mechanisms to activate or repress key sets of genes during plant colonization depending on several parameters, such

as bacterial growth, presence/absence of a host, host species and temperature. Although most of the virulence regulatory networks could be identified and constructed using artificial culture media, the importance of validating them *in planta* is evidenced. This is the case of the T3SS, which appeared to be induced in the plant at high cell densities, contrary to *in vitro* studies that suggested a T3SS induction only at early stages, when bacterial numbers are low. Finally, despite the wealth of *in planta* transcriptomic studies performed in *R. solanacearum*, to date all of them have only focused on the disease onset stage, without considering other infection stages that are equally relevant for disease establishment and progression. Therefore, exploring the gene expression dynamics of *R. solanacearum* in different *in planta* infection stages will contribute to a more detailed picture of the essential virulence mechanisms that direct the switch from one stage to the next.

chapter 2

OBJECTIVES

The objectives of this thesis are presented below:

Genome and methylome profiling of *R. solanacearum* UY031

1. Provide the complete genome sequence and its characterization of the phylotype IIB-1 strain *R. solanacearum* UY031.
2. Compare the methylome profiles of *R. solanacearum* UY031 to that of GMI1000.
3. Explore the possible contribution of DNA methylation to virulence gene expression.

Characterization of *repR*, a new candidate virulence gene in *R. solanacearum*

4. Characterize the involvement of RepR in *R. solanacearum* UY031 pathogenicity.
5. Understand the molecular basis of RepR using a genome-wide expression profiling.

Understanding the *R. solanacearum* UY031 transcriptomic changes during the infection process

6. Decipher the *R. solanacearum* UY031 transcriptome during root colonization of tolerant and susceptible wild potato plants.
7. Profile the expression of *R. solanacearum* virulence factors along the infective cycle in potato plants.

Identification of T3SS inhibitors to combat bacterial plant diseases – Proof of Concept Study

8. Identify potential T3SS inhibitors *in vitro* and *in vivo* using *R. solanacearum* as model organism.
9. Analyze the possible application of candidate T3SS inhibitors as plant disease protectants.

PUBLICATIONS

Informe del director de tesi del factor d'impacte dels articles publicats

La memòria de la tesi doctoral "Control strategies and gene expression dynamics of the plant pathogen *Ralstonia solanacearum*" (Estratègies de control i dinàmica d'expressió gènica en el fitopatogen *Ralstonia solanacearum*) presentada per Marina Puigvert Sanchez conté a la secció de publicacions 3 articles i 3 apartats en forma de manuscrit. La participació de la doctoranda en cadascun d'ells és la que es detalla a continuació:

Publicació 1

Títol: Complete genome sequence of the potato pathogen *Ralstonia solanacearum* UY031
Autors: Rodrigo Guarischi-Sousa, **Marina Puigvert**, Núria S. Coll, María Inés Siri, María Julia Pianzzola, Marc Valls i João C. Setubal.
Revista: Aquest article està publicat a la revista Standards in Genomic Sciences (2016).
Índex d'impacte a l'any de publicació: 1,189; Àrees: Genètica i Herència (Q4); Microbiologia (Q4)
Nombre de citacions: 7.

La participació de la Marina Puigvert ha consistit en la preparació de les mostres biològiques, així com també en l'elaboració de l'anàlisi bioinformàtica dels efectors de tipus III presents en *R. solanacearum* UY031 (descrit a la Taula 6). Ha col·laborat en l'anotació del genoma i ha participat activament en la planificació del projecte i l'elaboració del manuscrit. La resta d'anàlisis bioinformàtiques han estat dutes a terme pel col·laborador brasiler (R Guarischi-Souza). La resta d'autors externs han cedit materials o col·laborat en la direcció de la feina.

Publicació 2

Títol: Comparative analysis of *Ralstonia solanacearum* methylomes
Autors: Ivan Erill, **Marina Puigvert**, Ludovic Legrand, Rodrigo Guarischi-Sousa, Céline Vandecasteele, João C. Setubal, Stephane Genin, Alice Guidot i Marc Valls.
Revista: Aquest article està publicat a la revista Frontiers in Plant Science (2017).
Índex d'impacte (2016): 4,291; Àrees: Ciències de plantes (Q1).

La doctoranda Marina Puigvert és responsable de la part experimental d'aquest treball. També ha participat activament en la planificació del projecte, discussió dels resultats i elaboració del manuscrit. Les anàlisis bioinformàtiques les ha dutes a terme el primer autor (IP de grup col·laborador) i la resta d'autors externs han cedit materials o col·laborat en la direcció de la feina.

Publicació 3

Títol: Transcriptomes of *Ralstonia solanacearum* during Root Colonization of *Solanum commersonii*
Autors: **Marina Puigvert**, Rodrigo Guarischi-Sousa, Paola Zuluaga, Núria S. Coll, Alberto P. Macho, João C. Setubal i Marc Valls.
Revista: Aquest article està publicat a la revista Frontiers in Plant Science.
Índex d'impacte (2016): 4,291; Àrees: Ciències de plantes (Q1); Nombre de citacions: 1

En aquest article, la doctoranda Marina Puigvert ha dut a terme la totalitat del treball experimental. També ha realitzat gran part del treball bioinformàtic presentat en col·laboració amb el grup Brasiler. Ha participat activament en la planificació del projecte, la realització

d'experiments, interpretacions bioinformàtiques, la discussió dels resultats i l'elaboració del manuscrit.

Manuscrit 1

Títol: RepR, a MarR transcriptional regulator from *Ralstonia solanacearum* key for early stages of plant colonization.
Autors: **Marina Puigvert**, Pau Sebastià, Núria Sanchez-Coll, Marc Valls.

La doctoranda Marina Puigvert ha dut a terme la totalitat del treball experimental i bioinformàtic presentat, excepte les rèpliques d'alguns experiments, així com de la redacció d'aquest esborrany i de les figures presentades al manuscrit.

Manuscrit 2

Títol: Spatiotemporal transcriptomic changes of *Ralstonia solanacearum* UY031 during different potato infection stages.
Autors: **Marina Puigvert**, Pau Sebastià, Roger de Pedro, Alberto P. Macho, Rodrigo Guarischi-Sousa, Núria Sanchez-Coll, João C. Setubal, Marc Valls.

La doctoranda Marina Puigvert ha dut a terme la majoria del treball experimental presentat, en el qual ha estat assistida per un alumne de màster (Roger de Pedro) i el doctorand que continuarà la feina (Pau Sebastià). La doctoranda ha dut a terme també tota l'anàlisi bioinformàtica de les dades amb la supervisió i assessorament dels col·laboradors Brasilers, així com de la redacció d'aquest esborrany i de les figures presentades al manuscrit.

Manuscrit 3

Títol: Identification of inhibitors of the type III secretion system to combat bacterial plant diseases.
Autors: **Marina Puigvert**, Montserrat Solé, Belén López-Garcia, Núria S. Coll, Karren D. Beattie, Rohan A. Davis, Mikael Elofsson, Marc Valls.

La doctoranda Marina Puigvert ha dut a terme la totalitat del treball experimental presentat, excepte algunes rèpliques d'assajos de virulència, dutes a terme per la segona autora, així com de la redacció d'aquest esborrany i de les figures presentades al manuscrit.

El director,

Marc Valls Matheu

Barcelona, 11 d'Abril de 2018

chapter 3

PUBLICATION 1

Complete genome sequence of the potato pathogen *Ralstonia solanacearum* UY031

Resum de la publicació 1

"Complete genome sequence of the potato pathogen *Ralstonia solanacearum* UY031"

"Seqüència genòmica completa de *Ralstonia solanacearum* UY031, patogen de la patatera"

Rodrigo Guarischi-Sousa, Marina Puigvert, Núria S. Coll, María Inés Siri, María Julia Pianzzola, Marc Valls i João C. Setubal

Referència: Standards in Genomic Sciences 2016 11:7

Doi: https://doi.org/10.1186/s40793-016-0131-4

El bacteri fitopatogen *Ralstonia solanacearum* és l'agent causant del marciment bacterià en patateres. La soca UY031 de *R. solanacearum* correspon al filotip americà IIB sequevar 1; o també classificada com a raça 3 biovarietat 2. En aquest estudi es presenta el genoma completament seqüenciat d'aquesta soca, la primera del filotip IIB sequevar 1 amb el genoma complet, i la quarta del complexe d'espècies de *R. solanacearum*. A més de l'anotació estàndard del genoma, també s'ha dut a terme una anotació acurada dels gens efectors de tipus III, un tipus de gens molt importants involucrats en patogenicitat. S'han identificat 60 gens d'efectors i s'ha observat que aquest repertori d'efectors és diferent dels d'altres soques del filotip IIB. Onze efectors apareixen com a no-funcionals degut a mutacions disruptives. També es descriu una anàlisi del metiloma d'aquest genoma, el primer per a una soca de *R. solanacearum*. Aquesta anàlisi ha servit per a posar de manifest la presència d'un gen que codifica una toxina en una regió de probable origen fàgic, cosa que suggereix que aquest gen podria tenir un paper rellevant en la virulència d'aquesta soca.

Guarischi-Sousa et al. Standards in Genomic Sciences (2016) 11:7
DOI 10.1186/s40793-016-0131-4

Standards in Genomic Sciences

SHORT GENOME REPORT Open Access

Complete genome sequence of the potato pathogen *Ralstonia solanacearum* UY031

Rodrigo Guarischi-Sousa[1], Marina Puigvert[2], Núria S. Coll[2], María Inés Siri[3], María Julia Pianzzola[3], Marc Valls[2] and João C. Setubal[1,4*]

Abstract

Ralstonia solanacearum is the causative agent of bacterial wilt of potato. *Ralstonia solanacearum* strain UY031 belongs to the American phylotype IIB, sequevar 1, also classified as race 3 biovar 2. Here we report the completely sequenced genome of this strain, the first complete genome for phylotype IIB, sequevar 1, and the fourth for the *R. solanacearum* species complex. In addition to standard genome annotation, we have carried out a curated annotation of type III effector genes, an important pathogenicity-related class of genes for this organism. We identified 60 effector genes, and observed that this effector repertoire is distinct when compared to those from other phylotype IIB strains. Eleven of the effectors appear to be nonfunctional due to disruptive mutations. We also report a methylome analysis of this genome, the first for a *R. solanacearum* strain. This analysis helped us note the presence of a toxin gene within a region of probable phage origin, raising the hypothesis that this gene may play a role in this strain's virulence.

Keywords: Short genome report, Bacterial wilt, *Ralstonia solanacearum*, Bacterial plant pathogen, Methylome, Uruguay

Introduction

Ralstonia solanacearum is the causal agent of bacterial wilt, one of the most devastating plant diseases worldwide [1]. It is a highly diversified bacterial plant pathogen in terms of host range, geographical distribution, pathogenicity, epidemiological relationships, and physiological properties [2]. Strains are divided in four phylotypes, corresponding roughly to their geographic origin: Asia (phylotype I), the Americas (II), Africa (III), and Indonesia (IV) [3]. Strain UY031 belongs to phylotype IIB, sequevar 1 (IIB1), the group considered mainly responsible for bacterial wilt of potato in cold and temperate regions [4]. Phylotype IIB, sequevar 1 is also traditionally classified as race 3 biovar 2.

Strain UY031 was isolated in Uruguay from infected potato tubers in 2003 and displays high aggressiveness both on potato and tomato hosts [5]. This strain is being used as a model in plant-pathogen gene expression studies carried out by our group; having its genome available greatly facilitates the identification of pathogenicity-related genes. Four other IIB1 *R. solanacearum* strains have been partially sequenced: UW551 [6], IPO1609 [7], NCPPB909 [8], and CFIA906 [8]. This is the first genome of this group to be completely sequenced, and the fourth within the *R. solanacearum* species complex (the other three are strains GMI1000 [9], Po82 [10] , and PSI07 [11]).

Organism information

Classification and features

Ralstonia solanacearum UY031 strain is classified within the order *Burkholderiales* of the class *Betaproteobacteria*. It is an aerobic, non-sporulating, Gram-negative bacterium with rod-shaped cells ranging from 0.5 to 1.5 μm in length (Fig. 1, (a) and (b)). The strain is moderately fast-growing, forming 3–4 mm colonies within 2–3 days at 28 °C. On a general nutrient medium containing tetrazolium chloride and high glucose content, strain UY031 usually produces a diffusible brown pigment and develops pearly cream-white, flat, irregular, and fluidal colonies with characteristic pink whorls in the centre (Fig. 1, (c)). Strain UY031 was isolated from a naturally infected potato tuber showing typical brown rot symptoms (creamy exudates from the vascular rings and eyes of the tuber). This strain is highly pathogenic in different solanaceous hosts including important crops like tomato and potato [5]. Pathogenicity of this strain was also confirmed in several accessions

* Correspondence: setubal@iq.usp.br
[1]Instituto de Química, Universidade de São Paulo, São Paulo, Brazil
[4]Biocomplexity Institute, Virginia Tech, Blacksburg, VA, USA
Full list of author information is available at the end of the article

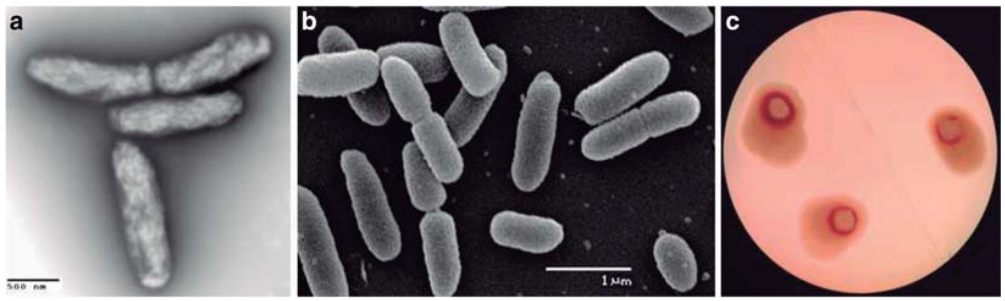

Fig. 1 Images of *Ralstonia solanacearum* strain UY031 using transmission (**a**) and scanning (**b**) electron microscopy, as well as light microscopy to visualize colony morphology on solid media (**c**)

Table 1 Classification and general features of *Ralstonia solanacearum* strain UY031according to the MIGS recommendations [27]

MIGS ID	Property	Term	Evidence code[a]
	Classification	Domain Bacteria	TAS [28]
		Phylum *Proteobacteria*	TAS [29]
		Class *Betaproteobacteria*	TAS [30, 31]
		Order *Burkholderiales*	TAS [31, 32]
		Family *Burkholderiaceae*	TAS [31, 33]
		Genus *Ralstonia*	TAS [34, 35]
		Species *Ralstonia solanacearum*	TAS [34, 35]
		Strain UY031	
	Gram stain	Negative	IDA
	Cell shape	Rod	IDA
	Motility	Motile	IDA
	Sporulation	Non sporulating	NAS
	Temperature range	Mesophile	IDA
	Optimum temperature	27 °C	IDA
	pH range; Optimum	5.5 – 8.0; 6.5	NAS
	Carbon source	Dextrose, lactose, maltose, cellobiose	IDA
MIGS-6	Habitat	potato plants, soil	TAS [5]
MIGS-6.3	Salinity	<2.0 %	TAS [36]
MIGS-22	Oxygen requirement	Aerobic	IDA
MIGS-15	Biotic relationship	free-living	IDA
MIGS-14	Pathogenicity	Pathogenic	TAS [5]
MIGS-4	Geographic location	Uruguay, San José	TAS [5]
MIGS-5	Sample collection	2003	TAS [5]
MIGS-4.1	Latitude	34°43′58.17″S	NAS
MIGS-4.2	Longitude	56°32′2.87″W	NAS
MIGS-4.4	Altitude	116.7 m	NAS

[a]Evidence codes - *IDA* Inferred from direct assay, *TAS* Traceable author statement (i.e., a direct report exists in the literature), *NAS* Non-traceable author statement (i.e., not directly observed for the living, isolated sample, but based on a generally accepted property for the species, or anecdotal evidence). These evidence codes are from the Gene Ontology project [37]

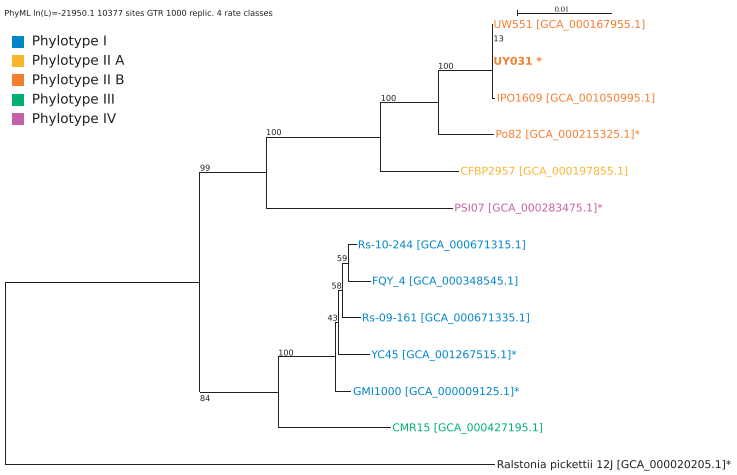

Fig. 2 Phylogenetic tree highlighting the position of the *Ralstonia solanacearum* UY031 (shown in bold) relative to other strains from the same species. The phylogenetic tree was constructed using four conserved prokaryotic marker genes, namely: recA, rpoA, rpoB and rpoC. Each gene was aligned individually with MUSCLE [25]; the resulting multiple alignments were concatenated. PhyML [26] was used to perform tree reconstruction using the GTR model and 1,000 bootstrap replicas. Strain names are colour-coded according to the correspondent phylotype. GenBank accession numbers are displayed within brackets. Strains whose genome was completely sequenced are marked with an asterisk. *Ralstonia pickettii* 12 J (NCBI accession NC_010682) was used as an outgroup

of *Solanum commersonii* Dunal, a wild species considered as a valuable source of resistance for potato breeding. Due to its great aggressiveness, strain UY031 is being used for selection of resistant germplasm as part of the potato breeding program developed in Uruguay. This strain has been deposited in the CFBP collection of plant-associated bacteria, and has received code CFBP 8401. Minimum Information about the Genome Sequence of *R. solanacearum* strain UY031 is summarized in Table 1, and a phylogenetic tree is shown in Fig. 2.

Genome sequencing information

Genome project history

This sequencing project was carried out in 2015; the result is a complete and finished genome. Project data is available from GenBank (Table 2). Accession codes for reads in the

Table 2 Project information

MIGS ID	Property	Term
MIGS 31	Finishing quality	Finished
MIGS-28	Libraries used	SMRT library (P5-C3 large insert library)
MIGS 29	Sequencing platforms	PacBio RS II
MIGS 31.2	Fold coverage	138×
MIGS 30	Assemblers	HGAP.2 workflow
MIGS 32	Gene calling method	Prokka v1.10 (ncRNAs search enabled)
	Locus tag	RSUY
	Genbank ID	CP012687 (chr), CP012688 (pl)
	GenBank date of release	September 28, 2015
	GOLD ID	NA
	BIOPROJECT	PRJNA278086
MIGS 13	Source material identifier	SAMN03402637
	Project relevance	Plant pathogen

Table 3 Summary of genome: one chromosome and one plasmid

Label	Size (Mb)	Topology	INSDC identifier	RefSeq ID
Chromosome	3.41	circular	NA	NA
Megaplasmid	1.99	circular	NA	NA

Sequence Read Archive are SRP064191, SRR2518086, and SRZ132405.

Growth conditions and genomic DNA preparation

R. solanacearum strain UY031 was routinely grown in rich B medium (10 g/l bactopeptone, 1 g/l yeast extract and 1 g/l casaminoacids). Genomic DNA was extracted from a bacterial culture grown to stationary phase to avoid over-representation of genomic sequences close to the origin of replication. Twelve ml of a culture grown for 16 h at 30 °C and shaking at 200 rpm (OD_{600} = 0.87) were used to extract DNA with Blood & Cell Culture DNA Midi kit (Qiagen), following manufacturer's instructions for gram-negative bacteria. DNA concentration and quality were measured in a Nanodrop (ND-8000 8-sample spectrophotometer).

Genome sequencing and assembly

Whole-genome sequencing was performed on the PacBio RS II platform at the Duke Center for Genomic and Computational Biology (USA). P5-C3 chemistry and a single SMRTcell were used, and quality control was performed with DUGSIM. The number of Pre-Filter Polymerase Read Bases was greater than 749 million (>130x genome coverage). Reads were assembled using RS_HGAP_Assembly.2 protocol from SMRT Analysis 2.3 [12]. This resulted in one circular chromosome (3,412,138 bp) and one circular megaplasmid (1,999,545 bp). These lengths are very similar to those of the corresponding replicons in *R. solanacearum* Po82, a IIB sequevar 4 strain, also a potato pathogen and which has also been completely sequenced [10]. The origin of replication was defined for both replicons based on the putative origin for reference strain GMI1000 [9].

An assembly quality assessment was performed before all downstream analyses. All reads were mapped back to the assembled sequences using RS_Resequencing.1 protocol from SMRT Analysis 2.3. This analysis revealed that chromosome and megaplasmid sequences had 100 % of bases called (percentage of assembled sequence with coverage > = 1) and 99.9999 % and 99.9992 %, respectively, of consensus concordance.

Genome annotation

Genome annotation was done using Prokka [13] with the option for ncRNA search. Type III effectors of strain UY031 were identified and annotated in three steps: First, 17 of the T3Es from the *R. solanacearum* species complex [14] were identified based on the Prokka annotations. Second, the 15 T3Es annotated as "Type III Effector Protein", "Probable Type III Effector Protein" or "Putative Type III Effector Protein" by Prokka were manually annotated using the first BLAST [15] hits (usually 100 % identity) of their DNA sequences against genome sequences of phylotype IIB strains MOLK2 and Po82. Third, the UY031 genome was uploaded to the "*Ralstonia* T3E" web interface tool [14] to search for additional T3Es not annotated as such with Prokka. The additional 28 T3E genes identified were manually annotated as above. Homologous Gene Group clustering was performed with get_homologues [16] using the orthoMCL program [17] and requiring a minimum sequence identity in BLAST query/subject pairs of 30 %.

The sequencing plataform used to assemble the genome (PacBio RS II) also gives kinectics information about the sequenced genome. The presence of a methylated base in the DNA template delays the incorporation of the complementary nucleotide; such modifications in the kinectics may be used to characterize modified bases by methylation including: 6-mA, 5-mC and 4-mC [18]. The analysis of these modifications in a genome-wide and single-base-resolution scale allowed us to characterize the 'methylome' of this strain. These epigenetic marks are commonly used by bacteria, and its implications vary from a defense mechanism, protecting the cell from invading bacteriophages or other foreign DNA, to the bacterial virulence itself [19–21]. We performed methylome analysis and motif detection using RS_Modification_and_Motif_analysis.1 protocol from SMRT Analysis 2.3. Such epigenetic marks arise from DNA methyl-transferases, sometimes coupled with a restriction endonuclease (a Restriction-Modification System). We

Table 4 Genome statistics

Attribute	Value	% of total
Genome size (bp)	5,411,683	100.00
DNA coding (bp)	4,737,274	87.5
DNA G + C (bp)	3,604,487	66.6
DNA scaffolds	2	100.00
Total genes	4,778	100.00
Protein coding genes	4,683	98.0
RNA genes	95	1.9
Pseudo genes	NA	NA
Genes in internal clusters	NA	NA
Genes with function prediction	3,566	74.6
Genes assigned to COGs	3,586	76.6
Genes with Pfam domains	3,892	83.1
Genes with signal peptides	501	10.6
Genes with transmembrane helices	1132	24.1
CRISPR repeats	0	-

Table 5 Number of genes associated with general COG functional categories

Code	Value	%	Description
J	160	3.4	Translation, ribosomal structure and biogenesis
A	2	<0.1	RNA processing and modification
K	273	5.8	Transcription
L	240	5.1	Replication, recombination and repair
B	3	<0.1	Chromatin structure and dynamics
D	28	0.6	Cell cycle control, Cell division, chromosome partitioning
V	45	1.0	Defense mechanisms
T	162	3.5	Signal transduction mechanisms
M	237	5.1	Cell wall/membrane biogenesis
N	119	2.5	Cell motility
U	61	1.3	Intracellular trafficking and secretion
O	154	3.3	Posttranslational modification, protein turnover, chaperones
C	226	4.8	Energy production and conversion
G	165	3.5	Carbohydrate transport and metabolism
E	342	7.3	Amino acid transport and metabolism
F	75	1.6	Nucleotide transport and metabolism
H	154	3.3	Coenzyme transport and metabolism
I	177	3.8	Lipid transport and metabolism
P	176	3.8	Inorganic ion transport and metabolism
Q	73	1.6	Secondary metabolites biosynthesis, transport and catabolism
R	352	7.5	General function prediction only
S	362	7.7	Function unknown
-	1097	23.4	Not in COGs

The total is based on the total number of protein coding genes in the genome

further characterized which genes give rise to the modified motifs using tools available at REBASE [22].

Genome properties

The genome of *R. solanacearum* strain UY031 has one chromosome (3,412,138 bp) and one circular megaplasmid (1,999,545 bp) (Table 3). The average GC content of the chromosome is 66.5 % while that of the megaplasmid is 66.7 %. A total of 4,778 genes (4,683 CDSs and 95 RNAs) were predicted. Of the protein-coding genes, 3,566 (76.1 %) had functions assigned while 1,212 were considered hypothetical (Table 4). Of all CDSs, 76.6 % could be assigned to one COG functional category and for 83.1 % one or more conserved PFAM-A domains were identified (Table 5).

Insights from the genome sequence

We performed a pan-genome analysis of the *R. solanacearum* UY031 genome, comparing it to four other genomes: two closely-related *R. solanacearum* strains (UW551 and IPO1609) and two others with complete genome sequences available (GMI1000 and Po82). The pan-genome consists of 7,594 HGGs while the core genome consists of 2,958 HGGs; the variable genome consists of 2,643 HGGs, and the number of strain-specific HGGs ranges from 193 to 774 (Fig. 3). We identified 193 HGGs that are UY031-specific; 75.1 % of them were annotated as hypothetical proteins.

Type III effector genes are among the most important for virulence determinants in bacterial plant pathogens such as *R. solanacearum* [14]. Based on comparisons with effector gene sequences in public databases (see above) we have identified 60 T3Es (Table 6), of which 11 appear to be nonfunctional due to frameshifts or other

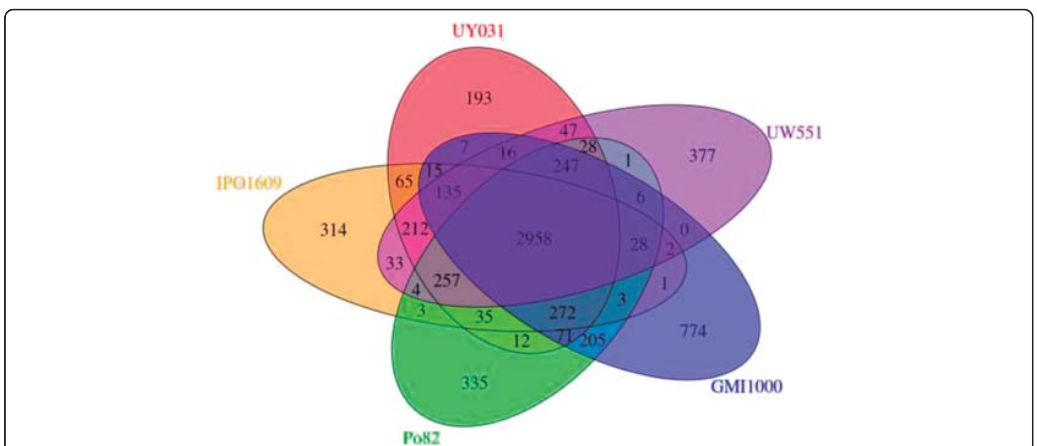

Fig. 3 Venn diagram of the *Ralstonia solanacearum* homologous gene groups. The *R. solanacearum* genomes compared were as follows: strains Po82, GMI1000, IPO1609, UW551, and UY031

Table 6 List of T3E genes identified in *R. solanacearum* UY031 genome and their orthologs

Former effector name	New effector name[a]	UY031(RSUY_)	GM1000(RS)	Po82(RSPO_)	IPO1609(RSIPO_)	UW551(RRSL_)
AWR2	RipA2	32720	p0099	m00080	03169	03418
AWR3	RipA3	40320	p0846	m01165	03901 + 05027[b]	-
AWR4	RipA4	40330/40[b]	p0847	m01166[b]	03902/3[b]	-
AWR5	RipA5_1	41860	p1024	m01289/90[b]	04049	01071
AWR5	RipA5_2	19780	-	c01821	01281	00546
Rip2	RipB	30390	c0245	c03161	00263	02573
Rip62	RipC1	42590	p1239	m01371	04123	03371
Rip34	RipD	33840	p0304	m01520	04484	00947
Rip26	RipE1	01190	c3369	c00070	03083	00852
-	RipE2	35100	-	c02513	04353	03923
PopF1	RipF1_1	45370	p1555	m01541	03403	04777
PopF2	RipF2	45510	-	m01557	05028/9[b]	04764
Gala2	RipG2	38790	p0672	m01007	04892	02264
Gala3	RipG3	32420	p0028	m00035	03202	00752
Gala4	RipG4	19910	c1800	c01835	01266/68[b]	00532
Gala5	RipG5	19920	c1801	c01836	01264	00531
Gala6	RipG6	17940	c1356	c01999	01463	01561
Gala7	RipG7	17950	c1357	c01998	01462	01562
HLK1	RipH1	19380	c1386	c01846	01319	00426
HLK2	RipH2	35470	p0215	m00201/2[c]	04317	03559
HLK3	RipH3	33320	p0160	m00157	03105	00041[b]
Rip1	RipI	00490 + 32050[b]	c0041	c03319	00098[b]	02976 + 02040[b]
Rip22	RipJ	24610[b]	c2132	c02749	-	-
Rip16	RipM	19180	c1475	c01871/2/3	01339 + 05024[b]	00705
Rip58	RipN	43290	p1130	m00869	04184	04736
Rip35	RipO1	34050	p0323	m01496	04463	00926
Rip63	RipQ	44390[b]	p1277	m00717	04287[b]	02855[b]
PopS	RipR	42640	p1281	m01376	04127	03375
SKWP1	RipS1	00860	c3401	c00036	00017	04182
SKWP2	RipS2	44630	p1374	m00690	04310	-
SKWP3	RipS3	41210	p0930	m01229	03993/4[b]	00237[b]
SKWP5	RipS5	10370 + 10840[b]	p0296	c02546[b]	-	-
SKWP7	RipS7	35110[b]	-	m00383	04352[b]	03921
Rip59	RipU	43920	p1212	m00805	04243	04660
Rip12	RipV1	17880	c1349	c02006	01470	01554
-	RipV2	19160[b]	-	c01875/76[b]	01341	00703
PopW	RipW	07010	c2775	c00735	02524	02682
PopA	RipX	40640	p0877	m01196	03933	02443
Rip3	RipY	30260	c0257	c03153	00276	01439
Rip57	RipZ	42040	p1031	m01312	04067	00271[b]
AvrA	RipAA	26380[b]	c0608	c02748	00659	01581
PopB	RipAB	40630	p0876	m01195	03932	02442
PopC	RipAC	40620	p0875	m01194	03931	02441
Rip72	ripAD	45790	p1601	m01585	03364	02518

Table 6 List of T3E genes identified in *R. solanacearum* UY031 genome and their orthologs *(Continued)*

Rip4	RipAE	29570	c0321	c03085	00343	01625
Rip41	RipAI	40230	p0838	m01156	03894	01021
Rip21	RipAJ	13300	c2101	c01332	04893	01260
Rip38	RipAL	39210[b]	-	m01053	-	02221
Brg40	RipAM	02270	c3272	c00191	02968	02810
Rip43	RipAN	40310	p0845	m01164	03900	01013
Rip50	RipAO	40750	p0879	m01206	03944	03105
Rip60	RipAP	43960	p1215[b]	m00800	04247	04655
Rip51	RipAQ	40810	p0885	-	03951	03113
Rip61	RipAR	44220[b]	p1236	m00770	04270	01136
Rip39	RipAV	39280	p0732	m01061	-	02213
Brg13	RipAX1	02040	c3290	m01221	02991	-
Rip55	RipAY	41810	p1022	m01283	04046	01066
-	RipBH	45880	-	m01600	03355	00782
-	RipBI	45200[b]	-	m00718	03419	00326
-	RipTPS	39290	p0731	m01062[b]	-	02212

[a]According to Peeters et al. [14]; [b]: these genes appear to be nonfunctional due to various reasons (frameshift, truncation, etc.); genes in other columns that appear in the form locus tag x + locus tag y are genes which also appear to be nonfunctional due to frameshifts. [c]:this gene is duplicated

mutations that disrupt the coding sequence. For example, the effector RipS5 is encoded by a gene that has been clearly interrupted by a 34 kbp prophage. Table 6 also shows the orthologs of these genes in the related strains GMI1000, Po82, IPO1609, and UW551. In the table it can be seen that the genes that code for RipAA and RipAR have frameshifts or truncations in strain UY031 only. The absence of a particular effector may be enough for a pathogen to avoid host defenses, and therefore cause disease. These two genes are therefore a good starting point for additional investigations of phenotypic differences between these strains. Other effector genes of interest are those that are present and do not have disrupting mutations in UY031 but are absent or appear to be nonfunctional in other strains. We have found several such cases (Table 6), but in all cases there is at least one other strain that also has the same gene in what appears to be a functional state.

Our modification analysis revealed two motifs that are essentially always methylated, namely: CAACRAC and GTWWAC. Both are fairly frequent in the genome, occurring respectively 2144 and 716 times. Motif CAACRAC is associated with the product of gene RSUY_11320 (R. Roberts, personal communication), which is hypothesized to be an enzyme of the Restriction-Modification System, with a restriction nuclease and a DNA methyltransferase role. This gene does not have homologs in other *R. solanacearum* strains and is located close to a region containing phage-related genes. This region contains gene RSUY_11410, which has been annotated as encoding a zonular occludens toxin. The provenance of this annotation is an enterotoxin gene found in *Vibrio cholera* [23]; in *R. solanacearum* the role of this toxin gene is still unclear [24]. Motif GTWWAC is probably associated with the product of gene RSUY_22890 (R. Roberts, personal communication), which is hypothesized to be a solitary DNA methyltransferase (no restriction endonuclease linked). This gene does have homologs in other *R. solanacearum* strains (GMI1000, IPO1609, Po82 and PSI07). To our knowledge this is the first *R. solanacearum* genome with a methylome profile available.

Conclusions

The complete sequence of *R. solanacearum* UY031 strain presented here should provide a rich platform upon which additional plant-pathogen studies can be carried out. Even though this is the fifth phylotype IIB1 sequenced, we found many differences with respect to the genomes of the other strains. In particular, the repertoire of T3E genes has many variations among these strains, and this may help explain some of the most relevant pathogenicity-related phenotypes described in the literature, opening the way to new control methods for bacterial wilt.

Abbreviations

IIB1: Phylotype IIB, sequevar 1; T3E: Type III effectors; HGG: Homologous gene groups.

Competing interests

The authors declare that they have followed all local, national and international guidelines and legislation and obtained the required permissions and/or licenses for this study.

The authors declare that they do not have any financial and non-financial competing interests.

Authors' contributions
Conceived the project: MV, JCS, RGS. Provided strains and metadata: MIS, MJP. Assembled and annotated the genome: RGS. Performed effector gene annotation: MP, NSC. Analyzed and interpreted results: JCS, MV, MP, NSC, RGS, MIS, MJP. Wrote the manuscript: JCS, MV, MP, RGS, MIS, MJP. All authors read and approved the final manuscript.

Acknowledgements
We thank Carlos Balsalobre and Cristina Madrid for their helpful advice and for kindly providing materials and protocols; and Carlos Morais for help with NCBI submission. We also thank COST action Sustain from the European Union for funding and Nemo Peeters and Stéphane Genin for hosting MP for a short stay to carry out UY031 effector annotation. RGS has a Ph.D. fellowship from FAPESP, Brazil. JCS has an investigator fellowship from the Conselho Nacional de Desenvolvimento Cientifico e Tecnologico, Brazil.

Author details
[1]Instituto de Química, Universidade de São Paulo, São Paulo, Brazil. [2]Department of Genetics, University of Barcelona and Centre for Research in Agricultural Genomics (CRAG), Bellaterra, Catalonia, Spain. [3]Departamento de Biociencias, Cátedra de Microbiología, Facultad de Química, Universidad de la República, Montevideo, Uruguay. [4]Biocomplexity Institute, Virginia Tech, Blacksburg, VA, USA.

Received: 29 September 2015 Accepted: 10 December 2015
Published online: 15 January 2016

References

1. Mansfield J, Genin S, Magori S, Citovsky V, Sriariyanum M, Ronald P, et al. Top 10 plant pathogenic bacteria in molecular plant pathology. Mol Plant Pathol. 2012;13(6):614–29.
2. Genin S, Denny TP. Pathogenomics of the *Ralstonia solanacearum* species complex. Annu Rev Phytopathol. 2012;50:67–89.
3. Fegan M, Prior P. How complex is the '*Ralstonia solanacearum*' species complex? In: Allen CP, editor. Bacterial wilt: The disease and the ralstonia solanacearum species complex. Prior, Hayward AC. St. Paul, MN: American Phytopathological Society; 2005. p. 449–61.
4. Janse JD, van den Beld HE, Elphinstone J, Simpkins S, Tjou-Tam-Sin NNA, van Vaerenbergh J. Introduction to Europe of *Ralstonia solanacearum* biovar 2, race 3 in *Pelargonium zonale* cuttings. J Plant Pathol. 2004;86(2):147–55.
5. Siri MI, Sanabria A, Pianzolla MJ. Genetic diversity and aggressiveness of *Ralstonia solanacearum* strains causing bacterial wilt of potato in Uruguay. Plant Dis. 2011;95(10):1292–301.
6. Gabriel DW, Allen C, Schell M, Denny TP, Greenberg JT, Duan YP, et al. Identification of open reading frames unique to a select agent: *Ralstonia solanacearum* race 3 biovar 2. MPMI. 2006;19(1):69–79.
7. Guidot A, Elbaz M, Carrere S, Siri MI, Pianzzola MJ, Prior P, et al. Specific genes from the potato brown rot strains of *Ralstonia solanacearum* and their potential use for strain detection. Phytopathology. 2009;99(9):1105–12.
8. Yuan KX, Cullis J, Levesque CA, Tambong J, Chen W, Lewis CT, et al. Draft genome sequences of *Ralstonia solanacearum* race 3 biovar 2 strains with different temperature adaptations. Genome Announc. 2015;3(4).
9. Salanoubat M, Genin S, Artiguenave F, Gouzy J, Mangenot S, Arlat M, et al. Genome sequence of the plant pathogen *Ralstonia solanacearum*. Nature. 2002;415(6871):497–502.
10. Xu J, Zheng HJ, Liu L, Pan ZC, Prior P, Tang B, et al. Complete genome sequence of the plant pathogen *Ralstonia solanacearum* strain Po82. J Bacteriol. 2011;193(16):4261–2.
11. Remenant B, Coupat-Goutaland B, Guidot A, Cellier G, Wicker E, Allen C, et al. Genomes of three tomato pathogens within the *Ralstonia solanacearum* species complex reveal significant evolutionary divergence. BMC Genomics. 2010;11:379.
12. Chin CS, Alexander DH, Marks P, Klammer AA, Drake J, Heiner C, et al. Nonhybrid, finished microbial genome assemblies from long-read SMRT sequencing data. Nat Methods. 2013;10(6):563–9.
13. Seemann T. Prokka: rapid prokaryotic genome annotation. Bioinformatics. 2014;30(14):2068–9.
14. Peeters N, Carrere S, Anisimova M, Plener L, Cazale AC, Genin S. Repertoire, unified nomenclature and evolution of the type III effector gene set in the *Ralstonia solanacearum* species complex. BMC Genomics. 2013;14:859.
15. Altschul SF, Madden TL, Schaffer AA, Zhang J, Zhang Z, Miller W, et al. Gapped BLAST and PSI-BLAST: a new generation of protein database search programs. Nucleic Acids Res. 1997;25(17):3389–402.
16. Contreras-Moreira B, Vinuesa P. GET_HOMOLOGUES, a versatile software package for scalable and robust microbial pangenome analysis. Appl Environ Microbiol. 2013;79(24):7696–701.
17. Li L, Stoeckert Jr CJ, Roos DS. OrthoMCL: identification of ortholog groups for eukaryotic genomes. Genome Res. 2003;13(9):2178–89.
18. Flusberg BA, Webster DR, Lee JH, Travers KJ, Olivares EC, Clark TA, et al. Direct detection of DNA methylation during single-molecule, real-time sequencing. Nat Methods. 2010;7(6):461–5.
19. Sanchez-Romero MA, Cota I, Casadesus J. DNA methylation in bacteria: from the methyl group to the methylome. Curr Opin Microbiol. 2015;25:9–16.
20. Garcia-Del Portillo F, Pucciarelli MG, Casadesus J. DNA adenine methylase mutants of *Salmonella typhimurium* show defects in protein secretion, cell invasion, and M cell cytotoxicity. Proc Natl Acad Sci U S A. 1999;96(20):11578–83.
21. Heithoff DM, Sinsheimer RL, Low DA, Mahan MJ. An essential role for DNA adenine methylation in bacterial virulence. Science. 1999;284(5416):967–70.
22. Roberts RJ, Vincze T, Posfai J, Macelis D. REBASE–a database for DNA restriction and modification: enzymes, genes and genomes. Nucleic Acids Res. 2015;43(Database issue):D298–9.
23. Di Pierro M, Lu R, Uzzau S, Wang W, Margaretten K, Pazzani C, et al. Zonula occludens toxin structure-function analysis. Identification of the fragment biologically active on tight junctions and of the zonulin receptor binding domain. J Biol Chem. 2001;276(22):19160–5.
24. Murugaiyan S, Bae JY, Wu J, Lee SD, Um HY, Choi HK, et al. Characterization of filamentous bacteriophage PE226 infecting Ralstonia solanacearum strains. J Appl Microbiol. 2011;110(1):296–303.
25. Edgar RC. MUSCLE: multiple sequence alignment with high accuracy and high throughput. Nucleic Acids Res. 2004;32(5):1792–7.
26. Guindon S, Dufayard JF, Lefort V, Anisimova M, Hordijk W, Gascuel O. New algorithms and methods to estimate maximum-likelihood phylogenies: assessing the performance of PhyML 3.0. Syst Biol. 2010;59(3):307–21.
27. Field D, Garrity G, Gray T, Morrison N, Selengut J, Sterk P, et al. The minimum information about a genome sequence (MIGS) specification. Nat Biotechnol. 2008;26(5):541–7.
28. Woese CR, Kandler O, Wheelis ML. Towards a natural system of organisms: proposal for the domains *Archaea*, *Bacteria*, and *Eucarya*. Proc Natl Acad Sci U S A. 1990;87(12):4576–9.
29. Garrity GM, Bell JA, Lilburn T. Phylum XIV. *Proteobacteria* phyl. nov. In: Garrity GM, Brenner DJ, Krieg NR, Staley JT, editors. Bergey's manual of systematic bacteriology, vol. 2. Second ed. New York: Springer; 2005. p. Part B:1.
30. Garrity GM, Bell JA, Lilburn T. Class II. *Betaproteobacteria* class. nov. In: Garrity GM, Brenner DJ, Krieg NR, Staley JT, editors. Bergey's manual of systematic bacteriology, vol. 2. Second ed. New York: Springer; 2005. p. 575. part C.
31. List Editor. Validation List Number 107. List of new names and new combinations previously effectively, but not validly, published. Int J Syst Evol Microbiol. 2006,56:1–6
32. Garrity GM, Bell JA, Lilburn T. Order I. *Burkholderiales* ord. nov. In: Garrity GM, Brenner DJ, Krieg NR, Staley JT, editors. Bergey's manual of systematic bacteriology, vol. 2. Second ed. New York: Springer; 2005. p. 575. part C.
33. Garrity GM, Bell JA, Lilburn T. Family I. *Burkholderiaceae* fam. nov. In: Garrity GM, Brenner DJ, Krieg NR, Staley JT, editors. Bergey's manual of systematic bacteriology, vol. 2. Second ed. New York: Springer; 2005. p. 575. part C.
34. Yabuuchi E, Kosako Y, Yano I, Hotta H, Nishiuchi Y. Transfer of two *Burkholderia* and an Alcaligenes species to *Ralstonia* gen. Nov.: proposal of *Ralstonia pickettii* (Ralston, Palleroni and Doudoroff 1973) comb. nov., *Ralstonia solanacearum* (Smith 1896) comb. nov. and *Ralstonia eutropha* (Davis 1969) comb. Nov. Microbiol Immunol. 1995;39(11):897–904.
35. List Editor. Validation List No. 57. Validation of the publication of new names and new combinations previously effectively published outside the IJSB. Int J Syst Bacteriol. 1996,46:625–626
36. Denny TP, Hayward AC, Schaad NW, Jones JB, Chun W. II. Gram negative bacteria. F. *Ralstonia*. In: Laboratory guide for identification of plant pathogenic bacteria. Thirdth ed. St. Paul, MN, USA: American Phytopathological Society Press; 2001.
37. Ashburner M, Ball CA, Blake JA, Botstein D, Butler H, Cherry JM, et al. Gene ontology: tool for the unification of biology. The gene ontology consortium. Nat Genet. 2000;25(1):25–9.

chapter 4

PUBLICATION 2

Comparative Analysis of *Ralstonia solanacearum* Methylomes

Resum de la publicació 2

"Comparative Analysis of *Ralstonia solanacearum* Methylomes"

"Anàlisi comparativa dels metilomes de *Ralstonia solanacearum*"

Ivan Erill, Marina Puigvert, Ludovic Legrand, Rodrigo Guarischi-Sousa, Céline Vandecasteele, João C. Setubal, Stephane Genin, Alice Guidot i Marc Valls

Referència: Front. Plant Sci. 8:504.
Doi: 10.3389/fpls.2017.00504

4

Ralstonia solanacearum és un important patogen transmès per terra, amb una àmplia distribució geogràfica i capaç de causar marciment bacterià en molts cultius de gran interès agrícola. La seqüenciació de múltiples genomes de diverses soques de *R. solanacearum* ha permès la identificació de trets genètics únics i compartits que han influït tant en la seva evolució com en la seva habilitat per a colonitzar plantes hostes. Estudis anteriors han demostrat que la metilació de l'ADN pot impulsar l'especiació i modular la virulència en bacteris, però l'impacte de les modificacions epigenètiques en la diversificació i patogenicitat de *R. solanacearum* continua sent desconegut. La seqüenciació de les soques GMI1000 i UY031 utilitzant la tecnologia *Single Molecule Real-Time* ens ha permès dur a terme una anàlisi comparativa dels metilomes de *R. solanacearum*. La nostra anàlisi ha identificat un nou motiu de metilació associat a una metilasa d'ADN que està conservada a tots els genomes del gènere *Ralstonia* i a tota la família *Burkholderiaceae,* així com un motiu de metilació associat a una metilasa de transmissió fàgica única a la soca *R. solanacearum* UY031. L'anàlisi comparativa del motiu de metilació conservat ha revelat que és majoritàriament predominant a les regions promotores de gens, on exhibeix un elevat grau de conservació detectable mitjançant l'empremta filogenètica. L'anàlisi de *loci* híper- i hipo- metilat ha identificat diversos gens involucrats en funcions reguladores globals i de virulència, l'expressió dels quals podria ser modulat per la metilació de l'ADN. L'anàlisi de patrons de modificació a tot el genoma ha detectat una correlació significativa entre la modificació de l'ADN i els gens de transposició en R. solanacearum UY031, impulsat per la presència d'un elevat nombre de còpies de seqüències d'inserció ISrso3 en aquest genoma, que senyala a un nou mecanisme de regulació de la transposició. Aquests resultats representen una base ferma per a futures investigacions experimentals envers el paper de la metilació de l'ADN en l'evolució de *R. solanacearum* i en la seva adaptació a diferents plantes.

frontiers in Plant Science

ORIGINAL RESEARCH
published: 13 April 2017
doi: 10.3389/fpls.2017.00504

Comparative Analysis of *Ralstonia solanacearum* Methylomes

Ivan Erill[1,2]*, *Marina Puigvert*[2,3], *Ludovic Legrand*[4], *Rodrigo Guarischi-Sousa*[5], *Céline Vandecasteele*[6], *João C. Setubal*[5], *Stephane Genin*[4], *Alice Guidot*[4] *and Marc Valls*[2,3]*

[1] Department of Biological Sciences, University of Maryland Baltimore County, Baltimore, MD, USA, [2] Center for Research in Agricultural Genomics, CSIC- IRTA- UAB -UB, Barcelona, Spain, [3] Department of Genetics, Universitat de Barcelona, Barcelona, Spain, [4] Laboratoire des Interactions Plantes Micro-organismes, INRA, Centre National de la Recherche Scientifique, Université de Toulouse, Castanet-Tolosan, France, [5] Departamento de Bioquímica, Instituto de Química, Universidade de São Paulo, São Paulo, Brazil, [6] INRA, US 1426, GeT-PlaGe, Genotoul, Castanet-Tolosan, France

Ralstonia solanacearum is an important soil-borne plant pathogen with broad geographical distribution and the ability to cause wilt disease in many agriculturally important crops. Genome sequencing of multiple *R. solanacearum* strains has identified both unique and shared genetic traits influencing their evolution and ability to colonize plant hosts. Previous research has shown that DNA methylation can drive speciation and modulate virulence in bacteria, but the impact of epigenetic modifications on the diversification and pathogenesis of *R. solanacearum* is unknown. Sequencing of *R. solanacearum* strains GMI1000 and UY031 using Single Molecule Real-Time technology allowed us to perform a comparative analysis of *R. solanacearum* methylomes. Our analysis identified a novel methylation motif associated with a DNA methylase that is conserved in all complete *Ralstonia* spp. genomes and across the *Burkholderiaceae*, as well as a methylation motif associated to a phage-borne methylase unique to *R. solanacearum* UY031. Comparative analysis of the conserved methylation motif revealed that it is most prevalent in gene promoter regions, where it displays a high degree of conservation detectable through phylogenetic footprinting. Analysis of hyper- and hypo-methylated loci identified several genes involved in global and virulence regulatory functions whose expression may be modulated by DNA methylation. Analysis of genome-wide modification patterns identified a significant correlation between DNA modification and transposase genes in *R. solanacearum* UY031, driven by the presence of a high copy number of ISrso3 insertion sequences in this genome and pointing to a novel mechanism for regulation of transposition. These results set a firm foundation for experimental investigations into the role of DNA methylation in *R. solanacearum* evolution and its adaptation to different plants.

Keywords: *Ralstonia*, methylome, comparative genomics, epigenomics, transcriptional regulation, transposon, nucleotide modification, genome

OPEN ACCESS

Edited by:
Adi Avni,
Tel Aviv University, Israel

Reviewed by:
Bryan Bailey,
United States Department of Agriculture, USA
Assaf Zemach,
Tel Aviv University, Israel

***Correspondence:**
Ivan Erill
erill@umbc.edu
Marc Valls
marcvalls@ub.edu

Specialty section:
This article was submitted to Plant Microbe Interactions, a section of the journal Frontiers in Plant Science

Received: *16 January 2017*
Accepted: *22 March 2017*
Published: *13 April 2017*

Citation:
Erill I, Puigvert M, Legrand L, Guarischi-Sousa R, Vandecasteele C, Setubal JC, Genin S, Guidot A and Valls M (2017) Comparative Analysis of Ralstonia solanacearum Methylomes. Front. Plant Sci. 8:504. doi: 10.3389/fpls.2017.00504

INTRODUCTION

Ralstonia solanacearum is a widely-distributed, soil-borne phytopathogen belonging to the Betaproteobacteria subclass (Peeters et al., 2013). Known primarily as the causative agent of bacterial wilt among solanaceous plants, *R. solanacearum* encompasses a highly heterogeneous group of organisms capable of infecting over 200 plant species from more than 50 different

families (Denny, 2007). Owing to its phylogenetic and host diversity, this group of organisms is conventionally known as the *R. solanacearum* species complex (RSSC) (Fegan and Prior, 2005). RSSC organisms share similar etiology, infecting and colonizing plant roots before invading xylem vessels and spreading to aerial plant parts. Extensive colonization of xylem vessels results in vascular dysfunction, leading to the signature wilting symptoms of *R. solanacearum* infections (Denny, 2007). Genomic analysis of sequenced *R. solanacearum* isolates has revealed that RSSC members share a similar genomic structure consisting of two circular replicons typically referred to as chromosome and megaplasmid (Remenant et al., 2010; Peeters et al., 2013). Multiple lines of evidence indicate that housekeeping genes reside predominantly in the chromosome, whereas environment- and pathogenicity-specific functions are encoded in the less-conserved megaplasmid (Genin and Denny, 2012). These include the main pathogenicity determinant of *R. solanacearum*, the type III secretion system (T3SS), as well as the extracellular polysaccharide (EPS) gene cluster and motility-associated determinants (Peeters et al., 2013). The notable phenotypic heterogeneity of *R. solanacearum* isolates has been primarily ascribed to the prevalence of genomic islands and genomic rearrangement events, frequently linked to the presence of prophages and transposable elements, as well as the ability of *R. solanacearum* to acquire exogenous DNA through natural transformation (Coupat et al., 2008; Remenant et al., 2010). Multi-locus sequence analyses, hybridization, genomic and phylogeographic methods have firmly established that the RSSC can be divided into four major phylotypes, further subdivided into sequevars and approximately corresponding to their known geographical origins (Guidot et al., 2007; Remenant et al., 2010; Wicker et al., 2012). However, the molecular mechanisms driving niche- and host-adaptation remain yet to be fully elucidated, prompting the need for novel approaches to understand their evolution.

DNA methylation is a chemical modification of DNA mediated by DNA methyltransferase (MTase) enzymes and known to directly regulate several processes in eukaryotic cells (Jones, 2012). DNA methylation is also prevalent in bacteria, in the form of 6-methyladenosine (m6A), 4-methylcytosine (m4C), and 5-methylcytosine (m5C) bases, and it is most frequently associated with the presence of restriction-modification (RM) systems. RM systems are composed of a restriction endonuclease (REase) and an MTase that preferentially bind to the same DNA sequence. They are broadly classified into four major types, according to their subunit composition, sequence recognition strategy, substrate specificity and cleavage position (Loenen et al., 2014). Methylation by MTases protects genomic DNA from cleavage and degradation by corresponding REases and, hence, RM systems are primarily envisaged as bacterial defense mechanisms against foreign DNA (Tock and Dryden, 2005). However, RM systems have also been shown to act as addiction molecules in plasmids and to help establish bacterial biotypes by preventing genetic exchange via conjugation or natural transformation (Handa and Kobayashi, 1999; Lindsay, 2010; Budroni et al., 2011). Furthermore, DNA methylation by RM systems and, more frequently, orphan MTases has been shown to be involved in coordinating replication initiation and cell-cycle progression, limiting transposition, regulating gene expression and phage packaging, and orchestrating phase-variation (Low and Casadesús, 2008).

The recent development of Single Molecule, Real-Time (SMRT) DNA sequencing allows detection of methylated bases in bacterial plasmids and chromosomes as characteristic delays in the real-time monitoring of the incorporation of nucleotides by individual DNA polymerase molecules (Schadt et al., 2013). For large DNA sequences, methylation motifs can be inferred as overrepresented patterns in the sequence context surrounding the modified base. Inferred motifs can then be matched to genome MTases on the basis of motif similarity to MTases with known specificity, via MTase subcloning or through resequencing of MTase mutants (Murray et al., 2012; Forde et al., 2015; Blow et al., 2016). The availability of SMRT sequencing has enabled the characterization of many new RM systems and their target motifs (Murray et al., 2012; Blow et al., 2016). It has also made it possible to identify additional phase-variation systems modulated by methylation (Blakeway et al., 2014), to identify RM systems that likely define clade boundaries (Nandi et al., 2015) and to trace evolutionary changes in MTase target recognition (Furuta et al., 2014). Here we used SMRT sequencing of the reference *R. solanacearum* GMI1000 strain (phylotype I, sequevar 18) and the highly-aggressive *R. solanacearum* UY031 strain (phylotype IIB, sequevar 1) to perform a comparative analysis of their DNA modification patterns. We identified the target motif of an m6A MTase conserved in both strains and across the *Burkholderiaceae*. Analysis of conserved methylation sites for this MTase revealed a clear enrichment in up- and downstream regions of coding sequences, and comparative analysis of their genetic context suggested that methylation targets are under strong purifying selection. Detection of hyper-methylated and non-methylated regions for this conserved m6A MTase identified several promoters where methylation could have a regulatory function. The modification profile of strain UY031 was found to correlate significantly with the presence of a multi-copy transposable element with a highly non-uniform modification pattern.

MATERIALS AND METHODS

Reference Genomes

Twelve complete genomes of the *R. solanacearum* species complex available through the NCBI RefSeq service (RefSeq, RRID:SCR_003496) were used as a reference for comparative genomics analyses (Supplementary Table 1). In addition to the *R. solanacearum* GMI1000 (phylotype I, sequevar 18) and UY031 (phylotype IIB, sequevar 1) strains, these genomes include several phylotype IIB representatives (Po82, UW163, and IBSBF1503), a phylotype I (FQY-4), a phylotype III (CMR15) and a phylotype IV (PSI07) representative, as well as three additional *Ralstonia* species (*R. insidiosa*, *R. pickettii*, and *R. mannitolilytica*).

Bacterial Growth and Genomic DNA Preparation

Bacterial growth and genomic DNA extraction for the *R. solanacearum* UY031 strain was performed as described previously (Guarischi-Sousa et al., 2016). Briefly, *R. solanacearum* strain UY031 was grown in liquid rich B medium (10 g/l bactopeptone, 1 g/l yeast extract and 1 g/l casaminoacids) to stationary phase ($OD_{600\ nm} = 0.87$). Genomic DNA was extracted from a bacterial culture grown to stationary phase to avoid overrepresentation of genomic sequences close to the origin of replication. Twelve ml of bacterial culture were used to extract DNA with the Blood and Cell Culture DNA Midi kit (QIAGEN, RRID:SCR_008539), following manufacturer's instructions for gram-negative bacteria. DNA concentration and quality were measured by spectrometry (Nanodrop 800; Thermo Fisher Scientific, RRID:SCR_013270). Bacterial growth and genomic DNA extraction for the *R. solanacearum* GMI1000 strain was performed in the present work. The protocol used to extract DNA from the GMI1000 strain was derived from the protocol described in Mayjonade et al. (2016). Briefly, bacteria were grown overnight in 50 ml MP minimal medium ($FeSO_4$, $7H_2O$, 1.25×10^{-4} g/l; $(NH_4)_2SO_4$, 0.5 g/l; $MgSO_4$. $7H_2O$, 0.05 g/l; KH_2PO_4, 3.4 g/l) supplemented with glucose 20 mM and a pH adjusted to 6.5 with KOH. When the culture reached an $OD_{600\ nm}$ of 0.5 (exponential phase), bacteria were centrifuged 10 min at 7,000 rpm, the pellet was washed with 50 ml sterile water and centrifuged again to resuspend the pellet in 600 µl of lysis buffer (NaCl 2.5 M, TrisHCl pH8 1 M, EDTA pH8 0.5 M, SDS 20%, Sodium Metabisulfite 0.1%) preheated at 72°C. A total of 6 µl RNAse (100 mg/ml) was added before incubation 30 min at 55°C with gentle agitation every 10 min. Then 200 µl potassium acetate 5M was added, mixed and the suspension was centrifuged 10 min 13,000 rpm at 4°C. A total of 500 µl of supernatant was transferred in a new tube and 500 µl binding buffer (PEG8000 200 mg/ml, NaCl 200 mg/ml) was added. Then 30 µl of carboxylated magnetic beads (Thermo Fisher Scientific, RRID:SCR_013270) was added, and mixed before incubation for 1 h at room temperature under gentle agitation. The tubes were transferred to a magnetic rack to wash the beads 3 times with 70% Ethanol. DNA was eluted from the beads by resuspension in 80 µl of elution buffer (TrisHCl pH8 1M) preheated at 55°C. DNA concentration and quality were measured by spectrometry (Nanodrop 2000; Thermo Fisher Scientific, RRID:SCR_013270) and fluorometry (Qubit 3.0 Fluorometer; Thermo Fisher Scientific, RRID:SCR_013270). DNA integrity was evaluated by performing pulsed-field electrophoresis, which showed that the DNA molecules ranged in size from ∼10 to ∼90 kb with a mean at ∼30 kb.

SMRT Sequencing

DNA libraries from strain UY031 were constructed using P5-C3 chemistry. The library preparation procedure followed the PacBio 128 standard for large insert library preparation with BluePippin size selection (Sage Science, 129 RRID:SCR_014808). The library insert size was 15 kb with size selection on the BluePippin using a 130 cut off of 6–50 kb for PacBioRSII. Whole-genome sequencing was performed using one single SMRTcell on PacBio RS II platform at Duke Center for Genomic and Computational Biology (USA). An assembly quality assessment was performed before all downstream analyses. All reads were mapped back to the assembled sequences using RS_Resequencing.1 protocol from SMRT Analysis 2.3. This analysis revealed that chromosome and megaplasmid sequences had 100% of bases called (percentage of assembled sequence with coverage $>= 1$) and 99.9999% and 99.9992%, respectively, of consensus concordance. More than 749 million of Pre-Filter Polymerase Read Bases were generated (>130x genome coverage) and deposited to NCBI Sequence Read Archive, RRID:SCR_004891 (SRP064191). Genomic DNA from the GMI1000 strain was sent to the Get-PlaGe core facility (INRA, Toulouse, France) where methylome data was obtained by SMRT technology. A 20-kb SMRTbell library was prepared according to manufacturer's protocols as described for the 20 kb template preparation with BluePippin size selections as follow: 5 µg of gDNA was sheared to an average length of 35 kb using Megaruptor system (Diagenode, RRID: SCR_014807), treated with DNA damage repair mix, end-repaired and ligated to hairpin adapters. Incompletely formed SMRTbell templates were digested using Exonuclease III and VII. Finally, the library was size selected with a 12 kb cutoff using BluePippin electrophoresis (Sage Science, RRID:SCR_014808). Sequencing was carried out on the PacBio RS II (INRA, Toulouse, France) from 0.25 nM of library loading on 3 SMRTCells, and using OneCellPerWell protocol on P6/C4 chemistry for 6 h movies, yielding mean genome coverage of 372x. All reads were mapped to the public GMI1000 reference genome using RS_Modification_and_Motif_analysis.1 protocol. This analysis revealed that both GMI1000 chromosome and megaplasmid sequences had 100% of bases called and 99.9952% and 99.9960%, respectively, of consensus concordance. 2.868.126.059 of Pre-Filter Polymerase Read Bases were generated (>450x genome coverage). Raw sequencing data was deposited on the NCBI Sequence Read Archive, RRID:SCR_004891 (SRP096275). Tet1-oxidation of DNA prior to SMRTbell library preparation, required for detection of m5C methylation (Clark et al., 2013), was not performed on either strain.

Modification Detection and Motif Analysis

The UY031 strain genome was assembled using RS_HGAP_Assembly.2 protocol from SMRT Analysis 2.3 (Chin et al., 2013) on one circular chromosome (3,412,138 bp) and one circular megaplasmid (1,999,545 bp). The origin of replication for both replicons was defined based on the putative origins of replication reported for reference strain GMI1000 (Salanoubat et al., 2002). The GMI1000 strain genome was assembled using the previously published GMI1000 genome as reference. Motif detection for both strains was performed using RS_Modification_and_Motif_analysis.1 protocol from SMRT Analysis using QV threshold of 30. The resulting modification files were deposited on the Gene Expression Omnibus (GEO) (GSE92982 and GSE93317; NCBI GEO DataSets, RRID:SCR_005012).

Mapping of Modification Marks to Genome Features

Genome features were extracted from the NCBI RefSeq sequences of *R. solanacearum* GMI1000 (NC 003296.1, NC 003295.1) and *R. solanacearum* UY031 (NZ CP012688.1, NZ CP012687.1) using the BioPython 1.66 GenBank parser (Cock et al., 2009). A mapping between locus tag identifiers from the current RefSeq annotation and those from previous annotations was generated to facilitate identification of referenced genes in previously published work (Supplementary Table 2). For species reported in Blow et al. (2016), a Python script was used to identify and parse RefSeq sequences from GenBank identifiers, to download methylome General Feature Format (GFF) files from the corresponding GEO record (GSE69872; NCBI GEO DataSets, RRID:SCR_005012) and to associate methylome references in GFF files to RefSeq identifiers based on an exact match between the reported sequence length of the GFF reference and the RefSeq accession (Supplementary Table 3). For all species under analysis, modification marks were parsed from the corresponding GFF file using a custom Python script. Modification marks were then mapped to relevant genome features (CDS, tRNA, rRNA, tmRNA, ncRNA, mobile_element, and repeat_region) if their mark position overlapped the annotated feature positions. For coding features (CDS, tRNA, rRNA, tmRNA, and ncRNA), modification marks were annotated as *intragenic* if their positions mapped within the annotated coding segment, *upstream* if they mapped to the first non-coding 375 bp before the annotated feature start position, *downstream* if they mapped to the first non-coding 100 bp after the annotated feature end, and *intergenic* otherwise.

Analysis of Modification Density

Modification density for a given type of modification mark was computed as the number of relevant modification marks within the region of interest divided by the length of said region. To account for correlation between sequencing coverage in a given region and its mark count, modification density within a given region was normalized with the ratio of genome-wide average coverage to region-wide average coverage for the mark type under analysis. Modification density plots were generated by analyzing normalized modification density using a sliding window of 1,000 bp with a step size of 100 bp.

Analysis of Conserved Methylation Marks

Conservation of detected methylation marks in the *R. solanacearum* GMI1000 and *R. solanacearum* UY031 genomes was assessed through alignment of their sequence context using a custom Python script. Bona fide orthologs between *R. solanacearum* GMI1000 and UY031 genes were obtained from a full-genome alignment with Mauve (Darling et al., 2004). For each ortholog pair, a pairwise gapless alignment was performed between the contexts of all modification marks mapping to the corresponding gene in either strain. Modification marks were labeled as conserved if their gapless context alignment had at least 70% identity and non-conserved otherwise. Modification marks not mapping to an ortholog pair were annotated as such. To assess modification mark conservation across the assembled panel of reference *Ralstonia* genomes, the sequence context of conserved modification marks in *R. solanacearum* GMI1000 was aligned with all reference genomes using BLASTN with modified gap penalties to avoid gapped alignments (Altschul et al., 1997). Modification marks were considered to be conserved in a particular reference species when the best BLASTN gapless alignment of their sequence context showed at least 70% identity. For each mark, the number of species against which valid alignments were obtained, the number of valid alignments with an intact 6 bp stretch in positions 17–22 (corresponding to the G<u>T</u>AW**A**C motif) and the number of alignments spanning the full mark context (41 bp) were compiled. For full alignments, the number of mismatches with respect to the *R. solanacearum* GMI1000 sequence in each alignment position was also computed.

Identification of Non-methylated, Hyper-Methylated and Highly-Conserved Motifs

Non-methylated motif instances in the *R. solanacearum* GMI1000 and *R. solanacearum* UY031 genomes were identified following the protocol outlined in Blow et al. (2016). Essentially, a motif instance (detected through regular-expression search on the genome) was considered to be non-methylated if its inter-pulse duration ratio (ipdR) score fell below the under-methylated motif ipdR threshold, defined as (0.1*average motif ipdR)+(0.9*average non-motif ipdR), using only modifications of the same type (e.g., m6A) to compute the average non-motif ipdR. Motif and non-motif average ipdR values were computed on the central 60% of ranked ipdR scores to minimize the effect of outliers. For the palindromic motifs under analysis, motif instances were considered non-methylated if their ipdR ratios were below the under-methylated motif ipdR threshold on both strands and had at least twenty-fold SMRT sequence coverage. Hyper-methylated loci were detected as those with a number of motif instances in their upstream region larger than two standard deviations above the mean number of motif instances for all genome upstream regions (Mou et al., 2014). Highly-conserved motif instances were identified as those presenting fully aligned sequence contexts (41 bp) in all the species making up the panel of reference genomes.

Non-supervised Orthologous Groups and Annotated Feature Analysis

Protein sequences for each RefSeq identifier were parsed from the genome GenBank-format file and used to query the eggNOG database (4.5). eggNOG identifiers, categories, and descriptions were retrieved from the eggNOG database (eggNOG, RRID:SCR_002456) using HMMER (Hmmer, RRID:SCR_005305) (Eddy, 2011; Powell et al., 2014) and used to annotate extracted genome features. NOG (Non-supervised Orthologous Groups) category enrichment for a subset of methylation marks (e.g., conserved G<u>T</u>WW**A**C marks) in a given region relative to annotated protein coding genes (upstream, intragenic or downstream) was assessed by performing a Fisher exact test on NOG categories, using the presence of at least one

such methylation mark in the region of interest as an indicator function for all genome protein coding genes with annotated NOGs. Modification mark enrichment for specific NOGs and gene-relative regions was assessed through permutation analysis, generating 10,000 NOG replicates containing the same number of genes mapping to the NOG and assessing their normalized modification density in the region under study. Modification mark enrichment for a specific annotated feature (e.g., genes with "transposase" in their product/NOG description) was assessed by performing a Mann-Whitney *U*-test on the normalized modification density of genes containing the annotated feature vs. all other genome genes, and by computing the point-biserial correlation coefficient between normalized modification densities in contiguous 1,000 bp sequence chunks and the presence of the annotated feature within said chunks. Statistical computations were performed using the Python SciPy library (SciPy, RRID:SCR_008058). When appropriate, *p*-values were adjusted for multiple hypothesis testing using the Bonferroni procedure (Dunn, 1961). Statistical significance was determined at significance level $\alpha = 0.01$ for all tests reported in this work.

Promoter Analysis

Upstream regions of interest were analyzed for the presence of promoter elements using three different prediction tools: the Phi-Site Promoter Hunter (phiSITE, RRID:SCR_014754) (Klucar et al., 2010), PePPER (PePPER Prokaryote Promoter Prediction, RRID:SCR_014740) (de Jong et al., 2012) and BPROM (SoftBerry, RRID:SCR_000902). Only the strongest prediction of each method on each strand, when applicable, was considered.

RESULTS

Identification of Methylation Motifs in *R. solanacearum*

SMRT sequencing of *R. solanacearum* GMI1000 and UY031 strains yielded different total numbers of statistically significant modification marks (229,207 for *R. solanacearum* GMI1000 and 22,732 for *R. solanacearum* UY031). These numbers correlate with a threefold difference in average sequencing coverage for detected modification marks between both strains (177.35 ± 19.46 for GMI1000 vs. 51.53 ± 23.99 for UY031) (**Table 1**). It is of note that most of the additional identified marks in GMI1000 correspond to m4C modifications, whereas the number of m6A modifications appears to be constant between both strains. This is consistent with lower detection yields for m4C methylation with reduced coverage (Schadt et al., 2013; Blow et al., 2016). Motif analysis of the modification profiles identified two m6A and two m4C novel methylation motifs. The two m4C motifs (C**C**CAKNAVCR and YG**C**CGGCRY) were only detected in *R. solanacearum* GMI1000, while one of the m6A methylation motifs (CAACR**A**C) was identified only in *R. solanacearum* UY031. The remaining m6A motif (GTWW**A**C) was consistently detected in both strains.

TABLE 1 | Summary statistics for modification profiles of *R. solanacearum* GMI1000 and *R. solanacearum* UY031 strains.

Modification type	Motif	UY031	GMI1000
Not determined	–	17,989	202,350
	CAACRAC	38	0
	GTWWAC	10	1
	CCCAKNAVCR	0	358
	YGCCGGCRY	0	2,296
	All	18,094	205,005
m6A	–	373	880
	CAACRAC	2,100	0
	GTWWAC	689	779
	All	3162	1659
m4C	–	1,293	17,916
	CCCAKNAVCR	0	77
	YGCCGGCRY	0	922
	All	1,293	18,915
Expected	–	160	0
	CAACRAC	6	0
	GTWWAC	17	4
	CCCAKNAVCR	0	712
	YGCCGGCRY	0	2912
	All	183	3,628
All		22,732	229,207

Reported numbers are for statistically significant modification marks on either DNA strand.

Motif-Methylase Assignment and Distribution of Predicted RM Systems

Of the four detected novel motifs, only the two m6A motifs could be reliably assigned to predicted methylases in REBASE (**Table 2**). The CAACR**A**C motif is most likely the target of the Rso31ORF11320P fused RM system of *R. solanacearum* UY031, which has no detectable homologs in the reference panel of complete *Ralstonia* genomes. In contrast, the GTWW**A**C motif was assigned to the M.Rso31ORF22890P/M.RsoORF1982P MTase (encoded by RS_RS09960 and RSUY_RS11230, respectively, in *R. solanacearum* GMI1000 and *R. solanacearum* UY031), which is conserved in the reference panel of *Ralstonia* spp. genomes and across the *Burkholderiaceae*. Methylome analysis of *Burkholderia pseudomallei* strains had previously identified a similar type II motif (GTAW**A**C), which is likely the target of the M.Rso31ORF22890P/M.RsoORF1982P MTase homolog in *B. pseudomallei* (Nandi et al., 2015). The distribution of RM systems in both strains is similar and consistent with the overall distribution of RM systems predicted by REBASE in *Ralstonia* (Supplementary Table 4). Both strains harbor a type I RM system conserved among all *R. solanacearum* reference genomes, as well as two well-conserved type II MTases (in addition to M.Rso31ORF22890P/M.RsoORF1982P). It is worth noting that these two tightly linked MTases reside in the megaplasmid of *R. solanacearum* UY031, but are located in the

TABLE 2 | REBASE annotated methylases and associated motifs in *R. solanacearum* GMI1000 and *R. solanacearum* UY031.

R. solanacearum UY031				*R. solanacearum* GMI1000					RM system			
Replicon	Locus tag	Protein ID	REBASE ID	Replicon	Locus tag	Protein ID	REBASE ID	R/M	Type	Motif	% detect.	Cons.
NZ_CP012687.1	RSUY_RS00445	WP_003261699.1	Rso31ORF920P	NC_003295.1	RS_RS17020	WP_011003276.1	RsoORF3394P	R	I	–	–	9
NZ_CP012687.1	RSUY_RS00435	WP_003261701.1	M.Rso31ORF920P	NC_003295.1	RS_RS17010	WP_011003274.1	M.RsoORF3394P	M	I	–	–	9
NZ_CP012688.1	RSUY_RS22775	WP_039562516.1	M1.Rso31ORF46860P	NC_003295.1	RS_RS04210	WP_011000797.1	M1.RsoORF844P	M	II	–	–	7
NZ_CP012688.1	RSUY_RS22780	WP_039562519.1	M2.Rso31ORF46860P	NC_003295.1	RS_RS04215	WP_011000798.1	M2.RsoORF844P	M	II	–	–	10
NZ_CP012687.1	RSUY_RS11230	WP_020957142.1	M.Rso31ORF22890P	NC_003295.1	RS_RS09960	WP_011001918.1	M.RsoORF1982P	M	II	GTWW**A**C	95.5/99.5	12
NZ_CP012687.1	RSUY_RS05525	WP_039558712.1	Rso31ORF11320P	–	–	–	–	RM	II	CAACR**A**C	97.0	1
NZ_CP012687.1	RSUY_RS05480	WP_003264976.1	M.Rso31ORF11220P	–	–	–	–	M	II	–	–	1
NZ_CP012687.1	RSUY_RS05495	WP_049280918.1	Rso31ORF11260P	–	–	–	–	R	II	(GA**N**TC)	–	1
NZ_CP012687.1	–	–	M.Rso31ORF11260P	–	–	–	–	M	II	(GA**N**TC)	–	1
–	–	–	–	NC_003295.1	RS_RS17175	(pseudo)	M.RsoORF3438P	M	II	(Y**GCC**GGCRY)	32.8	1
–	–	–	–	NC_003295.1	RS_RS25190	WP_011003318.1	V.RsoORF3438P	V	II	–	–	1
–	–	–	–	NC_003296.1	RS_RS19865	WP_011003871.1	M.RsoORF570P	M	II	–	–	1
–	–	–	–	NC_003295.1	–	–	M.RsoORF869P	M	II	(**CC**CAKNAVCR)	17.3	4

R denotes restriction enzymes, M methylases and V nicking enzymes associated with m5C–MTases. Bracketed motifs indicate tentative, unconfirmed mappings to RM systems. "% detect." indicates the percentage of motif instances detected as methylated through the SMRT sequencing in either strain. "Cons." indicates the number of species from the reference panel in which the components of the RM system are conserved, as determined through reciprocal BLAST. The "–" symbol indicates missing RM components or their missing annotation in RefSeq records. (pseudo) indicates that the corresponding locus has been annotated as a pseudogene in RefSeq.

chromosome of *R. solanacearum* GMI1000. Besides the fused RM system targeting the CAACR**A**C motif, *R. solanacearum* UY031 also harbors a type II RM system predicted by REBASE to target a GA**N**TC motif, although this motif was not detected by SMRT sequencing. *R. solanacearum* GMI1000 carries an additional type II RM system, as well as two type II MTases, but the C**C**CAKNAVCR and YG**CC**GGCRY motifs could not be reliably assigned to predicted methylases in this strain. In general, the RM systems and MTases not conserved between *R. solanacearum* GMI1000 and UY031 do not present homologs among other *Ralstonia* species and thus appear to have been independently acquired by each strain.

Gene-Relative Distribution of Methylation Marks

An analysis of mark distribution with respect to annotated gene features in *R. solanacearum* strains GMI1000 and UY031 revealed that GTWW**A**C marks show a clear preference for the upstream regions of annotated genes (38% of GTWW**A**C marks vs. 8% of other motif marks) in both strains. Marks for all other identified motifs show a strong association with intragenic regions, as expected under a uniform model for methylation activity (Supplementary Image 1). The skew observed for GTWW**A**C marks cannot be explained simply by a difference in the %GC-content of the GTWW**A**C motif, since such a dramatic tendency is not observed for intergenic regions or among non-motif associated marks. To contextualize the preference of GTWW**A**C marks for upstream regions, we analyzed the distribution of modification marks with respect to annotated genes across the two *R. solanacearum* strains and a panel of 208 publicly available methylomes (Blow et al., 2016). Our results indicate that the preference of GTWW**A**C marks for upstream regions is exceptional among previously reported methylomes (**Figure 1**). Even though there is substantial correlation between motif %GC content and the fraction of marks mapping to upstream and downstream regions (Pearson $r = -0.41$ and $r = -0.34$, respectively; Supplementary Image 2), the preference of GTWW**A**C marks for upstream regions is distinctly high even when controlling for %GC content. Furthermore, among all the previously reported motifs showing strong (1st percentile) preference for upstream regions, only the GTWW**A**C motifs of *R. solanacearum* strains GMI1000 and UY031 show also heavy differential enrichment in upstream regions vs. downstream ones, suggesting that upstream GTWW**A**C marks may play a functional role in these *R. solanacearum* strains (Supplementary Table 5).

Analysis of Conserved Methylation Marks

The presence of a conserved MTase associated with a GTWW**A**C motif in both *R. solanacearum* GMI1000 and UY031 indicates that the GTWW**A**C methylome most likely predates the split between these two strains, enabling us to perform a comparative analysis of detected methylation marks associated with this motif (Supplementary Table 6). After detecting bona fide gene orthologs between both strains, we identified their conserved GTWW**A**C marks as those presenting at least 70% identity in a gapless alignment of the methylation mark sequence

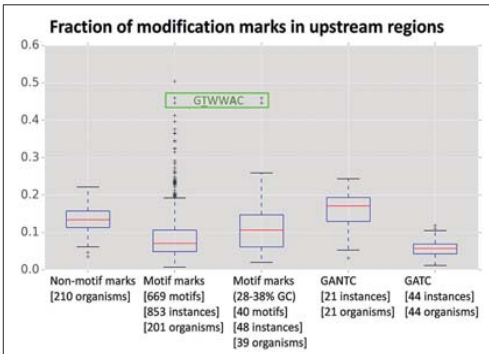

FIGURE 1 | Fraction of modification marks mapping to upstream regions of annotated genes across a panel of 210 methylomes. The fraction of upstream marks is relative to the sum of marks mapping to upstream, downstream, and intragenic regions of annotated genes in each genome. The boxplot columns designate different datasets: non-motif associated modification marks, motif-associated modification marks, %GC-controlled (28–38% GC) motif-associated modification marks, and marks associated with the widely distributed GTN**A**C and GT**A**C motifs. For each column, the bracketed numbers in the abscissa legend indicate the number of unique motifs in the dataset, the number of instances of those motifs identified in the complete set of methylomes and the number of organisms on which such instances were detected. The data points corresponding to the *R. solanacearum* GMI1000 and *R. solanacearum* UY031 GTWW**A**C motifs are boxed.

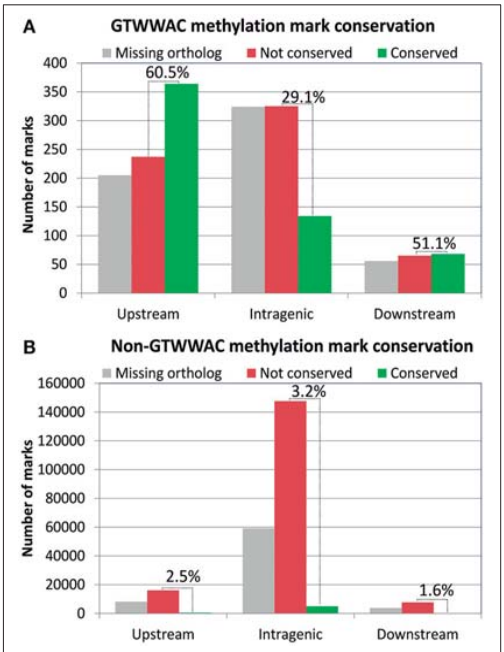

FIGURE 2 | Distribution of GTWWAC methylation marks conserved in *R. solanacearum* GMI1000 and *R. solanacearum* UY031 as a function of their location relative to annotated genes. The plot shows the number of GTWW**A**C methylation marks conserved in each location category. Non-conserved marks are distinguished from those mapping to genes lacking an identifiable ortholog in either strain. The relative conservation of GTWW**A**C methylation marks in each region (excluding marks mapping to genes lacking orthologs) is indicated on top of the bars. **(A)** GTWWAC methylation marks. **(B)** Non-GTWWAC methylation marks.

context (41 bp) of both strains. Analysis of mark conservation based on their location relative to annotated genes revealed that GTWW**A**C marks located upstream and downstream of annotated genes were much more likely to be conserved than those mapping to intragenic regions (**Figure 2A**). For marks mapping to conserved orthologs, 60.5% were conserved between both strains for upstream regions, 29.1% for intragenic regions and 51.1% for downstream regions. This association between mark location and conservation was not observed in marks not associated to the GTWW**A**C motif (**Figure 2B**). Among these, only intragenic regions showed a moderate amount of conservation (3.21%), most likely arising from increased sequence conservation within coding regions. The high fraction of GTWW**A**C marks mapping to upstream regions in both strains and their remarkable inter-strain conservation is hence highly suggestive of a functional role.

To investigate the putative functional role of upstream GTWW**A**C marks, we performed a comparative analysis of conserved GTWW**A**C marks across a panel of 12 *Ralstonia* species with complete sequenced genomes, using conserved non-GTWW**A**C marks as a control. The results of this analysis were in broad agreement with those obtained in the comparison between *R. solanacearum* GMI1000 and *R. solanacearum* UY031 (Supplementary Table 6). The contexts of GTWW**A**C marks were more frequently conserved than those of non-GTWW**A**C marks in both upstream and downstream regions, although the difference is significant (Mann-Whitney U p-value < 0.01) only for upstream marks (**Figure 3**). Furthermore, among conserved mark contexts the 6 bp region corresponding to the GTWW**A**C mark is significantly well-preserved for upstream marks, but not for intragenic or downstream ones (Supplementary Image 3). Analysis of the mutational profile along fully aligned mark contexts revealed a clear pattern of sequence conservation surrounding the GTWW**A**C mark region (positions 17–22) in upstream regions (**Figure 4**). This pattern can also be observed in downstream regions, but is completely absent in intragenic regions and it was not observed in any region among non-GTWW**A**C conserved modification marks. This is consistent with a scenario of purifying selection acting on GTWW**A**C marks in upstream and downstream regions.

Distribution of Upstream Sites in Hyper-Methylated and Non-methylated Loci

It has been proposed that the presence of upstream sites matching a methylation motif but with no apparent methylation may be indicative of an interplay between transcription factors

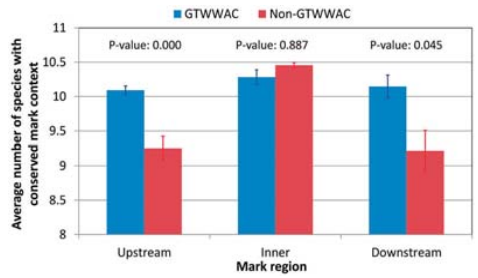

FIGURE 3 | Conservation of GTWWAC and non-GTWWAC associated marks across a panel of 12 reference complete *Ralstonia* genomes. The plot shows the average number of genomes in which the *R. solanacearum* GMI1000 context of a methylation mark is considered to be conserved (alignment identities above 70%) for different regions (upstream, intragenic, and downstream) relative to genes with orthologs in *R. solanacearum* GMI1000 and *R. solanacearum* UY031. Vertical bars indicate the standard error of the mean. The *p*-values of a two-tailed Mann Whitney *U*-test between GTWW**A**C and non-GTWW**A**C associated marks are provided on top of the bars.

and MTases, as evidenced by the well-studied *Escherichia coli* Pap system (Braaten et al., 1994; Low and Casadesús, 2008; Blow et al., 2016). Conversely, an overabundance of upstream methylation marks in certain loci might also be indicative of a functional role, as in the case of DNA replication control (Løbner-Olesen et al., 2003; Blow et al., 2016). To further explore the functional role of upstream GTWW**A**C sites, we identified loci with non-methylated GTWW**A**C motifs in strains GMI1000 and/or UY031, as well as upstream gene regions with an overabundance of conserved GTWW**A**C sites and with highly conserved GTWW**A**C motifs. Only five genomic loci presented more than one methylated GTWW**A**C site conserved upstream of orthologous genes in the GMI1000 and UY031 strains (**Figure 5**; Supplementary Table 7). These loci corresponded to the shared upstream region of RS_RS16825 (a SET domain-containing protein) and RS_RS16830 (a HU-like transcriptional regulator), the megaplasmid replication protein RepA (RS_RS17200), the tricarboxylate transporter component TctC (RS_RS14850), the AidB isovaleryl-coenzyme A dehydrogenase homolog (RS_RS01370) and the exopolysaccharide repressor EpsR (RS_RS18775). In two of these upstream regions, the conserved GTWW**A**C sites overlap (5 out of 6 positions) with the −35 boxes of predicted RNA polymerase binding sites (**Figure 5**). This is particularly true for the upstream region shared between the divergently transcribed RS_RS16825and RS_RS16830 genes, where GTWW**A**C sites overlap with high-confidence promoter elements in both strands. An analysis of all GTWW**A**C sites detected in upstream regions with predicted promoters revealed that more than 15% overlap predicted promoter elements (5% of them in 5 out of 6 positions), indicating that such arrangements are much more frequent than expected by chance (Supplementary Image 4). In hypermethylated upstream regions where GTWW**A**C sites do not show a clear overlap with −35 elements, they often define (RS_RS18775) or are part of larger (RS_RS01370) palindromic elements that might be targeted by transcription factors.

Most GTWW**A**C motif instances in both *R. solanacearum* GMI1000 and *R. solanacearum* UY031 were detected as methylated by SMRT sequencing. Our analysis revealed only seven upstream regions with non-methylated GTWW**A**C sites in either strain (Supplementary Table 8). Of these, only three were conserved in both strains, but they displayed different methylation states (**Figure 5**). The GTWW**A**C site upstream of RS_RS12840, a putative DUF3313 domain-containing lipoprotein, was non-methylated in both strains and overlapped the −35 region of a putative promoter. In contrast, the site upstream of RS_RS15735, a HipB-like transcriptional regulator, was non-methylated in strain GMI1000, but hemi-methylated in UY031. Lastly, the site upstream of RS_RS17560, a predicted RelB antitoxin, was fully methylated in GMI1000, but non-methylated in UY031. This site also overlapped a predicted −35 element and was found to be adjacent to an additional GTWW**A**C site in strain GMI1000 that is not conserved in UY031. Analysis of GTWW**A**C site conservation across the reference genome panel revealed two sites with fully aligned sequence contexts in all reference genomes (Supplementary Table 6). One of these sites mapped to the shared upstream region of the divergently transcribed *metK* (RS_RS00660) and *lpxL* (RS_RS00665) genes, where it overlaps the −35 element of a predicted *metK* promoter (**Figure 5**).

NOG Category Enrichment Analysis

To elucidate whether MTases with associated motifs preferentially target a functional subset of genes, we performed a functional category enrichment of motif-associated methylation marks based on their location (upstream, intragenic and downstream) relative to the protein-coding genes mapping to each Non-supervised Orthologous Group (NOG). Analysis of both conserved and strain-specific GTWW**A**C marks revealed no statistically significant enrichment in any NOG category. In contrast, intragenic CAACR**A**C marks showed significant enrichment for the M functional category (Cell wall/membrane/envelope biogenesis) (Supplementary Table 9). Analysis of the protein coding genes mapping to this NOG category showed that the observed enrichment was mainly driven by porins and membrane transporters, with a substantial presence of RHS repeat-containing proteins (PF05593; Pfam, RRID:SCR_004726) linked to type IV and type VI secretion systems (Koskiniemi et al., 2013). Such association could not be attributed to a simple overlap between repeat motifs and the CAACR**A**C target motif, since the codons encoding the signature motifs of RHS repeats (YD, RY and GR dipeptides) are not contained within the CAACR**A**C pattern (Hill et al., 1994).

Genome-Wide Analysis of Modification Profiles

Even when restricting the analysis to modification marks with significant coverage, the fraction of modifications detected by SMRT sequencing-based analyses that can be unambiguously mapped to MTase activity remains consistently small (Schadt et al., 2013; Blow et al., 2016). As it can be seen in **Table 1**, in both

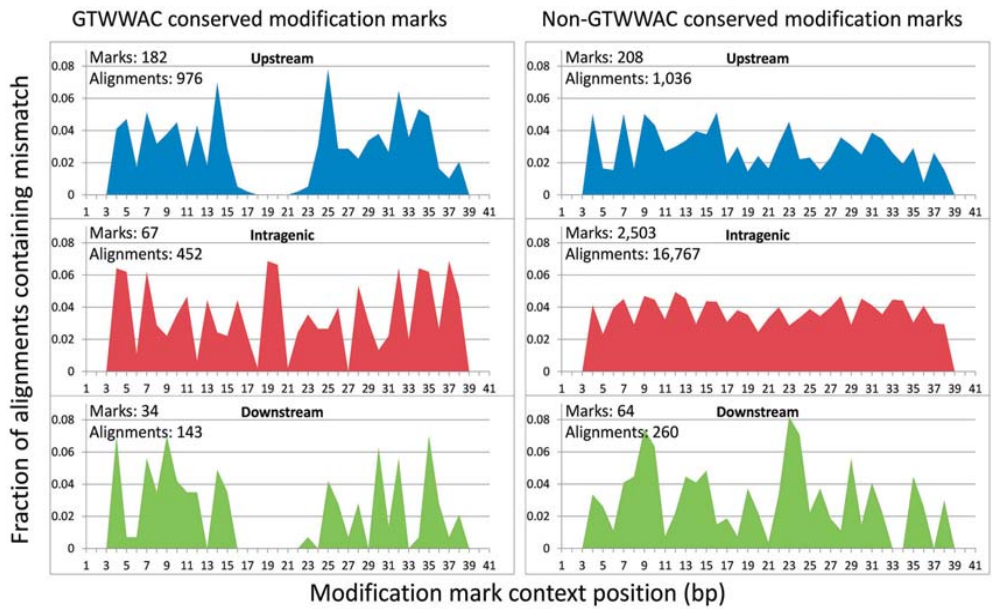

FIGURE 4 | Positional distribution of nucleotide changes with respect to *R. solanacearum* GMI1000 in gapless alignments of conserved modification marks. The plots show the fraction of alignments containing mismatches at each alignment position for marks conserved in *R. solanacearum* GMI1000 and UY031 strains located in upstream, downstream and intragenic regions. The fraction is computed based on cumulative alignment mismatch counts for full gapless BLAST alignments (100% coverage) against a panel of 12 complete *Ralstonia* genomes. The number of conserved marks in each region, and the number of full alignments used to tally mismatches are provided. Mismatches on the first and last two positions of the alignment are not expected due to the greedy nature of the BLAST hit extension process.

strains the majority (99%) of these modifications correspond to unresolved modifications (i.e., SMRT sequencing was not able to assign a specific modification type (m4C or m6A)). To investigate whether these unassigned modifications might have a functional role, we first performed a comparative analysis of unassigned modification density for protein coding genes assigned to NOGs in *R. solanacearum* strains GMI1000 and UY031. We identified NOGs with unusually high unassigned modification density in their upstream, intragenic and downstream regions as those with a normalized modification density within the 5th percentile for that region in both strains. This procedure identified 27 NOGs with unusually high modification density in each of the analyzed regions (9 upstream, 15 intragenic and 3 downstream) (Supplementary Table 10), but revealed no apparent functional association among them. To further explore the possibility of a functional role for unassigned modification density, we analyzed the normalized modification density profile for the chromosome and megaplasmid of the GMI1000 and UY031 strains, computed on overlapping 1,000 bp segments. Inspection of highly-modified segments (3 standard deviations above the average modification density) revealed a consistent association between high modification density and annotated transposase genes in *R. solanacearum* UY031 (**Figure 6**). This association was positive and statistically significant in strain UY031 (Mann-Whitney U p-value < 0.01, point-biserial correlation coefficient $r = 0.21$, $p < 0.01$ (chromosome) and $r = 0.25$, $p < 0.01$ (megaplasmid), but was not detectable in GMI1000 [$r = -0.03$, $p < 0.01$ (chromosome) and $r = -0.09$, $p < 0.01$ (megaplasmid)]. A systematic analysis of publicly available methylomes (Blow et al., 2016) revealed that very few prokaryotic species show a consistent association between hyper-modification and annotated transposase genes. When detectable, this association is strongest within the intragenic and downstream regions of these genes, but this phenomenon was remarkably more pronounced in *R. solanacearum* UY031 than in any other species (Supplementary Table 11).

An examination of transposase genes in the *R. solanacearum* UY031 genome showed that it contains a high copy number of transposases (86) associated with the insertion sequence ISrso3 (Jeong and Timmis, 2000). This number was much higher than that observed in other *R. solanacearum* strains and corresponded to 76% of all annotated transposase genes in the UY031 genome (Supplementary Table 12). Accordingly, a permutation analysis of normalized modification density for the NOG associated with the ISrso3 transposase (ENOG4105F2I) in strain UY031 confirmed that this NOG presented an unusually

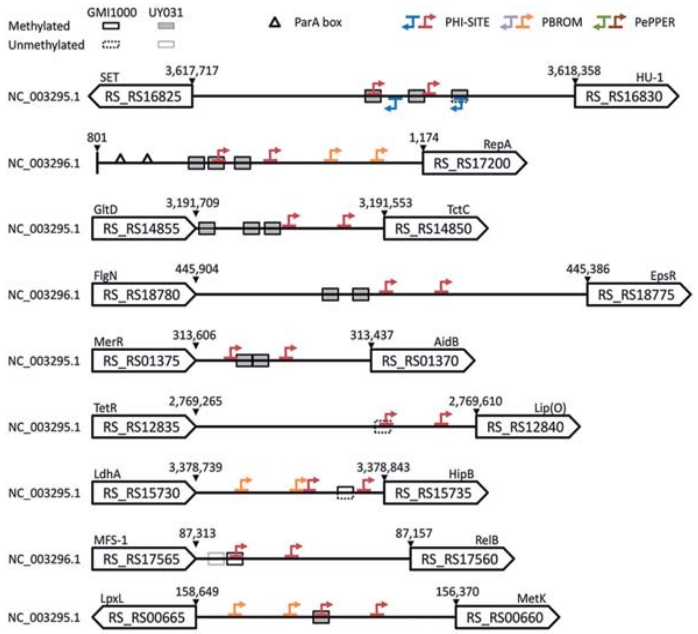

FIGURE 5 | Schematic representation of the upstream region for conserved loci enriched in methylated, non-methylated and highly-conserved GTWWAC sites. Accessions, locus tags and coordinates are provided for the *R. solanacearum* GMI1000 genome. A mapping to old GMI1000 locus tag identifiers is provided in Supplementary Table 2. When not annotated in *R. solanacearum* GMI1000, gene acronyms are derived from homology searches against the *E. coli* genome or from representative domains (uppercase). GTWW**A**C sites are denoted by boxes, with their methylation state in *R. solanacearum* GMI1000 indicated by solid/dotted outlines and their methylation state in *R. solanacearum* UY031 indicated by white/shaded fillings. Triangles denote ParA boxes annotated in the *R. solanacearum* GMI1000 genome. Arrows indicate directional −35 and −10 promoter elements predicted by Phi-Site, BPROM, and PePPER. When predictions overlap, the results are shown using the following coloring precedence: Phi-Site, BPROM, and PePPER.

high modification density (p-value < 0.01) in its intragenic and downstream regions, consistent with the aforementioned association between modification density and transposase genes. A positional analysis of modification marks on the 86 copies of the ISrso3 transposase revealed a highly uneven pattern of modification in these genes, with two large modification peaks in their intragenic and downstream regions (**Figure 7**). Analysis of these two modification peaks revealed that they are primarily led by modification of positions 487 and 1,049. The context of these two modification loci displayed only weak sequence identity (TCNGATNNANNHNNGG), but the presence of modification marks in 85 of the 86 ISrso3 transposase genes at these positions suggested that they are the result of a systematic modification process.

DISCUSSION

Distribution and Possible Roles of RM Systems in *Ralstonia solanacearum*

Even though the nature of RM systems as primary bacterial defense mechanisms has been firmly established (Tock and Dryden, 2005), there is substantial evidence supporting many additional roles for DNA methylation in bacteria (Low and Casadesús, 2008). Moreover, the nature and scope of their impact on bacterial lifestyle and evolution has not been fully elucidated (Vasu and Nagaraja, 2013). Several studies have taken advantage of SMRT sequencing to analyze and compare the methylation profile of closely related bacteria (Budroni et al., 2011; Krebes et al., 2014; Mou et al., 2014; Nandi et al., 2015). Here, we leveraged SMRT sequencing data for two relatively distant *R. solanacearum* strains (Wicker et al., 2012) to shed light on the diversity and possible roles of DNA methylation in this agriculturally important plant pathogen. Our analysis reveals a conserved architecture of RM systems across *R. solanacearum* strains, which harbor a conserved type I RM system and three conserved type II orphan MTases. The absence of this type I RM system in other *Ralstonia* species, which contain an unrelated type I RM system annotated in REBASE, points to a major evolutionary event in the divergence of species within this genus. Divergence in type I RM systems has been shown to forestall genetic exchange and drive the evolution in *Staphylococcus aureus* strains (Lindsay, 2010) and it seems

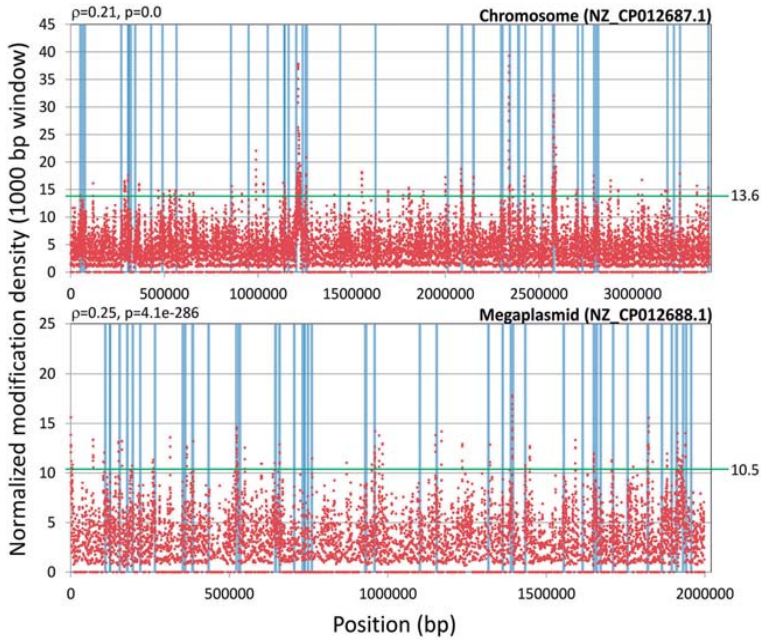

FIGURE 6 | Association of normalized modification mark density with transposable elements. The plot shows the genomic distribution of normalized modification mark density using a 1,000 bp window with a 100 bp step size on the *R. solanacearum* UY031 chromosome and megaplasmid. The presence of transposable elements within the sliding window is indicated by light blue bars. The point-biserial correlation coefficient and its *p*-value are provided for each replicon. A green horizontal line indicates the threshold for high modification density (three standard deviations above the mean normalized modification density).

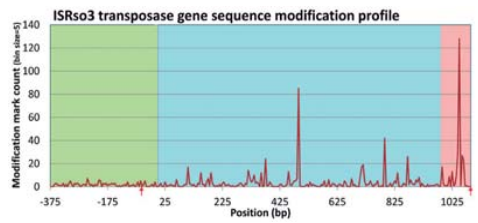

FIGURE 7 | Distribution of modification marks along the ISRso3 transposase [WP_003261205.1; ENOG4105F2I] of *R. solanacearum* UY031. The plot shows aggregated modification mark counts in upstream, intragenic and downstream regions of the 86 genes coding for WP_003261205.1 in *R. solanacearum* UY031. Mark counts were computed on 5 bp bins. Upstream, intragenic and downstream regions are delineated by shading color. Red arrows designate the location of the inverted repeats (IR) targeted by the ISrso3 transposase.

therefore plausible that a similar role may have been played by type I RM systems in the evolution of *Ralstonia* species. Beyond the presence of conserved RM elements, *R. solanacearum* strains also display a similar amount of non-conserved RM systems and orphan MTases (Supplementary Table 4), that have been presumably independently acquired by each strain. The functional role of these systems remains to be elucidated, but our analysis sheds some light onto their possible origin and function. *R. solanacearum* UY031 harbors a type II fused RM system targeting a novel m6A motif (CAACRAC). The gene encoding this RM system (RSUY_RS05525) is located in a prophage region identified by PHAST (PHAge Search Tool, RRID:SCR_005184) as being similar to *R. solanacearum* phiRS603, a filamentous phage of *R. solanacearum* (Zhou et al., 2011; Van et al., 2014; Guarischi-Sousa et al., 2016). The protein product of RSUY_RS05525 has no homologs among completely sequenced *R. solanacearum* genomes, but is present in the draft genomes of seven other *R. solanacearum* strains. This supports the notion that this fused RM system is phage-borne and has been recently acquired by *R. solanacearum*. Given its recent acquisition, it is unlikely that this RM system has been coopted for host-specific functions in *R. solanacearum* UY031. However, the preferential targeting of membrane-associated genes by the CAACRAC motif (Supplementary Table 9), including several systems known to mediate in intercellular competition (Koskiniemi et al., 2013), suggests that it could potentially play a role in strain differentiation and virulence.

A Conserved Type II MTase in *Ralstonia* spp. Targeting Gene Promoter Regions

The detection and independent assignment of an identical m6A methylation motif (GTWW**A**C) to orthologous loci in *R. solanacearum* strains GMI1000 and UY031 (RS_RS09960 and RSUY_RS11230, respectively) allows us to conclusively determine the association of this methylation motif with a type II orphan MTase conserved in all completely sequenced *Ralstonia* spp. genomes. Furthermore, reciprocal BLAST analyses indicate that this MTase is conserved across the *Burkholderiaceae*, consistent with the recent identification of a similar methylation motif in *B. pseudomallei* (Nandi et al., 2015). The broad conservation of this orphan MTase across the *Burkholderiaceae* family is suggestive of a functional role for GTWW**A**C methylation. Consistent with this hypothesis, genome-wide analyses of the distribution of GTWW**A**C methylation marks relative to annotated genes in both *R. solanacearum* strains revealed a highly pronounced preference for regions upstream of annotated genes (**Figure 1**; Supplementary Image 1). Several lines of evidence indicate that this preference does not stem solely from the relatively low %GC content of the GTWW**A**C motif. In particular, motifs with similar %GC content do not display this bias (**Figure 1**), and the GTWW**A**C motif does not exhibit such a pronounced preference for intergenic or downstream regions (Supplementary Tables 4, 5). Together, these data indicate that the observed preferential targeting of upstream regions by the GTWW**A**C motif is unique among previously reported motifs. Intriguingly, the association of GTWW**A**C with upstream regions is three- and seven-fold higher than the one observed in motifs with well-established roles in gene regulation (GANTC and GATC, respectively; **Figure 1**) (Low and Casadesús, 2008; Marinus and Casadesus, 2009), suggesting a functional role for GTWW**A**C methylation in upstream regions.

The hypothesis of a functional role driving the association of the GTWW**A**C motif with upstream gene regions suggests that upstream GTWW**A**C methylation marks should also be preferentially conserved. Comparison of GTWW**A**C mark context conservation mapping to orthologous loci in *R. solanacearum* GMI1000 and UY031 revealed that it is twice more likely to be conserved in upstream regions than in intragenic regions. This trend is not observed for non-GTWW**A**C mark contexts, which tend to be more conserved in intragenic regions (**Figure 2**). Furthermore, analysis of conserved mark contexts across a reference panel of complete *Ralstonia* spp. genomes reveals that GTWW**A**C mark contexts are also significantly more conserved in upstream regions (**Figure 3**). This effect could be partly ascribed to a biased distribution of upstream GTWW**A**C marks targeting highly conserved (e.g., housekeeping) genes, but NOG category enrichment of conserved GTWW**A**C marks did not reveal such a systematic bias. Moreover, the positional distribution of mismatches across a collection of fully aligned GTWW**A**C mark context hits on reference panel genomes revealed a clear footprint of sequence conservation surrounding the GTWW**A**C motif in upstream regions (**Figure 4**), suggesting that conservation of upstream contexts is largely driven by purifying selection on GTWW**A**C marks. Taken together, the preferential association of the GTWW**A**C motif with upstream regions and the higher conservation of GTWW**A**C marks when mapping to upstream regions provide strong support for a functional role of GTWW**A**C methylation in gene promoter regions.

Possible Functions of GTWWAC Methylation

Hyper-methylation and hypo-methylation of loci have been both put forward as possible indicators of a functional interplay between methylation and biological processes operating on the DNA sequences. For instance, attenuation of leucine-reponsive regulatory protein (Lrp) binding to hemi-methylated target sites and competition between Lrp and the Dam methylase for GA**T**C sites overlapping Lrp-binding sites is known to modulate expression of the *pap* pilin promoter, driving phase variation in *E. coli* (Braaten et al., 1994; Marinus and Casadesus, 2009). In a different context, competition for hemi-methylated GA**T**C sites between SeqA and Dam near the *E. coli* origin of replication (*oriC*) and in the promoter region of the *dnaA* gene is used to synchronize chromosomal replication with cell division (Løbner-Olesen et al., 2003; Marinus and Casadesus, 2009). Similarly, the CcrM methylase of *Caulobacter crescentus* (targeting the GANTC motif but unrelated to Dam) orchestrates the morphological differentiation of *C. crescentus* cells by modulating a transcriptional cascade involving three different regulators (DnaA, GcrA and CtrA) and occluding access to the origin of replication (Marczynski and Shapiro, 2002; Marinus and Casadesus, 2009). Although several of the precise mechanisms behind these regulatory processes involving DNA methylation remain to be fully elucidated, the presence of multiple methylation target sites in upstream regions and their hemi- or non-methylated state are shared elements in all known instances of DNA methylation interplay with cellular processes (Low and Casadesús, 2008; Marinus and Casadesus, 2009). In the context of a comparative analysis, highly-conserved methylation sites also appear as likely candidates for a functional role of DNA methylation.

Analysis of loci with conserved non- and hemi-methylated GTWW**A**C sites, loci containing multiple conserved GTWW**A**C sites in their upstream regions and loci harboring highly-conserved GTWW**A**C sites identified several genes that could potentially be regulated by the GTWW**A**C MTase (**Figure 5**). It is worth noting that GTWW**A**C marks overlap predicted −35 or −10 hexamers corresponding to RNA-polymerase binding sites in seven out of the nine upstream regions identified in the analysis, a fact known to play a role in modulating gene expression via Dam and CcrM methylation (Marinus and Casadesus, 2009). Among conserved non- and hemi-methylated sites, GTWW**A**C sites overlap the −35 region of a predicted lipoprotein (RS_RS12840) and a putative RelBE-like toxin-antitoxin (TA) system (RS_RS17560-RS_RS17555). This promoter region of this TA system is hemi-methylated in *R. solanacearum* GMI1000 and non-methylated in strain UY031, hinting at a differential process in DNA methylation that might be linked to cell state. Regulation of TA systems through DNA

methylation has not been reported to date. If confirmed, it could provide a causative mechanism for programmed switching into the viable but non-culturable (VBNC) state that *R. solanacearum* is known to enter in certain soil conditions (Grey and Steck, 2001). In this context, the presence of a highly-conserved G<u>T</u>WW**A**C site overlapping the −35 element of the predicted promoter of a *metK* homolog is also intriguing. MetK synthetizes SAM, the main methyl donor in *E. coli*, and its regulation through DNA methylation could therefore define a feedback loop governing DNA methylation in *R. solanacearum*. Moreover, *E. coli metK* mutants are known to undergo filamentation (Newman et al., 1998), suggesting that *metK* regulation through DNA methylation could also be involved in cell cycle control. The possibility that G<u>T</u>WW**A**C methylation might be involved in cell-cycle control is substantiated by the identification of a cluster of three conserved G<u>T</u>WW**A**C sites overlapping a predicted −35 element upstream of the megaplasmid *repA* locus (RS_RS17200). Even though these G<u>T</u>WW**A**C sites do not overlap predicted ParA-binding sites, and hence seem unlikely to define a Dam/CcrM-like mechanism of replication control, they could potentially co-regulate *repA* expression and thus contribute to modulate the proper partitioning of *R. solanacearum* megaplasmids (Pinto et al., 2012).

The putative role of G<u>T</u>WW**A**C methylation in the regulation of broad cellular processes in *R. solanacearum* is further supported by the identification of three conserved sites in the shared upstream region of the divergently transcribed RS_RS16830 and RS_RS16825 genes. Given the large size of this intergenic region (640 bp), the precise arrangement of these G<u>T</u>WW**A**C sites, overlapping the −35 elements of high-confidence predicted promoters for both genes, is strongly suggestive of an interplay between G<u>T</u>WW**A**C methylation and transcriptional initiation at these loci. RS_RS16830 encodes a HU histone-like protein, annotated as DbhB in the *Burkholderia*. DbhB homologs are known to be involved in genome-wide DNA bending that modulates transcriptional regulation in multiple loci of *Pseudomonas aeruginosa* (Bartels et al., 2001). Furthermore, besides bending-mediated transcriptional regulation, the *E. coli* HU protein also participates in control of DNA replication through interaction with DnaA (Flashner and Gralla, 1988). In this setting, it is worth noting that the divergently transcribed RS_RS16825 encodes a predicted SET domain-containing protein-lysine N-methyltransferase. Lysine methylation of histones is known to play a key role in eukaryotic epigenetic regulation by modulating histone activity (Qian and Zhou, 2006), and a similar interaction could thus be conceivably attributed to RS_RS16825 and the DbhB histone-like protein. Lastly, DNA methylation has been shown to influence the activity of several determinants of bacterial virulence, including lipopolysaccharide synthesis (Fälker et al., 2007; Marinus and Casadesus, 2009). Our analysis revealed the presence of two conserved G<u>T</u>WW**A**C sites upstream of the exopolysaccharide repressor EpsR (RS_RS18775). These sites are close to (13 bp), but do not overlap the predicted −35 promoter. Interestingly, the two sites are only 6 bp apart and, together, define a perfect palindromic repeat with an AT-rich spacer, which could well be the target of a transcriptional regulator. These observations suggest that EpsR transcription might be modulated by G<u>T</u>WW**A**C methylation, which could represent an additional layer of control on the synthesis of exopolysaccharide-I, a major virulence determinant in *R. solanacearum* (Chapman and Kao, 1998; Schell, 2000).

Systematic Modification of Multi-Copy Transposase Genes

Regulation of transposition though DNA methylation has been experimentally described for several transposable elements (Casadesús and Low, 2006). In the well-studied Tn10 and Tn5 transposons, Dam methylation of target sites impacts transposition in two different ways (Dodson and Berg, 1989; Kleckner, 1990). On the one hand, a G<u>A</u>**T**C site overlapping the -10 promoter element of the transposase gene is known to activate transposase transcription when hemi-methylated. On the other hand, hemi-methylation of a second G<u>A</u>**T**C overlapping the transposase IR site immediately downstream of the transposase gene is also required for efficient binding of the transposase. The presumed rationale for this arrangement is to synchronize transposition with chromosome replication, thereby enhancing the transmission of transposase genes while limiting their impact on chromosome stability (Kleckner, 1990). Even though motif-associated methylation sites were not preferentially detected in transposases on either *R. solanacearum* strain, analysis of unassigned modification marks revealed a clear, genome-wide association between densely modified regions and transposase genes in strain UY031, but not in GMI1000 (**Figure 6**). A similar association can be identified in a few other available methylomes, but the effect is not as pronounced as in *R. solanacearum* UY031, suggesting that this is an unusual property of this particular strain. Closer inspection revealed that this association was driven primarily by the presence of a high number of ISrso3 transposases in the genome of strain UY031. Interestingly, the modification pattern on ISrso3 genes was found to be remarkably non-uniform, with two well defined peaks within both the intragenic region and the region immediately downstream of the transposase gene (**Figure 7**). These two peaks do not coincide with previously described targets of DNA methylation in transposases, pointing to a possible hitherto unknown mechanism of transposase regulation or to a systematic bias in the incorporation of modified bases during transposition.

Insights from Methylome Analyses into *R. solanacearum* Biology and Evolution

Beyond its economic impact on crops around the world, *R. solanacearum* is probably best known for its ability to infect a wide variety of plant hosts, fueled by rapid adaptation, changes in its effector repertoire and phylogeographic diversification. Recent advances in sequencing technology have enabled the analysis of genome-wide DNA modification profiles in bacteria, but the biological relevance of such modifications remains largely unknown. Our identification of a conserved m6A MTase in *Ralstonia* spp. preferentially targeting gene upstream regions and the observation that its methylation sites appear to be under positive selection indicate that DNA methylation is

likely playing an active role in modulating the expression of many genes, including major transcriptional regulators and several genes involved in virulence and cell-state regulation. These results support the notion that DNA methylation could act as an additional layer of control on the pathogenicity of *R. solanacearum*, paving the way for targeted experimental approaches to elucidate the nature and impact of DNA methylation on *R. solanacearum* pathogenesis and its interaction with different plant hosts. Our work also examines for the first time the possible biological role of unassigned DNA modifications. The observation that transposases from high-copy insertion sequences are systematically modified and the characterization of an active, phage-borne RM system in the highly-virulent UY031 strain indicates that DNA modification may be playing an active role in controlling horizontal transfer in *R. solanacearum*, thus influencing its evolution and phylogeographic diversification. Our findings hence indicate that DNA methylation may play an important role in the pathogenesis and adaptation of *R. solanacearum* strains to their plant hosts, and should help focus subsequent *in vitro* and *in vivo* studies aimed at determining the impact of DNA methylation in this important bacterial phytopathogen.

AUTHOR CONTRIBUTIONS

IE, MV, AG, and SG conceived the experiment and coordinated the research. LL and CV performed SMRT sequencing and motif analysis on *R. solanacearum* GMI1000. RG and JS performed SMRT sequencing and motif analysis on *R. solanacearum* UY031. IE and MP performed the comparative analyses. IE wrote the necessary scripts and performed the statistical analyses. IE, MP, MV, AG, and SG discussed the findings and interpreted the results. IE drafted the manuscript. All authors read and approved the manuscript.

FUNDING

This work was funded by the Spanish Ministry of Economy and Competitiveness projects AGL2013-46898-R and AGL2016-78002-R to MV and by a U.S. National Science Foundation (MCB-1158056) award to IE. We also acknowledge financial support from the CERCA Program of the Catalan Government (Generalitat de Catalunya), the University of Maryland, Baltimore County Office of Research, the "Severo Ochoa Program for Centers of Excellence in R&D" 2016–2019 (SEV-2015-0533) of the Spanish Ministry of Economy and Competitiveness and the COST Action SUSTAIN (FA1208) from the European Union. RG is the recipient of a doctoral fellowship [grant 2012/15197-1, São Paulo Research Foundation (FAPESP)]. JS has a researcher fellowship from CNPq (304881/2015-5). MP holds an APIF doctoral fellowship from Universitat de Barcelona. This work was also performed in collaboration with the GeT core facility, Toulouse, France (http://get.genotoul.fr), and was supported by France Génomique National infrastructure, funded as part of "Investissement d'avenir" program managed by Agence Nationale pour la Recherche (contract ANR-10-INBS-09).

ACKNOWLEDGMENTS

The authors wish to thank R. Gonzàlez-Duarte for her key role in the inception of this collaborative research project.

SUPPLEMENTARY MATERIAL

The Supplementary Material for this article can be found online at: http://journal.frontiersin.org/article/10.3389/fpls.2017.00504/full#supplementary-material

REFERENCES

Altschul, S. F., Madden, T. L., Schaffer, A. A., Zhang, J., Zhang, Z., Miller, W., et al. (1997). Gapped BLAST and PSI-BLAST: a new generation of protein database search programs. *Nucleic Acids Res.* 25, 3389–3402. doi: 10.1093/nar/25.17.3389

Bartels, F., Fernández, S., Holtel, A., Timmis, K. N., and de Lorenzo, V. (2001). The essential HupB and HupN proteins of *pseudomonas putida* provide redundant and nonspecific DNA-bending functions. *J. Biol. Chem.* 276, 16641–16648. doi: 10.1074/jbc.M011295200

Blakeway, L. V., Power, P. M., Jen, F. E.-C., Worboys, S. R., Boitano, M., Clark, T. A., et al. (2014). ModM DNA methyltransferase methylome analysis reveals a potential role for *Moraxella catarrhalis* phasevarions in otitis media. *FASEB J.* 28, 5197–5207. doi: 10.1096/fj.14-256578

Blow, M. J., Clark, T. A., Daum, C. G., Deutschbauer, A. M., Fomenkov, A., Fries, R., et al. (2016). The epigenomic landscape of prokaryotes. *PLoS Genet.* 12:e1005854. doi: 10.1371/journal.pgen.1005854

Braaten, B. A., Nou, X., Kaltenbach, L. S., and Low, D. A. (1994). Methylation patterns in pap regulatory DNA control pyelonephritis-associated pili phase variation in *E. coli*. *Cell* 76, 577–588. doi: 10.1016/0092-8674(94)90120-1

Budroni, S., Siena, E., Hotopp, J. C. D., Seib, K. L., Serruto, D., Nofroni, C., et al. (2011). *Neisseria meningitidis* is structured in clades associated with restriction modification systems that modulate homologous recombination. *Proc. Natl. Acad. Sci. U.S.A.* 108, 4494–4499. doi: 10.1073/pnas.1019751108

Casadesús, J., and Low, D. (2006). Epigenetic gene regulation in the bacterial world. *Microbiol. Mol. Biol. Rev.* 70, 830–856. doi: 10.1128/MMBR.00016-06

Chapman, M. R., and Kao, C. C. (1998). EpsR modulates production of extracellular polysaccharides in the bacterial wilt pathogen *Ralstonia* (Pseudomonas) *solanacearum*. *J. Bacteriol.* 180, 27–34.

Chin, C.-S., Alexander, D. H., Marks, P., Klammer, A. A., Drake, J., Heiner, C., et al. (2013). Nonhybrid, finished microbial genome assemblies from long-read SMRT sequencing data. *Nat. Methods* 10, 563–569. doi: 10.1038/nmeth.2474

Clark, T. A., Lu, X., Luong, K., Dai, Q., Boitano, M., Turner, S. W., et al. (2013). Enhanced 5-methylcytosine detection in single-molecule, real-time sequencing via Tet1 oxidation. *BMC Biol.* 11:4. doi: 10.1186/1741-7007-11-4

Cock, P. J. A., Antao, T., Chang, J. T., Chapman, B. A., Cox, C. J., Dalke, A., et al. (2009). Biopython: freely available Python tools for computational molecular biology and bioinformatics. *Bioinformatics* 25, 1422–1423. doi: 10.1093/bioinformatics/btp163

Coupat, B., Chaumeille-Dole, F., Fall, S., Prior, P., Simonet, P., Nesme, X., et al. (2008). Natural transformation in the *Ralstonia solanacearum* species complex: number and size of DNA that can be transferred. *FEMS Microbiol. Ecol.* 66, 14–24. doi: 10.1111/j.1574-6941.2008.00552.x

Darling, A. C. E., Mau, B., Blattner, F. R., and Perna, N. T. (2004). Mauve: multiple alignment of conserved genomic sequence with rearrangements. *Genome Res.* 14, 1394–1403. doi: 10.1101/gr.2289704

de Jong, A., Pietersma, H., Cordes, M., Kuipers, O. P., and Kok, J. (2012). PePPER: a webserver for prediction of prokaryote promoter elements and regulons. *BMC Genomics* 13:299. doi: 10.1186/1471-2164-13-299

Denny, T. (2007). "Plant pathogenic Ralstonia species," in *Plant-Associated Bacteria*, ed S. S. Gnanamanickam (Springer), 573–644. Available online at: http://link.springer.com/chapter/10.1007/978-1-4020-4538-7_16 (Accessed November 14, 2016).

Dodson, K. W., and Berg, D. E. (1989). Factors affecting transposition activity of IS50 and Tn5 ends. *Gene* 76, 207–213. doi: 10.1016/0378-1119(89)90161-3

Dunn, O. J. (1961). Multiple comparisons among means. *J. Am. Stat. Assoc.* 56, 52–64. doi: 10.1080/01621459.1961.10482090

Eddy, S. R. (2011). Accelerated profile HMM searches. *PLoS Comput. Biol.* 7:e1002195. doi: 10.1371/journal.pcbi.1002195

Fälker, S., Schilling, J., Schmidt, M. A., and Heusipp, G. (2007). Overproduction of DNA adenine methyltransferase alters motility, invasion, and the lipopolysaccharide O-antigen composition of *Yersinia enterocolitica*. *Infect. Immun.* 75, 4990–4997. doi: 10.1128/IAI.00457-07

Fegan, M., and Prior, P. (2005). "How complex is the *Ralstonia solanacearum* species complex?" in *Bacterial Wilt Disease and the Ralstonia solanacearum Species Complex*, eds C. Allen, P. Prior, and A. C. Hayward (St. Paul, MN: APS Press), 449–461.

Flashner, Y., and Gralla, J. D. (1988). DNA dynamic flexibility and protein recognition: differential stimulation by bacterial histone-like protein HU. *Cell* 54, 713–721. doi: 10.1016/S0092-8674(88)80016-3

Forde, B. M., Phan, M.-D., Gawthorne, J. A., Ashcroft, M. M., Stanton-Cook, M., Sarkar, S., et al. (2015). Lineage-specific methyltransferases define the methylome of the globally disseminated *Escherichia coli* ST131 Clone. *mBio* 6, e01602–e01615. doi: 10.1128/mBio.01602-15

Furuta, Y., Namba-Fukuyo, H., Shibata, T. F., Nishiyama, T., Shigenobu, S., Suzuki, Y., et al. (2014). Methylome diversification through changes in DNA methyltransferase sequence specificity. *PLoS Genet.* 10:e1004272. doi: 10.1371/journal.pgen.1004272

Genin, S., and Denny, T. P. (2012). Pathogenomics of the *Ralstonia solanacearum* species complex. *Annu. Rev. Phytopathol.* 50, 67–89. doi: 10.1146/annurev-phyto-081211-173000

Grey, B. E., and Steck, T. R. (2001). The viable but nonculturable state of *Ralstonia solanacearum* may be involved in long-term survival and plant infection. *Appl. Environ. Microbiol.* 67, 3866–3872. doi: 10.1128/AEM.67.9.3866-3872.2001

Guarischi-Sousa, R., Puigvert, M., Coll, N. S., Siri, M. I., Pianzzola, M. J., Valls, M., et al. (2016). Complete genome sequence of the potato pathogen *Ralstonia solanacearum* UY031. *Stand. Genomic Sci.* 11:7. doi: 10.1186/s40793-016-0131-4

Guidot, A., Prior, P., Schoenfeld, J., Carrère, S., Genin, S., and Boucher, C. (2007). Genomic structure and phylogeny of the plant pathogen *Ralstonia solanacearum* inferred from gene distribution analysis. *J. Bacteriol.* 189, 377–387. doi: 10.1128/JB.00999-06

Handa, N., and Kobayashi, I. (1999). Post-segregational killing by restriction modification gene complexes: observations of individual cell deaths. *Biochimie* 81, 931–938. doi: 10.1016/S0300-9084(99)00201-1

Hill, C., Sandt, C., and Vlazny, D. (1994). Rhs elements of *Escherichia coli*: a family of genetic composites each encoding a large mosaic protein. *Mol. Microbiol.* 12, 865–871. doi: 10.1111/j.1365-2958.1994.tb01074.x

Jeong, E.-L., and Timmis, J. N. (2000). Novel insertion sequence elements associated with genetic heterogeneity and phenotype conversion in *Ralstonia solanacearum*. *J. Bacteriol.* 182, 4673–4676. doi: 10.1128/JB.182.16.4673-4676.2000

Jones, P. A. (2012). Functions of DNA methylation: islands, start sites, gene bodies and beyond. *Nat. Rev. Genet.* 13, 484–492. doi: 10.1038/nrg3230

Kleckner, N. (1990). Regulation of transposition in bacteria. *Annu. Rev. Cell Biol.* 6, 297–327. doi: 10.1146/annurev.cb.06.110190.001501

Klucar, L., Stano, M., and Hajduk, M. (2010). phiSITE: database of gene regulation in bacteriophages. *Nucleic Acids Res.* 38, D366–D370. doi: 10.1093/nar/gkp911

Koskiniemi, S., Lamoureux, J. G., Nikolakakis, K. C., t'Kint de Roodenbeke, C., Kaplan, M. D., Low, D. A., et al. (2013). Rhs proteins from diverse bacteria mediate intercellular competition. *Proc. Natl. Acad. Sci. U.S.A.* 110, 7032–7037. doi: 10.1073/pnas.1300627110

Krebes, J., Morgan, R. D., Bunk, B., Spröer, C., Luong, K., Parusel, R., et al. (2014). The complex methylome of the human gastric pathogen *Helicobacter pylori*. *Nucleic Acids Res.* 42, 2415–2432. doi: 10.1093/nar/gkt1201

Lindsay, J. A. (2010). Genomic variation and evolution of *Staphylococcus aureus*. *Int. J. Med. Microbiol.* 300, 98–103. doi: 10.1016/j.ijmm.2009.08.013

Løbner-Olesen, A., Marinus, M. G., and Hansen, F. G. (2003). Role of SeqA and Dam in *Escherichia coli* gene expression: a global/microarray analysis. *Proc. Natl. Acad. Sci. U.S.A.* 100, 4672–4677. doi: 10.1073/pnas.0538053100

Loenen, W. A. M., Dryden, D. T. F., Raleigh, E. A., Wilson, G. G., and Murray, N. E. (2014). Highlights of the DNA cutters: a short history of the restriction enzymes. *Nucleic Acids Res.* 42, 3–19. doi: 10.1093/nar/gkt990

Low, D. A., and Casadesús, J. (2008). Clocks and switches: bacterial gene regulation by DNA adenine methylation. *Curr. Opin. Microbiol.* 11, 106–112. doi: 10.1016/j.mib.2008.02.012

Marczynski, G. T., and Shapiro, L. (2002). Control of chromosome replication in *caulobacter crescentus*. *Annu. Rev. Microbiol.* 56, 625–656. doi: 10.1146/annurev.micro.56.012302.161103

Marinus, M. G., and Casadesus, J. (2009). Roles of DNA adenine methylation in host-pathogen interactions: mismatch repair, transcriptional regulation, and more. *FEMS Microbiol. Rev.* 33, 488–503. doi: 10.1111/j.1574-6976.2008.00159.x

Mayjonade, B., Gouzy, J., Donnadieu, C., Pouilly, N., Marande, W., Callot, C., et al. (2016). Extraction of high-molecular-weight genomic DNA for long-read sequencing of single molecules. *BioTechniques* 61, 203–205. doi: 10.2144/000114460

Mou, K. T., Muppirala, U. K., Severin, A. J., Clark, T. A., Boitano, M., and Plummer, P. J. (2014). A comparative analysis of methylome profiles of *Campylobacter jejuni* sheep abortion isolate and gastroenteric strains using PacBio data. *Front. Microbiol.* 5:782. doi: 10.3389/fmicb.2014.00782

Murray, I. A., Clark, T. A., Morgan, R. D., Boitano, M., Anton, B. P., Luong, K., et al. (2012). The methylomes of six bacteria. *Nucleic Acids Res.* 40, 11450–11462. doi: 10.1093/nar/gks891

Nandi, T., Holden, M. T. G., Didelot, X., Mehershahi, K., Boddey, J. A., Beacham, I., et al. (2015). *Burkholderia pseudomallei* sequencing identifies genomic clades with distinct recombination, accessory, and epigenetic profiles. *Genome Res.* 25:608. doi: 10.1101/gr.177543.114

Newman, E. B., Budman, L. I., Chan, E. C., Greene, R. C., Lin, R. T., Woldringh, C. L., et al. (1998). Lack of S-adenosylmethionine results in a cell division defect in *Escherichia coli*. *J. Bacteriol.* 180, 3614–3619.

Peeters, N., Guidot, A., Vailleau, F., and Valls, M. (2013). *Ralstonia solanacearum*, a widespread bacterial plant pathogen in the post-genomic era. *Mol. Plant Pathol.* 14, 651–662. doi: 10.1111/mpp.12038

Pinto, U. M., Pappas, K. M., and Winans, S. C. (2012). The ABCs of plasmid replication and segregation. *Nat. Rev. Microbiol.* 10, 755–765. doi: 10.1038/nrmicro2882

Powell, S., Forslund, K., Szklarczyk, D., Trachana, K., Roth, A., Huerta-Cepas, J., et al. (2014). eggNOG v4.0: nested orthology inference across 3686 organisms. *Nucleic Acids Res.* 42, D231–239. doi: 10.1093/nar/gkt1253

Qian, C., and Zhou, M.-M. (2006). SET domain protein lysine methyltransferases: structure, specificity and catalysis. *Cell. Mol. Life Sci.* 63, 2755–2763. doi: 10.1007/s00018-006-6274-5

Remenant, B., Coupat-Goutaland, B., Guidot, A., Cellier, G., Wicker, E., Allen, C., et al. (2010). Genomes of three tomato pathogens within the *Ralstonia solanacearum* species complex reveal significant evolutionary divergence. *BMC Genomics* 11:379. doi: 10.1186/1471-2164-11-379

Salanoubat, M., Genin, S., Artiguenave, F., Gouzy, J., Mangenot, S., Arlat, M., et al. (2002). Genome sequence of the plant pathogen *Ralstonia solanacearum*. *Nature* 415, 497–502. doi: 10.1038/415497a

Schadt, E. E., Banerjee, O., Fang, G., Feng, Z., Wong, W. H., Zhang, X., et al. (2013). Modeling kinetic rate variation in third generation DNA sequencing data to detect putative modifications to DNA bases. *Genome Res.* 23, 129–141. doi: 10.1101/gr.136739.111

Schell, M. A. (2000). Control of virulence and pathogenicity genes of *Ralstonia solanacearum* by an elaborate sensory network. *Annu. Rev. Phytopathol.* 38, 263–292. doi: 10.1146/annurev.phyto.38.1.263

Tock, M. R., and Dryden, D. T. (2005). The biology of restriction and anti-restriction. *Curr. Opin. Microbiol.* 8, 466–472. doi: 10.1016/j.mib.2005.06.003

Van, T. T. B., Yoshida, S., Miki, K., Kondo, A., and Kamei, K. (2014). Genomic characterization of ΦRS603, a filamentous bacteriophage that is infectious to the phytopathogen *Ralstonia solanacearum*. *Microbiol. Immunol.* 58, 697–700. doi: 10.1111/1348-0421.12203

Vasu, K., and Nagaraja, V. (2013). Diverse functions of restriction-modification systems in addition to cellular defense. *Microbiol. Mol. Biol. Rev.* 77, 53–72. doi: 10.1128/MMBR.00044-12

Wicker, E., Lefeuvre, P., de Cambiaire, J.-C., Lemaire, C., Poussier, S., and Prior, P. (2012). Contrasting recombination patterns and demographic histories of the plant pathogen *Ralstonia solanacearum* inferred from MLSA. *ISME J.* 6, 961–974. doi: 10.1038/ismej.2011.160

Zhou, Y., Liang, Y., Lynch, K. H., Dennis, J. J., and Wishart, D. S. (2011). PHAST: a fast phage search tool. *Nucleic Acids Res.* 39, W347–W352. doi: 10.1093/nar/gkr485

Conflict of Interest Statement: The authors declare that the research was conducted in the absence of any commercial or financial relationships that could be construed as a potential conflict of interest.

The reviewer AZ and handling Editor declared their shared affiliation, and the handling Editor states that the process nevertheless met the standards of a fair and objective review.

Supplementary Data

4

Suplementary Figure 1

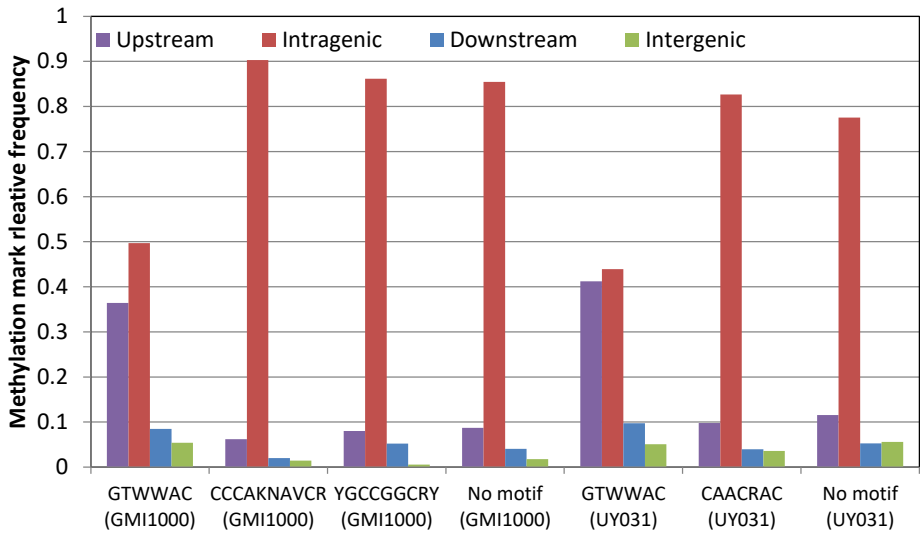

Relative frequency of motif and non-motif associated modification marks detected through SMRT sequencing as a function of their position relative to annotated genes.

Suplementary Figure 2

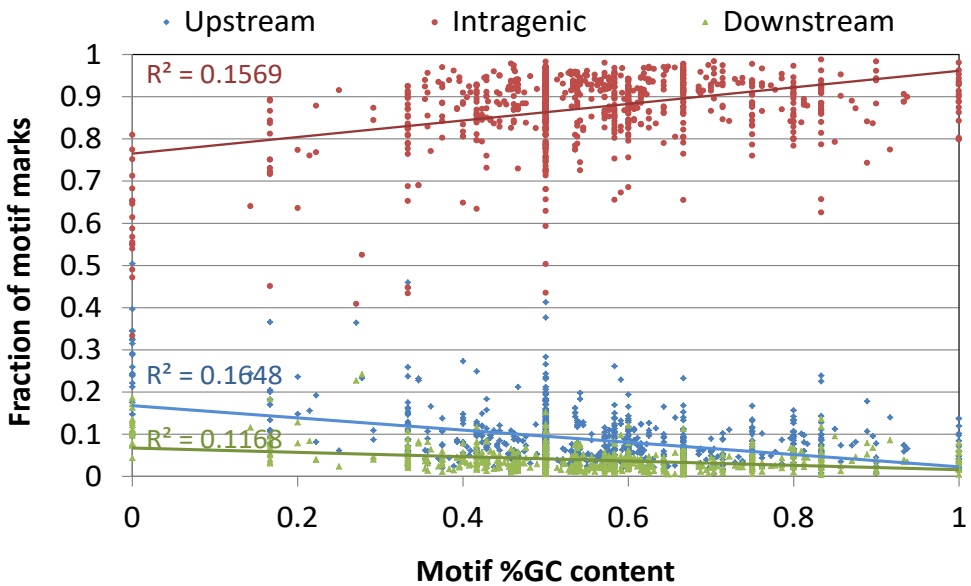

Fraction of motif marks mapping to upstream, intragenic and downstream regions of annotated genes in the methylomes of 210 bacteria, as a function of motif %GC content. The Pearson correlation coefficient (R^2) between both variables is provided for each gene-relative region. Pearson R values: $R_{upstream}$=-0.405, $R_{downstream}$=-0.341, $R_{intragenic}$=0.396.

Suplementary Figure 3

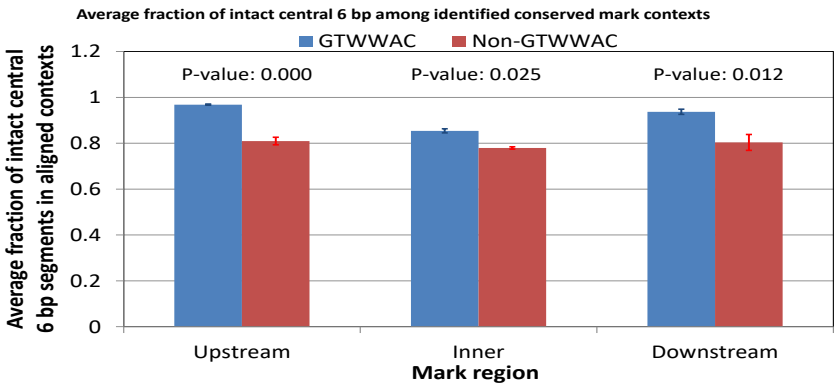

Conservation of the central 6 bp segment corresponding to the GTWWAC motif in alignments of GTWWAC and non-GTWWAC associated marks against a panel of 12 reference complete *Ralstonia* genomes. The plot shows the average fraction of genomes (relative to the total number of genomes in which a hit is identified) in which the central 6 bp segment of the methylation mark is fully conserved (with respect to the *R. solanacearum* GMI1000 context sequence) for different regions (upstream, intragenic and downstream) relative to genes with orthologs in *R. solanacearum* GMI1000 and *R. solanacearum* UY031. Vertical bars indicate the standard error of the mean. The p-values of a two-tailed Mann Whitney U test between GTWWAC and non-GTWWAC associated marks are provided on top of the bars.

Suplementary Figure 4

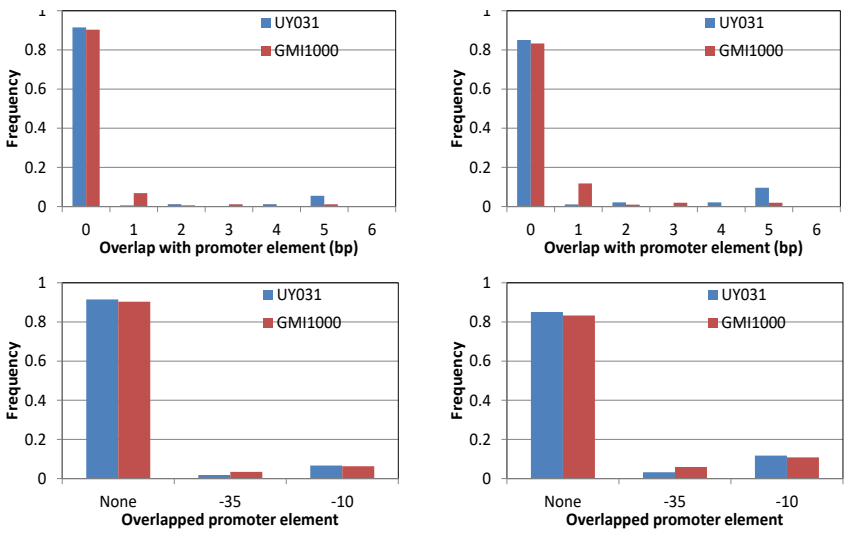

Distribution of overlaps between detected GTWWAC sites and promoters predicted using BPROM on all upstream sequences (>99 bp) containing GTWWAC sites. The plots show the distribution with respect to the amount of overlap (bp) and the type of element being overlapped (-35 or -10 region) when considering all sequences (left) or just those containing predicted promoters (right).

Due to their length, **Supplementary Tables** are only available online at:
https://www.frontiersin.org/article/10.3389/fpls.2017.00504/full#supplementary-material

Additional results

4

Additional results to publication 2

This section contains additional experimental results to the scientific publication entitled "Comparative Analysis of *Ralstonia solanacearum* Methylomes".

Effect of the MTase RSc1982 (GMI1000)/RSUY_RS11230 (UY031) in *eps* expression

The analysis of upstream regions in *R. solanacearum* GMI1000 and UY031 genomes with different methylation profiles in the GTWW**A**C motif, allowed the identification of several promoters of known genes These genes included the EpsR, an already described repressor of *eps* transcription (McWilliams et al. 1995), one of the main virulence factors in *R. solanacearum* (Denny and Baek 1991). Both strains, GMI1000 and UY031, appeared to have the same methylation pattern in the GTWW**A**C sites.

To test whether methylation of the GTWW**A**C motif in upstream gene regions could affect gene expression, the methyl-transferase (MTase) responsible for GTWW**A**C methylation was deleted in the two strains. To this end, 1 kb-flanking regions of both MTase genes were PCR amplified from genomic DNA, the kanamycin resistance gene from the pCM184 plasmid (provided by S. Genin) and the tetracycline cassette from the pG-T plasmid (Monteiro et al. 2012b). All amplifications were performed with the Platinum Pfx DNA polymerase (Thermo Fisher Scientific). Resistance cassettes were inserted between the side fragments of each gene by double-joint PCR (Yu et al. 2004). RSc1982 from *R. solanacearum* GMI1000 was replaced by kanamycin and RSUY_RS11230 from *R. solanacearum* UY031 with tetracycline after homologous recombination via natural transformation (Boucher C.A. 1985). The list of oligonucleotides used to create the two mutants are listed in Additional Table 1. To detect *eps* expression, the mutant constructions were introduced in the corresponding wild-type (WT) strain containing the *Peps::LuxCDABE* fusion.

WT and mutant strains were grown in liquid rich B medium to measure *eps* expression. Since *eps* transcription is dependent on bacterial density, a time-course experiment to monitor gene expression was performed at three different starting bacterial concentrations: 10^8, 10^7 and 10^6 CFU/ml. *Eps* expression is represented as Relative Luminescence Units (RLUs) normalized by bacterial density. As shown in Additional Figure 1, *eps* expression is not altered by the absence of the MTase in GMI1000 nor in UY031 at 10^8 nor 10^7 CFU/ml starting bacterial densities (Additional Figure 1 A,B,C,D). However, at the lowest starting cell density, *eps* expression was slightly reduced after 14 hpi in both mutants compared to their respective WT strains (Additional Figure 1 E, F). In either strain, *eps* expression was recovered to WT levels after 20 hpi.

These results suggest that the methylation state in *epsR* upstream region has an effect on *eps* gene expression at certain bacterial densities, seeming especially dramatic during exponential growth. The same behavior between GMI1000 and UY031 *eps* expression was expected, as both

strains shared the same methylation pattern. It remains to be tested, whether genes whose upstream regions show different methylation profiles in their GTWW**A**C motifs also have different expression patterns between the two *R. solanacearum* strains. Finally, this data provides a first hint of the potential epigenetic regulation on gene expression in *R. solancearum*. However, more experiments need to be performed in the future to shed more light on the implications that DNA methylation can have over virulence gene expression in this pathogen.

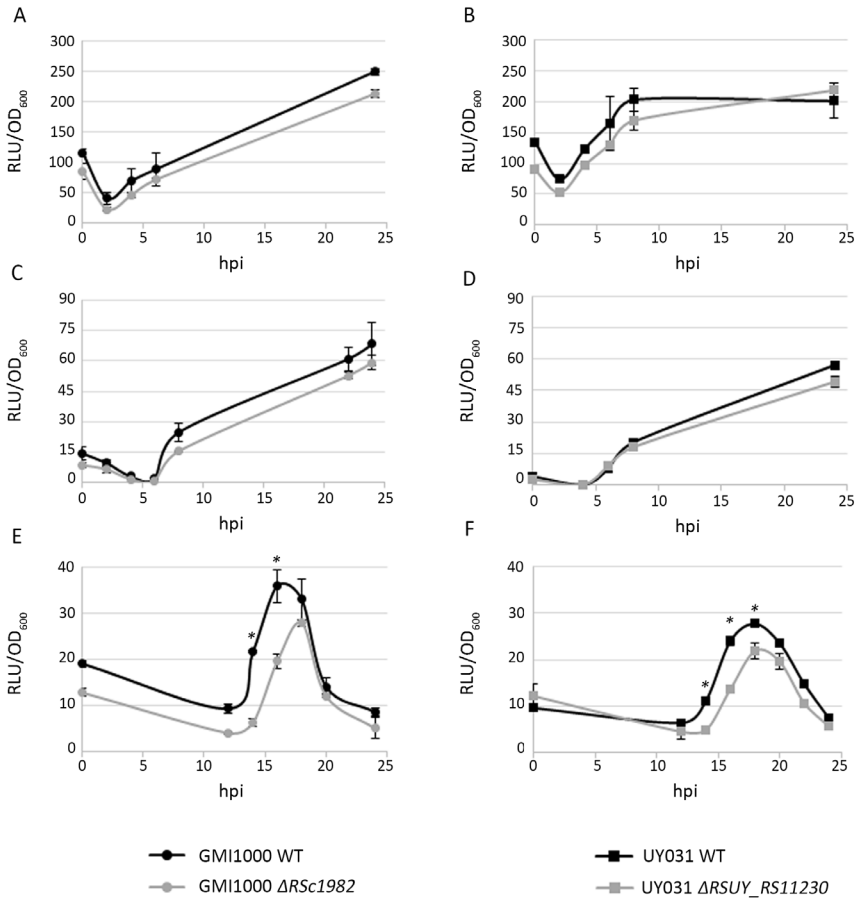

Additional Figure 1. Expression profile of the *eps* promoter in *R. solanacearum* strains GMI1000 and UY031 and their corresponding methyl-transferase mutants in rich medium.

The wild-type *R. solanacearum* strains GMI1000 (A, C, E) and UY031 (B, D, F) carrying the Peps::LuxCDABE construction (black lines) and their corresponding methylase mutants (RSc1982 and RSUY_RS11230 genes, grey lines), were grown in liquid rich B medium. Growth and luminescence were measured at different time points. Three starting bacterial concentrations were used: 10^8 CFU/ml (A,B), 10^7 CFU/ml (C,D) and 10^6 CFU/ml (E,F). Promoter activity is represented as relative luminescence units (luminometer values divided by 10^4) normalized by bacterial concentration, estimated by OD_{600}. Each value represents the average of 3 technical replicates and error bars indicate standard deviations. Time-points marked with an asterisk showed statistical reduction of *eps* expression in the MTase mutant compared to the WT. Experiments were repeated at least two times with similar results.

Additional Table 1. List of primers used to generate mutant constructs of RSc1982 and RSUY_RS11230.

Primer ID	Sequence	Properties
Tet-F2	CGTTAACCCTAGGGGATCCT	Tc cassette amplification from pG-T plasmid
Tet-R2	GCACTAGTGATTAGTACTTCAAT	
RecA-UY-F1	CATTTGATCCACAGGCCTTC	1st round PCR to amplify right-flank of RSUY_RS11230
RecA-UY-R1	CGCTGAGGATCCCCTAGGGTTAACGAACCTCTCCTATCCATGTCC	
RecB-UY-F3	CGATTGAAGTACTAATCACTAGTGCTTGCGTCAGAGCTCGATGCC	1st round PCR to amplify left-flank of RSUY_RS11230
RecB-UY-R3	GCGCCCACAAGGTGAACAAC	
nest-UY-F	GCGTTGCGACGGATCGGTCT	Nest primers for 3rd round PCR to replace RSUY_RS11230
nest-UY-R	GGGCAAGCCGCGCGTGATCG	
K-F2	TGGCGGCCGCATAACTTC	K cassette amplification from pCM184 plasmid
K-R2	AGCTGGATCCATAACTTCGTAT	
RecA-GMI-F1	CAAGCGCGAAGACCTGAACC	1st round PCR to amplify right-flank of RSc1982
RecA-GMI-R1	GCTATACGAAGTTATGCGGCCGCCAGCGTCAGAGATCGATGCCCG	
RecB-GMI-F3	ATTATACGAAGTTATGGATCCAGCTAACCTCTTCAATCCATGTCC	1st round PCR to amplify left-flank of RSc1982
RecB-GMI-R3	TCATGCGTACTCCTTGAATG	
nest-GMI-F	GGGCAAGCCGCGCGTGATC	Nest primers for 3rd round PCR to replace RSc1982
nest-GMI-R	CGAGCGCCTGGCGGATGTC	

chapter 5

PUBLICATION 3

Transcriptomes of *Ralstonia solanacearum* during Root Colonization of *Solanum commersonii*

Resum de la publicació 3

"Transcriptomes of *Ralstonia solanacearum* during Root Colonization of *Solanum commersonii*"

"Transcriptomes de *Ralstonia solanacearum* durant la colonització de l'arrel de *Solanum commersonii*"

Marina Puigvert, Rodrigo Guarischi-Sousa, Paola Zuluaga, Núria S. Coll, Alberto P. Macho, João C. Setubal i Marc Valls

Referència: Front. Plant Sci. 8:370.
doi: 10.3389/fpls.2017.00370

El marciment bacterià de les patateres, també anomenat podridura marró, és una malaltia devastadora causada pel patogen vascular *Ralstonia solanacearum* que provoca pèrdues econòmiques significatives. Com en altres interaccions planta-patogen, els primers contactes establerts entre el bacteri i la planta condicionen de forma important el resultat de la malaltia. En aquest treball s'estudia el transcriptoma de *R. solanacearum* UY031 poc després de la infecció en dues accessions de patatera salvatge, *Solanum commersonnii*, amb diferents nivells de resistència al marciment bacterià. Els ARNs total es van obtenir a partir d'arrels infectades asimptomàtiques, es van seqüenciar i se'n van recuperar per a 4609 gens dels 4778 gens anotats al genoma de la soca UY031. Només dos gens van resultar estar diferencialment expressats entre les accessions de patatera resistent i susceptible, suggerint que el component bacterià juga un paper minoritari en l'establiment de la malaltia. Per altra banda, 422 gens estaven expressats diferencialment (ED) en comparació amb els bacteris crescuts en medi ric sintètic. Només 73 d'aquests gens havien estat prèviament identificats com a ED en un transcriptoma de *R. solanacearum* a partir de bacteris extrets directament dels vasos xilemàtics de tomaqueres infectades. Alguns determinants de virulència, com per exemple el Sistema de Secreció de Tipus III i les seves proteïnes efectores, estructures de motilitat i enzims detoxificadors d'espècies reactives d'oxigen, estaven també induïts durant la infecció de *S. commersonii*. Per contra, les activitats metabòliques van resultar majoritàriament reprimides durant la colonització primerenca de l'arrel, amb l'excepció notable del metabolisme del nitrogen, la reducció del sulfat i l'absorció del fosfat. Molts gens de *R. solanacearum* identificats com a sobreexpressats durant la infecció no havien estat mai abans descrits com a factors de virulència. Aquest és el primer informe que descriu un transcriptoma de *R. solanacearum* obtingut directament de teixit infectat, així com el primer a analitzar l'expressió gènica bacteriana en les arrels, on té lloc la infecció de la planta per part d'aquest bacteri. També es demostra que el transcriptoma bacterià dins la planta pot ser estudiat inclús quan la quantitat de patogen és petita, mitjançant la seqüenciació de trànscrits de teixit infectat sense previ enriquiment d'ARN procariota.

frontiers in Plant Science

ORIGINAL RESEARCH
published: 20 March 2017
doi: 10.3389/fpls.2017.00370

Transcriptomes of *Ralstonia solanacearum* during Root Colonization of *Solanum commersonii*

Marina Puigvert[1,2], Rodrigo Guarischi-Sousa[3], Paola Zuluaga[1,2], Núria S. Coll[2], Alberto P. Macho[4], João C. Setubal[3] and Marc Valls[1,2]**

[1] Department of Genetics, University of Barcelona, Barcelona, Spain, [2] Centre for Research in Agricultural Genomics CSIC-IRTA, Autonomous University of Barcelona, Bellaterra, Spain, [3] Department of Biochemistry, University of São Paulo, São Paulo, Brazil, [4] Shanghai Center for Plant Stress Biology, CAS Center for Excellence in Molecular Plant Sciences, Shanghai Institutes of Biological Sciences, Chinese Academy of Sciences (CAS), Shanghai, China

OPEN ACCESS

Edited by:
Fabienne Vailleau, Centre Toulouse Midi-Pyrénées (INRA), France

Reviewed by:
Yasufumi Hikichi, Köchi University, Japan
Chiu-Ping Cheng, National Taiwan University, Taiwan

***Correspondence:**
João C. Setubal
joao.c.setubal@gmail.com
Marc Valls
marcvalls@ub.edu

Specialty section:
This article was submitted to Plant Microbe Interactions, a section of the journal Frontiers in Plant Science

Received: 17 January 2017
Accepted: 02 March 2017
Published: 20 March 2017

Citation:
Puigvert M, Guarischi-Sousa R, Zuluaga P, Coll NS, Macho AP, Setubal JC and Valls M (2017) Transcriptomes of Ralstonia solanacearum during Root Colonization of Solanum commersonii. Front. Plant Sci. 8:370. doi: 10.3389/fpls.2017.00370

Bacterial wilt of potatoes—also called brown rot—is a devastating disease caused by the vascular pathogen *Ralstonia solanacearum* that leads to significant yield loss. As in other plant-pathogen interactions, the first contacts established between the bacterium and the plant largely condition the disease outcome. Here, we studied the transcriptome of *R. solanacearum* UY031 early after infection in two accessions of the wild potato *Solanum commersonii* showing contrasting resistance to bacterial wilt. Total RNAs obtained from asymptomatic infected roots were deep sequenced and for 4,609 out of the 4,778 annotated genes in strain UY031 were recovered. Only 2 genes were differentially-expressed between the resistant and the susceptible plant accessions, suggesting that the bacterial component plays a minor role in the establishment of disease. On the contrary, 422 genes were differentially expressed (DE) *in planta* compared to growth on a synthetic rich medium. Only 73 of these genes had been previously identified as DE in a transcriptome of *R. solanacearum* extracted from infected tomato xylem vessels. Virulence determinants such as the Type Three Secretion System (T3SS) and its effector proteins, motility structures, and reactive oxygen species (ROS) detoxifying enzymes were induced during infection of *S. commersonii*. On the contrary, metabolic activities were mostly repressed during early root colonization, with the notable exception of nitrogen metabolism, sulfate reduction and phosphate uptake. Several of the *R. solanacearum* genes identified as significantly up-regulated during infection had not been previously described as virulence factors. This is the first report describing the *R. solanacearum* transcriptome directly obtained from infected tissue and also the first to analyze bacterial gene expression in the roots, where plant infection takes place. We also demonstrate that the bacterial transcriptome *in planta* can be studied when pathogen numbers are low by sequencing transcripts from infected tissue avoiding prokaryotic RNA enrichment.

Keywords: *Ralstonia solanacearum*, bacterial wilt, *Solanum commersonii*, RNA sequencing, transcriptomics, disease resistance, potato brown rot

INTRODUCTION

Changes in pathogen gene expression control the switch from a commensal to a parasitic relationship with the host, which may subvert the host metabolism or development to the pathogen's benefit (Stes et al., 2011). However, there is still limited information concerning how this is controlled. Understanding how these trophic relationships initiate and persist in the host requires deciphering the functional adaptations at the transcriptomic level. Pioneer studies of the expression profiles of bacterial animal pathogens in infected tissues showed that the genes induced more strongly contributed to bacterial virulence and/or survival in the host (reviewed in La et al., 2008).

Ralstonia solanacearum is the causal agent of the destructive bacterial wilt disease in tropical and subtropical crops, including tomato, tobacco, banana, peanut, and eggplant (Hayward, 1991; Peeters et al., 2013). The disease in potato is also called brown rot and is endemic in the Andean region, where potato is a staple food, causing an important impact on food production and the economy (Priou, 2004; Coll and Valls, 2013). Disease control of bacterial wilt is very challenging, because of the bacterium aggressiveness, its persistence in the field and the lack of resistant commercial varieties in any of its hosts. Potato breeding programs have used wild species related to *Solanum tuberosum*, such as *Solanum commersonii*, as sources of resistance against bacterial wilt (Kim-Lee et al., 2005; Siri et al., 2009).

As in most Gram-negative animal and plant pathogens, the major pathogenicity determinant in *R. solanacearum* is the type three secretion system (T3SS) (Boucher et al., 1987). This system injects bacterial proteins called effectors directly into the eukaryotic host cells to manipulate the host defenses and establish disease (Buttner, 2016; Popa et al., 2016a). Amongst other factors that contribute to *R. solanacearum* virulence are motility—either caused by flagella or type IV pili- and the reactive oxygen species (ROS)- detoxifying enzymes (Meng, 2013).

In vitro studies using microarrays allowed the study of *R. solanacearum* virulence gene expression and the discovery of novel regulatory networks (Occhialini et al., 2005; Valls et al., 2006). However, the first studies on gene expression *in planta* using quantitative reporters indicated that *R. solanacearum* virulence genes showed unexpected expression patterns (Monteiro et al., 2012). Contrary to what was believed based on *in vitro* studies, it was demonstrated that the genes encoding the T3SS genes and its associated effectors were transcribed *in planta* at late stages of infection (Monteiro et al., 2012). These findings were later confirmed in transcriptomic studies with *R. solanacearum* extracted from infected tomato and banana plants (Jacobs et al., 2012; Ailloud et al., 2016). However, these studies *in planta* could only be performed from heavily colonized plants, as limited pathogen biomass has hindered until recently the investigation of gene expression at the early stages of the interaction, when plants are still asymptomatic.

In a previous work, we demonstrated that rRNA-depleted RNAs obtained from infected roots could be used to determine the transcriptomic responses of *S. commersonnii* plants resistant or susceptible to bacterial wilt through RNA sequencing (Zuluaga et al., 2015). Here, we have used these sequences to extract *R. solanacearum* UY031 transcripts *in silico* and have compared them to the bacterial transcriptomes obtained in synthetic media to investigate the pathogen RNAs expressed during early infection. Our results reveal differential expression of a number of known and putative transcriptional regulators and virulence factors during early plant colonization, providing insight into their role in infection.

MATERIALS AND METHODS

Bacterial Strains, Plant Accessions, and Growth Conditions

The *R. solanacearum* isolate UY031, phylotype IIB, sequevar 1, originally isolated from potato (Siri et al., 2011), carrying the LUX-operon under the *psbA* promoter (Monteiro et al., 2012) was used for all experiments. Bacteria were routinely grown in rich B medium as described (Monteiro et al., 2012).

S. commersonnii accessions F97 (susceptible to bacterial wilt) and F118 (moderately resistant) obtained from a segregating population were used in this work and propagated *in vitro* as described (Zuluaga et al., 2015).

Sample Preparation

As a control condition, bacteria were grown for 2 days on rich solid medium without tetrazolium chloride or antibiotics at the appropriate dilution to obtain separate colonies. Bacteria were recovered from plates and mixed with 5% of an ice-cold transcription stop solution [5% (vol/vol) water-saturated phenol in ethanol]. Cells were centrifuged at 4°C for 2 min at maximum speed and the bacterial pellet was immediately frozen in liquid nitrogen.

For plant RNA samples, *S. commersonii* F97 and F118 roots were inoculated as described in Zuluaga et al. (2015). Briefly, plant roots from 2-week old plants grown in soil were injured with a 1 ml pipette tip and inoculated by soil drenching with a bacterial solution at 10^7 colony forming units (cfu)/ml. Control plants were mock-inoculated with water. After inoculation, plants were kept in a growth chamber at 28°C in long-day conditions. Luminescence quantification was used to select plants with comparable infection levels in the susceptible and the resistant accessions, corresponding to approximately 10^5 colony forming units per g of tissue (Cruz et al., 2014).

RNA Extraction, Sequencing, and Library Preparation

Total RNA from bacterial cultures was extracted using the SV Total RNA Isolation System kit (Promega) following the manufacturer's instructions for Gram-negative Bacteria. Infected plant RNA extractions were carried out as described (Cruz et al., 2014). RNA concentration and quality was measured using the Agilent 2100 Bioanalyzer. For rRNA depletion, 2.5 μg of RNA were treated with the Ribo-zero$^{(TM)}$ magnetic kit for bacteria (Epicenter). Three biological replicates per condition were subjected to sequencing on an Illumina-Solexa Genome Analyzer II apparatus in the Shanghai PSC Genomics facility using multiplexing and kits specially adapted to obtain 100 bp

paired-end reads in stranded libraries. Raw sequencing data is available in the Sequence Read Archive under the accession code SRP096020.

Read Mapping, Quantification, and Differential Gene Expression Analysis

FASTQC was used to evaluate the quality of the RNA-seq raw data. *R. solanacearum* reads were identified from total infected root sequences using Bowtie2 (version 2.2.6; Langmead and Salzberg, 2012) as described in the results section. The completely sequenced genome of strain UY031 (Guarischi-Sousa et al., 2016) was used as reference. For identification of *R. solanacearum* reads, the Burrows-Wheeler Alignment (BWA) tool was initially used. However, a high number of reads from mock-inoculated control samples mapped to the bacterial genome (**Table 1**). Visual evaluation of these mapped reads using the Integrative Genomics Viewer (IGV) tool (Robinson et al., 2011; Thorvaldsdottir et al., 2013) showed that most contained mismatches to the *R. solanacearum* genome sequence, indicating that they likely belonged to contaminating bacteria. BWA was thus assayed with more stringent parameters (-B 20-O 30-E 5-U 85), to increase penalties for mismatches, gap openings, gap extension, and unpaired read pairs, resulting in a reduction of only half of the reads mapping to the genome. Finally, Bowtie2 was assayed, once more using stringent parameters to penalize mismatches and gaps (–mp 30–rdg 25,15–rfg 25,15). In this case, mapped reads levels in mock-inoculated plants could be considered background compared to the high read numbers from inoculated samples, thus, Bowtie2 was finally used in all samples analyzed, including RNA-seq reads coming from *in vitro* grown bacteria (**Table 1**). Alignments were summarized by genes on counting tables using HTSeq-count (version 0.6.1 p1; Anders et al., 2015) and NCBI's reference annotation (genome features were extracted from NCBI's RefSeq sequences NZ_CP012687.1 and NZ_CP012688.1); alignments with quality lower than 10 were discarded. Differential expression (DE) analysis was carried out with the DESeq2 (version 1.12.3; Love et al., 2014) package in R (version 3.3.2). Benjamini–Hochberg procedure was used for multiple testing corrections. Genes with $\log_2$(fold-change) >0.5 and $q < 0.01$ were considered as differentially expressed. We used these thresholds to select for relevant and robust differentially expressed genes. Final annotation of the genome was defined based on the NCBI gene locus and the gene name and description of the reference *R. solanacearum* GMI1000 genome annotation (Supplementary Table 1).

Homology Analysis

get_homologs (version 2.0; Contreras-Moreira and Vinuesa, 2013) was used for searching *R. solanacearum* UY031 homologous genes on *R. solanacearum* GMI1000, *R. solanacearum* IPO1609 and *R. solanacearum* UW551 strains as well as in *Pseudomonas syringae* pv. syringae B728a; NCBI RefSeq sequences GCF_001299555.1, GCF_000009125.1, GCF_001050995.1, GCF_000167955.1, and GCF_000012245.1, respectively. Default algorithm of bidirectional best-hits was used on homologous genes search.

Functional Categories

R. solanacearum UY031's genes were functionally categorized using two different strategies. Firstly, functional categories from *Pseudomonas syringae* pv. *syringae* B728a as defined by Yu et al. (2013), were translated to *R. solanacearum* UY031 based on homology information between the two strains. Although the *P. syringae*-derived categories should be more specific and accurate for another bacterial plant pathogen, almost 70% of the *R. solanacearum* UY031 genes could not be classified using this method. Therefore, a second strategy based on Clusters of

TABLE 1 | Number and percentage of aligned reads to the *R. solanacearum* UY031 genome from mock-inoculated (Control) and inoculated *Solanum commersonii* accessions.

			BWA[a]		BWA_stringent[b]		Bowtie2_stringent	
Condition[c]	Replica	Total reads	Reads	%	Reads	%	Reads	%
Resistant mock-inoculated	1	83867508	110859	0.1	66083	0.1	601	0.0
	2	88913944	42040	0.0	25296	0.0	771	0.0
Resistant infected	1	71855042	348369	0.5	330968	0.5	290036	0.4
	2	96470501	943974	1.0	924297	1.0	879112	0.9
	3	23473454	249285	1.1	234153	1.0	183728	0.8
Susceptible mock-inoculated	1	100234418	70173	0.1	40797	0.0	300	0.0
	2	27594608	15060	0.1	8889	0.0	137	0.0
Susceptible infected	1	75368620	249382	0.3	232550	0.3	211561	0.3
	2	93023963	2103356	2.3	2010284	2.2	1867585	2.0
	3	24695183	518872	2.1	484873	2.0	410525	1.7

[a] *Burrows-Wheeler Alignment.*
[b] *Burrows-Wheeler Alignment using stringent parameters as described in methods.*
[c] *Samples from Zuluaga, Solé, Lu, BMC Genomics, 2015.*

Orthologous Groups (COG) categories was applied. Genome features were extracted from NCBI's RefSeq annotation and cdd2cog.pl script (version 0.1; Leimbach, 2016) was used to assign COG IDs and functional categories to the differentially expressed genes (Supplementary Table 1).

RESULTS

Obtaining *R. solanacearum* Sequences from Infected Root Tissues

cDNA libraries from rRNA-depleted RNAs isolated from *S. commersonii* roots inoculated with *R. solanacearum* were sequenced using Illumina technology as previously reported (Zuluaga et al., 2015). To generate the transcriptomic profile of the bacteria growing inside root tissues, *R. solanacearum* UY031 sequences were obtained following the pipeline detailed in **Figure 1**. First, reads from mock-inoculated plants were used as a control to determine the best alignment tool to map against the *R. solanacearum* UY031 reference genome (Guarischi-Sousa et al., 2016; see material and methods). The Bowtie2 alignment tool with stringent parameters was used, as it retained a number of *R. solanacearum* reads in mock-inoculated plants that could be considered background levels compared to the high read numbers from inoculated samples (**Table 1**). All samples were analyzed with Bowtie2, including RNA-seq reads coming from *in vitro* grown bacteria. We determined that around 1% of the total sequenced reads from plant tissues corresponded to *R. solanacearum* and these were retained for further analyses. *S. commersonnii* sequences accounted on average for 63.15% of the total reads sequenced and the remaining reads corresponded mostly to contamination by other bacterial endophytes. The retrieved bacterial sequences were quantified and differentially expressed (DE) genes comparing the different conditions were determined. Total RNAs from infected *S. commersonii* enabled transcript quantification for over 96% of *R. solanacearum* UY031 predicted genes (4,609 out of the 4,778; Guarischi-Sousa et al., 2016).

Similar *R. solanacearum* Genes Are Differentially Expressed upon Infection of Resistant and Susceptible *S. commersonii* Plants

In order to compare the *R. solanacearum* gene expression patterns during infection of resistant and susceptible wild potato

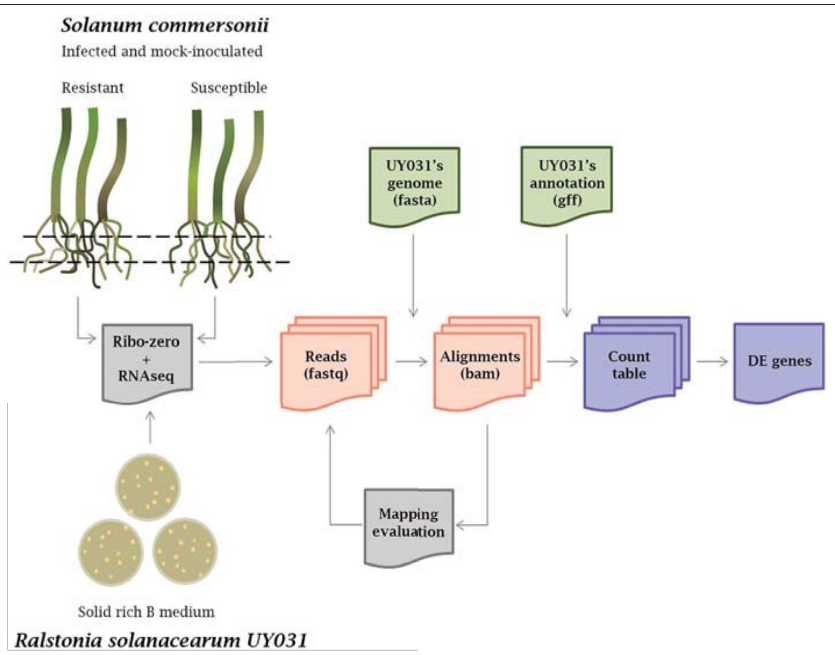

FIGURE 1 | Workflow of the transcriptomic analysis. RNAseq was carried out from roots of infected and mock-inoculated *Solanum commersonii* resistant and susceptible varieties and from bacteria grown in solid rich B medium. Three biological replicates were used for each condition. Total extracted RNAs were treated with Ribo-zero to remove rRNA and sequenced using Illumina technology. Raw reads were aligned against the *R. solanacearum* UY031 genome using different alignment tools and mapping was visually evaluated with the IGV Browser. Mapped reads were quantified using count tables and differential expression (DE) analysis was carried out.

plants, we analyzed separately the bacterial reads obtained from infected *S. commersonii* accessions F118 and F97, respectively. Surprisingly, only two out of the 4,609 genes for which expression was detected showed differential expression between the two genotypes. The differentially-expressed (DE) genes, RSUY_RS08455, and RSUY_RS16950, were both up-regulated in bacteria grown inside the resistant accession (**Table 2**). The first gene corresponds to an uncharacterized member of the MarR transcriptional regulator family, while the second encodes a hypothetical protein.

Since *R. solanacearum* showed extremely similar (>99.9%) transcriptional behavior during interaction with both *S. commersonii* accessions, bacterial reads from both accessions were treated as biological replicates in the rest of this study.

R. solanacearum Activates Stress-Related Genes and Shuts Down Metabolic Activities during Early Root Colonization

The *R. solanacearum in planta* gene expression dataset was compared to a reference condition consisting of bacteria grown on solid rich B medium. Bacteria grown on solid medium were used as the reference condition instead of liquid cultures. *R. solanacearum* colonies grown on solid media better mimic the biofilms and microcolonies formed by *R. solanacearum* during early infection, when most bacteria occupy plant intercellular spaces (Mori et al., 2016). A total of 422 genes were differentially expressed during pre-symptomatic infection (231 up-regulated and 191 down-regulated), compared to growth on rich medium (Supplementary Table 2). These DE genes were classified into the functional categories previously used for gene expression studies in the plant pathogenic bacterium *P. syringae* (Yu et al., 2013; Supplementary Table 3). The number of successfully classified genes in each category was quantified in differentially induced or repressed groups and in the whole genome as a reference (**Figure 2**). This analysis revealed four categories highly over-represented in the up-regulated genes and under-represented in down-regulated genes: stress, secretion, chemosensing, and motility and phage and insertion sequences (IS). These categories represent together approximately 20% of the total induced genes *in planta*. The opposite trend (under-representation in up-regulated and over-representation in down-regulated genes) is observed in the categories including genes for transport and metabolism of amino acids and carbohydrates. In addition, the categories replication and DNA repair, transport, fatty acid metabolism and cofactor metabolism are strongly under-represented amongst the up-regulated genes *in planta* (**Figure 2**).

We used the *P. syringae* categories because they were created to describe the genes of a bacterial plant pathogen and are thus very informative for this study. However, the same analysis was carried out using the widely used but more general COG categories, and the results confirmed the previously-described tendencies (Supplementary Figure 1). Genes involved in carbohydrate, amino acid, lipid, cofactor, and secondary metabolism were over-represented among those down-regulated *in planta*. A clear enrichment of replication, cell motility and recombination and repair (where IS elements are included) was observed in the up-regulated genes. Interestingly, a clear asymmetry was seen for unclassified genes in this case, for they represent 40% of the up-regulated but only 7% of the down-regulated genes.

Closer scrutiny of the up-regulated genes in the plant revealed that the category secretion included 11 genes encoding the T3SS and its associated effectors and four chemosensing and motility genes, coding for pilus assembly and flagellum transcriptional activators (**Table 3**).

Taken together, these results show a major induction of stress-related activities and an inhibition of the central metabolism when the bacterium grows *in planta* compared to synthetic media.

R. solanacearum Virulence Genes Are Differentially Expressed in Wild Potato Roots

Among the 422 genes DE during *S. commersonii* root colonization, 34% (80 induced and 65 repressed genes) had been identified in previous studies analyzing gene expression of *R. solanacearum* cells recovered from infected plant stems (see references below). Notably, 73 genes were also DE in microarray analyses of *R. solanacearum* UW551 -a phylotype IIB strain highly similar to UY031- isolated from tomato (Jacobs et al., 2012). Also, 42 genes have been shown to be induced in a temperature-dependent manner when bacteria grew in tomato xylem or rhizosphere (Bocsanczy et al., 2014; Meng et al., 2015). In addition, 31 DE genes (most of them induced *in planta*) are part of either the HrpB or HrpG regulons, which are known to trigger expression of the T3SS and other virulence genes in response to direct plant cell contact (Valls et al., 2006).

Amongst the *R. solanacearum* genes induced during plant colonization, 31 encode already reported virulence traits (**Table 3**). As expected, genes encoding the T3SS (*hrpY*, *hrpX*, *hrpK*, *hrcT)* and some of its related effectors *(ripV2*, *popC*, ripD, *popF1*, *awr5_1*, *popB,* and *popA*) were induced inside the

TABLE 2 | *R. solanacearum* UY031 genes differentially expressed in resistant vs. susceptible *S. commersonii*.

UY031 NCBI locus[a]	UY031 Prokka locus[b]	GMI1000 locus[c]	Gene product	Log_2FC	Adjusted *p*-value
RSUY_RS08455	*RSUY_17320*	*RSc1295*	MarR family transcriptional regulator	2.37	0.0004
RSUY_RS16950	*RSUY_34650*	*RSp0403*	hypothetical protein	2.53	0.0017

[a] *According to R. solanacearum UY031 genome annotation available at GenBank (NCBI).*
[b] *According to R. solanacearum UY031 genome annotation from Guarischi-Sousa et al. (2016).*
[c] *According to the homology Supplementary Table 1.*

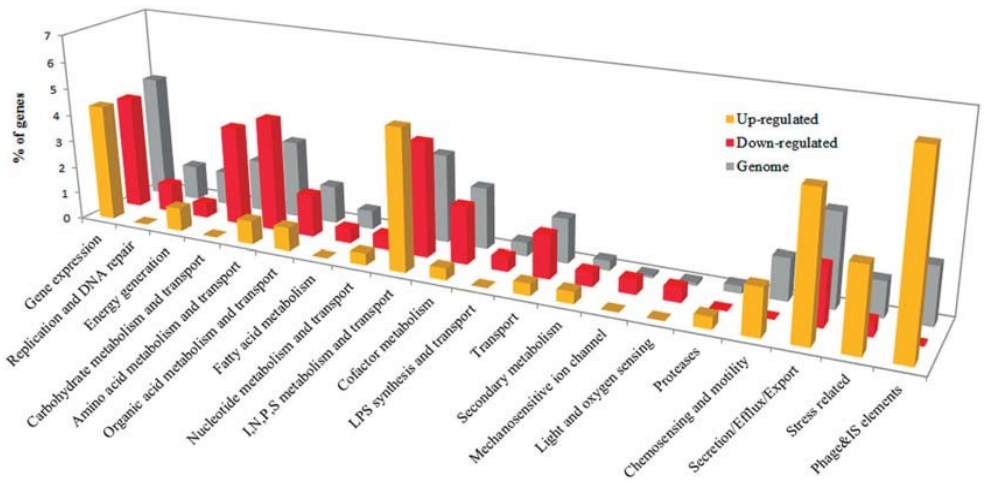

FIGURE 2 | Percentage of DE genes classified into *Pseudomonas syringae*-derived functional categories (Yu et al., 2013). Genes DE between growth *in planta* vs. rich medium were classified according to the functional categories described for *P. syringae* (Yu et al., 2013). Categories were grouped by function similarity for better visualization (Supplementary Table 4). As a reference, functional category distribution considering all annotated genes in the UY031 genome is shown.

plant (Boucher et al., 1987; Cunnac et al., 2004). Motility and adherence genes were also up-regulated, including type IV pili (*pilG*, *pilH*, *pilN*, *pilM*, *pilY*, *pilW*, and *fimV*), as well as the transcriptional activators of the flagellum genes *flhC* and *flhD* (Kang et al., 2002; Tans-Kersten et al., 2004). Other induced genes encoding described factors that are key for bacterial virulence included *hdfA* (Delaspre et al., 2007), *efe* (Valls et al., 2006), *metE* (Plener et al., 2012), and *rpoN1* (Lundgren et al., 2015; Ray et al., 2015; **Table 3**). Peroxidases, catalases (*katE, katG*) and alkyl hydroperoxide reductases (*ahpC1, ahpF*), which have been described to combat the oxidative stress response during plant infection (Rocha and Smith, 1999; Flores-Cruz and Allen, 2009; Ailloud et al., 2016) were also induced. Similarly, the flavohemoprotein *hmpX*, involved in NO-detoxification (Dalsing and Allen, 2014), was also induced.

In contrast, only 10 reported virulence determinants were down-regulated, including the type III effectors *ripQ, ripS2,* and *ripTPS,* the quorum sensing regulator *solI* (Flavier et al., 1997) and the Type II secretion system genes *gspE, gspJ* (**Table 3**).

R. solanacearum Genes for Plant Colonization Are Differentially Expressed in *S. commersonii* Roots

Thirty-six *R. solanacearum* genes previously described as related to plant colonization in gene expression studies in other plant species were also induced in potato. Few metabolic genes were induced *in planta*, being an exception *nadB2*, involved in the degradation of L-aspartate in the xylem (Brown and Allen, 2004) and the *ptsN* and *narL* nitrogen metabolism genes, known to be active during plant colonization (Dalsing and Allen, 2014; Dalsing et al., 2015; **Table 3**).

Amongst the down-regulated genes, 42 had also been described as specifically down-regulated during plant colonization (Jacobs et al., 2012). Most repressed genes encoded metabolic enzymes and transporters. Examples are the xylose transporters *xylF, xylG,* and *xylH*, glycine catabolism genes *gcvP*, *gcvT,* and *gcvA*, the adenilate cyclase coding gene RSUY_RS02845, four siderophore biosynthesis genes and 11 genes involved in amino acid metabolism (**Table 3**). Also, the stress response gene *speE2* and five transcriptional and response regulators were repressed *in planta.*

Novel Putative Virulence Genes and Metabolic Traits Involved in Early Stages of Wild Potato Infection by *R. solanacearum*

Transcriptomic analysis of *S. commersoni* early root infection revealed highly induced *R. solanacearum* virulence factors still uncharacterized in this pathogen that may play a role at this stage of the interaction with the host. An example of this is *suhB,* a global virulence regulator controlling the type III and type VI secretion systems, flagellum biosynthesis, and biofilm formation in the human pathogens *Burkholderia cenocepacia* and *Pseudomonas aeruginosa* (Rosales-Reyes et al., 2012; Li et al., 2013). Similarly, a *P. aeruginosa* orthologue of the *in planta* induced type IV secretion gene Rhs has been described as a virulence determinant (Kung et al., 2012).

Metabolic traits that might be key at this point of plant infection are the assimilatory sulfate reduction pathway and phosphate mobilization, since *cysD, cysN,* and *cysI* (sulfate

TABLE 3 | *R. solanacearum* UY031 genes differentially expressed in potato roots vs. solid rich medium.

Function	UY031 NCBI locus[a]	UY031 Prokka locus[b]	GMI1000 locus[c]	Log_2FC	Gene name	Gene product
***RALSTONIA SOLANACEARUM* VIRULENCE GENES**						
Type III secretion system and effectors	RSUY_RS19685	RSUY_40420	RSp0855	7.80	*hrpY*	Type III secretion system protein HrpY
	RSUY_RS19795	RSUY_40640	RSp0877	4.66	*popA*	Type III effector protein PopA
	RSUY_RS19790	RSUY_40630	RSp0876	4.27	*popB*	Type III effector protein PopB
	RSUY_RS20380	RSUY_41860	RSp1024	3.96	*awr5_1*	Type III effector protein AWR5
	RSUY_RS22080	RSUY_45370	RSp0900	3.94	*popF1*	Type III effector protein PopF1
	RSUY_RS16550	RSUY_33840	RSp0304	3.76	*ripD*	Type III effector protein RipD
	RSUY_RS19785	RSUY_40620	RSp0875	3.35	*popC*	Type III effector protein PopC
	RSUY_RS19735	RSUY_40520	RSp0865	3.08	*hrpK*	Type III secretion system protein HrpK
	RSUY_RS19690	RSUY_40430	RSp0856	2.86	*hrpX*	Type III secretion system protein HrpX
	RSUY_RS19770	RSUY_40590	RSp0872	2.69	*hrcT*	HrcT family type III secretion system export apparatus protein
	RSUY_RS09370	RSUY_19160	–	2.44	*ripV2*	Type III effector protein RipV2
	RSUY_RS19150	RSUY_39290	RSp0731	−2.61	*ripTPS*	Trehalose-6-phosphate synthase
	RSUY_RS21730	RSUY_44630	RSp1374	−2.88	*ripS2*	Type III effector protein SKWP2
	RSUY_RS21610	RSUY_44390	RSp1277	−3.50	*ripQ*	Type III effector protein RipQ
Motility	RSUY_RS04635	RSUY_09450	RSc0727	3.14	*pilV*	Type IV pilus modification protein PilV
	RSUY_RS22435	RSUY_46110	RSp1412	2.65	*flhC*	Transcriptional activator FlhC
	RSUY_RS02415	RSUY_04970	RSc2974	2.62	*pilN*	Tfp pilus assembly protein PilN
	RSUY_RS22440	RSUY_46120	RSp1413	2.47	*flhD*	Flagellar transcriptional activator FlhD
	RSUY_RS04630	RSUY_09440	RSc0726	2.30	*pilW*	Pilus assembly protein PilW
	RSUY_RS02410	RSUY_04960	RSc2975	2.28	*pilM*	Pilus assembly protein PilM
	RSUY_RS04330	RSUY_08850	RSc0668	2.20	*pilG*	Two-component system response regulator
	RSUY_RS04335	RSUY_08860	RSc0669	1.95	*pilH*	Two-component system response regulator
	RSUY_RS11250	RSUY_22930	RSc1986	1.24	*fimV*	Tfp pilus assembly protein FimV
	RSUY_RS04590	RSUY_09370	RSc0718	−3.56	*pilY*	Pilus assembly protein PilY
Stress responses	RSUY_RS22220	RSUY_45660	RSp1581	3.16	*katE*	Catalase katE
	RSUY_RS00425	RSUY_00900	RSc3398	3.10	*hmpX*	flavohemoprotein
	RSUY_RS17495	RSUY_35830	RSp0245	2.64	*ahpC1*	Peroxiredoxin
	RSUY_RS17500	RSUY_35840	RSp0246	2.21	*ahpF*	Alkyl hydroperoxide reductase subunit F
	RSUY_RS04770	RSUY_09720	RSc0754	1.96	–	Peroxidase
	RSUY_RS04870	RSUY_09930	RSc0775	1.82	*katGb*	Catalase katGb
	RSUY_RS01185	RSUY_02450	RSc3254	−3.11	–	alkyl hydroperoxide reductase
Other virulence factors	RSUY_RS18925	RSUY_38830	RSp0676	3.71	*metE*	Methionine synthase II (cobalamin-independent)
	RSUY_RS01465	RSUY_03030	RSp0693	3.38	*hdfA*	Dioxygenase
	RSUY_RS14015	RSUY_28660	RSc0408	2.22	*rpoN1*	RNA polymerase sigma-54 factor

(Continued)

TABLE 3 | Continued

Function	UY031 NCBI locus[a]	UY031 Prokka locus[b]	GMI1000 locus[c]	Log_2FC	Gene name	Gene product
	RSUY_RS17795	RSUY_36440	RSp1529	1.72	*efe*	2-oxoglutarate-dependentethylene/succinate-forming enzyme
	RSUY_RS04455	RSUY_09100	RSc0693	−2.19	*kdtA*	3-deoxy-D-manno-octulosonic-acid transferase
Type II Secretion System	RSUY_RS01675	RSUY_03470	RSc3109	−2.63	*gspJ*	General secretion pathway protein GspJ
	RSUY_RS16275	RSUY_33280	RSp0148	−3.19	*gspE*	General secretion pathway protein GspE
Type VI secretion system	RSUY_RS19215	RSUY_39440	RSp0746	2.25	–	Type VI secretion protein
Cofactor metabolism and transport	RSUY_RS04050	RSUY_08280	RSc2633	−2.92	*pabB*	aminodeoxychorismate synthase component I
Quorum sensing	RSUY_RS01010	RSUY_02100	RSc3286	−3.24	*solI*	Acyl-homoserine-lactone synthase
***RALSTONIA SOLANACEARUM* GENES INVOLVED IN PLANT COLONIZATION**						
Aminoacid metabolism	RSUY_RS21930	RSUY_45070	RSp1263	2.019462	*nadB2*	L-aspartate oxidase
	RSUY_RS04790	RSUY_09760	RSc0758	1.900185	–	Tryptophan 2,3-dioxygenase 1
	RSUY_RS01705	RSUY_03530	RSc3103	−1.93219	–	4-hydroxyphenylpyruvate dioxygenase
	RSUY_RS00955	RSUY_01990	RSc3295	−1.97096	*gcvP*	glycine dehydrogenase
	RSUY_RS00965	RSUY_02010	RSc3293	−2.1387	*gcvT*	aminomethyltransferase
	RSUY_RS08880	RSUY_18160	RSc1381	−2.22786	–	glutathione ABC transporter permease GsiC
	RSUY_RS02965	RSUY_06080	RSc2867	−2.45751	*dppD1*	peptide ABC transporter substrate-bindingprotein
	RSUY_RS19000	RSUY_38980	RSp0691	−2.63642	*hmgA*	homogentisate 1,2-dioxygenase
	RSUY_RS08860	RSUY_18120	RSc1377	−2.72373	–	transcriptional regulator
	RSUY_RS00950	RSUY_01980	RSc3296	−2.82715	*sdaA2*	L-serine ammonia-lyase / L-serine ammonia-lyase
	RSUY_RS18995	RSUY_38970	RSp0690	−2.93699	*hmgB*	fumarylacetoacetase
	RSUY_RS08895	RSUY_18190	RSc1384	−3.10843	–	D-aminopeptidase
	RSUY_RS08865	RSUY_18130	RSc1378	−3.44342	–	isoaspartyl peptidase
Carbohydrate metabolism	RSUY_RS22935	RSUY_47230	RSp1633	−1.90617	*xylF*	D-xylose ABC transporter substrate-bindingprotein
	RSUY_RS22945	RSUY_47250	RSp1635	−2.40016	*xylH*	xylose ABC transporter permease
	RSUY_RS21965	RSUY_45140	RSp1270	−2.4781	–	glycosyl hydrolase
	RSUY_RS22940	RSUY_47240	RSp1634	−2.98048	*xylG*	D-xylose ABC transporter ATP-binding protein
	RSUY_RS17060	RSUY_34910	RSp0423	−3.65067	–	aldolase
	RSUY_RS22950	RSUY_47260	RSp1636	−4.75552	–	NAD-dependent dehydratase
Transcriptional and response regulators	RSUY_RS08455	RSUY_17320	RSc1295	4.365537	–	MarR family transcriptional regulator
	RSUY_RS22955	RSUY_47270	RSp1637	−1.62836	–	LacI family transcriptional regulator
	RSUY_RS06090	RSUY_12470	RSc2209	−1.75486	–	LysR family transcriptional regulator
	RSUY_RS00225	RSUY_00480	RSc0040	−2.26596	–	two-component system response regulator
	RSUY_RS00910	RSUY_01900	RSc3301	−2.57757	*putA*	trifunctional transcriptional regulator
Siderophore biosynthesis	RSUY_RS17055	RSUY_34900	RSp0422	−2.30463	–	siderophore biosynthesis protein
	RSUY_RS03590	RSUY_07350	RSc2729	−2.4997	–	membrane protein / membrane protein

(Continued)

TABLE 3 | Continued

Function	UY031 NCBI locus[a]	UY031 Prokka locus[b]	GMI1000 locus[c]	Log_2FC	Gene name	Gene product
	RSUY_RS17040	RSUY_34870	RSp0419	−2.75083	–	siderophore biosynthesis protein
	RSUY_RS17050	RSUY_34890	RSp0421	−2.94313	–	siderophore biosynthesis protein
Nitrogen metabolism	RSUY_RS14025	RSUY_28680	RSc0406	2.27	*ptsN*	PTS IIA-like nitrogen-regulatory protein PtsN
	RSUY_RS17995	RSUY_36860	RSp0980	2.24	*narL*	DNA-binding response regulator
	RSUY_RS11470	RSUY_23380	RSc2031	−3.3167	*ureE*	urease accessory protein UreE
Transporters	RSUY_RS20760	RSUY_42660	RSp1283	2.005142	–	porin
	RSUY_RS11090	RSUY_22610	RSc1951	−2.22	–	cation acetate symporter
	RSUY_RS22930	RSUY_47220	RSp1632	−2.42488	*oprB*	porin
	RSUY_RS05795	RSUY_11880	RSc2274	−2.96894	*ragC*	Cation efflux protein
Organic acid metabolism	RSUY_RS19540	RSUY_40110	RSp0826	3.403389	–	5-dehydro-4-deoxyglucarate dehydratase
	RSUY_RS19480	RSUY_39990	RSp0814	2.44631	*mqo*	malate:quinone oxidoreductase
	RSUY_RS11960	RSUY_24410	RSc2358	−1.7429	*ppc*	phosphoenolpyruvate carboxylase
Proteases	RSUY_RS12475	RSUY_25460	RSc2465	2.359347	*clpS*	ATP-dependent Clp protease adaptor ClpS
	RSUY_RS18550	RSUY_38040	RSp0603	2.211049	–	serine protease
	RSUY_RS14120	RSUY_28870	RSc0388	−1.98903	–	zinc protease
Lipid metabolism	RSUY_RS17295	RSUY_35410	–	2.478807	–	Acyl-CoA synthetase
	RSUY_RS01975	RSUY_04090	RSc3052	−2.40887	*glpK*	glycerol kinase
Energy	RSUY_RS08510	RSUY_17430	RSc1305	3.640811	*fpr*	ferredoxin–NADP(+) reductase
	RSUY_RS08360	RSUY_17120	RSc1276	3.417949	–	cytochrome c oxidase, cbb3-type subunit I
Signal transduction	RSUY_RS23055	RSUY_47460	RSc0617	1.988909	–	signal peptidase
	RSUY_RS01700	RSUY_03520	RSc3104	1.73953	–	calcium sensor EFh
Stress related	RSUY_RS13090	RSUY_26760	RSc0582	2.610905	–	avrD-like protein
	RSUY_RS21705	RSUY_44580	RSp1306	−2.11404	*speE2*	spermidine synthetase
Cofactor metabolism and transport	RSUY_RS02845	RSUY_05840	RSc2886	−2.57058	–	adenylate cyclase
Recombination and repair	RSUY_RS07890	RSUY_16140	RSc1189	−2.09233	–	recombinase RecB
Translation	RSUY_RS15445	RSUY_31580	RSc0085	−2.70405	*cca*	multifunctional CCA protein
Hypothetical proteins	RSUY_RS19605	RSUY_40240	–	4.758974	–	hypothetical protein
	RSUY_RS17575	RSUY_35990	RSp0261	4.146986	–	membrane protein
	RSUY_RS16950	RSUY_34650	RSp0403	3.74634	–	hypothetical protein
	RSUY_RS22040	RSUY_45290	RSp0982	3.589851	–	hypothetical protein

(Continued)

TABLE 3 | Continued

Function	UY031 NCBI locus[a]	UY031 Prokka locus[b]	GMI1000 locus[c]	Log_2FC	Gene name	Gene product
	RSUY_RS12885	RSUY_26330	RSc0613	3.409348	–	hypothetical protein
	RSUY_RS08290	RSUY_16960	RSc1262	3.394474	–	hypothetical protein
	RSUY_RS06775	RSUY_13900	RSc0971	3.025981	–	hypothetical protein
	RSUY_RS20375	RSUY_41850	–	3.019263	–	hypothetical protein
	RSUY_RS01105	RSUY_02290	RSc3270	2.806237	–	hypothetical protein
	RSUY_RS15470	RSUY_31630	RSc0080	2.792044	–	hypothetical protein
	RSUY_RS14600	RSUY_29830	RSc0297	2.641501	–	hypothetical protein
	RSUY_RS05760	RSUY_11810	RSc2280	2.552951	–	hypothetical protein
	RSUY_RS10215	RSUY_20850	RSc1622	2.233892	–	hypothetical protein
	RSUY_RS12820	RSUY_26200	–	2.213444	–	hypothetical protein
	RSUY_RS22015	RSUY_45240	RSp1546	2.185718	–	hypothetical protein
	RSUY_RS01435	RSUY_02950	RSc0616	2.148496	–	hypothetical protein
	RSUY_RS06705	RSUY_13730	RSc0953	2.116755	–	hypothetical protein
	RSUY_RS01875	RSUY_03890	RSc3072	2.098485	–	hypothetical protein
	RSUY_RS04190	RSUY_08560	RSc2555	1.909667	–	membrane protein
	RSUY_RS05940	RSUY_12170	RSc2238	1.775776	–	hypothetical protein
	RSUY_RS04990	RSUY_10170	RSc0799	−1.56204	–	hypothetical protein
	RSUY_RS02135	RSUY_04410	RSc3030	−2.05111	–	hypothetical protein
	RSUY_RS20585	RSUY_42270	–	−2.22451	–	membrane protein
	RSUY_RS14980	RSUY_30600	RSc0211	−2.4077	–	membrane protein
	RSUY_RS17045	RSUY_34880	RSp0420	−2.58002	–	membrane protein
	RSUY_RS15175	RSUY_31000	RSc0146	−2.83465	–	hypothetical protein
PUTATIVE VIRULENCE GENES AND PLANT COLONIZATION METABOLIC ACTIVITIES						
Transporters	RSUY_RS00490	RSUY_01050	RSc3386	3.50	–	metal ABC transporter substrate-binding protein
	RSUY_RS17605	RSUY_36050	RSp0429	3.24	–	MFS transporter
	RSUY_RS20020	RSUY_41100	RSp0931	2.92	–	ABC transporter
	RSUY_RS19045	RSUY_39070	RSp0706	−1.77	–	metal-dependent hydrolase
	RSUY_RS18205	RSUY_37320	RSp0481	−2.03	–	ABC transporter substrate-binding protein
	RSUY_RS18195	RSUY_37300	RSp0479	−2.09	–	amino acid ABC transporter ATPase
	RSUY_RS21220	RSUY_43600	RSp1181	−2.11	–	transporter
	RSUY_RS18895	RSUY_38770	RSp0670	−2.14	–	acriflavine resistance protein B / transporter protein
	RSUY_RS17425	RSUY_35690	RSp0234	−2.37	–	MFS transporter
	RSUY_RS09885	RSUY_20190	RSc1738	−2.40	–	ABC transporter ATPbinding protein
	RSUY_RS21615	RSUY_44400	RSp1278	−2.49	–	MFS transporter
	RSUY_RS21315	RSUY_43800	RSp1200	−2.60	–	RND transporter
	RSUY_RS03020	RSUY_06190	RSc2856	−2.72	–	MFS transporter
	RSUY_RS01560	RSUY_03230	RSc3134	−2.94	–	MFS transporter
	RSUY_RS06940	RSUY_14230	RSc1002	−2.95	–	membrane protein

(Continued)

TABLE 3 | Continued

Function	UY031 NCBI locus[a]	UY031 Prokka locus[b]	GMI1000 locus[c]	Log_2FC	Gene name	Gene product
	RSUY_RS15855	RSUY_32410	–	−2.98	*oprM*	RND transporter
	RSUY_RS20395	RSUY_41890	–	−2.99	*ybtP*	ABC transporter ATP-binding protein
	RSUY_RS15985	RSUY_32660	RSp0078	−3.05	–	MFS transporter
	RSUY_RS18200	RSUY_37310	RSp0480	−3.17	–	amino acid ABC transporter permease
	RSUY_RS19050	RSUY_39080	RSp0707	−3.19	–	ABC transporter ATP-binding protein
	RSUY_RS21055	RSUY_43260	RSp1114	−3.35	–	RND transporter
	RSUY_RS01890	RSUY_03920	RSc3069	−3.50	–	MFS transporter
	RSUY_RS22255	RSUY_45730	RSp1595	−3.73	–	ABC transporter ATP-binding protein
	RSUY_RS04055	RSUY_08290	RSc2632	−3.85	–	ABC transporter ATP-binding protein
Lipid metabolism	RSUY_RS14075	RSUY_28780	RSc0396	3.29	*ipk*	4-diphosphocytidyl-2C-methyl-D-erythritolkinase
	RSUY_RS10705	RSUY_21830	RSc1540	3.14	–	acyltransferase
	RSUY_RS19325	RSUY_39670	–	2.15	–	Phosphatidylserine/phosphatidylglycerophosphate/cardiolipin synthase
	RSUY_RS09620	RSUY_19650	RSc1772	−2.06	–	alpha/beta hydrolase
	RSUY_RS14790	RSUY_30210	RSc0262	−2.17	–	glyoxylate/hydroxypyruvate reductase A
	RSUY_RS00675	RSUY_01440	RSc3346	−2.24	–	alpha/beta hydrolase
	RSUY_RS13905	RSUY_28430	RSc0427	−2.30	–	beta-ketoacyl-[acyl-carrier-protein] synthaseII
	RSUY_RS09090	RSUY_18590	–	−2.77	–	Lysophospholipase
	RSUY_RS01035	RSUY_02150	RSc3283	−2.82	*glxR*	2-hydroxy-3-oxopropionate reductase
	RSUY_RS10955	RSUY_22330	RSc1874	−2.82	–	NUDIX hydrolase
	RSUY_RS14265	RSUY_29170	RSc0357	−2.86	*gpsA*	glycerol-3-phosphate dehydrogenase (NAD(P)(+))
	RSUY_RS11775	RSUY_23990	RSc2091	−3.04	–	ABC transporter permease
	RSUY_RS15945	RSUY_32580	RSp0036	−3.05	–	acyl-CoA dehydrogenase
	RSUY_RS21855	RSUY_44890	RSp1245	−3.30	–	esterase
	RSUY_RS20415	RSUY_41930	–	−3.31	–	Acyl-coenzyme A synthetase
	RSUY_RS21590	RSUY_44350	–	−3.32	–	Dehydrogenases
	RSUY_RS20425	RSUY_41950	–	−3.60	–	Polyketide synthase
	RSUY_RS14720	RSUY_30070	RSc0275	−3.61	–	short-chain dehydrogenase
	RSUY_RS10105	RSUY_20630	RSc1643	−4.27	*ispD*	2-C-methyl-D-erythritol 4-phosphatecytidylyltransferase
Other putative virulence factors	RSUY_RS16085	RSUY_32860	RSp0112	2.09	–	carbonic anhydrase
	RSUY_RS00735	RSUY_01550	RSp0085	1.66	–	type IV secretion protein Rhs
	RSUY_RS00905	RSUY_01890	RSc3302	−2.04	*priA*	primosomal protein N'
	RSUY_RS15535	RSUY_31760	RSc0068	−2.06	*smf*	DNA processing protein DprA
	RSUY_RS14955	RSUY_30550	RSc0222	−2.29	*rtcR*	Fis family transcriptional regulator
	RSUY_RS17190	RSUY_35180	RSp0181	−3.10	–	activator of HSP90 ATPase
	RSUY_RS14940	RSUY_30520	RSc0226	−3.23	*rtcA*	RNA 3'-terminal phosphate cyclase
Sulfur metabolism and transport	RSUY_RS12265	RSUY_25040	RSc2425	3.22	*cysI1*	Sulfite reductase/sulfite reductase
	RSUY_RS07020	RSUY_14390	RSc1019	2.23	*nifS*	Cysteine desulfurase IscS

(Continued)

TABLE 3 | Continued

Function	UY031 NCBI locus[a]	UY031 Prokka locus[b]	GMI1000 locus[c]	Log_2FC	Gene name	Gene product
	RSUY_RS12250	RSUY_25010	RSc2422	2.14	*cysD*	Sulfate adenylyltransferase small subunit
	RSUY_RS12245	RSUY_25000	RSc2421	1.89	*cysN*	Sulfate adenylyltransferase
	RSUY_RS07025	RSUY_14400	RSc1020	1.60	*nifU*	Iron-sulfur cluster scaffold-like protein
	RSUY_RS17845	RSUY_36540	RSp1519	−3.36	–	Membrane protein
Cofactor metabolism and transport	RSUY_RS11705	RSUY_23850	RSc2077	1.85	*ilvI*	acetolactate synthase
	RSUY_RS18660	RSUY_38270	RSp0615	−2.97	*cbiA*	cobyrinic acid a,c-diamide synthase
	RSUY_RS18690	RSUY_38330	RSp0621	−2.97	*cbiL*	precorrin-2 C(20)-methyltransferase
	RSUY_RS18680	RSUY_38310	RSp0619	−3.00	*cbiG*	cobalamin biosynthesis protein CbiG
	RSUY_RS03905	RSUY_07990	RSc2663	−3.51	–	ATP:cob(I)alamin adenosyltransferase
Phosphate mobilization	RSUY_RS10765	RSUY_21950	RSc1529	2.01	*pstS1*	phosphate ABC transporter substrate-bindingprotein PstS
	RSUY_RS07715	RSUY_15790	RSc1160	1.63	*suhB*	Inositol monophosphatase
	RSUY_RS10750	RSUY_21920	RSc1532	1.52	*pstB*	phosphate ABC transporter ATP-binding protein

[a] *According to R. solanacearum UY031 genome annotation available at GenBank (NCBI).*
[b] *According to R. solanacearum UY031 genome annotation from Guarischi-Sousa et al. (2016).*
[c] *According to the homology Supplementary Table 1.*

reduction) and *pstB* and *pstS1* (phosphate mobilization) were induced during *S. commersonii* root infection. Also, carbonic anhydrase (*RSUY_RS16085*), which plays a role in disease establishment between potato and *Phytophthora infestans* (Restrepo et al., 2005), was also found to be up-regulated in the *R. solanacearum* interaction with wild potato.

The most important category amongst the *R. solanacearum* genes down-regulated in *S. commersonii* with so far no assigned functions in plant colonization or virulence was metabolite transporters. Almost half of these corresponded to the ABC-family, including five amino acid transporters. In contrast, the seven major facilitator superfamily (MFS) transporters found in this category are involved with carbohydrate transport. The rest of genes were classified as permeases or RND (Resistance-Nodulation-Division) efflux systems (**Table 3**). The major metabolic activities identified as repressed in planta for the first time were lipid mobilization and cofactor metabolism, such as the anaerobic cobalamin biosynthesis operon (*cbiA*, *cbiG,* and *cbiL*), and stress-response genes such as *rtcA* and *rtcR*, involved in RNA repair (Das and Shuman, 2013).

In sum, our work reflects important gene expression changes between parasitic life and growth in rich medium (see below). This was corroborated by the fact that seven genes annotated as response regulators were also DE, five of them induced (**Table 3**).

DISCUSSION

Some *R. solanacearum* Virulence and Stress-Responsive Genes are Induced Irrespective of the Plant Host

1/3 of the *R. solanacearum* genes DE during potato infection had been also found DE when the bacterium colonized other plant species and many of these correspond to virulence determinants. For instance, we found that genes encoding the type III secretion system and its associated effectors (*popA*, *popB*, *popC*, *popF1*, *ripD*, *ripV2*, and *awr5_1*) were induced in potato (**Table 3**). Except for *awr5_1*, all these effectors had already been described as up-regulated when the bacterium grew in tomato and in melon (Ailloud et al., 2016), likely indicating that they are part of the minimal gene set required for bacterial virulence. Similarly, the effector *ripTPS* was down-regulated both in potato (**Table 3**) and during the interaction with melon (Ailloud et al., 2016). Also sharing similar up-regulation in potato (**Table 3**) and tomato are the transcriptional activators *flhC* and *flhD* (Jacobs et al., 2012), which regulate flagellum-encoding genes (Tans-Kersten et al., 2004) and the nitrogen metabolism genes *narL, ptsN*, and *hmpX* (Dalsing and Allen, 2014; Dalsing et al., 2015), implying that they all play a key role during plant infection. Additional genes induced during potato colonization had been described as key for virulence on other plant hosts, including small molecule *hdfA* (Delaspre et al., 2007), the ethylene forming enzyme *efe* (Valls et al., 2006), the methionine metabolism gene *metE* (Plener et al., 2012) and the alternative sigma factor *rpoN1* (Lundgren et al., 2015; Ray et al., 2015). These factors may be also considered essential for growth *in planta*, irrespective of the infected species.

Several transposable elements had been identified in an *in vivo* screening for genes expressed during *R. solanacearum* growth in tomato plants (Brown and Allen, 2004), and we found 16 transposases up-regulated in potato (**Table 3**). This may reflect common stressing conditions in various plant hosts, as stress is known to turn on transcription of transposable elements in various organisms (Capy et al., 2000). Oxidative stress seems also a condition generally encountered by *R. solanacearum* in plant tissues, as peroxidases, catalases, and peroxiredoxins, required for the bacterium to combat this stress in different plants (Rocha and Smith, 1999; Flores-Cruz and Allen, 2009; Ailloud et al., 2016), were also induced in potato.

Changes in the Host Environment and/or the Disease Stage May Account for Opposing Bacterial Virulence Gene Expression in Different Plants

Some of the *R. solanacearum* virulence genes DE in potato showed opposite trends in other host plants. *ripQ* and *ripS2, two* of the three type III secreted effectors inhibited in potato were, respectively, upregulated and not DE in melon, tomato and banana (Ailloud et al., 2016). Interestingly, these two downregulated effectors, together with the also repressed stress response gene *speE2,* are located in a genomic region that is deleted in the avirulent *R. solanacearum* strain UY043 (Siri et al., 2014), which suggests their involvement in bacterial virulence. Similarly, the effector *awr5_1*, which was described to trigger hypersensitive response (HR) in tobacco and to inhibit the TOR pathway (Sole et al., 2012; Popa et al., 2016b), showed opposite regulation in potato when compared to tomato and melon (Ailloud et al., 2016), suggesting that it may play host-specific roles. Similarly, genes *pilG*, *pilH*, *pilN*, *pilM*, *pilY,* and *pilW,* coding for structural components of the type IV pili involved in twitching motility and adherence (Liu et al., 2001; Kang et al., 2002) were induced in the current work but repressed in other plant species (Jacobs et al., 2012).

In addition, some virulence determinants well-described as induced during growth *in planta* were repressed or not DE in potato. Remarkably, the exopolysaccharide synthesis and regulation genes (*eps*) as well as most known cell wall degrading enzymes (*pehA, pehB, pehC, egl,* and *cbhA*), which are virulence determinants (Schell, 2000) induced during tomato infection (UW551 strain) infection (Jacobs et al., 2012) were absent from the potato DE dataset.

Differences in the host environment or in the tissue environment and disease stage are the two most plausible reasons for the discrepancies between virulence gene expression data in potato and in other plant hosts. We favor the latter explanation, as our samples were collected from bacteria growing in the root (including apoplastic and xylematic bacteria) at early times after inoculation while all previous transcriptomic work had been performed from bacteria extracted from xylem at later infection stages.

Three independent observations support the existence of stage-specific environmental cues that differentially affect gene expression in this work compared to previous studies. First, genes that are induced at high bacterial densities are absent from the potato DE genes. Examples are the mentioned exopolysaccharide synthesis genes or the quorum sensing regulator *solI*, repressed in our conditions but slightly induced in bacteria isolated from the tomato shoot xylem (Jacobs et al., 2012). In the low bacterial cell densities in the roots the *phcA* cell-density regulator was not induced, impeding *solI* or *eps* expression (Huang et al., 1995; Flavier et al., 1997). Second, three out of the six type III effectors that are induced in potato were described as secreted at early stages (Lonjon et al., 2016), two of them (*popF1* and *popA)* also proposed to play an important role in the first steps of infection (Kanda et al., 2003). On the contrary, only two out of the 38 described as "late" effectors (*ripD* and *popC*) were induced in our root transcriptome. Third, the afore-mentioned transcriptional regulators *flhC* and *flhD* responsible for the activation of the flagellum genes were up-regulated in potato root samples (**Table 3**) and also in the tomato xylem (Jacobs et al., 2012), but only in the latter were the flagellum structural genes induced, suggesting that the potato transcriptome represents an earlier stage where complete activation of this regulon has not yet occurred. These observations imply that our transcriptome represents a snapshot of a precise stage of the genetic programs deployed consecutively during plant colonization.

Finally, we cannot rule out that changes in *R. solanacearum* DE genes in different studies are due to the use of different strains. Differing transcriptomes of two *R. solanacearum* strains in the same plant environment have already been reported (Ailloud et al., 2016). However, the fact that previous gene expression studies were performed with strain UW551, which is genetically extremely close to UY031 used here, render this explanation unlikely. Standardization of the plant inoculation and sampling procedures and a systematic analysis of plant-pathogen interactions dissecting gene expression over time in a defined strain-host pathosystem would clarify the nature of the observed discrepancies between transcriptomic studies.

The *R. solanacearum* Metabolic State during Potato Root Colonization

From the transcriptomic information gathered in this work, we can infer for the first time the environmental conditions encountered by *R. solanacearum* in the root, the site where plant infection takes place.

A first observation is that the bacterium seems to start to run out of O_2. An indication of this is the highly induced *Cbb3*-cco, a high affinity cytochrome c oxidase known to contribute to the growth of *R. solanacearum* and other bacteria in microaerobic or anoxic environments (Colburn-Clifford and Allen, 2010; Hamada et al., 2014), such as the plant xylem (Pegg, 1985). Upregulation of the low O_2 affinity cytochrome ubiquinol oxidase genes *cyoA1* and *cyoB1* reinforces the notion of a microaerobic rather than an anoxic environment. In agreement with this, *nrdB*, which is required for growth in aerobiosis (Casado et al., 1991), was up-regulated, and *nrdG* and *nrdD*, required in strict anaerobiosis (Garriga et al., 1996; Ailloud et al., 2016) were not induced. Further, the *cbiA*, *cbiL,* and *cbiG* genes, which are involved in anaerobic cobalamin synthesis

(Roessner and Scott, 2006), were repressed. Another indication of microaerobic conditions is the induction of genes driving nitrate and sulfate anaerobic respiration. Examples are the *cys* genes, involved in the assimilatory sulfate reduction pathway (Kredich, 1992), *ptsN*—a nitrogen-dependent regulatory protein, *rpoN1*, -the global nitrogen regulator- and *narL* -the nitrate/nitrite-responsive transcriptional regulator- were all induced in wild potato roots. All these findings suggest that during early root infection *R. solanacearum* is experiencing the transition from an aerobic environment to the anaerobic conditions established at the onset of disease during xylem colonization (Ailloud et al., 2016).

Another take home message from the root transcriptomes is that few central metabolic pathways seem to be active. It was previously described that a large proportion of the *R. solanacearum* genes involved in amino acid metabolism and transport was down-regulated during growth in the xylem (Ailloud et al., 2016) and we found that this was also the case during growth in the root tissues at early stages of infection. For instance, the glycine catabolism genes *gcvP*, *gcvT,* and *gcvA* as well as the dipeptide uptake gene *dppD1* were repressed in both cases (**Table 3**; Ailloud et al., 2016). Other *R. solanacearum* metabolic genes previously known to be repressed *in planta* also down-regulated here included carbohydrate metabolism genes such as the xylose transporter operon *xylFGH* and Glucosamine 6-phosphate synthetase, the key enzyme controlling amino sugar biosynthesis (Milewski, 2002; Jacobs et al., 2012). Lipid metabolism was also strikingly repressed during root colonization. Out of the 21 DE genes involved in lipid mobilization, only 2 have been found in previous gene expression studies in *R. solanacearum* (**Table 3**; Jacobs et al., 2012). Thus, the downregulation of lipid metabolism could be specific to early infection stages or to wild potato colonization. In this sense, lipid metabolism has been reported to play an important role during plant-host interactions by modulating defense responses in plants and pathogen infection (Casadevall and Pirofski, 2001; Wenk, 2006). Cofactor metabolism was also repressed including the folate synthesis gene *pabB* (**Table 3**), already known to be down-regulated *in planta* (Shinohara et al., 2005), the cobalamin biosynthesis genes and adenilate cyclase. Repression of adenylate cyclase, which is a global metabolic regulator in bacteria (Ullmann and Danchin, 1980), illustrates the magnitude of the metabolic shutdown experienced by *R. solanacearum* in the roots of *S. commersonii*.

In contrast with the global metabolic shutdown, aspartate and tryptophan catabolism genes were up-regulated when *R. solanacearum* grew in the plant roots. The aspartate catabolism gene *nadB2* had already been identified as an essential gene for in planta growth in an *in vivo* screening (Brown and Allen, 2004). Interestingly, aspartate is the second most abundant aminoacid in the tomato apoplast and less so in the xylem (Zuluaga et al., 2013), which is in agreement with the bacterium mostly thriving in the apoplastic root spaces at the early infection times analyzed. Also induced was the Tryptophan 2,3-dioxygenase. Concentrations of this aminoacid are high at lateral root emergence sites (Jaeger et al., 1999), and it was suggested that it is also present in the tomato apoplast (Yu et al., 2013). Induction of tryptophan catabolism would thus be indicative of early plant colonization.

These results likely indicate the existence of a trade-off between the expression of virulence and metabolic genes. This has already been described in a previous study where the quorum-sensing-dependent regulatory protein PhcA regulated a trade-off between production of *R. solanacearum* exopolysaccharides and bacterial proliferation (Peyraud et al., 2016).

Proposed New Virulence Determinants Important for Early Root Colonization

RSUY_RS08455 and *RSUY_RS16950* were found to be upregulated in a resistant *S. commersonii* accession compared to a susceptible one (**Table 2**), as well as during root colonization compared to rich medium (**Table 3**). Although these genes also appeared in the microarray transcriptome of bacteria extracted from infected tomato xylem vessels (Jacobs et al., 2012), they have not been characterized.

Similarly, the gene encoding an avrD-like protein was up-regulated in tomato xylem (Jacobs et al., 2012) and in wild potato (**Table 3**). AvrD is required in *P. syringae* for the synthesis of syringolide, small molecules that can elicit a hypersensitive response on resistant plants (Keen et al., 1990; Mucyn et al., 2014). In *R. solanacearum* the avrD-like protein encoding gene is activated by the master virulence regulator HrpG (Valls et al., 2006). Considering the persistence of these three genes among the up-regulated during plant colonization, we suggest that they encode for potential virulence factors, probably necessary independently of the host or the infection stage.

Three genes found up-regulated in *S. commersonii* (*suhB, rhs* and the carbonic anhydrase gene *RSUY_RS16085*, **Table 3**) have been involved in bacterial virulence on animals and constitute putative virulence genes in *R. solanacearum*. Although classified as a phosphate mobilization gene (**Table 3**), *suhB* is a super-regulator involved in the proper rRNA folding (Singh et al., 2016). It plays a role in virulence of animal bacterial pathogens, influencing T3SS, T6SS, flagellum and biofilm regulation and probably acts in opposite ways in different bacteria (Rosales-Reyes et al., 2012; Li et al., 2013). Interestingly, *SuhB* differential expression was also observed in two *R. solanacearum* strains (Meng et al., 2015). The function of Rhs (Rearrangement Hot Spot) proteins is ill-defined but they are considered to promote recombination (Lin et al., 1984). Interestingly, a member of the Rhs family was described to be induced during infection and associated with increased bacterial numbers and decreased survival in mice during pneumonia caused by *P. aeruginosa* (Kung et al., 2012). Finally, carbonic anhydrase catalyzes the inter-conversion between carbon dioxide and bicarbonate but is also required for growth of many animal pathogenic microorganisms (Capasso and Supuran, 2015). In addition, a role in disease establishment between potato and *Phytophthora infestans* was also reported (Restrepo et al., 2005), suggesting the possible implication of CAs during host colonization. These evidences suggest that *suhB*, *rhs,* and *RSUY_RS16085* encode putative virulence factors shared

between gram-negative bacterial pathogens that infect animals and plants.

The assimilatory sulfate reduction pathway (c*ysD, cysN,* and *cysI*) and the phosphate mobilization (*pstB* and *pstS1*) were also induced during root colonization (**Table 3**). *cysD* and *cysN*, encode an ATP sulfurylase that produces APS, which can be in turn reduced to PAPS to ultimately synthesize cysteine by *cysI*. A study carried out in a closely related plant pathogenic bacterium, *Xanthomonas oryzae* pv. *Oryzae,* was demonstrated that mutation of either *raxP* or *raxQ* (homologs of *cysD* and *cysN*) impaired production of APS and PAPS and were required for the correct activity of the avirulence protein AvrXa21 (Shen et al., 2002). Further, several studies demonstrated that mutations on the pst system, responsible for phosphate uptake, affected virulence in diverse animal pathogenic bacteria (Rao et al., 2004; Lamarche et al., 2005, 2008). Altogether, these studies suggest that both systems might be regulators of bacterial pathogenicity, which could also be conserved in plant pathogens.

Finally, the *rtcA* and its regulator *rtcR* are down-regulated *in planta* (**Table 3**). The *rtc* system is involved in the regulation of the RNA repair system for ribosome homeostasis through the activation of *rtcR* by different agents and genetic lesions which in turn activates the *rtcAB* genes (Das and Shuman, 2013). The *rtc* system was also involved in the functioning of chemotaxis and motility in *Escherichia coli* (Engl et al., 2016), as mutations in either *rtcA* or *rtcB* increased motility. Since *rtc* acts a repressor of motility, its down-regulation in *S. commersonii* colonization could influence bacterial motility, a key virulence determinant.

AUTHOR CONTRIBUTIONS

MP performed experiments, analyzed data and wrote the manuscript; RG analyzed data; PZ performed experiments; NC designed the research and wrote the manuscript; AM designed experiments and analyzed data; JS designed the research, analyzed data and wrote the manuscript; MV designed the research, performed experiments, analyzed data, and wrote the manuscript.

FUNDING

This work was funded by projects AGL2013-46898-R, AGL2016-78002-R, and RyC 2014-16158 from the Spanish Ministry of Economy and Competitiveness. We also acknowledge financial support from the "Severo Ochoa Program for Centres of Excellence in R&D" 2016-2019 (SEV-2015-0533) and the CERCA Program of the Catalan Government (Generalitat de Catalunya) and from COST Action SUSTAIN (FA1208) from the European Union. APM is funded by the Chinese Academy of Sciences and the Chinese 1000 Talents Program. MP holds an APIF doctoral fellowship from Universitat de Barcelona and received a travel fellowship allowed by Fundació Montcelimar and Universitat de Barcelona to carry out a short stay in JCS's lab. RGS holds a doctoral fellowship; grant 2012/15197-1, São Paulo Research Foundation (FAPESP) and JCS has a CNPq research fellowship.

ACKNOWLEDGMENTS

We thank R. de Pedro for helping in the solid rich medium sample preparation, I. Erill for helping in the transcriptomic data interpretation, S. Genin, and S. Lindow for inspiring discussions, C. Madrid, and C. Balsalobre for advice on transcriptome data interpretation, M. Solé for the potato infection set up and F. Vilaró, M. dalla Rizza, and M.J. Pianzzola for their advice and for providing the *S. commersonii* genotypes used in this study. We thank the Shanghai PSC Genomics facility for RNA sequencing.

SUPPLEMENTARY MATERIAL

The Supplementary Material for this article can be found online at: http://journal.frontiersin.org/article/10.3389/fpls.2017.00370/full#supplementary-material

REFERENCES

Ailloud, F., Lowe, T. M., Robene, I., Cruveiller, S., Allen, C., and Prior, P. (2016). **In planta comparative transcriptomics of host-adapted strains of Ralstonia solanacearum. *PeerJ*. 4:e1549. doi: 10.7717/peerj.1549**

Anders, S., Pyl, P. T., and Huber, W. (2015). HTSeq–a Python framework to work with high-throughput sequencing data. *Bioinformatics* 31, 166–169. doi: 10.1093/bioinformatics/btu638

Bocsanczy, A. M., Achenbach, U. C., Mangravita-Novo, A., Chow, M., and Norman, D. J. (2014). Proteomic comparison *of Ralstonia solanacearum* strains reveals temperature dependent virulence factors. *BMC Genomics* 15:280. doi: 10.1186/1471-2164-15-280

Boucher, C. A., Van Gijsegem, F., Barberis, P. A., Arlat, M., and Zischek, C. (1987). *Pseudomonas solanacearum* genes controlling both pathogenicity on tomato and hypersensitivity on tobacco are clustered. *J. Bacteriol.* 169, 5626–5632. doi: 10.1128/jb.169.12.5626-5632.1987

Brown, D. G., and Allen, C. (2004). *Ralstonia solanacearum* genes induced during growth in tomato: an inside view of bacterial wilt. *Mol. Microbiol.* 53, 1641–1660. doi: 10.1111/j.1365-2958.2004.04237.x

Buttner, D. (2016). Behind the lines-actions of bacterial type III effector proteins in plant cells. *FEMS Microbiol. Rev.* 40, 894–937. doi: 10.1093/femsre/fuw026

Capasso, C., and Supuran, C. T. (2015). Bacterial, fungal and protozoan carbonic anhydrases as drug targets. *Expert Opin. Ther. Targets* 19, 1689–1704. doi: 10.1517/14728222.2015.1067685

Capy, P., Gasperi, G., Biémont, C., and Bazin, C. (2000). Stress and transposable elements: co-evolution or useful parasites? *Heredity (Edinb).* 85, 101–106. doi: 10.1046/j.1365-2540.2000.00751.x

Casadevall, A., and Pirofski, L. (2001). Host-pathogen interactions: the attributes of virulence. *J. Infect. Dis.* 184, 337–344. doi: 10.1086/322044

Casado, C., Llagostera, M., and Barbe, J. (1991). Expression of nrdA and nrdB genes of *Escherichia coli* is decreased under anaerobiosis. *FEMS Microbiol. Lett.* 67, 153–157. doi: 10.1111/j.1574-6968.1991.tb04432.x-i1

Colburn-Clifford, J., and Allen, C. (2010). A cbb(3)-type cytochrome C oxidase contributes to *Ralstonia solanacearum* R3bv2 growth in microaerobic environments and to bacterial wilt disease development in tomato. *Mol. Plant Microbe Interact.* 23, 1042–1052. doi: 10.1094/MPMI-23-8-1042

Coll, N. S., and Valls, M. (2013). Current knowledge on the *Ralstonia solanacearum* type III secretion system. *Microb. Biotechnol.* 6, 614–620. doi: 10.1111/1751-7915.12056

Contreras-Moreira, B., and Vinuesa, P. (2013). GET_HOMOLOGUES, a versatile software package for scalable and robust microbial pangenome analysis. *Appl. Environ. Microbiol.* 79, 7696–7701. doi: 10.1128/aem.02411-13

Cruz, A. P., Ferreira, V., Pianzzola, M. J., Siri, M. I., Coll, N. S., and Valls, M. (2014). A novel, sensitive method to evaluate potato germplasm for bacterial wilt resistance using a luminescent *Ralstonia solanacearum* reporter strain. *Mol. Plant Microbe Interact.* 27, 277–285. doi: 10.1094/MPMI-10-13-0303-FI

Cunnac, S., Occhialini, A., Barberis, P., Boucher, C., and Genin, S. (2004). Inventory and functional analysis of the large Hrp regulon in *Ralstonia solanacearum*: identification of novel effector proteins translocated to plant host cells through the type III secretion system. *Mol. Microbiol.* 53, 115–128. doi: 10.1111/j.1365-2958.2004.04118.x

Dalsing, B. L., and Allen, C. (2014). Nitrate assimilation contributes to *Ralstonia solanacearum* root attachment, stem colonization, and virulence. *J. Bacteriol.* 196, 949–960. doi: 10.1128/JB.01378-13

Dalsing, B. L., Truchon, A. N., Gonzalez-Orta, E. T., Milling, A. S., and Allen, C. (2015). *Ralstonia solanacearum* uses inorganic nitrogen metabolism for virulence, ATP production, and detoxification in the oxygen-limited host xylem environment. *MBio* 6:e02471. doi: 10.1128/mBio.02471-14

Das, U., and Shuman, S. (2013). 2'-Phosphate cyclase activity of RtcA: a potential rationale for the operon organization of RtcA with an RNA repair ligase RtcB in *Escherichia coli* and other bacterial taxa. *RNA* 19, 1355–1362. doi: 10.1261/rna.039917.113

Delaspre, F., Nieto Penalver, C. G., Saurel, O., Kiefer, P., Gras, E., Milon, A., et al. (2007). The *Ralstonia solanacearum* pathogenicity regulator HrpB induces 3-hydroxy-oxindole synthesis. *Proc. Natl. Acad. Sci. U.S.A.* 104, 15870–15875. doi: 10.1073/pnas.0700782104

Engl, C., Schaefer, J., Kotta-Loizou, I., and Buck, M. (2016). Cellular and molecular phenotypes depending upon the RNA repair system RtcAB of *Escherichia coli*. *Nucleic Acids Res.* 44, 9933–9941. doi: 10.1093/nar/gkw628

Flavier, A. B., Ganova-Raeva, L. M., Schell, M. A., and Denny, T. P. (1997). Hierarchical autoinduction in *Ralstonia solanacearum*: control of Acyl-homoserine lactone production by a novel autoregulatory system responsive to 3-hydroxypalmitic acid methyl ester. *J. Bacteriol.* 179, 7089–7097. doi: 10.1128/jb.179.22.7089-7097.1997

Flores-Cruz, Z., and Allen, C. (2009). *Ralstonia solanacearum* encounters an oxidative environment during tomato infection. *Mol. Plant Microbe Interact.* 22, 773–782. doi: 10.1094/MPMI-22-7-0773

Garriga, X., Eliasson, R., Torrents, E., Barbé, J., Gibert, I., and Reichard, P. (1996). nrdD and nrdG genes are essential for strict anaerobic growth of *Escherichia coli*. *Biochem. Biophys. Res. Commun.* 229, 189–192. doi: 10.1006/bbrc.1996.1778

Guarischi-Sousa, R., Puigvert, M., Coll, N. S., Siri, M. I., Pianzzola, M. J., Valls, M., et al. (2016). Complete genome sequence of the potato pathogen *Ralstonia solanacearum* UY031. *Stand. Genomic Sci.* 11, 7. doi: 10.1186/s40793-016-0131-4

Hamada, M., Toyofuku, M., Miyano, T., and Nomura, N. (2014). cbb3-type cytochrome c oxidases, aerobic respiratory enzymes, impact the anaerobic life of *Pseudomonas aeruginosa* PAO1. *J. Bacteriol.* 196, 3881–3889. doi: 10.1128/jb.01978-14

Hayward, A. C. (1991). Biology and epidemiology of bacterial wilt caused by ***Pseudomonas solanacearum***. ***Annu. Rev. Phytopathol.*** **29, 65–87. doi: 10.1146/annurev.py.29.090191.000433**

Huang, J., Carney, B. F., Denny, T. P., Weissinger, A. K., and Schell, M. A. (1995). A complex network regulates expression of eps and other virulence genes of *Pseudomonas solanacearum*. *J. Bacteriol.* 177, 1259–1267. doi: 10.1128/jb.177.5.1259-1267.1995

Jacobs, J. M., Babujee, L., Meng, F., Milling, A., and Allen, C. (2012). The in planta transcriptome of *Ralstonia solanacearum*: conserved physiological and virulence strategies during bacterial wilt of tomato. *MBio* 3:e00114-12. doi: 10.1128/mBio.00114-12

Jaeger, C. H. III., Lindow, S. E., Miller, W., Clark, E., and Firestone, M. K. (1999). Mapping of sugar and amino acid availability in soil around roots with bacterial sensors of sucrose and tryptophan. *Appl. Environ. Microbiol.* 65, 2685–2690.

Kanda, A., Yasukohchi, M., Ohnishi, K., Kiba, A., Okuno, T., and Hikichi, Y. (2003). Ectopic expression of *Ralstonia solanacearum* effector protein PopA early in invasion results in loss of virulence. *Mol. Plant Microbe Interact.* 16, 447–455. doi: 10.1094/MPMI.2003.16.5.447

Kang, Y., Liu, H., Genin, S., Schell, M. A., and Denny, T. P. (2002). *Ralstonia solanacearum* requires type 4 pili to adhere to multiple surfaces and for natural transformation and virulence. *Mol. Microbiol.* 46, 427–437. doi: 10.1046/j.1365-2958.2002.03187.x

Keen, N. T., Tamaki, S., Kobayashi, D., Gerhold, D., Stayton, M., Shen, H., et al. (1990). Bacteria expressing avirulence Gene D produce a specific elicitor of the soybean hypersensitive reaction. *Mol. Plant Microbe Interact.* 3, 112–121. doi: 10.1094/MPMI-3-112

Kim-Lee, H., Moon, J. S., Hong, Y. J., Kim, M. S., and Cho, H. M. (2005). Bacterial wilt resistance in the progenies of the fusion hybrids between haploid of potato and *Solanum commersonii*. *Am. J. Potato Res.* 82, 129–137. doi: 10.1007/BF02853650

Kredich, N. M. (1992). The molecular basis for positive regulation of cys promoters in *Salmonella typhimurium* and *Escherichia coli*. *Mol. Microbiol.* 6, 2747–2753. doi: 10.1111/j.1365-2958.1992.tb01453.x

Kung, V. L., Khare, S., Stehlik, C., Bacon, E. M., Hughes, A. J., and Hauser, A. R. (2012). An rhs gene of *Pseudomonas aeruginosa* encodes a virulence protein that activates the inflammasome. *Proc. Natl. Acad. Sci. U.S.A.* 109, 1275–1280. doi: 10.1073/pnas.1109285109

La, M. V., Raoult, D., and Renesto, P. (2008). Regulation of whole bacterial pathogen transcription within infected hosts. *FEMS Microbiol. Rev.* 32, 440–460. doi: 10.1111/j.1574-6976.2008.00103.x

Lamarche, M. G., Dozois, C. M., Daigle, F., Caza, M., Curtiss, R. III., Dubreuil, J. D., et al. (2005). Inactivation of the pst system reduces the virulence of an avian pathogenic *Escherichia coli* O78 strain. *Infect. Immun.* 73, 4138–4145. doi: 10.1128/iai.73.7.4138-4145.2005

Lamarche, M. G., Wanner, B. L., Crepin, S., and Harel, J. (2008). The phosphate regulon and bacterial virulence: a regulatory network connecting phosphate homeostasis and pathogenesis. *FEMS Microbiol. Rev.* 32 461–473. doi: 10.1111/j.1574-6976.2008.00101.x

Langmead, B., and Salzberg, S. L. (2012). Fast gapped-read alignment with Bowtie 2. *Nat. Methods* 9, 357–359. doi: 10.1038/nmeth.1923

Leimbach, A. (2016). *Bac-Genomics-Scripts: Bovine E. coli Mastitis Comparative Genomics Edition [Data set]*. Zenodo. doi: 10.5281/zenodo.215824

Li, K., Xu, C., Jin, Y., Sun, Z., Liu, C., Shi, J., et al. (2013). SuhB is a regulator of multiple virulence genes and essential for pathogenesis of *Pseudomonas aeruginosa*. *MBio* 4, e00419–e00413. doi: 10.1128/mbio.00419-13

Lin, R. J., Capage, M., and Hill, C. W. (1984). A repetitive DNA sequence, rhs, responsible for duplications within the *Escherichia coli* K-12 chromosome. *J. Mol. Biol.* 177, 1–18. doi: 10.1016/0022-2836(84)90054-8

Liu, H., Kang, Y., Genin, S., Schell, M. A., and Denny, T. P. (2001). Twitching motility of *Ralstonia solanacearum* requires a type IV pilus system. *Microbiology (Reading., Engl).* 147, 3215–3229. doi: 10.1099/00221287-147-12-3215

Lonjon, F., Turner, M., Henry, C., Rengel, D., Lohou, D., van de Kerkhove, Q., et al. (2016). Comparative secretome analysis of *Ralstonia solanacearum* Type 3 secretion-associated mutants reveals a fine control of effector delivery, essential for bacterial pathogenicity. *Mol. Cell. Proteomics.* 15, 598–613. doi: 10.1074/mcp.M115.051078

Love, M. I., Huber, W., and Anders, S. (2014). Moderated estimation of fold change and dispersion for RNA-seq data with DESeq2. *Genome Biol.* 15:550. doi: 10.1186/s13059-014-0550-8

Lundgren, B. R., Connolly, M. P., Choudhary, P., Brookins-Little, T. S., Chatterjee, S., Raina, R., et al. (2015). Defining the metabolic functions and roles in virulence of the rpoN1 and rpoN2 Genes in *Ralstonia solanacearum* GMI1000. *PLoS ONE* 10:e0144852. doi: 10.1371/journal.pone.0144852

Meng, F. (2013). The virulence factors of the bacterial wilt pathogen *Ralstonia solanacearum*. *J. Plant Pathol. Microbiol.* 4:168. doi: 10.4172/2157-7471.1000168

Meng, F., Babujee, L., Jacobs, J. M., and Allen, C. (2015). Comparative transcriptome analysis reveals cool virulence factors of *Ralstonia solanacearum* Race 3 Biovar 2. *PLoS ONE* 10:e0139090. doi: 10.1371/journal.pone.0139090

Milewski, S. (2002). Glucosamine-6-phosphate synthase–the multi-facets enzyme. *Biochim. Biophys. Acta* 1597, 173–192. doi: 10.1016/S0167-4838(02)00318-7

Monteiro, F., Genin, S., van Dijk, I., and Valls, M. (2012). A luminescent reporter evidences active expression of *Ralstonia solanacearum* type III secretion system genes throughout plant infection. *Microbiology (Reading., Engl).* 158, 2107–2116. doi: 10.1099/mic.0.058610-0

Mori, Y., Inoue, K., Ikeda, K., Nakayashiki, H., Higashimoto, C., Ohnishi, K., et al. (2016). The vascular plant-pathogenic bacterium *Ralstonia solanacearum* produces biofilms required for its virulence on the surfaces of tomato

cells adjacent to intercellular spaces. *Mol. Plant Pathol.* 17, 890–902. doi: 10.1111/mpp.12335

Mucyn, T. S., Yourstone, S., Lind, A. L., Biswas, S., Nishimura, M. T., Baltrus, D. A., et al. (2014). Variable suites of non-effector genes are co-regulated in the type III secretion virulence regulon across the Pseudomonas syringae phylogeny. *PLoS Pathog.* 10:e1003807. doi: 10.1371/journal.ppat.1003807

Occhialini, A., Cunnac, S., Reymond, N., Genin, S., and Boucher, C. (2005). Genome-wide analysis of gene expression in *Ralstonia solanacearum* reveals that the hrpB gene acts as a regulatory switch controlling multiple virulence pathways. *Mol. Plant Microbe Interact.* 18, 938–949. doi: 10.1094/MPMI-18-0938

Peeters, N., Guidot, A., Vailleau, F., and Valls, M. (2013). Ralstonia solanacearum, a widespread bacterial plant pathogen in the post-genomic era. *Mol. Plant Pathol.* 15, 651–662. doi: 10.1111/mpp.12038

Pegg, G. F. (1985). Life in a black hole: the microenvironment of the vascular pathogen. *Trans. Brit. Mycol. Soc.* 85, 1–20. doi: 10.1016/S0007-1528(85)80043-2

Peyraud, R., Cottret, L., Marmiesse, L., Gouzy, J., and Genin, S. (2016). A resource allocation trade-off between virulence and proliferation drives metabolic versatility in the plant pathogen *Ralstonia solanacearum*. *PLoS Pathog.* 12:e1005939. doi: 10.1371/journal.ppat.1005939

Plener, L., Boistard, P., Gonzalez, A., Boucher, C., and Genin, S. (2012). Metabolic adaptation of *Ralstonia solanacearum* during plant infection: a methionine biosynthesis case study. *PLoS ONE* 7:e36877. doi: 10.1371/journal.pone.0036877

Popa, C., Coll, N. S., Valls, M., and Sessa, G. (2016a). Yeast as a heterologous model system to uncover type III effector function. *PLoS Pathog.* 12:e1005360. doi: 10.1371/journal.ppat.1005360

Popa, C., Li, L., Gil, S., Tatjer, L., Hashii, K., Tabuchi, M., et al. (2016b). The effector AWR5 from the plant pathogen *Ralstonia solanacearum* is an inhibitor of the TOR signalling pathway. *Sci. Rep.* 6:27058. doi: 10.1038/srep27058

Priou, S. (2004). *Integrated Management of Bacterial Wilt and Soil-Borne Diseases of Potato in Farmer Communities of the Inter-Andean Valleys of Peru and Bolivia*. Final Technical Report DFID-funded project CRF 7862(C), CIP, Lima.

Rao, P. S., Yamada, Y., Tan, Y. P., and Leung, K. Y. (2004). Use of proteomics to identify novel virulence determinants that are required for *Edwardsiella tarda* pathogenesis. *Mol. Microbiol.* 53, 573–586. doi: 10.1111/j.1365-2958.2004.04123.x

Ray, S. K., Kumar, R., Peeters, N., Boucher, C., and Genin, S. (2015). rpoN1, but not rpoN2, is required for twitching motility, natural competence, growth on nitrate, and virulence of *Ralstonia solanacearum*. *Front. Microbiol.* 6:229. doi: 10.3389/fmicb.2015.00229

Restrepo, S., Myers, K., del Pozo, O., Martin, G. B., Hart, A. L., Buell, C. R., et al. (2005). Gene profiling of a compatible interaction between Phytophthora infestans and *Solanum tuberosum* suggests a role for carbonic anhydrase. *Mol. Plant Microbe Interact.* 18, 913–922. doi: 10.1094/MPMI-18-0913

Robinson, J. T., Thorvaldsdottir, H., Winckler, W., Guttman, M., Lander, E. S., Getz, G., et al. (2011). Integrative genomics viewer. *Nat. Biotechnol.* 29, 24–26. doi: 10.1038/nbt.1754

Rocha, E. R., and Smith, C. J. (1999). Role of the alkyl hydroperoxide reductase (ahpCF) Gene in oxidative stress defense of the obligate. *J. Bacteriol.* 181, 5701–5710.

Roessner, C. A., and Scott, A. I. (2006). Fine-tuning our knowledge of the anaerobic route to cobalamin (vitamin B12). *J. Bacteriol.* 188, 7331–7334. doi: 10.1128/jb.00918-06

Rosales-Reyes, R., Saldias, M. S., Aubert, D. F., El-Halfawy, O. M., and Valvano, M. A. (2012). The suhB gene of *Burkholderia cenocepacia* is required for protein secretion, biofilm formation, motility and polymyxin B resistance. *Microbiology* 158, 2315–2324. doi: 10.1099/mic.0.060988-0

Schell, M. A. (2000). Control of virulence and pathogenicity genes of *Ralstonia Solanacearum* by an elaborate sensory network. *Annu. Rev. Phytopathol.* 38, 263–292. doi: 10.1146/annurev.phyto.38.1.263

Shen, Y., Sharma, P.,.da Silva, F.G., and Ronald, P. (2002). The Xanthomonas oryzae pv. oryzae raxP and raxQ genes encode an ATP sulphurylase and adenosine-5¢-phosphosulphate kinase that are required for AvrXa21avirulence activity. *Mol. Microbiol.* 44, 37–48. doi: 10.1046/j.1365-2958.2002.02862.x

Shinohara, R., Kanda, A., Ohnishi, K., Kiba, A., and Hikichi, Y. (2005). Contribution of folate biosynthesis to *Ralstonia solanacearum* proliferation in intercellular spaces. *Appl. Environ. Microbiol.* 71, 417–422. doi: 10.1128/AEM.71.1.417-422.2005

Singh, N., Bubunenko, M., Smith, C., Abbott, D. M., Stringer, A. M., Shi, R., et al. (2016). SuhB associates with nus factors to facilitate 30S ribosome biogenesis in *Escherichia coli*. *MBio* 7:e00114. doi: 10.1128/mBio.00114-16

Siri, M. I., Galván, G. A., Quirici, L., Silvera, E., Villanueva, P., Ferreira, F., et al. (2009). Molecular marker diversity and bacterial wilt resistance in wild *Solanum commersonii* accessions from Uruguay. *Euphytica* 165, 371–382. doi: 10.1007/s10681-008-9800-8

Siri, M. I., Sanabria, A., Boucher, C., and Pianzzola, M. J. (2014). New type IV pili-related genes involved in early stages of *Ralstonia solanacearum* potato infection. *Mol. Plant Microbe Interact.* 27 712–724. doi: 10.1094/MPMI-07-13-0210-R

Siri, M. I., Sanabria, A., and Pianzzola, M. J. (2011). Genetic diversity and aggressiveness of ralstonia solanacearumstrains causing bacterial wilt of potato in uruguay. *Plant Dis.* 95, 1292–1301. doi: 10.1094/pdis-09-10-0626

Sole, M., Popa, C., Mith, O., Sohn, K. H., Jones, J. D., Deslandes, L., et al. (2012). The awr gene family encodes a novel class of *Ralstonia solanacearum* type III effectors displaying virulence and avirulence activities. *Mol. Plant Microbe Interact.* 25, 941–953. doi: 10.1094/MPMI-12-11-0321

Stes, E., Vandeputte, O. M., El Jaziri, M., Holsters, M., and Vereecke, D. (2011). A successful bacterial coup d'etat: how *Rhodococcus fascians* redirects plant development. *Annu. Rev. Phytopathol.* 49, 69–86. doi: 10.1146/annurev-phyto-072910-095217

Tans-Kersten, J., Brown, D., and Allen, C. (2004). Swimming motility, a virulence trait of *Ralstonia solanacearum*, is regulated by FlhDC and the plant host environment. *Mol. Plant Microbe Interact.* 17, 686–695. doi: 10.1094/MPMI.2004.17.6.686

Thorvaldsdottir, H., Robinson, J. T., and Mesirov, J. P. (2013). Integrative Genomics Viewer (IGV): high-performance genomics data visualization and exploration. *Brief. Bioinform.* 14, 178–192. doi: 10.1093/bib/bbs017

Ullmann, A., and Danchin, A. (1980). Role of cyclic AMP in regulatory mechanisms in bacteria. *Trends Biochem. Sci.* 5, 95–96. doi: 10.1016/0968-0004(80)90257-1

Valls, M., Genin, S., and Boucher, C. (2006). Integrated regulation of the type III secretion system and other virulence determinants in *Ralstonia solanacearum*. *PLoS Pathog.* 2:e82. doi: 10.1371/journal.ppat.0020082

Wenk, M. R. (2006). Lipidomics of host-pathogen interactions. *FEBS Lett.* 580, 5541–5551. doi: 10.1016/j.febslet.2006.07.007

Yu, X., Lund, S. P., Scott, R. A., Greenwald, J. W., Records, A. H., Nettleton, D., et al. (2013). Transcriptional responses of Pseudomonas syringae to growth in epiphytic versus apoplastic leaf sites. *Proc. Natl. Acad. Sci. U.S.A.* 110, E425–E434. doi: 10.1073/pnas.1221892110

Zuluaga, A. P., Puigvert, M., and Valls, M. (2013). Novel plant inputs influencing *Ralstonia solanacearum* during infection. *Front. Microbiol.* 4:349. doi: 10.3389/fmicb.2013.00349

Zuluaga, A. P., Sole, M., Lu, H., Gongora-Castillo, E., Vaillancourt, B., Coll, N., et al. (2015). Transcriptome responses to *Ralstonia solanacearum* infection in the roots of the wild potato *Solanum commersonii*. *BMC Genomics* 16:246. doi: 10.1186/s12864-015-1460-1

Conflict of Interest Statement: The authors declare that the research was conducted in the absence of any commercial or financial relationships that could be construed as a potential conflict of interest.

Supplementary Data

5

Supplementary Figure 1. Percentage of *R. solanacearum* UY031 DE genes according to COG categories.

DE genes between in planta and rich medium growth were classified according to the COG categories assigned to each gene. Distribution of COG categories considering all annotated genes in the UY031 genome is shown as reference. Exact values for each category are shown in Supplementary Table 5.

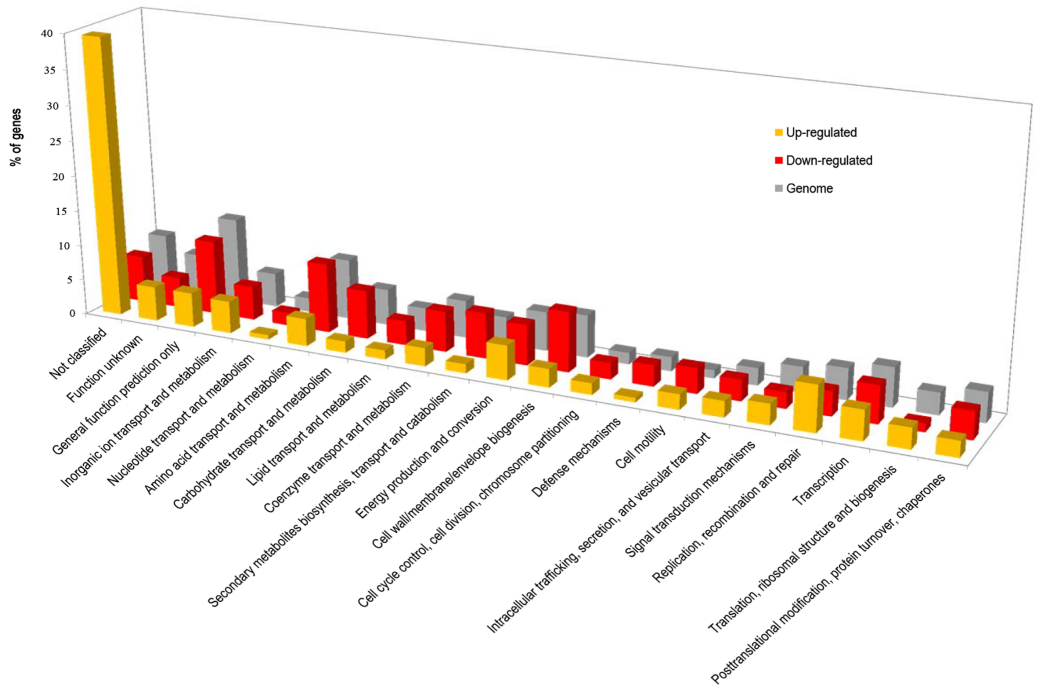

Due to their length,**Supplementary Tables** are available online at:
https://www.frontiersin.org/article/10.3389/fpls.2017.00370/full#supplementary-material

chapter 6

DRAFT 1

***repR*, a MarR transcriptional regulator from *Ralstonia solanacearum* key for early stages of plant colonization**

repR, a MarR transcriptional regulator from *Ralstonia solanacearum* key for early stages of plant colonization

M. Puigvert[1,2], P. Sebastià[2], N.S. Coll[2], M. Valls[1,2*]

[1]Department of Genetics, University of Barcelona, Barcelona, Catalonia, Spain

[2]Centre for Research in Agricultural Genomics (CSIC-IRTA-UAB-UB), Bellaterra, Catalonia, Spain

Abstract

The MarR-family of transcription factors comprises a wide array of bacterial transcriptional regulators that generally control cellular processes important for adaptation to varying environments. Different MarR members have been shown to provide resistance against antibiotics, act as catabolic repressors or participate in virulence in both human and plant pathogens. In a previous *in planta* transcriptome study in *R. solanacearum* during wild potato root colonization, a MarR-encoding gene appeared to be highly induced in tolerant compared to susceptible plant root infection. In this work, we further characterize this gene, that we have called RepR, for Repressor Regulator, and provide evidence that its expression is specifically induced in plants and not dependent on minimal medium. We also show that RepR is necessary for early apoplast colonization and that it contributes to virulence on potato and tomato plants, but is not required for HR elicitation in tobacco. To better elucidate RepR function in plant apoplast, we performed RNA-sequencing of the mutant strain in potato leaf apoplast and compared it to the transcriptome of a wild-type strain growing in this plant niche. We report that RepR directly or indirectly controls expression of at least 563 genes in the apoplast, including many transcription factors. Finally, we also provide evidence that RepR mainly acts as a metabolic repressor controlling amino acid, fatty acid and cofactor metabolic pathways within the apoplast, indicating that reprogramming of these metabolic pathways is potentially important for *R. solanacearum* fitness during adaptation to the initial steps of root colonization.

Introduction

Bacterial adaptation to different environments is controlled by multiple ligand-responsive transcription factors that regulate the expression of sets of genes required under certain conditions. An example of such regulators is the MarR family of transcription factors, named after the *Escherichia coli* Multiple Antibiotic Resistance Regulator (Cohen et al. 1989). These transcription factors are widespread among bacteria and archaea (Ellison and Miller 2006), and are specially abundant in microorganisms with complex lifestyles (Grove 2017). Since different MarR proteins have shown to provide many bacterial species with adaptation to certain conditions and stresses, they are regarded as responsive sensors to changing environments (Grove 2017). Many members of the MarR family described so far act as catabolic repressors, which can be derepressed by the presence of their specific ligand (Grove 2013). This system is an efficient mechanism to ensure expression of specific catabolic pathways only when the carbon source is available (Grove 2017). Lately, great attention is payed to MarR proteins for their potential applications in metabolic engineering as biological sensors (Grove 2017).

Nonetheless, MarRs can also control virulence gene expression in response to perception of host signals. In fact, many MarR proteins have been reported to regulate expression of virulence factors in human pathogens such as *Salmonella typhimurium*, *Staphylococcus aureus*, *Vibrio cholerae* and *Yersinia enterocolitica* (Ellison and Miller 2006). Interestingly, some MarR transcription factors controlling pathogenicity have been also found in bacterial plant pathogens. In soft rot producing bacteria, such as *Pectobacterium carotovorum* and *Dickeya dadantii*, the MarR proteins Hor, PecS and SlyA have been reported to regulate expression of cell wall degrading enzymes such as cellulase, polygalacturonase or pectate lyases, which produce tissue maceration (Sjoblom et al. 2008; Haque et al. 2009). Furthermore, SlyA from *D. dadantii* also regulates expression of other virulence factors such as resistance to oxidative stress, flagellar motility and type III secretion system (T3SS) (Haque et al. 2009; Zou et al. 2012; Haque et al. 2015). In *Xanthomonas campestris*, the MarR regulator HpaR also controls virulence and is positively regulated by HrpG and HrpX, the two main regulators of the T3SS signaling cascade (Qian et al. 2005; Wei et al. 2007; Pan et al. 2018). Finally, PrhN is another member of the MarR family that affects virulence in *Ralstonia solanacearum* by triggering the expression of HrpB and PrhG, two members of the T3SS cascade (Zhang et al. 2015).

R. solanacearum is the causal agent of bacterial wilt in many solanaceous crops (Hayward 1991). Due to its worldwide distribution, its wide range of hosts, the aggressiveness of the disease and the fact there is no control strategy to prevent or cure it, the bacterium was listed in the top 10 most destructive bacterial phytopathogens (Mansfield et al. 2012). The pathogen first enters the plant root system via natural openings and colonizes the intercellular spaces (also called apoplast), a key step for virulence (Hikichi et al. 2007). Cells that survive to the plant apoplast, advance through the endodermis and move to the xylem vessels. Within the xylem, bacteria

multiply extensively and produce exopolysaccharide (EPS), which finally occludes the vasculature and causes plant death (Genin 2010). Besides EPS production, *R. solanacearum* also bears a T3SS to hijack the plant defense responses by directly translocating effector proteins into the host cell (Macho and Zipfel 2015). A functional T3SS triggers disease in susceptible plants or a cell death reaction called Hypersensitive Response in resistant plants (Boucher et al. 1987).

In a previous study, we characterized the *R. solanacearum* UY031 transcriptome during root colonization of a tolerant and a susceptible wild potato accessions (Puigvert et al. 2017, chapter 5). Only two genes were differentially induced in the pathogen during infection of tolerant compared to susceptible accession plants. One of the genes encodes a hypothetical protein, while the other was predicted as a putative MarR family transcription factor. Here, we characterize the latter gene and propose that this MarR regulator mainly acts as a metabolic repressor, therefore renamed as RepR for Repressor Regulator, that provides metabolic adaptation to the host at early infection stages.

Results

A new *R. solanacearum* MarR transcriptional regulator conserved within the *R. solanacearum* species complex

In a previous *in planta* transcriptome study, our group identified a member of the MarR transcription factor family in *R. solanacearum* UY031 that appeared to be induced during the colonization of resistant wild potato roots in contrast to susceptible plants (RSUY_RS08455) (Puigvert et al. 2017). DNA sequence analysis of this gene (renamed RepR), showed that it is highly conserved within *R. solanacearum* species complex, sharing more than 95% identity in strains belonging to different phylotypes (Figure 1). The gene is also present in the closely related species *R. syzygii* and Blood Disease Bacterium. Outside the *Ralstonia solanacearum* species complex, the gene only appears in other *Ralstonia* spp, such as in *R. mannitolityca*, *R. picketii* and *R. insidiosa*. BLAST analysis also revealed that, although *R. solanacearum* UY031 encodes for more than 15 putative MarR-regulator proteins, RepR is unique and different from other MarRs.

Table 1. *repR* log_2FC values *in planta.*

Plant species	***S. commersonni* roots** [b]				***S. tuberosum*** [c]		
Condition	**Tolerant (T)**	**Susceptible (S)**	**T+S**	**T vs S**	**Leaf apoplast**	**Asymptomatic plant xylem**	**Dead plant xylem**
log_2FC[a]	5.49	3.09	4.37	2.37	4.69	2.83	1.81

[a] Expression values compared to bacteria grown on solid rich medium using $p<0.01$.

[b] Data published in Puigvert et al, 2017 (chapter 5).

[c] Unpublished data (Puigvert et al, chapter 7).

RepR is specifically induced *in planta*

In our previous *R. solanacearum* transcriptome in wild potato roots, we noticed that RepR was not only induced in tolerant plants compared to susceptible ones, but it was still up-regulated when we compared all the infected root samples (pooling together resistant and susceptible plants) to bacteria grown on solid rich medium (Puigvert et al. 2017, chapter 5), suggesting that this gene is generally induced *in planta.* Unpublished transcriptome data at different potato infection stages obtained in our lab (Puigvert et al, unpublished), also showed that the MarR regulator was induced in three other *in planta* conditions compared to solid rich medium as reference (Table 1). However, expression levels were higher in the first infection stage (leaf apoplast) and decreased along the infection process (xylem of dead plants), with the lowest fold-change in completely wilted plants (Table 1). Furthermore, *repR* expression was statistically induced in leaf apoplast compared to four different reference conditions: minimal and rich media in liquid cultures and solid plates (Puigvert et al, unpublished) (Supplementary Table 2). Taken together, these results strongly suggest that *repR* is specifically induced at early stages of *in planta* colonization independently of the type of *in vitro* medium used as reference.

A

PHYLOTYPE	III	I	I	I	I	I	IV	IV	IV	IIA	IIA	IIB	IIB	IIB	IIB
STRAINS	CMR15	EP1	OE1-1	RSCM	CQPS-1	GMI1000	R24	R229	PSI07	RS489	CFBP2957	UY031	RS488	UW163	PO82
CMR15	100	98	98	98	98	98	96	96	96	95	95	95	95	95	95
EP1	98	100	100	100	100	100	97	97	97	95	95	95	95	96	96
OE1-1	98	100	100	100	100	100	96	96	96	94	94	95	95	95	95
RSCM	98	100	100	100	100	100	96	96	96	94	94	95	95	95	95
CQPS-1	98	100	100	100	100	100	97	97	97	95	95	95	95	96	96
GMI1000	98	100	100	100	100	100	96	96	96	94	94	95	95	95	95
R24	96	97	96	96	97	96	100	99	99	96	96	97	97	97	97
R229	96	97	96	96	97	96	99	100	100	96	96	97	97	97	97
PSI07	96	97	96	96	97	96	99	100	100	96	96	97	97	97	97
RS489	95	95	94	94	95	94	96	96	96	100	100	97	97	98	98
CFBP2957	95	95	94	94	95	94	96	96	96	100	100	97	97	98	98
UY031	95	95	95	95	95	95	97	97	97	97	97	100	100	98	99
RS488	95	95	95	95	95	95	97	97	97	97	97	100	100	98	99
UW163	95	96	95	95	96	95	97	97	97	98	98	98	98	100	100
PO82	95	96	95	95	96	95	97	97	97	98	98	99	99	100	100

B

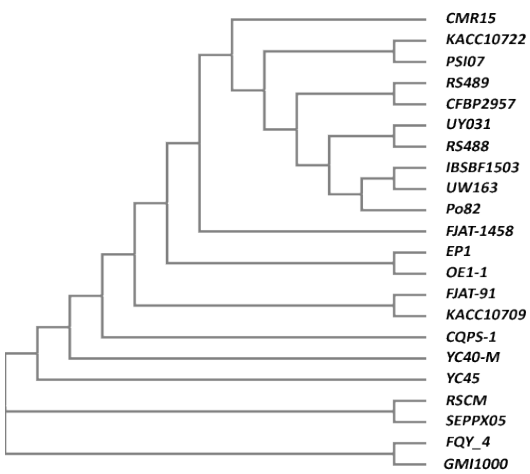

Figure 1. RepR conservation within the *Ralstonia solanacearum* species complex.

A) Percent identity matrix and

B) phylogenetic tree of *repR* in 15 *R. solanacearum* strains belonging to different phylotypes. Alignment was perfomed using the Clustal Omega tool from EMBL-EBI.

A repR deletion mutant is impaired in bacterial multiplication in leaf apoplast

To rule out the possibility that RepR is involved in housekeeping functions, we tested the ability of a RepR deletion mutant (*ΔrepR*) to grow in liquid rich medium. As shown in Supplementary Figure 1, both wild-type (WT) and *ΔrepR* strains grow equally in artificial rich medium. However, as suggested by our *R. solanacearum* transcriptomes *in planta* (Table 1), the genetic function of RepR seems to be especially important in the apoplastic environment, which corresponds to the initial stages of the colonization. To test whether RepR might have a function at this stage, we evaluated bacterial growth of the WT and the *ΔrepR* strains in potato leaf apoplast. Figures 2A and C show that *ΔrepR* growth is impaired during the first two days post inoculation (dpi), although it is able to recover and reach WT densities at 3 dpi. To identify the timing of RepR function *in planta* more precisely, we monitored *R. solanacearum* growth in potato leaf apoplast at shorter time points (Figure 2B). We determined that the RepR mutant has a defect in adapting to the new environment as early as 12 hours post inoculation (hpi), since bacterial densities at that time point are slightly reduced compared to 0 hpi. On the other hand, although the WT does not multiply much within the first 12 hpi, it keeps the same population as in 0 hpi (Figure 2B). These findings demonstrate that RepR contributes to full *R. solanacearum* growth *in planta*.

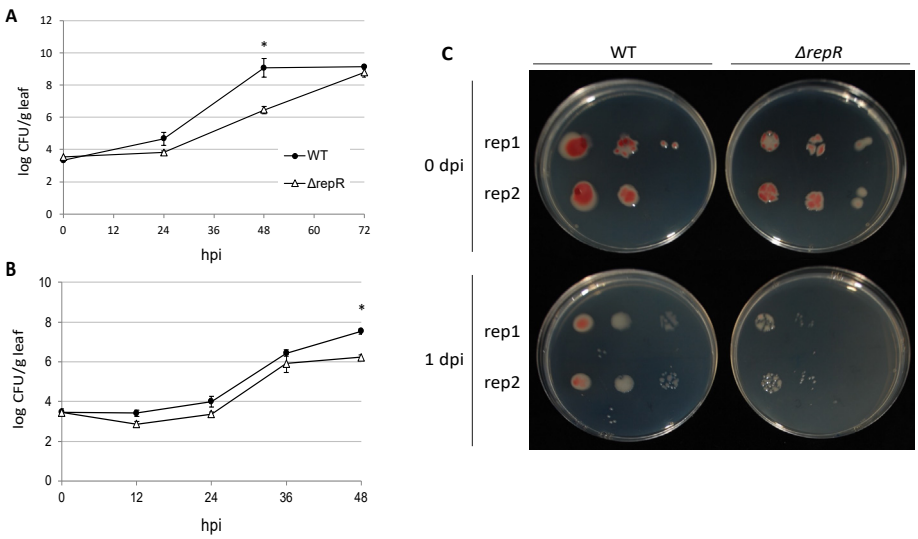

Figure 2. Growth of *R. solanacearum* WT and *ΔrepR* in potato leaf apoplast.

R. solanacearum UY031 WT and *ΔrepR* strains were vacuum infiltrated in potato leaves at a starting bacterial denisity of 10^5 CFU/ml. Bacterial growth curves in potato leaf apoplast were monitored for 3 days every 24 h (A) or for 2 days every 12 h (B). Apoplast fluid from infected potato leaves was collected and 10-fold dilutions were plated onto solid rich medium plates. Growth is represented as the logarithm of CFUs/g leaf. Measurements correspond to the average of three replicates, each one consisting on two leaves from different plants. The experiment was repeated three times with similar results. Statistical differences between WT and *ΔrepR* strains are indicated with an asterisk. C) 20 µl drops of 10-fold apoplast diltuions plated onto rich medium plates for both strains at day 0 and day 1 post-inoculation. At 0 dpi dilutions 0,-1 and-2 were plated, while at 1 dpi dilutions 0,-1,-2,-3 and-4 were evaluated.

RepR is required for virulence in *R. solanacearum* UY031 but not for HR elicitation

Since RepR was necessary for full bacterial growth in plant apoplast, we decided to test the contribution of RepR on pathogenicity in potato and tomato plants, two hosts of *R. solanacearum* UY031. To this end, potato roots were injured followed by soil inoculation with the WT or the *ΔrepR* strains (Figure 3A). In few cases, a slight delay in wilting symptoms could be observed during the first days post inoculation, suggesting that RepR is involved in pathogenicity. To better visualize the effect of RepR on virulence, soil inoculation assays were repeated in potato plants without previous root injury. As shown in Figure 3B, deletion of *repR* had a more striking effect on virulence than in root-wounded plants and a great proportion of plants did not wilt after 3 weeks-post-inoculation. Similar results were obtained in uninjured soil-inoculated tomato plants (Figure 3C).

R. solanacearum UY031 is able to elicit a HR in tobacco plants, which is dependent on a functional T3SS. To determine whether RepR affects T3SS functionality, we infiltrated *Nicotiana benthamiana* leaves with different dilutions of the WT and *ΔrepR* strains. No differences in HR elicitation could be observed between the WT and the RepR mutant at the tested dilutions (Figure 4), suggesting that RepR is not necessary for T3SS *in vivo* functionality.

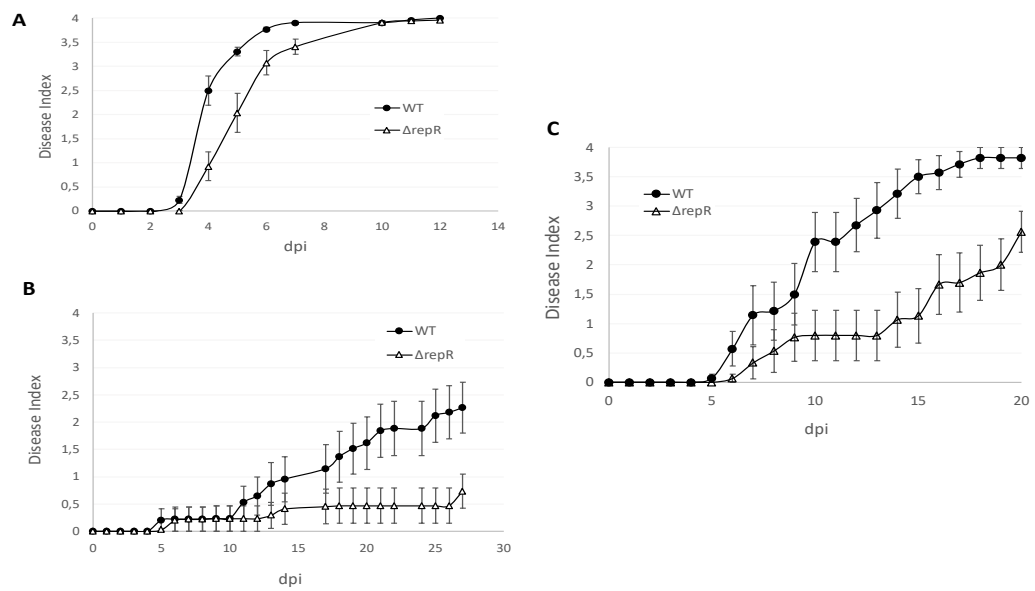

Figure 3. *R. solanacearum* UY031 pathogenicity tests.
Soil inoculation tests on A) potato with root wounding, B) potato without root wounding and C) tomato without root wounding.

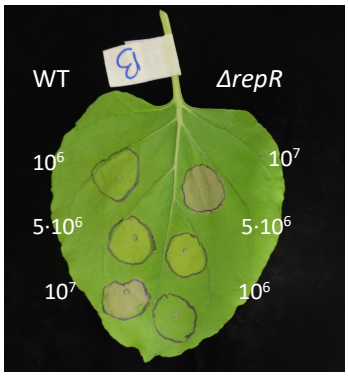

Figure 4. Hypersensitive response test in *Nicotiana benthamiana* plants.

WT and *ΔrepR* strains were grown overnight in liquid rich medium and serially diluted 5-fold in water (10^7, $5{\cdot}10^6$ and 10^6 CFUs/ml) and leaf-infiltrated in *Nicotiana benthamiana*. HR responses were photographed at 5 dpi.

RepR acts as a metabolic repressor in the apoplast

As RepR is a member of the MarR family of transcription factors, we hypothesized that it might regulate expression of downstream genes. To elucidate its function in the apoplast, we performed an RNA-sequencing analysis of the WT (Puigvert et al, unpublished, chapter 7) and *ΔrepR* strains in potato leaf apoplast, since this appeared to be the most relevant condition for RepR functionality. To identify the *in planta* RepR-regulated genes, the same bioinformatic pipeline developed in our previous *R. solanacearum* root trancriptome was applied ((Puigvert et al. 2017), chapter 5). More than 20 million reads mapped onto the *R. solanacearum* UY031 reference genome in each sample (Supplementary Table 3), and the principal component analysis showed that data was robust enough to capture differences between the strains (Supplementary Figure 2). Gene expression was considered statistically significant when $p<0.01$ and $|\log_2(FC)|> 0.5$. With this parameters, the analysis revealed that RepR is responsible for direct and indirect transcriptional regulation of 563 genes, from which 170 are down-regulated and 393 are up-regulated in the *ΔrepR* (Supplementary Table 4). Although this result reflects that RepR can both induce and repress gene transcription in the apoplast, approximately 70% of the total differentially expressed (DE) genes are repressed by RepR, suggesting that it mainly acts as a repressor. Interestingly, almost 20% of the down-regulated genes in wild potato roots (Puigvert et al. 2017) are RepR-repressed in potato leaf apoplast. We also compared the RepR-regulated genes dataset to already published *R. solanacearum* gene expression data *in planta* (Brown and Allen 2004; Jacobs et al. 2012; Meng et al. 2015; Khokhani et al. 2017; Puigvert et al. 2017) or to a list of described virulence factors (Supplementary Table 5). We found that 40% of the RepR-regulated genes have been identified in previous studies, either during *in planta* colonization or because they are key for disease development. We also detected that RepR is negatively regulated by PhcA *in vitro* and *in* planta (Khokhani et al. 2017; Perrier et al. 2018). To further investigate the role of RepR, we classified the 563 DE genes into functional categories (Table 2), and found a small proportion of previously defined virulence factors such as secretion systems, motility, and Reactive Oxygen Species (ROS) detoxification enzymes, among others. However, the analysis indicates that RepR is a major regulator controlling the expression of 37 other transcription factors and two-component

systems. Among the RepR-induced genes there is a vast majority of hypothetical proteins and transposases. On the other hand, RepR-repressed genes are enriched with transporter and metabolic-related genes, in addition to cyctochromes, methyltransferases and hypothetical proteins. To better characterize the RepR-regulated metabolic pathways, we represented them by mapping the RepR-induced and repressed genes onto the IPATH3 metabolic map. As highlighted in blue in Figure 5, RepR mainly represses Lipopolysaccharide (LPS) biosynthesis, the Phosphotransferase system (PTS) for sucrose uptake and utilization, fatty acid and several amino acid degradation pathways and cofactor metabolism, such as biosynthesis of biotin, porphyrin, riboflavin and thiamine. In contrast, RepR-induced pathways (highlighted in yellow) only include benzoate degradation and tyrosine metabolism. Altogether, our results indicate that RepR is a major metabolic repressor controlling the expression of different metabolic traits in *R. solanacearum* during apoplast colonization.

Table 2. Functional categories enriched in the RepR-induced and repressed genes in leaf apoplast.
Numbers indicate the percentage of genes in each category.

Functional category	RepR-induced	RepR-repressed
Secretion	2.9	2.5
Motility	0.6	1.8
ROS-detoxification	1.8	0.5
Other virulence	0.6	1.0
Methyltransferases	0.6	2.0
Cytochromes	0.0	1.8
Transcriptional regulators	6.5	6.9
Transposases	27.1	1.0
Transporters	10.0	12.5
Metabolism	12.4	43.5
Hypothetical/others	37.6	26.5

Figure 5. Metabolic pathway representation of the differentially RepR-induced and repressed genes.
R. solanacearum DE genes involved in metabolism were mapped onto Kegg pathways using IPATH3. RepR-induced and repressed pathways are highlighted in yellow and blue, respectively.

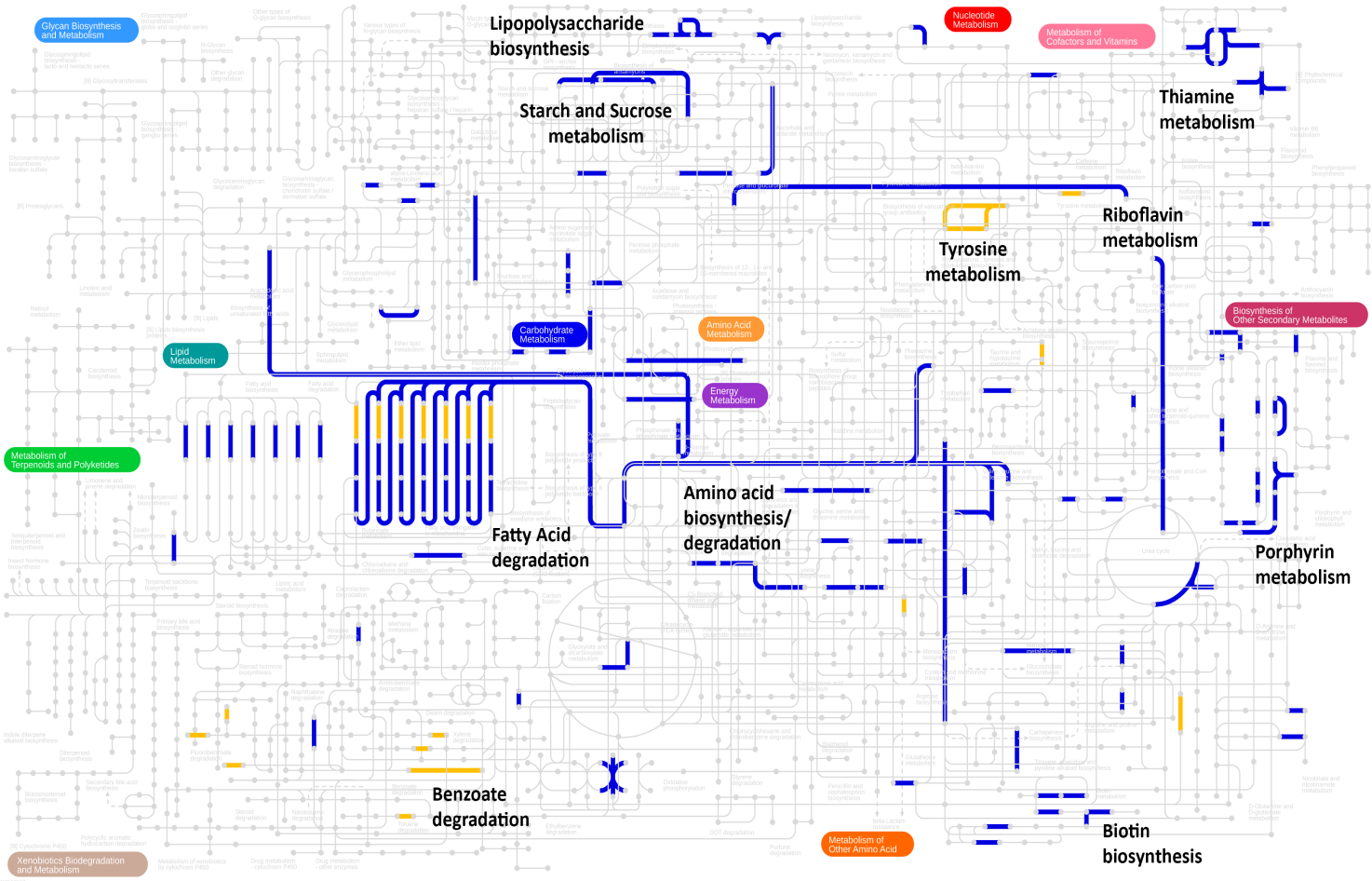
Glycan Biosynthesis and Metabolism
Lipopolysaccharide biosynthesis
Nucleotide Metabolism
Metabolism of Cofactors and Vitamins
Starch and Sucrose metabolism
Thiamine metabolism
Riboflavin metabolism
Tyrosine metabolism
Biosynthesis of Other Secondary Metabolites
Carbohydrate Metabolism
Amino Acid Metabolism
Lipid Metabolism
Energy Metabolism
Metabolism of Terpenoids and Polyketides
Amino acid biosynthesis/ degradation
Fatty Acid degradation
Porphyrin metabolism
Benzoate degradation
Biotin biosynthesis
Metabolism of Other Amino Acid
Xenobiotics Biodegradation and Metabolism

Discussion

RepR, a conserved MarR regulator in *R. solanacearum*, is specifically induced at early stages of plant infection

A MarR transcription regulator from *R. solanacearum* UY031, renamed RepR, was identified in a previous transcriptome during root colonization of wild potato plants ((Puigvert et al. 2017), chapter 5). High RepR conservation among the *R. solanacearum* species complex suggested that this gene might provide the pathogen with some biological advantage at least at certain stages of its life cycle (Figure 1). Interestingly, RepR was highly induced in *R. solanacearum* during root colonization compared to solid rich medium (Table 1). Actually, RepR expression was always induced during plant colonization compared to any reference condition (Supplementary Table 2). Induction was maintained when we compared *in planta* expression to minimal medium, a condition that is known to induce virulence gene expression (Arlat et al. 1992). In addition, the role of RepR appeared to be important at early infection stages, since its expression was highest during apoplast colonization and decreased as the disease progressed (Table 1). Since tolerant plants limit bacterial spread (Prior et al. 1994), the pathogen behavior in resistant plants might be more similar to that of initial colonization stages in susceptible hosts. This is probably the reason why RepR appeared to be more induced in infected tolerant plant roots versus susceptible plants (Puigvert et al. 2017). In line with this hypothesis, we found that RepR is negatively controlled by the master regulator PhcA both *in vitro* and *in planta* (Khokhani et al. 2017; Perrier et al. 2018). PhcA is known to be strongly induced at higher bacterial densities (Schell 2000), thus enabling RepR expression at initial infection stages and repressing its transcription later on. Altogether, these data strongly suggest that RepR plays an important role in the early *in planta* colonization by *R. solanacearum*.

RepR contributes to virulence in the first plant colonization steps

Since MarR regulators have been generally defined as sensors of changing environments (Grove 2017), we hypothesize that RepR is necessary for *R. solanacearum* adaptation to the apoplastic plant niche. To demonstrate that RepR function is especially important at early plant colonization steps, we first checked the ability of the *ΔrepR* strain to grow in apoplast, the plant environment that appeared to be more relevant for RepR function. Since *R. solanacearum* behaves similarly in root and plant apoplast (Hikichi 2016), bacterial growth was monitored in potato leaf apoplast to obtain increased reproducibility between experiments. We report that RepR contributes to bacterial fitness in plant apoplast, since the mutant exhibited a delay in growth during the first two days post-inoculation. The fact that the mutant is unable to maintain its original population within the first 12 hpi but it recovers its multiplication capacity later on (Figure 2), further supports the notion that RepR contributes to early adaptation in the apoplast, and in consequence, it might affect *R. solanacearum* pathogenicity. In fact, colonization of apoplast, or intercellular spaces, is a key step for virulence in *R. solanacearum* (Hikichi et al. 2007). Moreover, several MarR transcription

regulators have been described to act as virulence factors in many bacterial phytopathogens such as *X. campestris*, *D. dadantii* or *P. carotovorum* (Qian et al. 2005; Wei et al. 2007; Sjoblom et al. 2008; Haque et al. 2009). In *R. solanacearum*, the MarR regulator PrhN was also described to play a role in tomato and tobacco pathogenicity by controlling expression of the T3SS and T3Es (Zhang et al. 2015). We thus tested whether RepR also contributed to *R. solanacearum* virulence on host plants, and we found out that, similar to PrhN, *ΔrepR* was slightly less virulent than the WT when plant roots were wounded (Figure 3A), and even less virulent when plants were soil-inoculated without disturbing the roots (Figure 3B and C). The same virulence delay was observed independently on the host plant used, since both potato and tomato plants wilted to the same extent (Figure 3B and C). On the contrary, deletion of RepR caused no effect on the ability of *R. solanacearum* to elicit a HR in tobacco plants (Figure 4). Although a few T3SS genes appeared to be repressed by RepR (Supplementary Table 4), our data suggests that RepR-downregulation of some *hrp* genes might be insufficient to produce a detectable effect. In summary, these results indicate that RepR participates in *R. solanacearum* virulence by contributing to colonization of intercellular spaces, and does not completely affect T3SS function as measured by HR elicitation in resistant plants.

Metabolic reprogramming in *R. solanacearum* by RepR during apoplast colonization

MarR-transcription regulators usually control the expression of sets of genes that are necessary for adaptation by acting as environmental sensors and genetic switches (Grove 2017). Our RNAseq data revealed that RepR is able to reprogram more than 10% of the *R. solanacearum* genome in the apoplast, including 37 transcription regulators and two component systems, such as PehR, which is known to regulate the expression of some virulence factors in *R. solanacearum* (Allen et al. 1997). In fact, among the RepR-DE genes there are few previously described virulence factors: motility, secretion systems and ROS detoxification enzymes (Table 2, Supplementary Table 4). The RepR-induced genes include a majority of hypothetical proteins and transposases, which we already reported to be induced during root colonization (Puigvert et al. 2017), suggesting a genetic reprogramming to adapt to the new conditions (Casacuberta and Gonzalez 2013). RepR also induces tyrosine metabolism and benzoate degradation pathways (Figure 5). It is well known that plants accumulate phenolic compounds not only for growth but also as defense mechanism. Interestingly, it was recently described that the vascular pathogen *X. campestris* requires degradation of 4-Hydroxybenzoate for full virulence (Wang et al. 2015).

Although RepR both activates and represses genetic transcription, it appears to mainly act as a repressor since more than 70% of the DE genes were RepR-repressed. Among the RepR-repressed genes we found cytochromes, methyltransferases and a vast majority of genes involved in metabolism. When the metabolic pathways encoded by these genes were graphically represented, a clear enrichment in cofactor (biotin, thiamine, porphyrin and riboflavin) metabolism, the PTS system for sucrose utilization and fatty acid and amino acid degradation was found. Cofactors are needed for the proper function of some enzymes, thus, an arrest of their synthesis together

with a repression in fatty acid degradation suggests that these reactions might not be essentially needed during survival in plant apoplast. Since sucrose levels are higher in xylem sap than in apoplastic fluid (Jacobs et al. 2012; Zuluaga et al. 2013) it is expected that the *scr* genes from the PTS system will be induced at a later stage. Amino acids, on the other hand, are a carbon and nitrogen source that *R. solanacearum* metabolizes fast during growth in leaf apoplastic fluid (see annex (Zuluaga et al. 2013)). In our metabolic analysis we found that valine, leucine, proline, arginine and histidine are RepR-repressed, probably indicating that they were catabolized within the first few hours independently of RepR. Furthermore, RepR down-regulated genes account for almost 20% of the genes found repressed in the root apoplast in our previous root transcriptome analysis ((Puigvert et al. 2017, chapter 5). This observation further endorses the idea that RepR plays a key role at this stage of plant colonization and places leaf apoplast as a robust mimic condition of the root infection stage.

Recently, a catabolic repressor called EfpR, was described to provide *R. solanacearum* metabolic versatility through the acquisition of evolved mutations (Perrier et al. 2016). In fact, loss of function mutations are a common event in bacterial adaptation to challenging conditions (Hottes et al. 2013). Our dynamic gene expression analyses demonstrate that *repR* induction decreases in advanced disease stages (Table 1). Whether this decrease in expression is due to evolved mutation, mediated by PhcA or another mechanism, remains to be tested. In any case, our observations suggest that, similarly to EfpR, RepR inactivation might allow the bacterium to expand its metabolic capabilities as the disease progresses. This hypothesis is further supported by the fact that sucrose utilization, repressed by RepR in the apoplast, has been described to be highly induced at later infection stages (Jacobs et al. 2012).

Future experiments will be addressed at validating *repR* induction in root apoplast and the actual metabolic capabilities of *ΔrepR* using a Biolog plate assay. Nonetheless, this study shows that RepR is a novel player in the regulation of *R. solanacearum* metabolic adaptation to early infection stages.

Materials and Methods

Bacterial strains and plant growth conditions

The reporter *Ralstonia solanacearum* strain UY031 (Guarischi-Sousa et al. 2016) carrying the *psbA* promoter fused to the LUX operon (Cruz et al. 2014) was regularly grown in solid rich B medium supplemented with gentamycin 75 µg/ml.

Solanum tuberosum cv. Desirée plants were propagated *in vitro* as described (Zuluaga et al. 2015), transferred to peat soil and grown at 22ºC in long day conditions (16h/8h light/dark) for two weeks prior to acclimation for *R. solanacearum* inoculation. *Solanum lycopersicum* cv. Marmande and *Nicotiana benthamiana* plants were grown for three weeks in pots containing peat soil in the greenhouse under long day conditions (16h/8h, light/dark, 25 ºC/22ºC).

Construction of *repR* mutant and complemented strains

To delete the *repR* gene (RSUY_RS08455) from *R. solanacearum* UY031, 1kb-flanking regions were PCR amplified from genomic DNA using the Platinum Pfx DNA polymerase (ThermoFisher Scientific). The tetracyclin resistance cassette was amplified from the pG-T plasmid (Monteiro et al. 2012b) and inserted between the two fragments by double-joint PCR as described (Yu et al. 2004) to replace the wild-type gene locus by homologous recombination after natural transformation (Boucher C.A. 1985).

To construct the complemented *ΔrepR* strain, the complete *repR* open reading frame (plus 322 bp upstream of the ORF) was PCR amplified using primers PrepR-F and repR-R, inserted into the pENTR/TOPO/SD vector (Invitrogen, ThermoFisher Scientific) following manufacturer's instructions and transformed by heat-shock into chemically competent *E. coli* MACH1 cells. The Promoter::gene construction was introduced by an LR reaction in the destination vector pRCG::GWY (Monteiro et al. 2012b) to generate pRCG::PrepR::repR, which was stably integrated into *R. solanacearum*'s genome (Monteiro et al. 2012b).

The list of primers used to construct the mutant and the complemented strains is listed in Supplementary Table 1. New strains were always validated by PCR.

Hypersensitive response tests in tobacco plants

R. solanacearum UY031 WT and *ΔrepR* strains were grown overnight in liquid rich medium, washed and adjusted to 10^7, $5{\cdot}10^6$ and 10^6 CFUs/ml with sterile distilled water. Bacterial suspensions were leaf-infiltrated in *N. benthamiana* plants using a 1ml needleless syringe. Plants were left under continuous light and hypersensitive responses were recorded at 6 days post infiltration.

Virulence assays on potato plants

Potato and tomato plants used for pathogenicity tests were pre-acclimated for 3 days at 28ºC and 12/12 hour-photoperiod prior to *R. solanacearum* inoculation. Virulence tests were perfomed with and without root wounding. In the first case, roots were wounded with a 1 ml tip by digging 4-5 times in the peat soil. In both types of assays, each plant was watered with 40 ml of a 10^7 bacterial cells/ml solution. Wilting symptoms were recorded every day for each plant according to the following wilting scale: 0 – no wilting, 1 – 25 % wilted leaves, 2 – 50%, 3 – 75% and 4- dead plant.

Bacterial growth in leaf apoplast

Bacterial growth in potato leaf apoplast was assessed for *R. solanacearum* UY031 WT and *ΔrepR* strains as follows: 10^5 CFUs/ml bacterial suspensions were vacuum infiltrated in potato leaves for 30sec-1min. Before each sample collection, some leaves were detached from the plants and vacuum infiltrated with sterile water. Each biological replicate consisted on two leaves from different plants, and three biological replicates were used per strain and time point. 24 plants were used in total in each experiment. Water-infiltrated leaves were dried with towel paper, rolled and centrifuged at 2000 rpm inside 10 ml cut tips placed in 50 ml tubes. Apoplastic fluid from each replicate was collected in separate tubes and luminescent levels were measured. Apoplast was 10-fold diluted and 20 µl of each dilution were plated onto rich medium plates supplemented with gentamycin 75 µg/ml (WT strain selection) or tetracyclin 10 µg/ml (*ΔrepR*). Colonies were counted 24 hours after incubation.

Sample preparation, RNA extraction and sequencing

Experimental conditions for *in planta* gene expression data for *R. solanacearum* UY031 WT were obtained from Puigvert et al, unpublished. The same protocol was followed to obtain *ΔrepR* samples from potato leaf apoplast. Briefly, leaves from potato plants were vacuum-infiltrated using an initial inoculum of $5 \cdot 10^8$ cells/ml. Plants were incubated at 28ºC 12/12 hour-photoperiod for 6 hours, and apoplastic fluid enriched with bacteria was recovered as described before. Luminescence and colony forming units (CFU) were measured for each sample before the final centrifugation step at 4ºC for 1 minute at maximum speed. Samples from 12 plants were pooled together in each biological replicate. Bacterial pellets were immediately frozen in liquid nitrogen and routinely kept at-80ºC.

Total RNA was extracted using the SV Total Isolation kit (Promega) and RNA concentration was measured with a Nanodrop ND-8000. RNA integrity was evaluated using the Agilent 2100 Bioanalyzer, and only samples with an RNA Integrity Number > 8.5 were used for sequencing. To deplete ribosomal rRNA, 2.5 µg of total RNA were treated with the Ribo-Zero rRNA Removal Kit for Gram-Negative bacteria, followed by library preparation using TruSeq Stranded Total RNA Sample Prep Kit. Three biological replicates for each condition were used for sequencing using the Illumina HiSeq2000 platform in Macrogen Inc. (Seoul). 100-bp paired-end sequences in stranded libraries were obtained. Raw data will be available in the Sequence Read Archive.

Bioinformatic analysis of RNA-seq data

Prior to the analysis, raw data quality was checked with FASTQC (version 0.11.4). RNA-seq reads were mapped using Bowtie2 (version 2.2.6; (Langmead and Salzberg 2012) with already defined stringency parameters (Puigvert et al. 2017) onto *R. solanacearum* UY031 complete genome sequence (Guarischi-Sousa et al. 2016). Quantification of aligned reads was carried out using HTSeq-count (version 0.6.1; (Anders et al. 2015). To compare gene expression between WT and *ΔrepR*, RNAseq data corresponding to the same apoplast condition obtained with the WT UY031 strain (Puigvert et al, unpublished) was used. DE analysis was performed using the R (version 3.3.2) DESeq2 package (version 1.12.3; (Love et al. 2014) on high quality RNAseq reads considering genes with a $|\log2(\text{fold-change})| > 0.5$ and $q < 0.01$ as differentially expressed.

Metabolic pathway detection

To obtain diagrams of RepR-regulated metabolic pathways, aminoacid sequences of the differentially expressed genes were uploaded into the Kegg Mapper tool (http://www.kegg.jp/kegg/tool/annotate_sequence.html). Protein sequences were extracted from Genbank accessions CP012687.1 (chromosome) and CP012688.1 (megaplasmid). Kegg-Orthology identifiers were used to vizualize the metabolic pathways enriched in the DE gene lists with IPATH3 (Yamada et al. 2011).

Acknowledgements

We thank C. Balsalobre and C. Madrid for their advice in the interpretation of metabolic data. This work was funded by projects AGL2013-46898-R and RyC 2014-16158 from the Spanish Ministry of Economy and Competitiveness. We also acknowledge financial support from the "Severo Ochoa Program for Centres of Excellence in R&D" 2016-2019 (SEV-2015-0533) and the CERCA Program of the Catalan Government (Generalitat de Catalunya) and from COST Action SUSTAIN (FA1208) from the European Union. MP holds an APIF doctoral fellowship from Universitat de Barcelona.

Supplementary Data

6

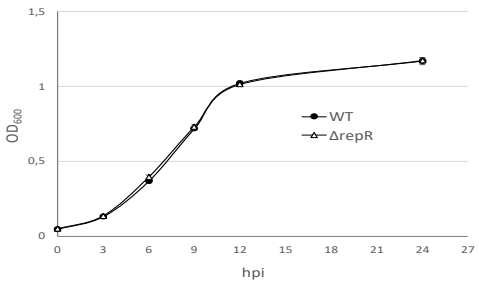

Supplementary Figure 1. Bacterial growth curves in liquid rich medium.

R. solanacearum UY031 WT and *ΔrepR* strains were grown in liquid rich medium cultures at a starting OD_{600}= 0.05 for 24 hours post inoculation (hpi).

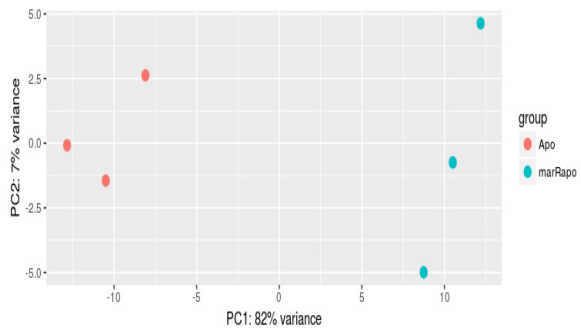

Supplementary Figure 2. Principal component analysis of *R. solanacearum* mapped reads.

Supplementary Table 1. List of primers used to generate mutant and complemented constructs of *repR* (RSUY_RS08455).

Primer ID	Sequence	Properties
Tet-F2	CGTTAACCCTAGGGGATCCT	Tc cassette amplification from pG-T plasmid
Tet-R2	GCACTAGTGATTAGTACTTCAAT	
RepR-RecA- F1	GATCAGGTCGATGCTCAGGTGG	1st round PCR to amplify right-flank of repR
RepR-RecA- R1	CGCTGAGGATCCCCTAGGGTTAACGCACCGCATTGCCCCGACTTT	
RepR-RecB- F3	CGATTGAAGTACTAATCACTAGTGCGCGGTAGTCCTCCACCCGGA	1st round PCR to amplify left-flank of repR
RepR-RecB- R3	CGATCTTGCCGACGTAGCTC	
RepR-nest-F	CTCGTCCACCTGTTCCAGTTC	Nest primers for 3rd round PCR to replace repR
RepR-nest-R	GAGGATGGTCTCGAACAGCG	
PrepR-F	CACCTGGGTATGAACTCGGAAACGAC	Amplification of 322 bp of the promoter region plus the repR coding sequence
repR-R	TCAGCTGCCGGCCGGGCG	

Supplementary Table 2. *repR* log_2FC values in leaf apoplast compared to four in vitro reference conditions [a]

Plant species	*S. tuberosum* leaf apoplast			
Reference condition	**Solid plates rich medium**	**Liquid culture rich medium**	**Solid plates minimal medium**	**Liquid culture minimal medium**
log_2FC[b]	4.69	4.72	3.61	4.07

[a] Unpublished data (Puigvert et al, chapter 7).

[b] Expression values compared to bacteria grown on leaf apoplast in relation to each in vitro reference condition using p<0.01

Supplementary table 3. Total and mapped sequencing reads from *R. solanacearum* UY031 WT and *ΔrepR* strains in potato leaf apoplast.

Sample ID	Total reads	Aligned reads	% mapping
Apoplast-WT1	21879209	18225945	83.30
Apoplast-WT2	26766576	22641780	84.59
Apoplast-WT3	24945027	20106785	80.60
Apoplast-RepR1	31824044	24196383	76.03
Apoplast-RepR2	33698251	27153421	80.58
Apoplast-RepR3	30944153	23157570	74.84

Supplementary Table 4. List of RepR-regulated genes in leaf apoplast

UY031 NCBI locus	Gene name	LOG_2FC	Description
MOTILITY			
RSUY_RS13200	pilA	-2,09	type 4 fimbrial pilin signal peptide protein
RSUY_RS07745	-	1,34	signal peptide protein
RSUY_RS16735	flgA	1,64	flagellar basal body P-ring biosynthesis protein FlgA
RSUY_RS09670	pilZ	1,69	putative type 4 fimbrial biogenesis protein
RSUY_RS16905	fliI	1,77	flagellum-specific ATP synthase
RSUY_RS20895	tadD	2,05	lipoprotein transmembrane
RSUY_RS16900	fliH	2,42	flagellar assembly protein FliH
RSUY_RS16820	fliO	3,18	flagellar biosynthesis protein FliO
SECRETION			
RSUY_RS12910	RipAA	-2,19	type III effector avra protein
RSUY_RS00730	-	-1,91	putative RHS-related protein
RSUY_RS00735	-	-1,67	putative RHS-related protein
RSUY_RS17090	-	-1,54	rhs-related protein
RSUY_RS17095	-	-1,37	putative RHS-related protein
RSUY_RS02580	tatB	1,42	sec-independent translocase
RSUY_RS01665	gspL	1,60	general secretory pathway L transmembrane protein
RSUY_RS19715	hrcQ	2,01	Hrp conserved protein HRCQ
RSUY_RS09380	RipM	2,07	hypothetical protein RipM type III effector
RSUY_RS19695	hrpW	2,13	HRPW transmembrane protein
RSUY_RS19660	prhR	2,37	component PRHR transmembrane protein
RSUY_RS19755	hrpF	3,06	type III secretion system protein HrpB
RSUY_RS19765	hrpD	3,38	hypothetical protein
RSUY_RS01655	gspN	3,67	general secretory pathway N transmembrane protein
RSUY_RS19750	hrpH	4,12	HRPH protein
ROS DETOXIFICATION			
RSUY_RS22220	katE	-1,87	catalase hydroperoxidase HpiI oxidoreductase

RSUY_RS17495	ahpC1	-1,63	alkyl hydroperoxide reductase subunit C
RSUY_RS12705	sodB	-1,56	superoxide dismutase [Fe] protein
RSUY_RS12010	sodC	1,76	superoxide dismutase Cu-Zn precursor protein
RSUY_RS01145	soxF	2,51	sulfide dehydrogenase flavocytochrome C oxidoreductase
EFFLUX PUMPS/PORINS/TRANSPORTERS			
RSUY_RS08440	emrB	-2,75	multidrug resistance B (translocase) transmembrane protein
RSUY_RS08310	ugpE	-2,72	SN-glycerol-3-phosphate transmembrane ABC transporter
RSUY_RS17125	-	-2,41	ABC-type uncharacterized transport system
RSUY_RS03765	-	-2,12	porin signal peptide protein
RSUY_RS17750	-	-2,03	lysine-specific permease protein
RSUY_RS12830	-	-1,90	sugar translocase
RSUY_RS03760	-	-1,87	Permease of the drug/metabolite transporter (DMT) superfamily
RSUY_RS22835	-	-1,87	Predicted permease, DMT superfamily
RSUY_RS08305	ugpA	-1,86	glycerol-3-phosphate transmembrane ABC transporter protein
RSUY_RS18295	czcA	-1,81	cation efflux system transmembrane protein
RSUY_RS05185	-	-1,77	sulfate transporter
RSUY_RS10755	pstA	-1,67	ABC-type phosphate transporter permease subunit
RSUY_RS00360	-	-1,67	amino acid-binding periplasmic (PBP) ABC transporter protein
RSUY_RS15085	-	-1,53	multidrug transport system
RSUY_RS06550	-	-1,41	ABC-type metal ion transport system
RSUY_RS11525	-	-1,32	branched-chain amino acid ABC transportersubstrate-binding
RSUY_RS17525	feoB	-1,22	ferrous IRON transport B transmembrane protein
RSUY_RS21905	-	1,39	multidrug MFS transporter
RSUY_RS04740	-	1,46	ABC-type uncharacterized transport system
RSUY_RS14675	-	1,47	ABC-type Fe3+-hydroxamate transport system
RSUY_RS01855	czcD	1,51	cation transporter
RSUY_RS10810	-	1,63	leucine export protein LeuE
RSUY_RS02690	-	1,65	putative IRON transport-sensory transduction transmembrane
RSUY_RS04895	-	1,71	aankyrin repeat-containing protein, MFS transporter
RSUY_RS21045	-	1,71	transmembrane multidrug efflux system transmembrane protein
RSUY_RS16600	mexC	1,71	multidrug efflux system protein
RSUY_RS16470	dinF	1,74	DNA-damage-inducible F transmembrane protein
RSUY_RS04060	-	1,74	transmembrane ABC transporter protein
RSUY_RS21315	-	1,75	putative outer membrane CHANEL lipoprotein transmembrane
RSUY_RS01500	-	1,84	ABC-type branched-chain amino acid transport systems
RSUY_RS18670	cobW	1,85	Low-affinity zinc transport protein
RSUY_RS18730	-	1,88	phosphate ABC transporter ATP-binding protein
RSUY_RS08675	ssuA2	1,90	alkanesulfonates binding protein precursor, ABC transporter
RSUY_RS01890	-	1,97	Arabinose efflux permease
RSUY_RS17335	-	2,00	amino acid ABC transporter permease

RSUY_RS17485	-	2,01	hemin transport protein
RSUY_RS12650	-	2,06	ABC transporter permease
RSUY_RS09230	-	2,07	Arabinose efflux permease
RSUY_RS12160	btuC	2,09	transmembrane ABC transporter protein
RSUY_RS04055	-	2,13	ABC transporter ATP-binding protein
RSUY_RS09715	-	2,15	ABC transporter ATP-binding protein
RSUY_RS13455	-	2,15	Predicted branched-chain amino acid permease
RSUY_RS21055	-	2,17	putative outer-membrane drug efflux protein
RSUY_RS13425	-	2,17	multidrug DMT transporter permease
RSUY_RS19435	-	2,21	probable abc transporter, atp-binding protein
RSUY_RS18740	-	2,23	amino acid transmembrane protein
RSUY_RS06865	-	2,24	Permeases of the drug/metabolite transporter (DMT) superfamily
RSUY_RS18735	-	2,26	amino-acid transmembrane protein
RSUY_RS22255	-	2,36	Arabinose efflux permease
RSUY_RS13140	rarD	2,36	Predicted permeases
RSUY_RS21100	-	2,38	ABC transporter ATP-binding protein
RSUY_RS08695	ssuB	2,44	aliphatic sulfonate ABC transporter ATP-binding protein
RSUY_RS12135	btuF	2,49	substrate-binding periplasmic (PBP) ABC transporter protein
RSUY_RS17045	-	2,53	multidrug resistance 1 transmembrane protein
RSUY_RS17480	-	2,54	abc-type transporter, periplasmic component protein
RSUY_RS13145	-	2,54	branched-chain amino acid transporter
RSUY_RS13965	-	2,60	Putative threonine efflux protein
RSUY_RS14495	-	2,63	ABC-type uncharacterized transport system, auxiliary component
RSUY_RS17330	-	2,64	ABC-type amino acid transmembrane protein
RSUY_RS12155	btuD	2,65	ABC transporter ATP-binding protein
RSUY_RS18430	-	2,66	putative outer membrane cation efflux system protein
RSUY_RS17215	-	2,80	Arabinose efflux permease
RSUY_RS18885	-	3,00	outer membrane CHANEL lipoprotein, RND transporter
RSUY_RS17470	-	3,12	iron ABC transporter
RSUY_RS17475	-	3,36	hemin ABC transporter permease
RSUY_RS19065	-	3,46	Predicted permease, DMT superfamily
OTHER VIRULENCE RELATED			
RSUY_RS00995	aidA	-2,09	conserved hypothetical protein
RSUY_RS05870	pacF	1,59	beta-ketoadipyl CoA thiolase
RSUY_RS21015	ohr	1,91	organic hydroperoxide resistance protein
RSUY_RS17380	vdh	2,20	vanillin dehydrogenase oxidoreductase protein
RSUY_RS05875	pcaB	3,14	3-carboxy-cis,cis-muconate cycloisomerase
TRANSCRIPTION/ TRANSCRIPTION REGULATORS/TWO-COMPONENT SYSTEM			
RSUY_RS08455	-	-12,58	putative MarR transcription regulator protein (RepR)
RSUY_RS17505	fur2	-2,24	Fur family transcriptional regulator

RSUY_RS22840	-	-2,02	LysR transcription regulator protein
RSUY_RS14995	-	-1,94	extracytoplasmic function sigma factor protein
RSUY_RS21275	-	-1,86	transcription regulator protein
RSUY_RS18185	-	-1,83	HxlR putative transcription regulator transcription regulator protein
RSUY_RS01430	-	-1,68	Transcriptional regulator, MarR family
RSUY_RS18255	czcR	-1,65	response regulator for cobalt zinc cadmium resistance
RSUY_RS03725	-	-1,57	Transcriptional regulator
RSUY_RS18130	-	-1,53	Transcriptional regulator
RSUY_RS15550	-	-1,46	LysR transcription regulator protein
RSUY_RS00225	-	1,40	response regulator transcription regulator protein
RSUY_RS14905	-	1,47	AraC transcription regulator protein
RSUY_RS14835	-	1,52	transcription regulator protein
RSUY_RS03270	pehR	1,53	Fis response regulator transcription regulator protein
RSUY_RS08630	-	1,57	IclR family transcriptional regulator
RSUY_RS21080	-	1,59	transcription regulator protein
RSUY_RS12195	-	1,67	LysR transcription regulator protein
RSUY_RS21290	-	1,77	two component transmembrane sensor kinase
RSUY_RS20850	-	1,81	probable transcription regulator protein
RSUY_RS00395	-	1,81	two-component sensor kinase transcription regulator protein
RSUY_RS22475	-	1,85	LysR transcription factor transcription regulator protein
RSUY_RS19035	-	1,87	IclR transcription regulator protein
RSUY_RS13305	-	1,93	TetR putative transcription regulator protein
RSUY_RS08180	-	1,99	LacI-related transcriptional regulator protein
RSUY_RS00390	-	2,06	XRE response regulator transcription regulator protein
RSUY_RS16570	-	2,06	LysR transcription regulator protein
RSUY_RS09695	-	2,13	LacI transcription regulator protein
RSUY_RS11415	-	2,16	LysR family transcriptional regulator
RSUY_RS15645	-	2,20	Fur family transcriptional regulator
RSUY_RS22070	-	2,21	transmembrane two-component sensor kinase
RSUY_RS11420	-	2,24	LysR transcription regulator protein
RSUY_RS22075	-	2,28	two-component response regulator
RSUY_RS19365	-	2,48	LysR family transcriptional regulator
RSUY_RS16010	-	2,49	LysR transcriptional regulatory dna-binding protein
RSUY_RS09900	-	2,50	two-component transmembrane sensor kinase
RSUY_RS17560	-	2,60	PadR family transcriptional regulator
RSUY_RS22085	hexR	2,68	putative transcription regulation repressor HEXR
TRANSPOSASES, PHAGE-RELATED, DNA REPLICATION			
RSUY_RS00295	TIS1021	-3,31	TIS1021 transposase
RSUY_RS18490	TIS1021	-3,04	TIS1021 transposase
RSUY_RS12915	tISRso10a	-2,93	ISRSO10-transposase ORFA protein

RSUY_RS22830	-	-2,91	putative bacteriophage related protein
RSUY_RS22920	TIS1021	-2,89	TIS1021 transposase
RSUY_RS05305	TIS1021	-2,88	TIS1021 transposase
RSUY_RS05165	-	-2,77	DNA transposition protein
RSUY_RS16520	TIS1021	-2,76	TIS1021 transposase
RSUY_RS14860	-	-2,76	Transposase
RSUY_RS05715	TIS1021	-2,69	TIS1021 transposase
RSUY_RS04720	TIS1021	-2,67	TIS1021 transposase
RSUY_RS18545	TIS1021	-2,63	TIS1021 transposase
RSUY_RS11070	TIS1021	-2,50	TIS1021 transposase
RSUY_RS20725	TIS1021	-2,49	TIS1021 transposase
RSUY_RS21750	TIS1021	-2,45	TIS1021 transposase
RSUY_RS06535	TIS1021	-2,40	TIS1021 transposase
RSUY_RS22705	TIS1021	-2,37	TIS1021 transposase
RSUY_RS05150	-	-2,31	putative phage-related dna-binding protein
RSUY_RS05095	-	-2,28	putative bacteriophage mu g-like protein
RSUY_RS22000	TIS1021	-2,26	TIS1021 transposase
RSUY_RS09775	-	-2,20	transposase protein
RSUY_RS05470	TIS1021	-2,19	TIS1021 transposase
RSUY_RS18460	-	-2,19	isrso8-transposase orfa protein
RSUY_RS19155	TIS1021	-2,16	TIS1021 transposase
RSUY_RS05100	-	-2,10	putative bacteriophage mu gp30-like protein
RSUY_RS18370	TIS1021	-2,09	TIS1021 transposase
RSUY_RS05110	-	-2,07	putative phage uncharacterized protein, c- terminal
RSUY_RS18455	-	-2,07	isrso8-transposase orfb protein
RSUY_RS16185	tISRso7	-2,05	ISRSO7-transposase protein
RSUY_RS00230	TIS1021	-2,04	TIS1021 transposase
RSUY_RS05225	-	-2,04	Mu-like prophage major head subunit gpT
RSUY_RS01770	TIS1021	-2,03	TIS1021 transposase
RSUY_RS18610	TIS1021	-2,00	TIS1021 transposase
RSUY_RS20825	-	-1,96	transposase (partial sequence) protein
RSUY_RS05265	-	-1,95	phage tail tape measure protein tp901, core region
RSUY_RS12505	TIS1021	-1,95	TIS1021 transposase
RSUY_RS03770	-	-1,92	transposase (partial sequence) protein
RSUY_RS00260	TIS1021	-1,90	TIS1021 transposase
RSUY_RS10485	-	-1,87	probable resolvase protein
RSUY_RS01200	TIS1021	-1,87	TIS1021 transposase
RSUY_RS20135	-	-1,85	probable phage replication cri-related protein
RSUY_RS00335	TIS1021	-1,81	TIS1021 transposase
RSUY_RS00320	-	-1,80	transposase (partial sequence) protein

RSUY_RS17745	-	-1,76	DNA helicase
RSUY_RS10440	-	-1,57	isrso8-transposase orfb protein
RSUY_RS05565	-	-1,40	probable bacteriophage protein
RSUY_RS07890	-	1,36	recombinase RecB
RSUY_RS07895	-	1,51	ATP-dependent exonuclease
RSUY_RS23190	-	1,53	integrase
RSUY_RS03965	recN	1,66	DNA repair protein
METHYLTRANSFERASES			
RSUY_RS00030	-	-1,82	putative isoprenylcysteine carboxyl methyltransferase
RSUY_RS02765	-	1,51	methyltransferase protein
RSUY_RS17415	-	1,81	probable methyltransferase protein
RSUY_RS15500	rrmB	1,94	putative RNA methyltransferase (SUN protein)
RSUY_RS06160	-	2,06	SPOUT methyltransferase superfamily protein
RSUY_RS11885	-	2,07	DNA mismatch repair protein MutS
RSUY_RS04115	ada	2,11	bifunctional methylated-DNA-protein-cysteine methyltransferase
RSUY_RS01125	-	2,31	Predicted methyltransferases
RSUY_RS04135	-	2,96	putative methylated-DNA--protein-cysteine methyltransferase
CYTOCHROMES			
RSUY_RS12530	-	1,73	Cytochrome c peroxidase
RSUY_RS09325	coxG	2,02	hypothetical protein
RSUY_RS09330	coxE	2,05	hypothetical protein
RSUY_RS21805	-	2,12	cbb3-type cytochrome C oxidase subunit III
RSUY_RS01140	-	2,16	Cytochrome c553
RSUY_RS20855	-	2,32	Cytochrome P450
RSUY_RS22135	coxO	3,08	cytochrome-C oxidase oxidoreductase protein
METABOLISM/ENERGY PRODUCTION			
RSUY_RS09425	-	-2,85	probable benzoate 1,2-dioxygenase beta subunit protein
RSUY_RS21820	-	-2,54	hydrolase /ayltransferase (alpha/beta hydrolase superfamily)
RSUY_RS06480	-	-2,36	NADP-dependent alcohol dehydrogenase oxidoreductase protein
RSUY_RS11385	-	-2,29	gst-related protein
RSUY_RS03740	-	-2,20	putative oxidoreductase protein
RSUY_RS18940	-	-2,19	putative diaminopimelate decarboxylase protein
RSUY_RS11455	-	-2,12	Fatty acid desaturase
RSUY_RS18945	trpC2	-2,07	indole-3-glycerol phosphate synthase protein
RSUY_RS05130	-	-2,01	putative lytic transglycosylase, catalytic protein
RSUY_RS01475	-	-2,01	putative tryptophan 2-monooxygenase oxidoreductase protein
RSUY_RS12820	-	-1,96	3'-hydroxymethylcephem-o-carbamoyltransferaseprotein
RSUY_RS03755	aldH	-1,92	aldehyde dehydrogenase
RSUY_RS08465	-	-1,85	C-5 sterol desaturase
RSUY_RS03750	-	-1,84	dihydrodipicolinate synthase

RSUY_RS09555	-	-1,76	trifunctonal enoyl-CoA hydratase/delta3-cis- delta2-trans-enoyl-CoA isomerase/3-hydroxyacyl-CoA dehydrogenase
RSUY_RS18770	-	-1,60	polyketide synthase
RSUY_RS10890	mel	-1,56	tyrosinase oxidoreductase protein
RSUY_RS09385	-	-1,42	nadph nitroreductase protein
RSUY_RS11145	exbB1	-1,42	biopolymer transport transmembrane protein
RSUY_RS21495	-	-1,40	Lactoylglutathione lyase
RSUY_RS05660	-	-1,36	putative acyl-coa dehydrogenase protein
RSUY_RS17535	-	1,26	histidine kinase
RSUY_RS13475	pepP	1,37	XAA-Pro aminopeptidase
RSUY_RS21285	-	1,37	proline rich transmembrane protein
RSUY_RS04455	kdtA	1,39	3-deoxy-D-manno-octulosonic-acid transferase
RSUY_RS20840	-	1,39	putative hemolysin activating-like protein
RSUY_RS07530	-	1,41	Transglutaminase-like
RSUY_RS06115	-	1,41	Lipid A core- O-antigen ligase
RSUY_RS08755	ilvG	1,44	acetolactate synthase 2 catalytic subunit
RSUY_RS05820	-	1,45	D-amino acid dehydrogenase small subunit
RSUY_RS06695	-	1,45	glycosyl transferase
RSUY_RS00665	-	1,46	cation-transporting ATPase transmembrane protein
RSUY_RS12310	-	1,47	putative oxidoreductase protein
RSUY_RS22090	glk	1,48	glucokinase protein
RSUY_RS06960	-	1,48	ferredoxin
RSUY_RS12300	-	1,49	chloride channel protein
RSUY_RS00650	-	1,50	ornithine cyclodeaminase
RSUY_RS15805	-	1,50	putative voltage-gated ClC-type chloride channel ClcB
RSUY_RS18875	-	1,53	putative CYNX-related transport transmembrane protein
RSUY_RS13450	-	1,53	Predicted phosphotransferase
RSUY_RS08705	-	1,55	diguanylate phosphodiesterase
RSUY_RS18300	hit	1,55	putative HIT-like protein
RSUY_RS15515	fmt	1,58	methionyl-tRNA formyltransferase
RSUY_RS12150	cobT	1,60	nicotinate-nucleotide--dimethylbenzimidazolephosphoribosyl transferase
RSUY_RS06325	-	1,60	putative deoxyribonucleotide triphosphate pyrophosphatase
RSUY_RS13690	-	1,60	Phosphatidylserine
RSUY_RS16640	-	1,61	metal-transporting P-type ATPase transmembrane protein
RSUY_RS21040	-	1,61	lipase protein
RSUY_RS21145	RS05425	1,62	lipoprotein signal peptide
RSUY_RS09630	-	1,64	N-acetyltransferase
RSUY_RS20160	-	1,64	putative thiol:disulfide interchange protein
RSUY_RS16565	-	1,65	oxidoreductase protein
RSUY_RS19545	-	1,66	ketoglutarate semialdehyde dehydrogenase protein

RSUY_RS17440	-	1,66	putative maltooligosyl trehalose trehalohydrolase protein
RSUY_RS11645	tpiA	1,66	triosephosphate isomerase
RSUY_RS10105	ispD	1,66	2-C-methyl-D-erythritol 4-phosphate cytidylyltransferase
RSUY_RS14735	-	1,66	Predicted sulfurtransferase
RSUY_RS12145	cobS	1,68	cobalamin synthase
RSUY_RS14165	trpD3	1,69	Anthranilate phosphoribosyltransferase
RSUY_RS06825	-	1,70	Chromate transport protein
RSUY_RS04050	pabB	1,72	putative PARA-aminobenzoate synthetase component I protein
RSUY_RS18645	-	1,72	rhodanese-like proteine
RSUY_RS12725	lpxK	1,73	tetraacyldisaccharide 4'-kinase
RSUY_RS13605	ttuD2	1,74	putative hydroxypyruvate reductase oxidoreductase protein
RSUY_RS08850	-	1,75	putative racemase transmembrane protein
RSUY_RS15360	thiG	1,76	thiazole synthase
RSUY_RS15445	cca	1,76	multifunctional tRNA nucleotidyl transferase/2'3'-cyclic phosphodiesterase/2'nucleotidase/phosphatase
RSUY_RS21235	-	1,77	putative fructokinase-like protein (sugar kinase)
RSUY_RS01895	-	1,77	Small-conductance mechanosensitive channel
RSUY_RS13435	pdxA	1,78	4-hydroxythreonine-4-phosphate dehydrogenase
RSUY_RS14760	-	1,78	enoyl-CoA hydratase
RSUY_RS15130	-	1,78	short chain dehydrogenase
RSUY_RS07970	-	1,79	Protein-L-isoaspartate carboxylmethyltransferase
RSUY_RS14940	rtcA	1,80	RNA 3'-terminal-phosphate cyclase
RSUY_RS18650	-	1,83	cystathionine beta-lyase (cysteine lyase) protein
RSUY_RS08555	-	1,83	lipoprotein transmembrane
RSUY_RS13115	purE	1,85	phosphoribosylaminoimidazole carboxylase catalytic subunit
RSUY_RS12125	cbiB	1,86	cobalamin biosynthesis protein
RSUY_RS04125	alkB	1,86	alkylated DNA repair protein
RSUY_RS14265	gpsA	1,86	NAD(P)H-dependent glycerol-3-phosphate dehydrogenase
RSUY_RS05010	-	1,87	Membrane-bound serine protease
RSUY_RS08925	-	1,88	Adenylate cyclase
RSUY_RS18700	cbiXC	1,89	Precorrin isomerase
RSUY_RS01600	eutC	1,90	ethanolamine ammonia-lyase small subunit
RSUY_RS06020	-	1,91	Geranylgeranyl pyrophosphate synthase
RSUY_RS21710	-	1,91	Amine oxidase
RSUY_RS08225	-	1,91	putative myo-inositol 2-dehydrogenase protein
RSUY_RS02680	ggt2	1,92	gamma-glutamyltranspeptidase precursor
RSUY_RS12130	cobD	1,94	putative threonine-phosphate decarboxylase
RSUY_RS03450	thiL	1,94	thiamine monophosphate kinase
RSUY_RS13055	-	1,95	putative amidohydrolase involved in phosphonate metabolism
RSUY_RS07615	-	1,95	Predicted metal-dependent phosphoesterase

RSUY_RS11950	-	1,95	bifunctional uroporphyrinogen-III synthetase/uroporphyrin-III C-methyltransferase
RSUY_RS13485	-	1,96	amino acid dehydrogenase transmembrane protein
RSUY_RS17555	-	1,98	Siderophore-interacting protein
RSUY_RS04800	-	1,99	Predicted metal-dependent hydrolase
RSUY_RS21855	-	2,00	putative arylesterase protein
RSUY_RS08710	-	2,01	esterase
RSUY_RS18310	serA2	2,02	2-hydroxyacid dehydrogenase
RSUY_RS09445	bioF	2,02	8-amino-7-oxononanoate synthase
RSUY_RS20520	-	2,03	putative n-acetyltransferase transferase protein
RSUY_RS08685	ssuD	2,04	alkanesulfonate monooxygenase
RSUY_RS20440	-	2,06	putative 2,3-dihydroxybenzoate-amp ligase protein
RSUY_RS12230	-	2,06	cobalamin biosynthesis protein CbiX
RSUY_RS15425	-	2,06	5-formyltetrahydrofolate cyclo-ligase
RSUY_RS21655	-	2,07	S-adenosylmethionine decarboxylase
RSUY_RS20425	-	2,07	probable polyketide synthetase protein
RSUY_RS18680	cbiG	2,11	cobalamin biosynthesis protein CbiG
RSUY_RS18710	chlID	2,12	chelatase protein
RSUY_RS14670	-	2,13	short chain dehydrogenase
RSUY_RS06170	-	2,15	nicotinic acid mononucleotide adenylyltransferase
RSUY_RS03805	proC	2,15	pyrroline-5-carboxylate reductase
RSUY_RS18570	paaD	2,18	phenylacetic acid degradation protein
RSUY_RS12595	-	2,18	glucose-1-dehydrogenase
RSUY_RS18225	-	2,19	putative hydrolase phosphatase protein
RSUY_RS11020	-	2,20	putative acyl coenzyme A thioester hydrolase protein
RSUY_RS11465	ureF	2,20	urease accessory protein UreF
RSUY_RS08155	iolI	2,23	protein implicated in myo-inositol catabolique pathway
RSUY_RS20505	-	2,23	cog0665, glycine/d-amino acid oxidase (deaminating) protein
RSUY_RS22990	-	2,25	Predicted nucleoside-diphosphate-sugar epimerases
RSUY_RS08205	iolD	2,25	putative acetolactate synthase protein
RSUY_RS08200	iolC	2,26	transferase kinase protein
RSUY_RS08760	menG	2,28	ribonuclease activity regulator protein RraA
RSUY_RS17210	-	2,28	D-alanine ligase
RSUY_RS13880	-	2,29	Acyl-coenzyme A synthetase
RSUY_RS13315	fabG	2,31	3-ketoacyl-(acyl-carrier-protein) reductase
RSUY_RS06990	-	2,32	putative ribokinase protein
RSUY_RS14840	-	2,32	putative gcn5-related n-acetyltransferase; protein
RSUY_RS20465	-	2,33	metal-dependent hydrolase
RSUY_RS06280	ahs2	2,33	Allophanate hydrolase subunit 2
RSUY_RS09740	-	2,33	pyruvate decarboxylase E1 (Beta subunit) oxidoreductase

RSUY_RS15045	-	2,34	2-dehydropantoate 2-reductase
RSUY_RS15930	-	2,35	oxidoreductase protein
RSUY_RS21270	ribB	2,36	3,4-dihydroxy-2-butanone 4-phosphate synthase protein
RSUY_RS08865	-	2,36	L-asparaginase precursor protein
RSUY_RS12040	-	2,37	formate dehydrogenase
RSUY_RS18810	-	2,37	enoyl-CoA hydratase
RSUY_RS17060	-	2,37	aldolase protein
RSUY_RS04140	-	2,39	putative acetyltransferase protein
RSUY_RS22500	-	2,40	6-phosphogluconate dehydrogenase protein
RSUY_RS17430	-	2,40	maltooligosyl trehalose synthase transmembrane protein
RSUY_RS03995	-	2,43	arginase
RSUY_RS07765	mesJ	2,47	putative cell cycle protein
RSUY_RS00075	gor	2,47	glutathione reductase oxidoreductase protein
RSUY_RS11470	ureE	2,47	urease accessory protein UreE
RSUY_RS12140	cobC	2,48	Fructose-2,6-bisphosphatase
RSUY_RS22095	pgl	2,49	6-phosphogluconolactonase oxidoreductase protein
RSUY_RS13885	-	2,50	Predicted acyltransferase
RSUY_RS08670	-	2,50	NADPH-dependent FMN reductase oxidoreductase protein
RSUY_RS14720	-	2,50	short chain dehydrogenase
RSUY_RS17435	-	2,51	putative 4-alpha-glucanotransferase (amylomaltase) protein
RSUY_RS20185	-	2,52	putative unsaturated glucuronyl hydrolase protein
RSUY_RS03890	glcE	2,53	glycolate oxidase FAD binding subunit
RSUY_RS14830	-	2,54	Phosphatidylserine decarboxylase
RSUY_RS18685	cbiF	2,55	precorrin-4 C11-methyltransferase protein
RSUY_RS20565	-	2,55	hippurate hydrolase protein
RSUY_RS14520	-	2,57	pantothenate kinase
RSUY_RS07705	-	2,64	glutamine amidotransferase
RSUY_RS19380	imuB	2,64	Nucleotidyltransferase
RSUY_RS15945	-	2,64	acyl-CoA dehydrogenase oxidoreductase protein
RSUY_RS14515	birA	2,69	biotin--protein ligase
RSUY_RS08220	-	2,70	putative isomerase-like tim barrel; protein
RSUY_RS20525	-	2,70	d-isomer specific 2-hydroxyacid dehydrogenase, nad-binding;
RSUY_RS13045	-	2,71	amidase
RSUY_RS11485	ureJ	2,73	urease accessory UREJ transmembrane protein
RSUY_RS19445	-	2,75	hydrolase protein
RSUY_RS11730	-	2,75	putative lipase transmembrane protein
RSUY_RS20545	-	2,76	putative oxidoreductase protein
RSUY_RS01030	ttuD1	2,77	hydroxypyruvate reductase protein
RSUY_RS09965	-	2,79	Predicted sugar kinase
RSUY_RS08135	iolG	2,79	oxidoreductase myo-inositol 2-dehydrogenase protein

RSUY_RS13915	-	2,86	Predicted 3-hydroxylacyl-(acyl carrier protein) dehydratase
RSUY_RS08145	-	2,87	pyridine nucleotide-disulphide oxidoreductase, classI protein
RSUY_RS13345	-	2,90	Monoamine oxidase
RSUY_RS18660	cbiA	2,95	cobyrinic acid a,c-diamide synthase
RSUY_RS09255	-	2,98	putative hydrolase protein
RSUY_RS09745	-	2,98	branched-chain alpha-keto acid dehydrogenase subunit E2
RSUY_RS15120	-	3,00	arginase
RSUY_RS13480	ubiH	3,02	2-octaprenyl-6-methoxyphenyl hydroxylase
RSUY_RS15355	-	3,03	sulfur carrier protein ThiS
RSUY_RS13320	-	3,09	Acyl dehydratase
RSUY_RS13465	-	3,13	putative mannose-1-phosphate guanyltransferase- related protein
RSUY_RS19455	-	3,23	fad flavoprotein transmembrane
RSUY_RS18900	-	3,28	enoyl-CoA hydratase
RSUY_RS15365	thiE1	3,39	thiamine-phosphate pyrophosphorylase protein
RSUY_RS07070	-	3,66	short chain dehydrogenase
RSUY_RS15600	-	3,99	Dienelactone hydrolase
RSUY_RS09450	bioD	4,90	dithiobiotin synthetase
RSUY_RS08640	moaD	5,28	molybdopterin MPT converting factor subunit 1
RSUY_RS02985	fruA	1,92	PTS system, fructose-specific IIBC component (EIIBC-fru) (fructose-permease IIBC component) transmembrane protein
RSUY_RS02995	fruB	1,97	multiphosphoryl transfer protein
RSUY_RS02990	fruK	1,54	1-phosphofructokinase protein
UNKOWN FUNCTION/HYPOTHETICAL PROTEINS			
This group comprises a total of 168 genes.			

Supplementary Table 5. References used to identify virulence factors in *R. solanacearum* UY031

Ailloud et al. 2015	Gonzalez et al. 2007	Meng et al. 2011	Tans-Kersten et al. 2001
Ailloud et al. 2016	Huang and Allen 2000	Meng 2013	Valls et al. 2006
Brown and Allen 2004	Jacobs et al. 2012	Meng et al. 2015	Wairuri et al. 2012
Brown et al. 2007	Khokhani et al. 2017	Peeters et al. 2013	Yao and Allen 2006
Dalsing et al. 2014	Li et al. 2016	Perrier et al. 2016	Zhang et al. 2011
Dalsing et al. 2015	Lowe et al. 2015	Plener et al. 2012	Zhang et al. 2013
Delaspre et al. 2007	Lowe-Power et al. 2017	Ray et al. 2015	Zhang et al. 2014
Flores-Cruz and Allen 2009	Lundgren et al. 2015	Schell 2000	Zhang et al. 2015
Flores-Cruz and Allen 2011			

chapter 7

DRAFT 2

Spatiotemporal transcriptomic changes of *Ralstonia solanacearum* UY031 during different potato infection stages

Spatiotemporal transcriptomic changes of *Ralstonia solanacearum* UY031 during different potato infection stages

M. Puigvert[1,2], P. Sebastià[2], R. de Pedro[1,2], A.P. Macho[3], R. Guarischi-Sousa[4], N. Sánchez-Coll[2], J.C. Setubal[4], M. Valls[1,2*]

[1]Department of Genetics, University of Barcelona, Barcelona, Catalonia, Spain

[2]Centre for Research in Agricultural Genomics (CSIC-IRTA-UAB-UB), Bellaterra, Catalonia, Spain

[3]Shanghai Center for Plant Stress Biology (PSC), Shanghai Institutes for Biological Sciences (SIBS), Chinese Academy of Sciences (CAS), Shanghai, China

[4] Departamento de Bioquímica, Universidade de São Paulo, São Paulo, Brazil

Abstract

R. solanacearum is the causal agent of the bacterial brown rot, a devastative plant disease responsible for serious economic losses especially on potato, tomato and other solanaceaous plant species in temperate countries. Many virulence determinants as well as their regulatory networks have been already identified in *R. solanacearum* through gene expression assays in minimal medium and, more recently, *in planta.* To date, most of the *in planta* transcriptomic studies performed in *R. solanacearum* focused on bacteria colonizing the xylem vessels at the onset of the disease. However, little is known about the genetic program that coordinates virulence gene expression and metabolic adaptation along the different plant colonization phases. To this end, we performed an RNA-sequencing transcriptome analysis of three different potato infection stages corresponding to early, mid and late phases of plant colonization. We further explored the impact of several reference conditions on data interpretation, including liquid or solid rich and minimal media. Our results show a dynamic expression of many virulence factors including the type III secretion system (T3SS) and effectors, motility and exopolysaccharide synthesis. Finally, we also investigated the metabolic changes of the pathogen throughout the infection process. This is the first report describing a dynamic transcriptome of a bacterial plant pathogen within the plant during the infection process, and our data not only corroborates previous results, but also adds new knowledge on the pathogen physiology during plant colonization.

Introduction

Brown rot of potato is a vascular disease caused by the bacterial phytopathogen *Ralstonia solanacearum*. This pathogen can infect over 200 different plant species, including many important crops such as potato, tomato, peanut, eggplant and banana, and is endemic of the tropical areas of the globe (Hayward 1991). However, strains classified as phylotype IIB-1 are acclimated to lower temperatures and grow optimally at 27ºC (Ciampi and Sequeira 1980) Although these strains presumably originated in the Andean highlands (Janse 2012), they were accidentally introduced in temperate European countries, where they could establish in waterways and reservoir weeds (Janse et al. 2004). As a result, several outbreaks affecting potato fields were reported in the early 1990s (Janse 1996), placing these strains as a major thread in Europe and North America (Champoiseau et al. 2009).

R. solanacearum has a complex life cycle. The pathogen survives in soil and water as saprophyte and enters the plant through root wounds or secondary root emerging points. Bacteria colonize the root intercellular spaces, or apoplast, which is the first plant hostile environment encountered by bacterial phytopathogens (Du et al. 2016). Attachment to host cells and colonization of the apoplast is key for *R. solanacearum* pathogenicity (Hikichi et al. 2007). Successful bacteria move to the xylem vessels, where the pathogen multiplies extensively and produce high amounts of exopolysaccharide (EPS). Occlusion of the vasculature due to massive EPS production and bacterial multiplication ultimately causes wilting symptoms and plant death (Vasse et al. 1995; Genin 2010).

To progress across the different plant tissues, the pathogen needs a large battery of virulence determinants, whose expression must be well orchestrated and tightly regulated. To date, many virulence factors have been described to play a role in *R. solanacearum* pathogenicity. These include the delivery of effector proteins inside the host cell by the type III secretion system (T3SS), EPS secretion, production of cell wall degrading enzymes and expression of protective enzymes against the oxidative burst (Meng 2013; Peeters et al. 2013). Most of the virulence genes in *R. solanacearum* were identified in *in vitro* studies using minimal medium conditions, which mimics bacterial behavior in the plant (Arlat et al. 1992). Nonetheless, gene expression studies performed *in planta* have been key to elucidate plant-dependent regulatory networks and led to the discovery of novel features involved in host adaptation, such as nitrogen assimilation, detoxification and the host's sucrose utilization (Jacobs et al. 2012; Dalsing and Allen 2014; Dalsing et al. 2015). However, most of the *R. solanacearum in planta* gene expression analyses only considered bacteria extracted from infected xylem vessels at the onset of the disease (Brown and Allen 2004; Jacobs et al. 2012; Meng et al. 2015; Ailloud et al. 2016; Khokhani et al. 2017).

Gene expression profiling throughout the infection cycle is essential to understand how the pathogen switches from one stage to the other. Lifestyle transitions have been well studied in

hemibiotrophic fungi such as *Colletotrichum higginisianum* (*Arabidopsis thaliana*), *C. graminicola* (maize) (O'Connell et al. 2012), *Dothistroma septosporum* (*Pinus radiata*) (Bradshaw et al. 2016), was well as in the oomycete *Phytophtora infestans* (tomato) (Zuluaga et al. 2016). However, the closest transcriptome dynamic studies performed in phytopathogenic bacteria correspond to *Xanthomonas oryzae* at different hours-post-incubation in rice leaf extracts (Kim et al. 2016), and very recently to *Pseudomonas syringae* in *A. thaliana* leaves (Nobori et al. 2018). *In planta* bacterial transcriptomes at different lifestyle phases are challenging, in the first place because lifestyle transitions are not as clear as in fungi (Kraepiel and Barny 2016). Besides, the need to enrich for bacterial RNAs, in particular at early infection stages at which bacterial yields are extremely low compared to the plant, represents an additional technical constraint (Van Vliet 2009). We previously proved that it is possible to analyze bacterial RNAs from infected plant tissue by bioinformatically selecting bacterial transcripts (Puigvert et al. 2017). This is especially interesting for incipient infections, but it is still cost-ineffective and it is preferable to enrich samples with bacterial cells prior to RNA isolation (Nobori et al. 2018).

To elucidate how *R. solanacearum* deploys its genetic program throughout the infection process, the transcriptome of a potato phylotype IIB-1 strain, *R. solanacearum* UY031, was analyzed at three different potato infection stages. The *in planta* conditions were set up with sufficient bacterial densities to perform subsequent bacterial isolation from the plant and RNA-sequencing. Early (leaf apoplast), mid (xylem from asymptomatic plants) and late infection stages (xylem from completely wilted plants) were determined. Furthermore, to understand how the reference condition used could impact our results, four reference conditions were analyzed: bacteria grown in rich and minimal medium in liquid cultures and solid plates. Our data validates previous results and shows that expression of the T3SS and effectors is inversely proportional, with a majority of effectors being massively induced at advanced disease stages. We also show that, unexpectedly, EPS synthesis is highly induced during apoplast colonization. Our results provide for the first time a profiling of *R. solanacearum* gene expression in different time points of the infection process.

Results

Reproducible transcriptome conditions can be obtained in the different infection stages

Symptom variability in *R. solanacearum* infected plants is very high due to stochastic variations such as the physiological state of the plant or the amount of vessels colonized (Cruz et al. 2014). Therefore, we first set up reproducible conditions to analyze the *R. solanacearum in planta* transcriptome at different points of the infection. To this end, we used a *R. solanacearum* UY031 luminescent reporter strain previously developed in our group, since it provides a more robust quantitative measurement of bacterial colonization than only annotation of wilting symptoms (Cruz et al. 2014). Three different potato infection stages were defined so that the pathogen could

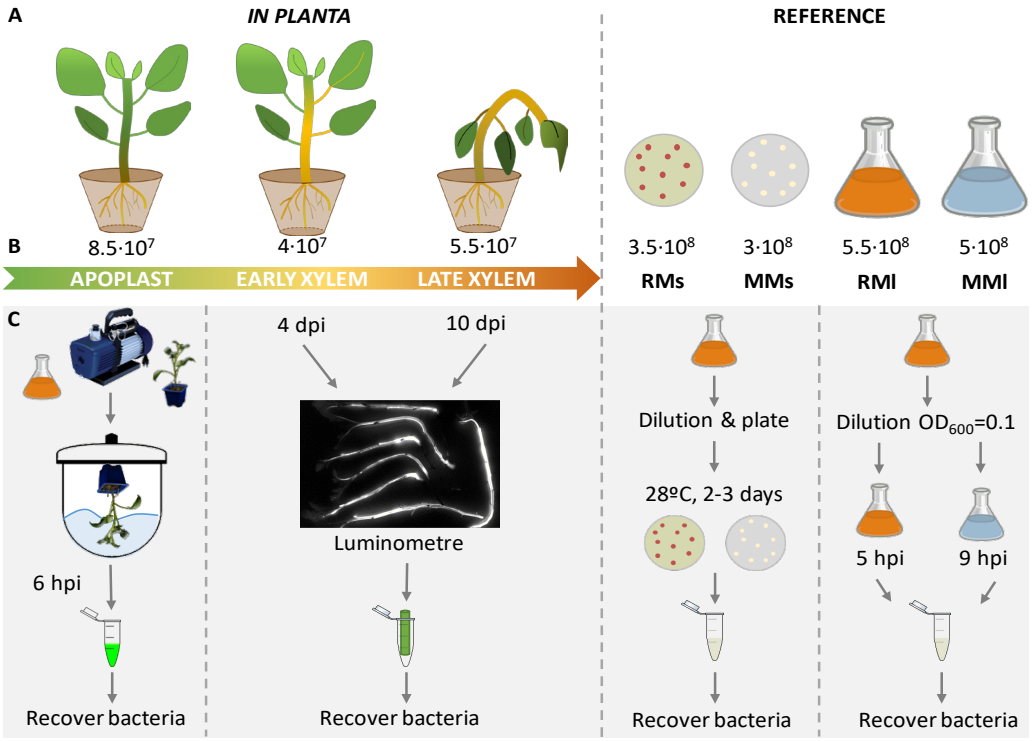

Figure 1. Conditions defined for the *R. solanacearum* in planta and in vitro transcriptome.

A) The three *in planta* conditions correspond to an early (leaf apoplast), mid (xylem from asymptomatic plants) and late stages (xylem from dead plants) of the disease. Reference conditions correspond to bacteria grown in rich and minimal media in liquid cultures or solid plates. B) Average of bacterial yields recovered in each condition are indicated as CFU/ml. C) Representation of bacterial enrichment in each condition.

be easily isolated from the plant, thus enabling the enrichment of sufficient bacterial mRNA (Figure 1). The initial stage corresponded to bacteria incubated in leaf apoplast, as it has been described that bacteria first colonize the apoplastic fluid of the intercellular spaces in the root (Vasse et al. 1995). To obtain more reproducible samples, leaf instead of root apoplast was used as a mimic condition since it has been reported that *R. solanacearum* equally behaves in both cases (Hikichi 2016). In our second and last infection stages, bacteria were isolated from colonized xylem vessels of nearly asymptomatic or completely wilted potato plants, respectively. To assess bacterial colonization levels especially in asymptomatic plants, stems were placed under a luminometer to visualize bacterial densities within the vascular system, and only plants showing luminescence were used. To avoid bias of quorum sensing signals in the xylem stages and not in the apoplast, similar bacterial yields were infiltrated in potato leaves for the initial stage. Finally, to identify the best time point at bacterial colonization within xylem vessels of almost asymptomatic plants was most similar to that in dead plants, we monitored bacterial growth, luminescence and

disease symptoms over time (Supplementary Figure 1). As shown in Figure 1, bacterial densities recovered from the three *in planta* conditions are in the same order of magnitude (between 10^7 and 10^8 CFUs/ml). *In vitro* reference conditions, corresponding to bacteria grown on solid or liquid rich or minimal media, were also obtained to better define *R. solanacearum* gene expression. Final bacterial yields from *in vitro* cultures were only one log more than *in planta* (Figure 1). These conditions allowed us to obtain enough *R. solanacearum* RNA-seq reads to have a robust representation of the whole genome (Supplementary Table 1). Principal component analysis revealed that these conditions are consistent among biological replicates and sensitive enough to detect biological differences between conditions (Supplementary Figure 2).

Table 1. Transcriptome profiling of the *R. solanacearum* virulence factors in the different *in planta* conditions.

Numbers indicate the percentage of genes in each category. Color-code was performed with Conditional Formatting of Microsoft Excel and applied to all categories except Transposases and Hypothetical proteins.

RM liquid						RM solid						MM liquid						MM solid						
Induced			Repressed			Induced			Repressed			Induced			Repressed			Induced			Repressed			
Apoplast	Early xylem	Late xylem	Apoplast	Early xylem	Late xylem	Apoplast	Early xylem	Late xylem	Apoplast	Early xylem	Late xylem	Apoplast	Early xylem	Late xylem	Apoplast	Early xylem	Late xylem	Apoplast	Early xylem	Late xylem	Apoplast	Early xylem	Late xylem	
7	8.5	2	0	0	0	14	4	3	0	0	0	5	0	0	0	0	0	1	2	2	0	0	0	Flagellum
0	0	1	0	0	0	1	1	2	0	0	0	0	0	0	0	0	0	1	2	2	0	0	0	Chemotaxis
5	0	0	0	1	1	4	3	2	1	0	1	5	0	0	0	0	0	3	2	2	0	1	2	PilT4A
0	0	0	3	0	1	0	0	1	4	1	1	0	0	0	0	0	1	0	1	1	1	0	1	PilT4B
1	10	5	0	0	0	6	7	8	0	0	0	0	0	0	1	1	1	0	0	2	1	1	1	T3E
1	1.7	0	0	0	0	3	2	1	0	0	0	0	0	0	2	3	2	0	0	0	3	2	2	T3SS
1	0	1	0	1	0	1	1	1	1	2	1	1	0	0	0	1	1	2	2	2	0	2	1	T2SS, CWDE
0	0	0	1	1	1	0	0	0	2	0	1	0	0	0	1	0	0	0	0	0	1	0	1	T6SS
0	0	1	0	3	2	1	1	0	1	3	2	0	0	0	0	0	2	1	1	0	0	0	2	QS, EPS, Biofilms
0	1.7	0	1	1	1	0	0	0	1	1	1	0	0	0	0	1	1	0	0		1	1	1	ROS detoxification
1	0	0	0	0	0	0	0	0	0	0	0	1	0	0	0	0	0	1	0	0	0	0	0	Sucrose uptake
0	3.4	1	1	0	0	0	2	2	1	0	0	0	6	7	1	0	1	1	4	2	1	0	1	Nitrogen metabolism
0	1.7	1	0	0	0	0	0	0	1	0	0	0	12	0	1	1	0	0	0	0	1	1	1	HCA degradation
2	1.7	4	0	0	2	8	11	11	0	0	0	1	0	0	0	2	6	6	11	11	0	0	1	Transposases, Phage-related
19	44	34	29	20	28	27	29	27	24	17	25	16	29	21	26	29	33	21	36	76	37	38	31	Hypothetical, Unknown function
450	59	158	336	177	701	208	283	364	191	209	485	527	17	14	468	142	324	297	183	263	278	100	326	
Number of DE genes																								

In planta transcriptome interpretation is influenced by the *in vitro* reference condition

To date, all available *R. solanacearum in planta* transcriptomes have based their interpretations by using a reference *in vitro* condition that corresponded to either rich or minimal medium liquid cultures (Jacobs et al. 2012; Meng et al. 2015; Ailloud et al. 2016; Khokhani et al. 2017). In our group, we also proved that using bacteria grown on rich medium plates as reference was also informative and allowed the detection of important genes specifically induced *in planta* ((Puigvert et al. 2017) and chapter 5). To better understand how rich or minimal media and solid or liquid state can influence *R. solanacearum* gene expression, we first compared the *in vitro* references among themselves. Interestingly, to obtain similar amounts of differentially expressed (DE) genes, different $\log_2$FC cutoffs had to be used when solid or liquid cultures were included in the analysis. For bacteria grown on solid plates $|\log_2 FC|>0.5$ was used, detecting 78 DE genes. 48 genes were up-regulated in minimal medium (MM) and mainly encoded amino acid and carbohydrate metabolism-related genes, whereas the 30 down-regulated genes comprised 10

T3SS genes (including the regulator HrpB), 6 T3Es (PopA, PopB, PopC, RipD, PopF1 and RipM), the T3 chaperone (T3C) HpaG and some other described virulence genes such as MetE and HdfA. On the other hand, when liquid cultures were used as reference, a $|\log_2 FC|>2$ was employed. In this case 129 DE genes were obtained and, again, the 67 down-regulated genes in MM encoded metabolic genes including the *scr* operon, whilst among the 62 genes induced in MM we found 9 T3SS genes (including HrpB and HrpG), 9 T3Es (PopA, PopB, PopC, RipD, PopF1, GALA7, RipV2 and the hypothetical T3E Hyp9 (Peeters et al. 2013), the T3C HpaB and the HrpB-dependent diffusible factor HdfA (Supplementary Table 2). These results show that not many genes are differentially expressed between RM and MM, with the exception of few metabolic-related genes and as expected the T3SS. This data validated the consistency of our control conditions.

Next, we compared the three *in planta* conditions to each reference. In general, *in planta* conditions were better mimicked by solid RM or MM reference conditions since we used a lower $\log_2 FC$ cutoff than with liquid RM or MM to obtain similar amounts of DE gene. As depicted in Table 1, xylem samples were best mimicked by MM in solid plates, since the comparison only retrieved 17 and 14 up-regulated genes in early and late xylem, respectively. In contrast, apoplast appeared to be slightly more similar to liquid RM.

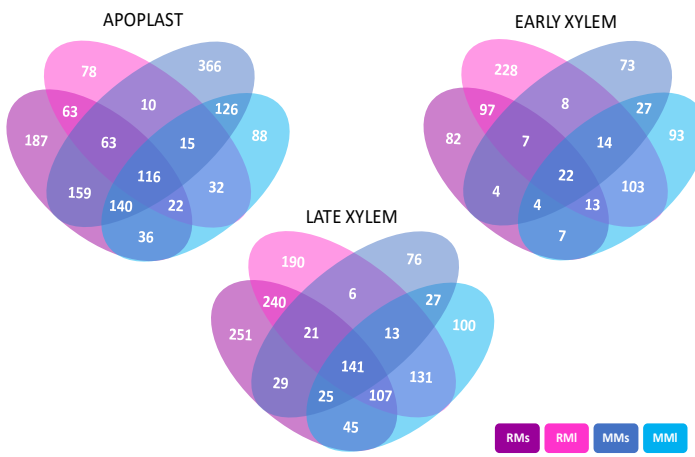

Figure 2. Overlap of DE genes *in planta* compared to the four in vitro references.

Venn Diagram representing the amount of common DE genes in each *in planta* condition when compared to the different reference conditions. RMs-solid rich medium, RMl-liquid rich medium, MMs-solid minimal medium, MMl-liquid minimal medium.

To better reflect the influence of reference conditions, we then classified the DE genes belonging to previously reported virulence factors (Table 1). Major differences could be observed with the T3SS and T3E, which were highly induced *in planta* when compared to any rich medium (RM) reference but repressed when MM was used. In few exceptions, some reference-dependent

tendencies could be observed, for instance: type IVb pili showed contrasting expression patterns in early xylem when compared to liquid RM or MM. In addition, the flagellum was induced in apoplast in all cases but in a lesser extent when compared to liquid MM cultures, indicating that it is induced by liquid MM. We also overlapped the different DE gene lists in each infection stage to the four references to obtain Venn diagrams. As shown in Figure 2, only 116, 22 and 141 DE genes were always present in a reference-independent manner in the apoplast, early and late xylem, respectively. In fact, most of the flagellum and type IVa pili genes, which are homogeneously highly induced in apoplast compared to most reference conditions, are lost in the common gene list. Altogether, these results show that a great proportion of genes is influenced by the type and state of the culture in which bacteria were grown.

Table 2. Proportion of up- and down-regulated genes in apoplast, early and late xylem using rich medium liquid as reference in relation to other *R. solanacearum* transcriptomes.

Percentage of common DE genes in each *in planta* condition compared to previous *in planta* gene expression analyses (A-Meng et al. 2015; B-Brown and Allen 2004, C-Occhialini et al. 2005 and Valls et al. 2006, D-Jacobs et al. 2012, E-Puigvert et al. 2017, F-Khokhani et al. 2017). Colors were plotted using the Conditional Formatting in Microsoft Excel.

Induced			Repressed			
Apoplast	Early xylem	Late xylem	Apoplast	Early xylem	Late xylem	
8	11	10	5	2	3	RNAseq -Tº-dependent factors tomato xylem (A)
3	2	1	4	3	3	IVET-tomato xylem (B)
7	10	9	2	0	0	Microarray- MM B-reg (C)
6	4	2	2	0	2	Microarray- MM G-reg (C)
0	0	0	0	0	0	Microarray- MM BG-reg (C)
37	36	28	6	4	3	Microarray-tomato xylem UW551 UP (D)
1	1	1	31	42	30	Microarray-tomato xylem UW551 DOWN (D)
17	20	15	5	4	2	Microarray-tomato xylem GMI1000 UP (D)
1	1	1	16	25	18	Microarray-tomato xylem GMI1000 DOWN (D)
16	11	6	16	10	8	RNAseq-Wild potato root (E)
14	14	11	22	14	16	RNAseq-tomato xylem phcA-regulated (F)

Apoplast and late xylem produce high genetic reprogramming in *R. solanacearum*

We then explored the DE gene lists from an *in planta* point of view. As shown in Figure 2, apoplast and late xylem are the most extreme *in planta* conditions, since they produced a strong genetic reprogramming evidenced by the amount of DE genes in both cases. We also compared our DE lists to those published from previous *R. solanacearum* gene expression analyses. Table 2 (and Supplementary Table 3) shows the proportion of genes in our transcriptome that previously appeared in other studies. Interestingly, between 30-50% of the early xylem DE genes match with published microarray data from *R. solanacearum* in infected tomato xylem samples at the onset of the disease. Furthermore, 15% of the apoplast DE genes and between 10-30% (depending on the reference used) of the early xylem DE genes were reported in our previous root transcriptome

study. Taken together, these results suggest that: I) our previous root transcriptome contained genes induced both at the apoplast and early xylem conditions, II) many *R. solanacearum* genes DE *in planta* during colonization are necessary irrespectively of the host, III) our transcriptome analysis is validated, since genes that were up- or down-regulated in tomato xylem at the beginning of symptom development correlated well with our data in similar conditions.

Finally, we investigated whether similar genes would be necessary at the three infection stages by overlapping the DE gene lists in Venn Diagrams. As shown in Supplementary Figure 3, very few genes are actually shared during apoplast and early xylem colonization, while a great proportion of genes are found in both xylem conditions. In contrast, a large number of DE genes in apoplast and late xylem were unique to those conditions, confirming that they are extreme and dissimilar environments.

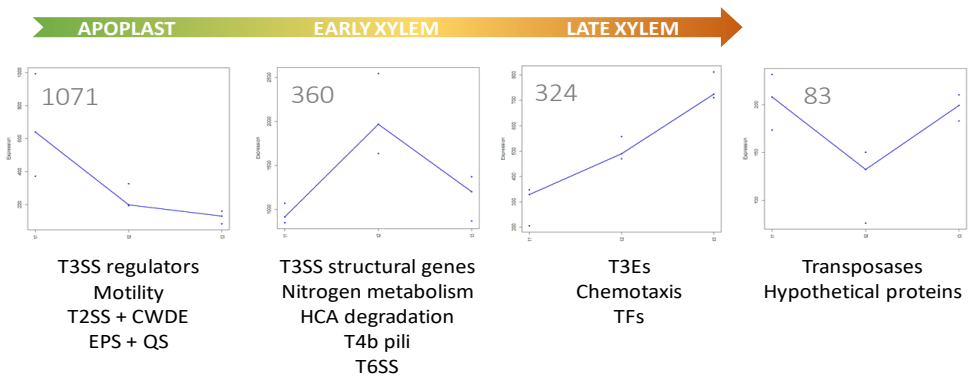

Figure 3. Clusters of dynamic gene expression profiles throughout the infection process

R. solanacearum gene expression data in apoplast, early and late xylem conditions was subjected to clustering according to dynamic gene expression patterns. Expression profiles are represented by the gene with highest fit value within each cluster. The number on the top left corner of each plot indicates the amount of genes following that pattern. A summary of the most relevant features within each cluster is shown under the plots. Abbreviations: CWDE (cell wall degrading enzymes), QS (quorum sensing), TF (transcription factor).

Bacterial metabolic landscape during brown rot disease

To examine the *in planta* metabolic behavior of *R. solanacearum*, we compared the metabolic pathways *in planta* to those in liquid RM or MM. Since metabolism is strongly dependent on the type of medium in which bacteria grow, we could only extract a general idea of the bacterial behavior in those artificial media. For instance, bacteria induce the Etner-Doudoroff pathway in RM and MM compared to apoplast. Besides, pectin degradation was up-regulated in the three *in planta* conditions compared to RM, but only in the apoplast when compared to MM, indicating that this trait is already slightly induced in MM (Supplementary Figure 4 A and B). Generally, bacterial metabolism *in planta* is reduced compared to that in artifical media.

To better understand how *R. solancearum* modulates its metabolism along with the disease, we performed a clustering analysis in the three infection stages considering the whole *R. solanacearum* UY031 genome. Four clusters were obtained and the expression profile of the gene with highest score within each cluster was depicted as example (Figure 3). Numbers in the left top corner of each plot indicate the total number of genes classified in each cluster. With this analysis, we could assign a cluster to 1838 out of the 4639 genes without 0 reads in any condition in the *R. solanacearum* UY031 genome. The first cluster (left) corresponds to genes whose expression levels are high at initial infection stages and decrease as disease advances. The next two clusters comprise genes with higher expression levels in early or late xylem, respectively, and the last cluster (right) includes genes that are active both in apoplast and in completely wilted plants. As numbers indicate, most of the genes with a dynamic expression throughout the infection process are highly induced at early stages and their expression levels decrease with time. We then identified metabolic related genes within each cluster by using BlastKOALA, and represented the corresponding metabolic pathways using IPATH3. 688/1071 genes in the apoplast cluster were identified using the KEGG Blast tool, indicating an enrichment in metabolic-related genes at initial colonization stages (Figure 4, highlighted in green). Early xylem contained 185/360 genes involved in metabolism (yellow), and 130/324 late xylem genes were attributed to a metabolic pathway (red). These observations indicate that there is a general tendency to diminish transcription as the disease progresses, and that few metabolic pathways are reprogrammed during colonization of dead plants.

When we explored the bacterial metabolic pathways altered along the infection (Figure 4), the following pathways appeared to be induced at initial infection stages: lipopolysaccharide (LPS) biosynthesis, fatty acid biosynthesis and oxidation, gluconeogenesis and reductive pentose phosphate, TCA cycle, nitrogen assimilation, pectin degradation, purine and pyrimidine biosynthesis, sulfur metabolism, urea cycle, Shikimate pathway and biosynthesis of valine, leucine, isoleucine, phenylalanine, tyrosine and many cofactors. However, when bacteria reach the xylem vessels, a completely different metabolic landscape is found: only the urea cycle, LPS and initiation of fatty acid biosynthesis are maintained, and on the other hand, the Etner-Doudoroff pathway is induced, together with arginine biosynthesis and degradation of histidine, tyrosine, alanine, leucine and isoleucine. Finally, when plants are dead, bacteria only induce benzoate degradation, polyamine biosynthesis and sulfur assimilation pathways. Overall, these observations demonstrate that *R. solanacearum* adapts metabolically to the different *in planta* environments by deploying or dampening specific metabolic pathways at each infection stage.

Sequential expression of the different members in the T3SS cascade

Since the T3SS regulatory pathway is well characterized in *R. solanacearum*, we investigated the gene expression pattern of the T3SS components and the T3E repertoire in *R. solanacearum* UY031 throughout our time-course transcriptome. We explored the presence of different members of

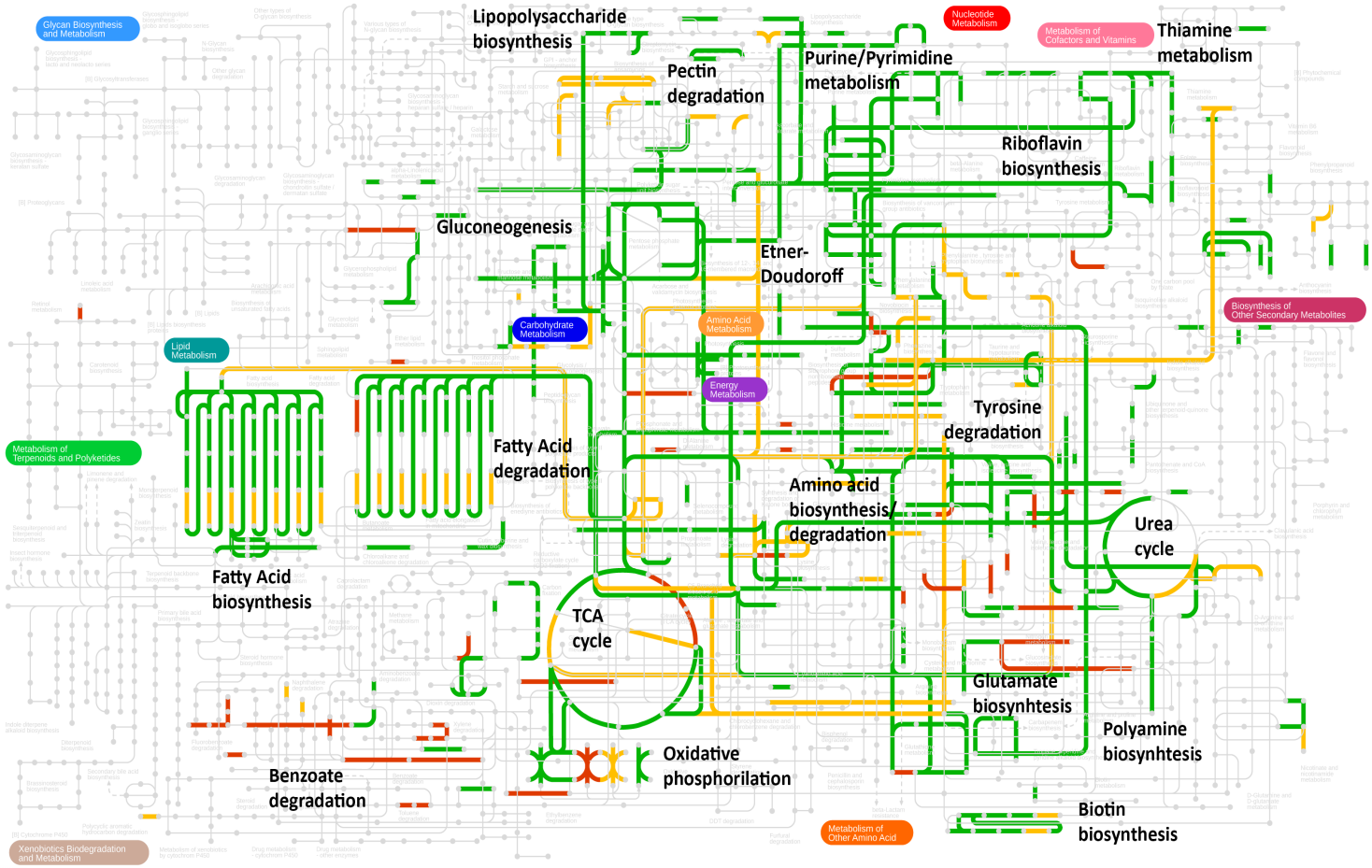
Glycan Biosynthesis and Metabolism
Lipopolysaccharide biosynthesis
Nucleotide Metabolism
Metabolism of Cofactors and Vitamins
Thiamine metabolism
Pectin degradation
Purine/Pyrimidine metabolism
Riboflavin biosynthesis
Gluconeogenesis
Etner-Doudoroff
Biosynthesis of Other Secondary Metabolites
Carbohydrate Metabolism
Amino Acid Metabolism
Lipid Metabolism
Energy Metabolism
Tyrosine degradation
Metabolism of Terpenoids and Polyketides
Fatty Acid degradation
Amino acid biosynthesis/ degradation
Urea cycle
Fatty Acid biosynthesis
TCA cycle
Glutamate biosynthesis
Polyamine biosynthesis
Oxidative phosphorilation
Benzoate degradation
Biotin biosynthesis
Metabolism of Other Amino Acid
Xenobiotics Biodegradation and Metabolism

7

Figure 4. Metabolic pathway induction at each potato infection stage.

R. solanacearum DE genes involved in metabolism were mapped onto Kegg pathways using IPATH3. Pathways highlighted in green, yellow or red denote induction in the apoplast, early or late xylem, respectively.

the T3SS cascade within the dynamic gene expression clusters (Figure 3). In Figure 5 we depicted the classical T3SS signaling cascade described in the literature (Valls et al. 2006), and show the condition in our transcriptome at which each member is differentially expressed. As expected, the *prh* genes are highly induced at the initial infection stage, or apoplast, since these are the upstream members of the T3SS signaling that sense the plant cell signal. *Hrp* genes, on the other hand, encode first for regulatory proteins named HrpG and HrpB, which ultimately trigger the expression of the T3SS structural proteins and T3Es. Figure 6 shows how HprG expression, which is dependent on the plant-cell contact signal, is induced in apoplast, while HrpB, which also senses a MM signal, is highly induced in early xylem together with other *hrp* genes encoding structural units of the T3SS pilus. Interestingly, some sets of T3Es appeared to be induced specifically at some points of the infection although there was a clear enrichment of T3Es at later infection stages. Similar results were obtained when we examined the DE lists of the three *in planta* conditions compared to liquid RM.

To investigate the exact expression pattern of the complete T3E repertoire in *R. solanacearum* UY031, we performed a clustering analysis of this subset of genes and obtained 7 different clusters (Figure 6). Patterns correspond to the relative expression of the three *in planta* conditions normalized by expression in liquid rich medium. Each cluster shows the expression profile for the gene with the highest score value within that cluster.

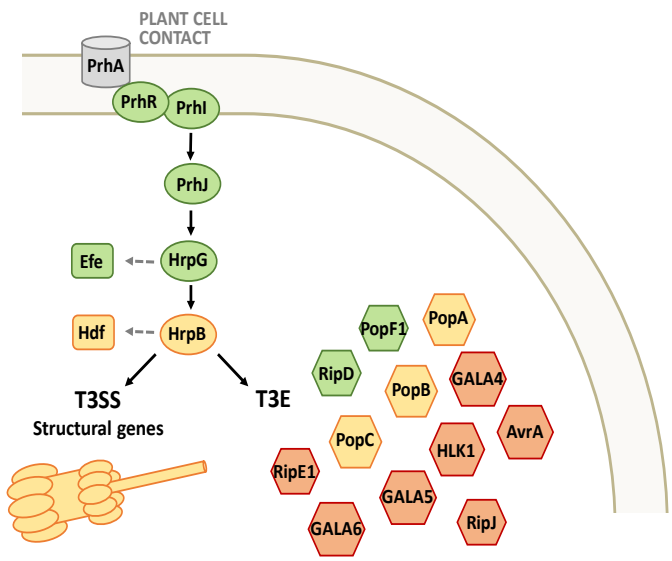

Figure 5. *R. solanacearum* expression of the T3SS signaling cascade along the infection process.

T3SS signaling cascade (adapted from Valls et al. 2006). Circles represent regulatory proteins, boxes represent downstream products and hexagons represent T3Es. Colors indicate the infection stage at which each gene is induced: apoplast (green), early xylem (yellow) and late xylem (red).

As previously detected, some T3Es are specifically induced at unique points of the infection process. For instance, T3Es in Cluster 1 and 2 (RipD, PopF1, PopS and RipAD) can be clearly classified as “early effectors” since their expression is highly induced in the apoplast compared to the other infection stages. Effectors classified in Cluster 4 (PopA, PopB and PopC) can be considered as “early xylem effectors”, since they appear to be specifically induced in the xylem of alive plants. T3Es grouped in Cluster 5 can be considered as “xylem” effectors, as their expression levels are maintained in the two xylem conditions. Surprisingly, most of the T3Es in *R. solanacearum* UY031 are grouped in Clusters 6 and 7 corresponding to “late effectors” and whose expression increases in completely wilted compared to asymptomatic plants. Altogether, these results demonstrate that our *in planta* conditions are robust enough to capture sequential inductions of the most well studied regulatory pathway in *R. solanacearum*, the T3SS. Furthermore, we also provide evidence that, contrary to what was expected, most T3Es are expressed during the last stage of the disease.

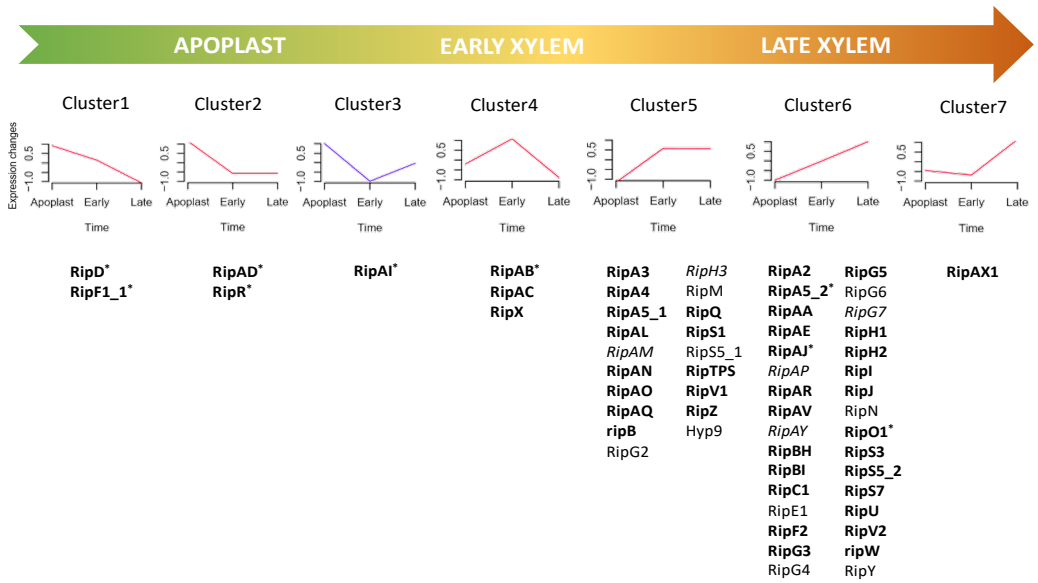

Figure 6. Gene expression patterns of theT3Es in *R. solanacearum* UY031 during brown rot disease development.

Effectors highlighted in bold were detected with the highest thereshold (α=0.75) and with and asterisk were found in at least 10/50 runs. T3Es without effect were detected at α=0.5 and in italics at α=0.25.

Virulence gene expression is dynamic along the infection process

We next investigated the expression profiles of known virulence determinants in *R. solanacearum* during potato colonization. To this end, we examined the presence of different virulence factors in each gene expression cluster (Figure 3, Supplementary Table 4). Within the cluster corresponding to genes induced in apoplast, we found many virulence determinants such as: motility (flagellum-encoding genes), attachment (LecM and Type IVa pili), ROS detoxification enzymes, T2SS and

a cell wall degrading enzyme (PglA), Exopolysaccharide (EPS) biosynthesis and quorum sensing signals, upstream members of the T3SS cascade (*prhI*, *prhJ*, *prhR*, *hrpG*) and two "early" effectors (RipD and PopF1). The ethylene encoding gene *efe,* the metabolic repressors EfpR and RepR and the alternative sigma factor RpoN1, responsible for twitching motility and growth on nitrate, are also included in the cluster. Interestingly, among the genes specifically induced in the early xylem stage we found other virulence factors: many *hrp* genes (encoding for structural units of the T3SS pilus as well as the HrpB regulator), few T3Es including RipQ, RipTPS and the above mentioned "early xylem effectors", Type IVb pili, the T6SS, the *hdf* operon and Hydroxycinnamic Acid (HCA) degradation enzymes. In contrast, genes belonging to chemotaxis and some others T3Es are grouped in the cluster of genes induced at late disease stages. In this case, we noticed that 12% of these genes encode for transcription factors, suggesting that the pathogen is preparing itself for the next stage if its life cycle. In line with this hypothesis, the last cluster comprises genes that are induced both in apoplast and in wilted plants. This group of genes might be deployed by the pathogen to adapt to extreme conditions, and they mainly include hypothetical proteins and transposases, which have been described to play an adaptive role to new environments (Casacuberta and Gonzalez 2013). These results indicate that the already described virulence factors in *R. solanacearum* are necessary at different stages of the disease.

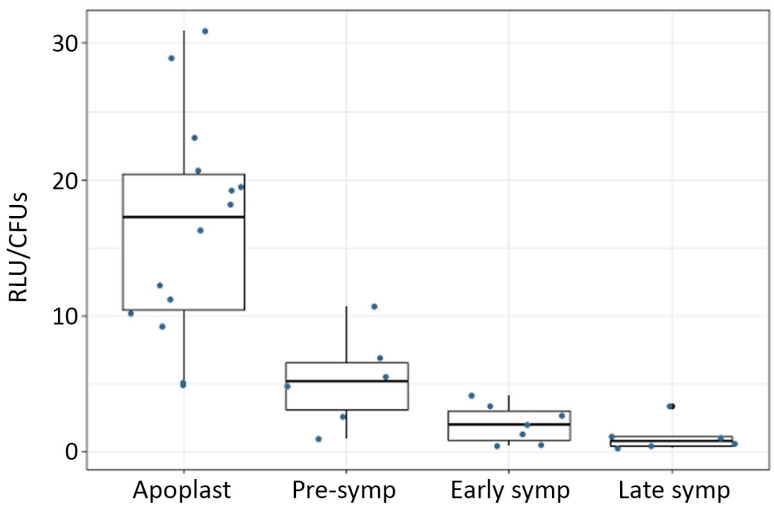

Figure 7. *eps* expression at different potato infection stages.

Eps expression was quantified by measuring light emission (Relative Luminescent Units) of a *R. solanacearum* UY031 strain containing the *Peps::lux* construct in its genome and normalized by the amount of bacteria present in each sample (CFUs). Expression was evaluated by recovering bacteria from leaf apoplast (6 hpi) and from xylem vessels at three infection stages: pre-symptomatic (Disease Index=0), early symptomatic (DI=0.5-1), and late symptomatic (DI=4). Data was plotted using the ggplot package in R. The experiment was repeated two times with similar results.

Early induction of exopolysaccharide production

Exopolysaccharide (EPS) production is one of the main virulence determinants in *R. solanacearum* and is controlled by quorum sensing signals that trigger the expression of the *eps* operon at high cell densities (Clough et al. 1997a). Contrary to what was expected, the *eps* operon is induced at early infection stages in our time-course transcriptome (Figure 3, Supplementary Table 4). The main regulator controlling EPS expression (PhcA) and other regulators in this signaling network (PhcQ, PhcS, PhcB, VsrC, VsrD, XpsR and WecC) are also highly expressed in the apoplast. Since it was traditionally assumed, however, that EPS and related quorum sensing networks would be only active during xylem colonization at which EPS is accumulated in high amounts, we validated this unexpected result using a different technique. To this end, we used a luminescent reporter strain of the *eps* biosynthesis operon and monitored its expression at four infection stages, including the conditions of our *in planta* transcriptome. Expression levels are represented as Relative Luminescent Units (RLU) normalized by the amount of bacteria in each plant. As shown in Figure 7, bacteria incubated in potato leaf apoplast show maximum expression levels compared to the rest of the conditions, which correspond to xylem colonization at different points of the infection process. Although the amount of EPS was notably increasing, EPS expression per cell decreased as disease progressed, suggesting that, when similar bacterial loads are present EPS is strongly induced in the intercellular spaces.

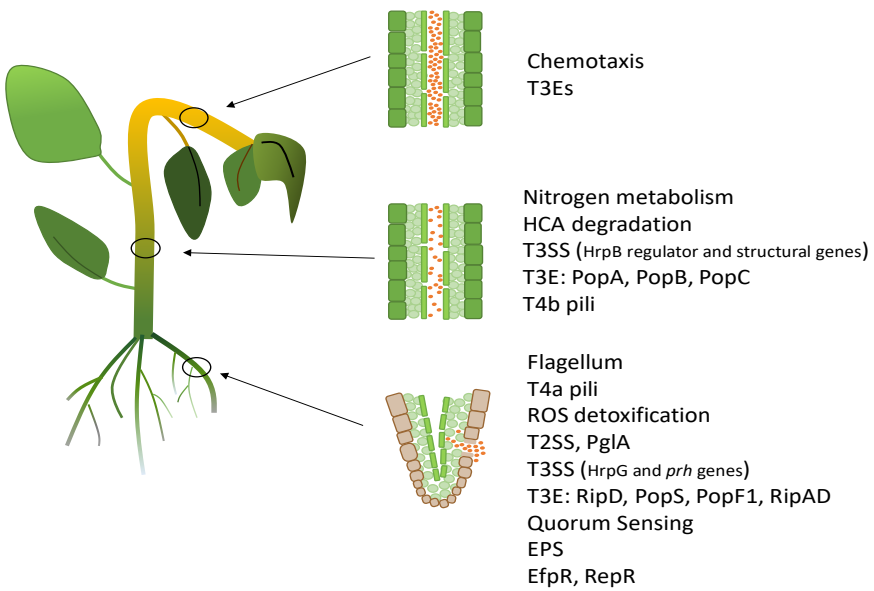

Figure 8. Dynamic virulence gene expression model in *R. solanacearum* during potato colonization.

Expression of known virulence factors in *R. solanacearum* at the tested *in planta* conditions. Bacteria are represented as orange dots. Conditions from top to bottom: xylem of wilted plants, xylem of alive plants and apoplast. Pathogenicity factors induced at each stage are indicated at the right. Abbreviations are explained in the text.

Discussion

Previous studies in *R. solanacearum* have identified many virulence factors involved in plant colonization and disease development. Recently, several *in planta* transcriptomes have become available, providing new insights on bacterial aspects essential for the emergence of wilting symptoms (Jacobs et al. 2012; Meng et al. 2015; Ailloud et al. 2016; Khokhani et al. 2017). However, understanding their expression profiles in the context of the pathogen life cycle has been more challenging. Although we already proved that it was possible to successfully analyze the bacterial transcriptome from total infected tissue (Puigvert et al. 2017), it is still cost-ineffective and it is preferred to isolate bacteria prior to RNA extraction (Nobori et al. 2018). Therefore, most of these works have focused at the disease onset stage, in which bacterial densities within the xylem vessels are extremely high.

To unravel the changes that *R. solanacearum* undergoes during the disease, we set up a time-course transcriptome at three different potato infection stages with enough bacterial densities to obtain robust transcriptomes and avoid biased expression by quorum sensing effects. Besides, four different reference conditions were included in the analysis: bacteria grown on solid or liquid rich and minimal medium (RM and MM, respectively) (Figure 1). To identify the genes that were up- or down-regulated between the conditions, we performed a differential expression (DE) analysis. Interestingly, the analysis showed that bacteria grown on solid media (RM or MM), had less DE genes with the *in planta* conditions than when liquid cultures were used as reference (Figure 2). This result further reinforces the idea that solid cultures mimic better the actual state of bacteria within the plant, as it was recently reported that they produce biofilms and microcolonies in the plant intercellular spaces (Mori et al. 2016).

We also assigned functional categories to the DE gene lists and, as expected, T3SS and T3E expression were induced in all *in planta* conditions compared to RM but repressed when compared to MM (Table 1). Finally, we examined the differential expression (DE) in apoplast, early and late xylem compared to each *in vitro* reference with that of previous *in planta* transcriptome analyses (Jacobs et al. 2012; Meng et al. 2015; Ailloud et al. 2016; Khokhani et al. 2017; Puigvert et al. 2017). As Table 2 and Supplementary Table 3 show, approximately 30% of the DE genes in our transcriptome appeared already in other studies. Data correlated especially well between *R. solanacearum* UY031 in early xylem conditions and the closely related strain UW551 in infected tomato xylem vessels (Jacobs et al. 2012). Furthermore, the strong overlap between our apoplast and early xylem conditions with our previous transcriptome in wild potato roots, might indicate that root samples contained a mixture of bacterial populations (Supplementary Table 3). Taken together, these observations validated our time-course transcriptome and provided evidence that our *in planta* conditions were dissimilar enough to detect relevant biological differences.

The analysis of MM versus RM revealed that, besides T3SS induction, several genes related to metabolism were also affected by the type of medium in which bacteria were grown

(Supplementary Table 2). This dependency was obvious when the metabolic pathways up- and down-regulated in apoplast, early and late xylem compared to liquid RM or MM were plotted onto KEGG pathways (Supplementary Figure 4). The analysis also unveiled that bacterial metabolism in MM and early xylem is highly similar and that *R. solanacearum* metabolism tended to diminish at late disease stages. This observation was clearer when we clustered the *R. solanacearum* genome according to gene expression profiles and represented the metabolic pathways induced at each infection stage (Figure 4). The decreasing amount of genes clustered in each expression profile further demonstrates this tendency (Figure 3). In this sense, the pathogen strongly activates its metabolism during apoplast colonization, inducing carbohydrate, lipid, cofactor, sulfur and nucleotide metabolism, as well as nitrogen assimilation pathways and biosynthesis of many aromatic amino acids. In contrast, when bacteria colonize the xylem vessels, they activate the Etner-Doudoroff pathway to get energy from carbon sources, synthesize arginine and degrade other amino acids such as histidine, tyrosine, leucine and isoleucine. Interestingly, this result is supported by a previous study in which we show that during growth in tomato xylem sap, which might have a similar composition to that in potato plants, *R. solanacearum* accumulates arginine while it consumes leucine, isoleucine, tyrosine and histidine (see annex (Zuluaga et al. 2013)). Finally, when plants are dead, the pathogen has already turned off most of its primary metabolic pathways but deploys polyamine biosynthesis and benzoate degradation pathways.

Besides metabolism, many virulence factors were also included in the gene expression clusters (Figure 3). When we looked at the T3SS, the main virulence factor and most well studied signaling pathway in *R. solanacearum* we realised that its expression pattern correlated well to the previously described signaling cascade (Valls et al. 2006). Initially, *prh* and *hrpG* genes, which trigger the plant cell contact signal (Brito et al. 1999), are up-regulated in apoplast. Subsequently, the *hrp* genes encoding structural T3SS units and the HrpB regulator, which senses the MM signal (Plener et al. 2010), are induced in early xylem (Figure 5). Interestingly, expression of T3Es appeared to take place in sets of genes at different infection stages. For instance, RipD, PopF1, PopS and RipAD were strongly induced in plant apoplast, and their expression decreased afterwards (Figures 5 and 6). In fact, different studies show that RipD, PopF1 and PopS single mutants are non-virulent or produce delayed disease symptoms (Cunnac et al. 2004; Meyer et al. 2006; Jacobs et al. 2013). Since suppression of a single T3E rarely results in delay or loss of virulence (Deslandes and Genin 2014), these reports further support the idea that these T3Es play key roles at early infection stages. Although it was expected that most T3E were induced during colonization of the xylem vessels, the preferred niche of *R. solanacearum*, it was surprising that a large amount of T3E were up-regulated in completely wilted plants (Figure 6). This result was especially unusual, considering that relatively few genes were induced in our latest disease stage (Figure 3). Conversely to the traditional notion of an exclusively early role of the T3SS, our *in planta* results further support the notion that the T3SS is active at advanced disease stages (Jacobs et al. 2012; Monteiro et al. 2012a) and that many T3Es might have a function at this disease. Previous *in planta* studies already addressed the possibility of different T3Es playing distinct roles in the infection process

(Turner et al. 2009). Accordingly, a recent *in vitro* approach exploring the secretion pattern of T3E in *R. solanacearum*, relevealed that a fine control of effector delivery mediated by T3C exists in the pathogen (Lonjon et al. 2016). In their study, Lonjon and collaborators suggest that T3Es whose secretion is T3C-independent might be secreted earlier, while those that depend on T3C for translocation might be secreted at later stages. When we compared their lists of putatively early/ late effectors to ours (Figure 6), few matches were found. Actually, this result is not surprising since effector translocation and its effect on the host cell might depend on many factors, including the host species, the T3E repertoire in the given bacterial strain, and expression of the T3E, the T3C and the T3SS pilus. With the development of the split-GFP system to monitor spatiotemporal translocation of T3Es (Henry et al. 2017; Park et al. 2017), future experiments will be addressed at characterizing the *in planta* translocation pattern of candidate "early" and "late" effector sets.

In addition to the T3SS, we also analyzed the expression dynamics of other virulence determinants described in *R. solanacearum* (Figure 3). In line with previous studies, we demonstrate that expression of the sigma factor RpoN1, Type IVa pili, the flagellum, T2SS and ROS detoxification enzymes takes place in the apoplast, thus validating their biological role at the establishment of the infection (Kang et al. 1994; Tans-Kersten et al. 2001; Kang et al. 2002; Flores-Cruz and Allen 2011; Lundgren et al. 2015; Ray et al. 2015). Besides, two HrpG-induced genes, *efe* and *lecM*, were also up-regulated in apoplast (Valls et al. 2006). Furthermore, we also detected the induction of two regulators involved in bacterial metabolic adaptation: EfpR and RepR ((Perrier et al. 2016), chapter 6). Interestingly, RepR was induced in apoplast compared to the four reference conditions.

In the subsequent infection stage, *R. solancearum* induces nitrogen respiration genes, a trait already demonstrated to play a role during xylem colonization (Dalsing et al. 2015), the *hdf* operon, which was described as HrpB-induced (Delaspre et al. 2007), and the T6SS –a novel virulence determinant in *R. solanacearum* whose expression is known to decrease transcription of flagellar genes (Zhang et al. 2012; Zhang et al. 2014). Moreover, it is known that HCA and derivates are released by the plants into the xylem lumen as a defense mechanism (Beckman 2000). It was recently reported that HCA degradation enzymes encoded by *R. solanacearum* also contribute to virulence (Lowe et al. 2015). It was hypothesized that HCA degradation might be involved during root colonization. However, in our time-course transcriptome we show that genes encoding HCA degradation enzymes are actually induced during early xylem colonization, where we propose they might develop their function. Within the xylem vessels of wilted plants, we show that *R. solanacearum* still induces expression of chemotaxis, a trait that was believed to be mainly involved in root colonization at the rhizosphere (Yao and Allen 2006), many T3E and a surprising large amount transcription factors. Altogether, these results indicate that, far from dying, bacteria might be preparing themselves for the coming environment beyond the disease. Finally, a group of 83 genes appeared to be induced both in apoplast and late xylem conditions, the most extreme conditions in our transcriptome. Not surprisingly, these genes include hypothetical proteins

and transposases, which are known to be involved in stress conditions and adaptation to new environments (Capy et al. 2000; Casacuberta and Gonzalez 2013).

Unexpectedly, our data also showed an early induction of quorum sensing networks and EPS production, which were further validated using promoter::reporter fusions (Figure 7). This challenges the notion that the quorum sensing pathways are specifically induced in the xylem (Schell 2000), showing that they can be induced at higher levels in the apoplast provided sufficient bacterial concentration is present. Interestingly, recent data indicate that *R. solanacearum* produces biofilm more abundantly in apoplast extracts than in xylem sap (Mori et al. 2016). The same study reports that the pathogen can form microcolonies in the apoplastic spaces, which could represent microenvironments with high EPS production. Further analyses will be needed to confirm this hypothesis.

Recently, growing knowledge on phenotypic heterogeneity in bacterial subpopulations during infection has revealed that this event is responsible for increased bacterial fitness and virulence (Weigel and Dersch 2018). This event has been already described in the plant pathogen *P. syringae*, which displays two T3SS-distinct populations within plant apoplast (Rufian et al. 2016). We hypothesize that during root colonization, *R. solanacearum* may also be differentiated into distinct populations with phenotypic heterogeneity, caused either by the presence of different microenvironments in the infected tissue or driven by transcription factors that affect positive feedback loops. The development of novel dual reporters in *R. solanacearum* targeting expression of *eps* together with a constitutively expressed gene will clarify whether bistable *eps* expression also takes place at early infection stages.

Although new questions arose during this work, our system has contributed to a global understanding of the modulation in *R. solanacearum* virulence gene expression along the infection process (Figure 8). Future research will shed light on the functional aspects of our novel observations.

Materials and Methods

Bacterial strains and plant growth conditions

The *R. solanacearum* strain UY031 isolated from potato tubers in Uruguay (Siri 2011) carrying the reporter LUX-operon under control of the *psbA* promoter was used. Luminescence expression allowed us to indirectly quantify the amount of bacteria present in each sample (Cruz et al. 2014).

Bacteria were grown in rich B medium supplemented with glucose (10g/l bactopeptone, 1g/l yeast extract, 1 g/l casaminoacids, 0.5% glucose) or in Boucher's Minimal Medium (BMM) supplemented with glutamate (200g/l KH_2PO_4, 50g/l $(NH_4)_2SO_4$, 10g/l $MgSO_4$-$7H_2O$, KOH 10N, 1.26g/l $FeSO_4$-$7H_2O$, 20mM glutamate), and incubated at 30ºC.

Solanum tuberosum cv. Desire plants were propageted *in vitro* (Zuluaga et al. 2015) and 2-week old apexes were transferred to pots containing a mixture of soil:silica sand in a 1:1 ratio and grown at 22ºC in long day (16h/8h light/dark) conditions. 3-week-old plants were used in all the experiments.

Bacterial sampling

For solid rich B or BMM samples, bacteria were grown for 2 or 3 days, respectively, as separated colonies and recovered with sterile water (Puigvert et al. 2017). For liquid samples, bacterial cultures at a starting OD_{600}=0.1 were grown for 5 h in rich B medium or 9 h in BMM, until they reached exponential growth phase (OD_{600}≈0.4-0.5). In either case, bacteria were centrifuged at 4ºC for 2 min at maximum speed and immediately frozen in liquid nitrogen.

To obtain leaf apoplast samples, bacterial cells from an overnight culture were washed with water and resuspended to a final concentration of $5 \cdot 10^8$ CFU/ml. The whole aerial part of the plants was vacuum-infiltrated for 30sec-1min and leaves were dried in paper towel before incubating the plants in the inoculation chamber (28ºC, 12/12). After 6 hours, leaves were vacuum-infiltrated with sterile distilled water, dried in paper towel, rolled in a cut 10 ml tip and centrifuged inside a 50 ml tube at 4ºC for 5 min at 2000 rpm. Apoplast fluid extract was pooled (each pool representing approximately 15 plants) and centrifuged at 4ºC at maximum speed for 2 min. Bacterial pellets were frozen in liquid nitrogen.

For early and late xylem samples, potato roots were injured with a 1 ml pipette tip before inoculation. 40 ml of a 10^8 CFU/ml *R. solanacearum* suspension was used to soil-inoculate each plant. After inoculation, plants were kept in the inoculation chamber (28ºC, 12/12) for 6 days (mean disease index=0-1) or 10 days (disease index=4 in 100% of the plants), respectively. Plants were photographed in a LAS4000 Luminometre to check individual infection levels and approximately 30 plants were used for each early xylem sample, while 7 plants were used for every late xylem sample. 2 cm-long stem pieces were cut from each plant, placed in a 1.5 ml tube containing 500 µl of sterile distilled water and centrifuged 2 min at maximum speed at 4ºC to release bacteria from the xylem vessels. All bacterial pellets were pooled together for each biological replicate and frozen in liquid nitrogen.

In all cases, bacterial densities were measured by luminescence and dilutions were plated to count CFUs before addition of 5% of an ice-cold transcriptional stop solution (5% [vol/vol] water-saturated phenol in ethanol).

RNA extraction, sequencing and library preparation

Total RNA was extracted using the SV Total RNA Isolation System kit (Promega) following manufacturer's instructions for Gramnegative Bacteria. RNA concentration was measured with a ND-8000 Nanodrop and RNA integrity was validated for all samples using the Agilent 2100 Bioanalyzer. For rRNA deplition, 2.5µg of total RNA were treated with the Ribo-zero$^{(TM)}$ magnetic kit for bacteria (Epicentre). Three biological replicates per condition were subjected to sequencing on a HiSeq2000 Illumina System apparatus using multiplexing and kits specially adapted to obtain 100 bp paired-end reads in stranded libraries. Liquid reference samples were sequenced by Macrogen Inc. (Seoul). In all other cases, RNA-sequencing was performed in the Shanghai PSC Genomics facility. Raw sequencing data will be available in the Sequence Read Archive under an accession code.

Read alignment, mapping and differential gene expression analysis

RNA-seq raw data quality was evaluated using FASTQC (version 0.11.4). The completely sequenced genome of strain UY031 (Guarischi-Sousa et al. 2016) was used as reference and *R. solanacearum* reads were mapped using Bowtie2 (version 2.2.6; (Langmead and Salzberg 2012) with stringent parameters (Puigvert et al. 2017). Alignments were quantified with HTSeq-count (version 0.6.1; (Anders et al. 2015) using NCBI's RefSeq sequences NZ_CP012687.1 and NZ_CP012688.1. DESeq2 (version 1.12.3; (Love et al. 2014) package in R (version 3.3.2) was employed to perform differential expression (DE) analysis of high quality RNAseq reads. Genes with $|\log_2(\text{fold-change})| > 0.5$ and $q < 0.01$ were considered as differentially expressed *in planta* when compared to bacteria grown on solid medium. When liquid cultures were used as reference conditions, $|\log_2(\text{fold-change})| > 2$ and $q < 0.01$ parameters were used. Common and unique differentially expressed gene lists, as well as Venn diagrams, were obtained using the online tool http://bioinformatics.psb.ugent.be/webtools/Venn/.

Gene expression pattern clusterization

EBSeqHMM package (version 1.12.0, (Leng et al. 2015)) in R (version 3.4.4) was used to cluster global *R. solanacearum* UY031 gene expression according to expression profile similarity along the different conditions. Non-prenormalized raw data of liquid rich medium, apoplast, early and late xylem samples was used as input. Expression profile clustering was estimated by applying a median normalization, 100 iterations and a False Discovery Rate (FDR) < 0.05. Only genes with a PP value ≥ 0.5 were taken into account.

To obtain expression profiles of the *R. solanacearum* UY031 T3E genes, a soft clustering analysis was performed using Mfuzz package (version 2.38.0, (Futschik and Carlisle 2005; Kumar and M 2007) in R (version 3.4.4). Input data corresponds to the expression ratios obtained by DEseq2 of apoplast, early and late xylem samples compared to liquid rich medium as reference condition. Fuzzifier parameter *m* was directly estimated as recommended in the Mfuzz manual and cluster number was set at c=8. In a first round of 50 iterations only genes with a $\mu \geq 0.75$ were considered. To classify the rest of T3Es present in strain UY031, a $\mu \geq 0.5$ was set for 20 additional iterations and at $\mu \geq 0.25$ for 4 iterations. RipE2 is not included in the list since it is not present in the annotation provided by NCBI.

Metabolic pathway detection

Amino acid sequences of differentially expressed genes were obtained from GenBank accessions CP012687.1 (chromosome) and CP012688.1 (megaplasmid) and uploaded in the Kegg Mapper tool (http://www.kegg.jp/kegg/tool/annotate_sequence.html) to obtain KO identifiers. These were plotted in IPATH3 (Yamada et al. 2011) to visualize metabolic pathways enriched in the different conditions.

In planta monitoring of *eps* gene expression

To validate RNAseq data, a reporter strain of *R. solanacearum* UY031 with the *eps* promoter fused to LUX genes (Cruz et al. 2014) was used. Bacteria were inoculated into potato plants as previously described for all the conditions, and after sample collection, luminescence and CFUs were measured separately for each plant. *eps* expression levels are expressed as Relative Luminescent Levels divided by 10000 (R.L.U.) and normalized by the amount of CFUs per plant. Samples from 6 different plants were used in each condition.

Acknowledgements

We thank C. Balsalobre and C. Madrid for their useful advice on bacterial metabolism interpretation. This work was funded by projects AGL2013-46898-R, AGL2016-78002-R and RyC 2014-16158 from the Spanish Ministry of Economy and Competitiveness. We also acknowledge financial support from the "Severo Ochoa Program for Centres of Excellence in R&D" 2016-2019 (SEV-2015-0533) and the CERCA Program of the Catalan Government (Generalitat de Catalunya). MP received an APIF doctoral fellowship from Universitat de Barcelona and travel fellowship funded by Fundació Montcelimar and Universitat de Barcelona to carry out a short stay in JCS's lab. PS has an INPhINIT- Obra Social La Caixa Ph.D. fellowship. JCS has CNPq research fellowship. APM is funded by the Chinese Academy of Sciences and the Chinese 1000 Talents Program.

Supplementary Data

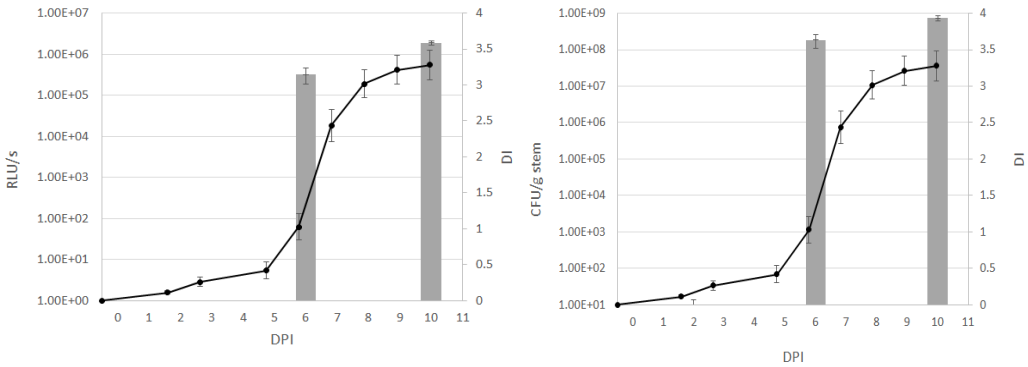

Supplementary Figure 1. *R. solanacearum* growth curve, luminescence and symptom development in potato plants.

A) Luminescence levels or B) bacterial growth and symtpom development in potato plants were monitored over time to detect the precise time points at which similar bacterial yields but different symtpoms could be detected.

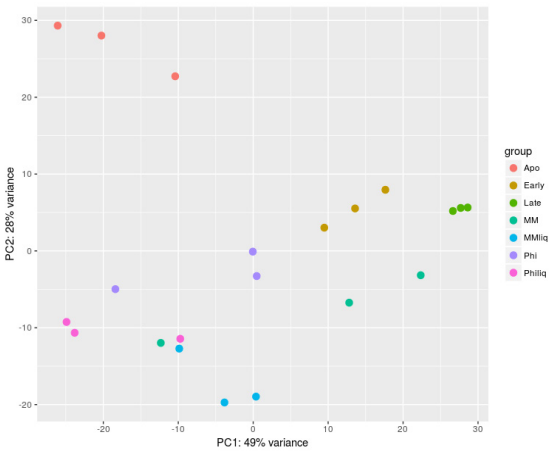

Supplementary Figure 2. PCA analysis of the different biological replicates in all the conditions tested.

MM-MM solid, MMliq- MM liquid, Phi- RM solid, Philiq- RM liquid

Supplementary Figure 3. Venn diagrams showing overlap of DE genes in the three *in planta* conditions when compared to each *in vitro* reference.

Venn Diagram representing the amount of common DE genes between the three *in planta* conditions when compared to the *in vitro* reference conditions.

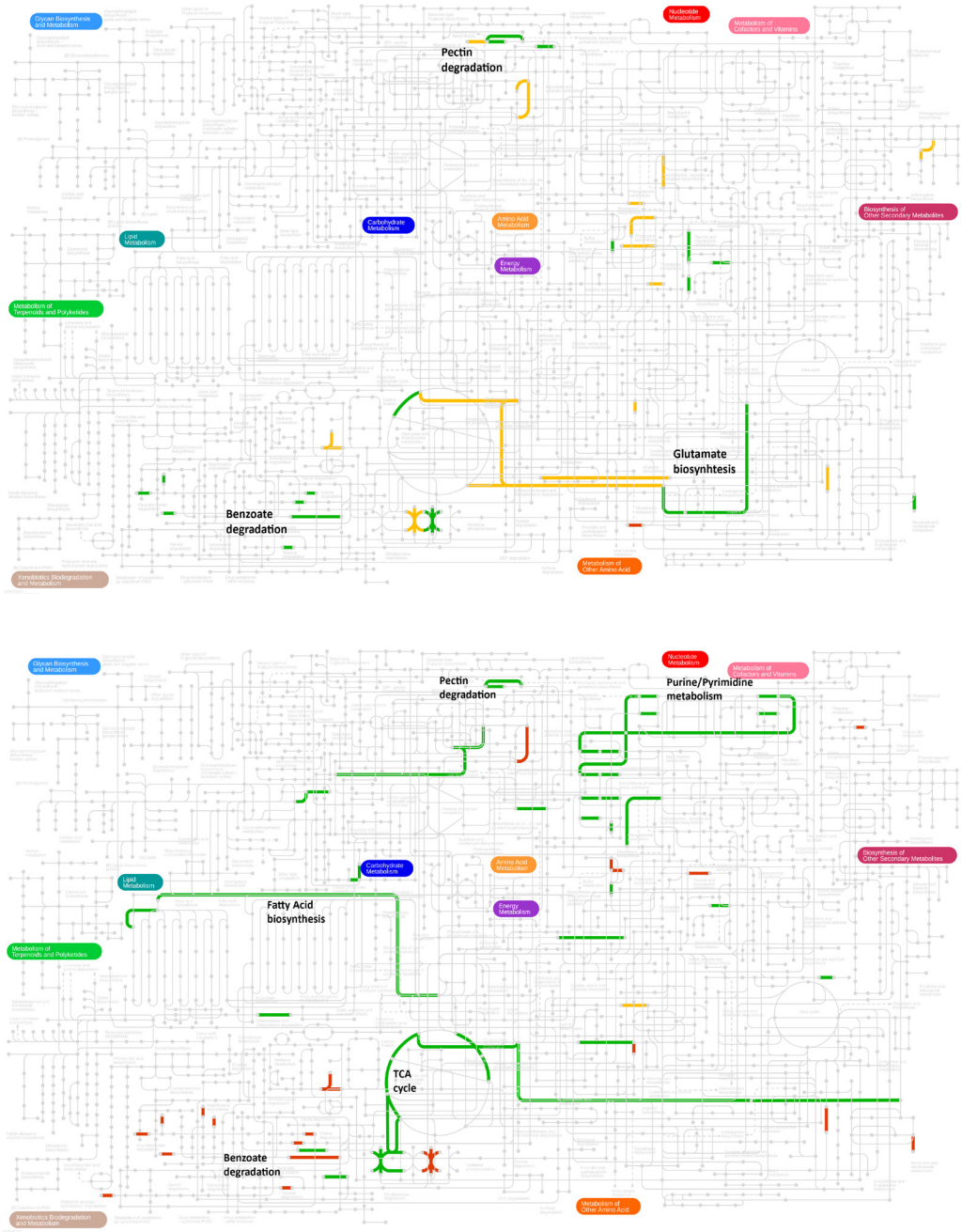

Supplementary Figure 4A. Metabolic pathways induced *in planta* compared to liquid RM or MM.

R. solanacearum up-regulated genes in apoplast, early or late xylem compared to liquid RM (top) or MM (bottom) were mapped onto Kegg pathways using IPATH3. Pathways highlighted in green, yellow or red are found in apoplast, early or late xylem, respectively.

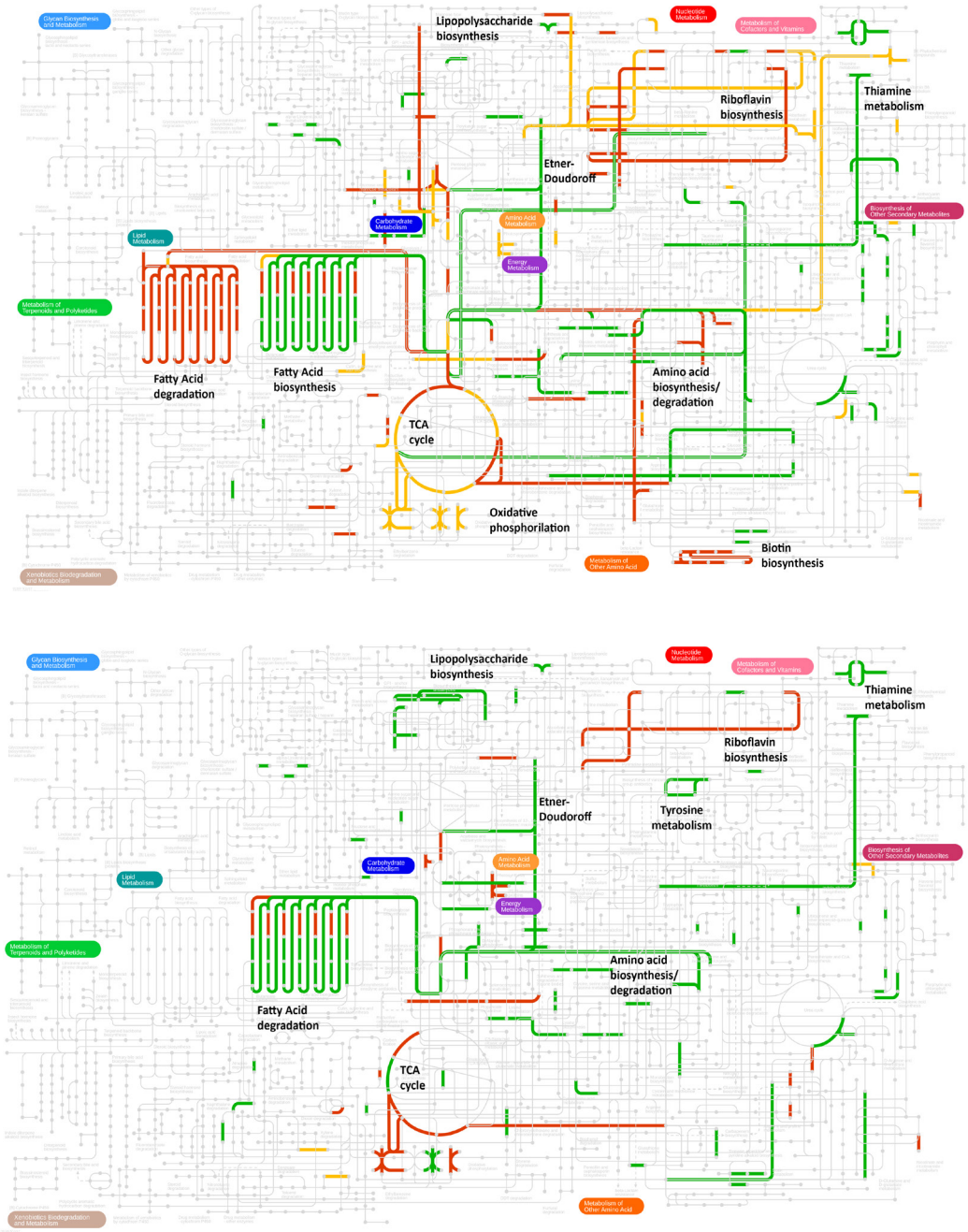

Supplementary Figure 4B. Metabolic pathways repressed *in planta* compared to liquid RM or MM.

R. solanacearum down-regulated genes in apoplast, early or late xylem compared to liquid RM (top) or MM (bottom) were mapped onto Kegg pathways using IPATH3. Pathways highlighted in green, yellow or red are found in apoplast, early or late xylem, respectively.

Supplementary Table 1. Number of mapped reads onto the *R. solanacearum* UY031 genome.

Sample ID	Total reads	Aligned reads	% Aligned reads
Apoplast1	21879209	18225945	83.30
Apoplast2	26766576	22641780	84.59
Apoplast3	24945027	20106785	80.60
Early xylem1	23554394	19887599	84.43
Early xylem2	24102624	20115780	83.46
Early xylem3	25157995	18506738	73.56
Late xylem1	23270138	21909969	94.15
Late xylem2	23309741	21562241	92.50
Late xylem3	24741904	23166640	93.63
MMsolid1	18148670	15865759	87.42
MMsolid2	24947872	23442027	93.96
MMsolid3	25550113	22916162	89.69
RMsol1	31412280	27487884	87.51
RMsol2	36020885	32022483	88.90
RMsol3	51577420	46015394	89.22
MMliq1	30460739	17716297	58.16
MMliq2	30516094	20299314	66.52
MMliq3	29553234	18911203	63.99
RMliq1	28623378	20467036	71.50
RMliq2	32546088	28018378	86.09
RMliq3	30741621	26841635	87.31

Supplementary table 2. DE genes in minimal compared to rich medium in solid plates and liquid cultures.

UY031_NCBI	log_2FC	padj	Gene name	Description
MMs vs RMs				
RSUY_RS18280	-3,72	2,16E-5	-	conserved hypothetical protein
RSUY_RS18995	-3,64	2,78E-8	hmgB	fumarylacetoacetase
RSUY_RS01705	-3,54	2,38E-11	-	4-hydroxyphenylpyruvate dioxygenase oxidoreductase protein
RSUY_RS14695	-3,54	2,30E-12	-	acyl-CoA dehydrogenase oxidoreductase protein
RSUY_RS22930	-3,20	3,33E-12	oprB	putative porin B precursor outer (glucose porin) transmembrane protein
RSUY_RS22935	-3,05	6,28E-9	xylF	D-xylose-binding periplasmic ABC transporter
RSUY_RS14705	-3,05	2,80E-9	-	carbonic anhydrase protein
RSUY_RS22940	-2,87	6,13E-10	xylG	xylose transporter ATP-binding subunit

RSUY_RS19000	-2,86	5,99E-3	hmgA	homogentisate 1,2-dioxygenase
RSUY_RS22960	-2,60	2,96E-5	-	hypothetical protein
RSUY_RS00965	-2,51	8,86E-9	gcvT	glycine cleavage system aminomethyltransferase T
RSUY_RS18215	-2,45	7,40E-3	-	ornithine cyclodeaminase
RSUY_RS22045	-2,38	5,36E-3	-	transcription regulator protein
RSUY_RS19885	-2,36	5,84E-7	-	putative oxidoreductase protein
RSUY_RS00955	-2,30	5,13E-6	gcvP	glycine dehydrogenase
RSUY_RS18985	-2,26	8,02E-3	-	hypothetical protein
RSUY_RS22950	-2,23	5,60E-3	-	putative oxidoreductase protein
RSUY_RS11045	-2,20	2,80E-9	-	two-component system response regulator
RSUY_RS22945	-2,06	4,61E-4	xylH	xylose transmembrane ABC transporter protein
RSUY_RS00635	-2,05	5,84E-7	phhA	phenylalanine 4-monooxygenase
RSUY_RS19890	-1,97	2,30E-12	kbl	2-amino-3-ketobutyrate coenzyme A ligase
RSUY_RS01980	-1,97	6,78E-4	-	putative signal peptide protein
RSUY_RS03990	-1,85	4,30E-3	hutH	histidine ammonia-lyase
RSUY_RS14690	-1,83	5,36E-3	-	putative transcription regulator protein
RSUY_RS12745	-1,83	5,44E-4	-	3-hydroxyacyl-CoA dehydrogenase type II oxidoreductase
RSUY_RS14700	-1,71	7,62E-3	aceK	bifunctional isocitrate dehydrogenase kinase/phosphatase
RSUY_RS21760	-1,68	4,08E-3	-	-
RSUY_RS10580	-1,66	6,81E-4	-	3-hydroxybutyrate dehydrogenase
RSUY_RS09910	-1,57	2,31E-4	-	putative lipoprotein signal peptide
RSUY_RS14730	-1,50	8,40E-3	-	putative 2-hydroxychromene-2-carboxylate isomerase
RSUY_RS15260	1,18	2,99E-3	-	hypothetical protein
RSUY_RS07585	1,24	4,94E-3	-	hypothetical protein
RSUY_RS12260	1,42	7,62E-3	-	hypothetical protein
RSUY_RS12310	1,54	2,13E-6	-	putative oxidoreductase protein
RSUY_RS14540	1,55	8,78E-5	-	putative glutathione peroxidase transmembrane protein
RSUY_RS23040	1,62	7,86E-3	-	hypothetical transmembrane protein
RSUY_RS22085	1,66	5,20E-4	hexR	transcription regulation repressor HEXR
RSUY_RS22075	1,83	2,16E-5	-	two-component response regulator transcription regulator
RSUY_RS08345	2,09	5,99E-3	-	putative lipoprotein
RSUY_RS19620	2,16	8,64E-3	hpaG	leucine-rich-repeat protein
RSUY_RS00210	2,18	4,72E-4	-	hypothetical protein
RSUY_RS17010	2,34	5,98E-3	-	hypothetical protein
RSUY_RS02860	2,41	9,03E-4	-	putative signal peptide protein
RSUY_RS17480	2,49	2,33E-3	-	abc-type transporter, periplasmic component protein
RSUY_RS05740	2,54	3,69E-3	-	hypothetical protein
RSUY_RS14710	2,55	7,56E-3	TIS1021	TIS1021 transposase
RSUY_RS19755	2,66	4,53E-3	hrpF	type III secretion system protein HrpB
RSUY_RS19760	2,72	9,45E-5	hrcN	type III secretion system ATPase

RSUY_RS19535	2,74	1,25E-3	-	hypothetical protein
RSUY_RS17485	2,80	1,25E-3	-	hemin transport protein
RSUY_RS19745	2,84	1,21E-3	hrcJ	Hrp conserved lipoprotein HRCJ transmembrane
RSUY_RS19785	2,85	2,63E-4	RipAC	type III effector protein popc
RSUY_RS19735	2,89	4,49E-3	hrpK	HRPK protein
RSUY_RS10220	2,91	5,43E-3	-	hypothetical protein
RSUY_RS17475	2,91	5,51E-4	-	transmembrane protein
RSUY_RS19700	2,92	6,10E-3	hrpV	hypothetical protein
RSUY_RS01465	2,92	6,78E-4	hdfA	hypothetical protein
RSUY_RS19615	2,99	8,27E-5	-	putative lipoprotein
RSUY_RS17055	3,02	7,32E-3	-	siderophore biosynthesis protein
RSUY_RS19775	3,05	2,77E-3	hrpB	regulatory HRPB transcription regulator protein
RSUY_RS19695	3,07	2,99E-3	hrpW	HRPW transmembrane protein
RSUY_RS19750	3,17	3,77E-3	hrpH	HRPH protein
RSUY_RS09380	3,18	1,59E-4	RipM	hypothetical protein RipM type III effector
RSUY_RS05745	3,23	1,97E-3	-	putative signal peptide protein
RSUY_RS17655	3,32	4,72E-4	-	hydrolase transmembrane protein
RSUY_RS09375	3,39	1,36E-6	-	hypothetical protein
RSUY_RS19690	3,44	2,56E-4	hrpX	hypothetical protein
RSUY_RS17060	3,47	8,08E-5	-	aldolase protein
RSUY_RS12040	3,73	1,02E-10	-	putative transmembrane protein
RSUY_RS19605	3,88	5,34E-8	-	hypothetical protein
RSUY_RS16550	4,02	4,78E-6	RipD	type III effector protein
RSUY_RS19790	4,04	1,39E-5	RipAB	type III effector protein popb
RSUY_RS05760	4,12	9,85E-4	-	signal peptide protein
RSUY_RS18925	4,37	2,34E-5	metE	5-methyltetrahydropteroyltriglutamate-- homocysteine methyltransferase
RSUY_RS22080	4,42	9,46E-7	RipF1_1	secreted protein POPF2 type III effector
RSUY_RS19795	5,18	8,86E-9	RipX	type III effector protein popa1 [contains: popa2 protein; popa3 protein].
RSUY_RS19685	6,68	1,36E-11	hrpY	Hrp pilus subunit HRPY protein
MMl vs RMl				
RSUY_RS19000	-6,51	2,41E-29	hmgA	homogentisate 1,2-dioxygenase
RSUY_RS18995	-5,97	2,41E-29	hmgB	fumarylacetoacetase
RSUY_RS00965	-3,96	3,22E-12	gcvT	glycine cleavage system aminomethyltransferase T
RSUY_RS07380	-3,96	9,83E-9	nagH	putative salicylate-5-hydroxylase small oxygenase component oxidoreductase protein
RSUY_RS01995	-3,95	1,02E-13	-	-
RSUY_RS01990	-3,91	2,81E-13	-	transmembrane ABC transporter protein
RSUY_RS08185	-3,90	1,49E-18	mocB	rhizopine-binding protein precursor
RSUY_RS18280	-3,80	9,73E-3	-	conserved hypothetical protein

RSUY_RS11560	-3,71	6,96E-7	-	hypothetical protein
RSUY_RS08215	-3,69	5,36E-10	iolB	putative myo-inositol catabolism protein
RSUY_RS07375	-3,66	6,63E-7	nagAb	ferredoxin subunit of A ring-hydroxylating dioxygenase oxidoreductase protein
RSUY_RS00955	-3,65	2,35E-22	gcvP	glycine dehydrogenase
RSUY_RS08210	-3,59	2,08E-8	iolE	putative myo-inositol catabolism protein
RSUY_RS18560	-3,57	9,64E-6	paaB	phenylacetate-CoA oxygenase subunit PaaB
RSUY_RS01985	-3,54	2,16E-4	-	hypothetical protein
RSUY_RS08190	-3,46	5,83E-7	-	sugar atp-binding protein
RSUY_RS11620	-3,45	9,76E-12	nuoC	NADH dehydrogenase subunit C
RSUY_RS08200	-3,44	1,64E-5	iolC	transferase kinase protein
RSUY_RS11110	-3,44	6,32E-11	fumA	fumarate hydratase protein
RSUY_RS01980	-3,41	8,32E-9	-	putative signal peptide protein
RSUY_RS20765	-3,40	6,33E-9	scrB	putative sucrose-6-phosphate hydrolase (Sucrase invertase)
RSUY_RS18505	-3,35	5,81E-4	-	general secretion pathway GSPG-like transmembrane
RSUY_RS07435	-3,29	5,73E-7	-	hypothetical protein
RSUY_RS07385	-3,27	2,48E-6	nagG	putative salicylate-5-hydroxylase oxygenase component
RSUY_RS11280	-3,24	7,00E-5	-	hypothetical protein
RSUY_RS11295	-3,19	2,74E-3	sdhD	succinate dehydrogenase hydrophobic subunit
RSUY_RS07430	-3,18	1,16E-3	-	cytochrome p-450-like monooxygenase protein
RSUY_RS08205	-3,17	6,94E-5	iolD	putative acetolactate synthase protein
RSUY_RS11285	-3,14	6,29E-6	sdhB	succinate dehydrogenase iron-sulfur subunit
RSUY_RS08145	-3,12	6,94E-5	-	pyridine nucleotide-disulphide oxidoreductase
RSUY_RS20770	-3,12	1,84E-6	scrA	PTS system, sucrose-specific (IIBC component) protein
RSUY_RS11570	-3,11	1,88E-4	nuoM	NADH dehydrogenase subunit M
RSUY_RS11575	-3,10	1,44E-4	nuoL	NADH dehydrogenase subunit L
RSUY_RS08195	-3,10	6,72E-4	-	sugar transmembrane protein
RSUY_RS20760	-3,08	9,24E-4	-	porin transmembrane protein
RSUY_RS22930	-3,06	9,73E-3	oprB	porin B precursor outer (glucose porin)
RSUY_RS22940	-3,04	1,91E-8	xylG	xylose transporter ATP-binding subunit
RSUY_RS22950	-3,03	3,31E-3	-	putative oxidoreductase protein
RSUY_RS11565	-3,02	1,63E-4	nuoN	NADH dehydrogenase subunit N
RSUY_RS11625	-3,01	1,23E-3	nuoB	NADH dehydrogenase subunit B
RSUY_RS02000	-3,00	1,25E-10	-	ABC transporter ATP-binding protein
RSUY_RS20695	-3,00	2,99E-6	-	transmembrane aldehyde dehydrogenase oxidoreductase
RSUY_RS20215	-3,00	6,94E-5	-	conserved hypothetical protein
RSUY_RS08220	-2,99	2,67E-3	-	putative isomerase-like tim barrel; protein
RSUY_RS00635	-2,94	2,09E-3	phhA	phenylalanine 4-monooxygenase
RSUY_RS20180	-2,94	3,41E-4	-	conserved hypothetical protein
RSUY_RS22945	-2,91	1,14E-5	xylH	xylose transmembrane ABC transporter protein

RSUY_RS00950	-2,88	9,24E-4	sdaA2	L-serine dehydratase
RSUY_RS04415	-2,88	4,57E-4	rfbC	dTDP-4-dehydrorhamnose 3,5-epimerase protein
RSUY_RS02010	-2,87	1,36E-8	glpD	glycerol-3-phosphate dehydrogenase
RSUY_RS08225	-2,87	5,54E-4	-	putative myo-inositol 2-dehydrogenase protein
RSUY_RS18770	-2,85	1,18E-3	-	hypothetical protein
RSUY_RS11290	-2,84	8,03E-4	sdhA	succinate dehydrogenase flavoprotein subunit
RSUY_RS11615	-2,84	2,53E-3	nuoD	NADH dehydrogenase subunit D
RSUY_RS11600	-2,81	1,10E-4	nuoG	NADH dehydrogenase subunit G
RSUY_RS20700	-2,79	5,52E-3	-	beta alanine--pyruvate transaminase
RSUY_RS11340	-2,77	1,96E-4	acnA	aconitate hydratase
RSUY_RS18940	-2,76	7,86E-3	-	putative diaminopimelate decarboxylase protein
RSUY_RS11595	-2,73	8,53E-3	nuoH	NADH dehydrogenase subunit H
RSUY_RS11610	-2,68	1,81E-3	nuoE	NADH dehydrogenase subunit E
RSUY_RS11590	-2,65	1,04E-4	nuoI	NADH dehydrogenase subunit I
RSUY_RS20775	-2,63	7,89E-4	scrR	DNA-binding sucrose operon transcription regulator
RSUY_RS11555	-2,61	2,21E-4	-	hypothetical protein
RSUY_RS02005	-2,60	8,03E-4	-	putative sugar-phosphate ATP-binding ABC transporter
RSUY_RS08050	-2,59	1,81E-4	hlfX	hypothetical protein
RSUY_RS09870	-2,53	3,13E-5	-	putative isomerase rotamase signal peptide protein
RSUY_RS00910	-2,49	4,31E-8	putA	trifunctional transcriptional regulator
RSUY_RS10860	2,19	3,66E-3	-	hypothetical protein
RSUY_RS10885	2,26	2,36E-3	-	hypothetical protein
RSUY_RS18240	2,53	2,89E-3	-	hydrolase transmembrane protein
RSUY_RS09370	2,61	1,29E-3	RipV2	probable type III effector protein RipV2
RSUY_RS19075	2,61	1,12E-3	-	hypothetical protein
RSUY_RS12565	2,66	8,25E-9	-	hypothetical protein
RSUY_RS20605	2,75	3,58E-4	-	signal peptide protein
RSUY_RS16300	2,80	4,56E-3	-	putative transmembrane protein
RSUY_RS05740	2,83	3,33E-6	-	hypothetical protein
RSUY_RS14975	2,92	6,71E-4	-	-
RSUY_RS22285	2,92	4,09E-3	-	hypothetical protein
RSUY_RS22300	3,07	1,00E-5	-	hypothetical protein
RSUY_RS10890	3,08	7,30E-5	mel	tyrosinase oxidoreductase protein
RSUY_RS16975	3,09	7,86E-3	-	hypothetical protein
RSUY_RS16650	3,11	6,78E-5	-	hypothetical protein
RSUY_RS18580	3,13	1,07E-3	-	hypothetical protein
RSUY_RS22305	3,24	1,65E-3	-	hypothetical protein
RSUY_RS23055	3,29	1,73E-3	-	signal peptide protein
RSUY_RS17025	3,36	4,89E-5	-	ferric siderophore receptor outer membrane signal peptide
RSUY_RS19770	3,41	1,62E-3	hrcT	Hrp conserved HRCT transmembrane protein

RSUY_RS22310	3,47	1,91E-5	-	hypothetical protein
RSUY_RS17045	3,47	1,65E-3	-	multidrug resistance 1 transmembrane protein
RSUY_RS01425	3,49	6,14E-3	-	hypothetical protein
RSUY_RS01465	3,66	2,16E-4	hdfA	hypothetical protein
RSUY_RS17060	3,84	3,13E-5	-	aldolase protein
RSUY_RS17020	3,85	1,57E-9	-	sigma factor transcription regulator protein
RSUY_RS11155	3,86	1,57E-4	hemP	putative hemin uptake protein
RSUY_RS05000	3,86	7,57E-3	-	putative lipoprotein transmembrane
RSUY_RS19535	3,93	1,94E-4	-	hypothetical protein
RSUY_RS17040	4,01	3,03E-7	-	putative siderophore biosynthesis protein
RSUY_RS16550	4,08	2,40E-12	RipD	type III effector protein
RSUY_RS19670	4,10	3,06E-17	hrpG	response regulator transcription regulator protein
RSUY_RS17015	4,16	1,72E-9	-	ferric siderophore receptor protein
RSUY_RS17065	4,21	7,87E-16	-	diaminopimelate decarboxylase protein
RSUY_RS17655	4,26	4,50E-18	-	hydrolase transmembrane protein
RSUY_RS17050	4,34	3,14E-14	-	siderophore biosynthesis protein
RSUY_RS08775	4,34	2,54E-7	RipG7	type III effector gala7 protein
RSUY_RS20405	4,37	1,52E-4	-	transcription activator transcription regulator protein
RSUY_RS19785	4,40	4,25E-14	RipAC	type III effector protein popc
RSUY_RS05745	4,42	4,25E-14	-	putative signal peptide protein
RSUY_RS17055	4,46	3,14E-14	-	siderophore biosynthesis protein
RSUY_RS10220	4,48	5,12E-21	-	hypothetical protein
RSUY_RS19775	4,49	1,29E-5	hrpB	regulatory HRPB transcription regulator protein
RSUY_RS19605	4,55	2,71E-5	-	hypothetical protein
RSUY_RS17010	4,75	7,88E-14	-	hypothetical protein
RSUY_RS19740	4,80	4,42E-7	hrpJ	HRPJ protein
RSUY_RS19675	4,92	4,77E-11	hpaB	hypothetical protein
RSUY_RS17510	4,94	3,46E-14	-	hypothetical protein
RSUY_RS17505	5,09	7,88E-14	fur2	ferric uptake transcriptional transcription regulator
RSUY_RS17035	5,27	2,58E-25	-	ornithine cyclodeaminase protein
RSUY_RS17030	5,35	3,75E-23	cysM2	cysteine synthase A protein
RSUY_RS19680	5,38	1,03E-14	hrpZ	HRPY-like protein
RSUY_RS19710	5,50	1,96E-11	hrcR	type III secretion system protein
RSUY_RS17480	5,57	2,09E-5	-	abc-type transporter, periplasmic component protein
RSUY_RS19690	5,60	2,36E-9	hrpX	hypothetical protein
RSUY_RS22080	5,66	8,03E-21	RipF1_1	secreted protein POPF2 type III effector
RSUY_RS19705	5,90	2,39E-11	hrcS	Hrp conserved HRCS transmembrane protein
RSUY_RS17485	6,32	3,85E-8	-	hemin transport protein
RSUY_RS17490	6,99	2,29E-11	-	outer membrane hemin receptor signal peptide protein
RSUY_RS19795	7,30	5,70E-19	RipX	type III effector protein popA
RSUY_RS19685	7,84	3,37E-24	hrpY	Hrp pilus subunit HRPY protein
RSUY_RS19790	8,63	3,77E-48	RipAB	type III effector protein popb

Supplementary Table 3. Proportion of up- and down-regulated genes in apoplast, early and late xylem (versus RMs, MMl and MMs) in relation to other *R. solanacearum* gene expression analyses. Percentage of common DE genes in each *in planta* condition compared to previous *in planta* gene expression analyses (A-Meng et al. 2015; B-Brown and Allen 2004, C-Occhialini et al. 2005 and Valls et al. 2006, D-Jacobs et al. 2012, E-Puigvert et al. 2017, F-Khokhani et al. 2017). Colors were plotted using the Conditional Formatting in Microsoft Excel.

RM solid						MM liquid						MM solid						
Induced			Repressed			Induced			Repressed			Induced			Repressed			
Apoplast	Early xylem	Late xylem	Apoplast	Early xylem	Late xylem	Apoplast	Early xylem	Late xylem	Apoplast	Early xylem	Late xylem	Apoplast	Early xylem	Late xylem	Apoplast	Early xylem	Late xylem	
5	14	13	7	4	4	8	12	12	10	6	6	4	35	0	8	5	6	RNAseq -Tº-dependent factors tomato xylem (A)
3	3	3	4	2	2	1	1	1	3	3	2	4	0	0	3	5	2	IVET-tomato xylem (B)
1	15	6	2	0	0	1	1	2	6	5	3	0	0	0	6	5	4	Microarray- MM B-reg (C)
5	7	4	3	2	3	4	3	2	5	7	4	3	0	0	3	5	3	Microarray- MM G-reg (C)
0	0	0	0	0	0	0	0	0	0	0	0	0	0	0	0	0	0	Microarray- MM BG-reg (C)
16	54	25	9	2	4	12	19	15	15	13	10	8	53	7	11	6	9	Microarray-tomato xylem UW551 UP (D)
6	2	4	26	33	24	9	4	3	15	28	18	13	0	7	11	20	15	Microarray-tomato xylem UW551 DOWN (D)
7	41	20	5	2	1	8	15	13	8	2	3	5	41	14	5	2	2	Microarray-tomato xylem GMI1000 UP (D)
4	0	1	10	19	15	6	2	2	4	8	9	9	0	0	4	6	7	Microarray-tomato xylem GMI1000 DOWN (D)
17	36	8	15	14	10	10	5	7	9	9	11	9	24	7	11	11	15	RNAseq-Wild potato root (E)
11	24	9	21	18	14	7	5	6	24	27	25	6	18	0	11	9	18	RNAseq-tomato xylem phcA-regulated (F)

Supplementary Table 4. Heatmap of the functional categories present in the *in planta* clusters.

Numbers indicate the percentage of genes of each category in the four clusters. Color-code is applied to all categories except Metabolism, Transposases and Hypothetical proteins. D-Down, U-Up.

D-D	U-D	U-U	D-U	
1.8	-	-	-	**Flagellum**
-	-	4.6	-	**Chemotaxis**
2.1	0.6	1.2	1.2	**PilT4A**
-	2.5	1.9	-	**PilT4B**
0.2	1.7	2.2	-	**T3E**
0.5	4.7	-	-	**T3SS**
1.0	-	-	1.2	**T2SS +CWDE**
0.2	2.5	-	-	**T6SS**
1.4	0.3	0.3	-	**QS, EPS, Biofilms**
0.7	0.6	0.3	-	**ROS**
4.0	4.7	12.3	2.4	**TF, Regulators**
0.5	2.2	0.3	-	**Nitrogen**
1.4	1.7	0.3	-	**Cytochrome**
2.0	3.3	7.7	8.4	**Transporters, Porins**
-	1.1	-	-	**HCA degradation**
43	33	22	12	**Metabolism,Energy,Translation**
35	40	43	53	**Hypothetical, Unknown function**
5	1	3	20	**Transposases, Phage-related**
1071	**360**	**324**	**83**	
Number of genes				

chapter 8

DRAFT 3

Identification of inhibitors of the type III secretion system to combat bacterial plant diseases

Identification of inhibitors of the type III secretion system to combat bacterial plant diseases

Marina Puigvert[1,2], Montserrat Solé[2], Belén López-Garcia[2], Núria S. Coll[2], Karren D. Beattie[3], Rohan A. Davis[3], Mikael Elofsson[4], Marc Valls[1,2*]

[1]Department of Genetics, University of Barcelona, Barcelona, Catalonia, Spain
[2]Centre for Research in Agricultural Genomics (CSIC-IRTA-UAB-UB), Bellaterra, Catalonia, Spain
[3]Griffith Institute for Drug Discovery, Griffith University, Queensland, Australia
[4]Department of Chemistry, Umeå University, Umeå, Sweden

Abstract

Finding chemical compounds that prevent and combat bacterial diseases is fundamental for crop production. Bacterial virulence inhibitors are a promising alternative to classical control treatments, such as bactericides or copper-based products, because they preserve the host microbiome, they have a low environmental impact and they are less likely to generate bacterial resistance. The major virulence determinant of most animal and plant bacterial pathogens is the Type III Secretion System (T3SS), which is increasingly regarded as an attractive target of novel antimicrobial molecules. In this work, we screened 9 plant extracts and 12 isolated compounds –including molecules effective against human pathogens– for their capacity to inhibit the T3SS of plant pathogens and their applicability as virulence inhibitors for crop protection. The screen was performed using a luminescent reporter system developed in the model pathogenic bacterium *Ralstonia solanacearum.* Five synthetic molecules, one natural product and two plant extracts were found to downregulate T3SS transcription, most of them through inhibition of the regulator *hrpB,* without altering transcription of control genes nor substantially affecting bacterial growth. In addition, for three of the molecules, corresponding to salicylidene acylhydrazide derivatives, the inhibitory effect caused a dramatic decrease in the T3SS capacity, which was translated in impaired plant hypersensitive response to the pathogen. These candidate virulence inhibitors were then tested for their ability to protect plants against *R. solanacearum* and *Pseudomonas syringae*. We demonstrate that salicylidene acylhydrazides can suppress T3SS functionality in these two plant pathogens, limiting *R. solanacearum* multiplication *in planta* and protecting tomato plants from bacterial speck caused by *P. syringae*. Our work validates the efficiency of transcription reporters to discover compounds (natural or synthetic) or natural product extracts that can be potentially applied to prevent bacterial plant diseases.

Introduction

Few effective management options are available against bacterial plant diseases, such as bacterial wilt caused by *Ralstonia solanacearum* or bacterial speck caused by *Pseudomonas syringae.* Antibiotics and copper-based compounds had traditionally been used (Zaumeyer 1958), however their application is now restricted in many countries (Duffy et al. 2005), due to their environmental impact. An important emerging strategy to combat pathogens seeks to block the ability of bacteria to harm the host by inhibiting bacterial virulence factors (Rasko and Sperandio 2010). Unlike antibiotics, virulence inhibitors do not kill the pathogen and should thus preserve the host endogenous microbiome and exert little selective pressure, avoiding the rapid appearance of resistance (Clatworthy et al. 2007).

The type III secretion system (T3SS) is an attractive target for antimicrobial compounds since it is essential for virulence in many pathogenic gram-negative bacteria (Puri and Bogyo 2009). This system injects bacterial effector proteins into host cells to subvert its defences (Buttner 2016). In bacterial plant pathogens, the T3SS is encoded by the *hrp* genes, so called because they play a key role both in the hypersensitive response (HR) elicitation and in pathogenicity (Boucher et al. 1987). The HR is a programmed cell death reaction that takes place locally in plants upon pathogen recognition at the site of infection (Huysmans et al. 2017). In the model phytopathogenic bacterium *R. solanacearum,* the regulator HrpB directly activates transcription of the genes encoding the structural units of the T3SS and its associated effectors (Genin et al. 1992; Occhialini et al. 2005; Valls et al. 2006). Amongst the genes controlled by HrpB is ***hrpY***, that codes for the major constituent of the T3SS pilus (Van Gijsegem et al. 2000).

As a strategy to block bacterial virulence, interdisciplinary efforts have identified some small molecules that can specifically inhibit the synthesis or the functionality of the T3SS in human pathogens of the genera *Yersinia*, *Salmonella, Chlamydia* and *Pseudomonas* (Kauppi et al. 2003; Muschiol et al. 2006; Hudson et al. 2007; Yamazaki et al. 2012). Compounds with such activity include salicylidene acylhydrazides, N-hydroxybenzimidazoles, cytosporone B, ***p***-coumaric acid and (–)-hopeaphenol (Kauppi et al. 2003; Kim et al. 2009; Li et al. 2009; Li et al. 2013; Zetterstrom et al. 2013; Davis et al. 2014). Most of these anti-virulence agents lack bacteriocidal activity and have been proven in *in vitro* or *in vivo* studies to inhibit symptoms or infection showing no toxic effects on the host (Duncan et al. 2012). Treatment of infected animals has shown promising results for *Citrobacter rodentium* (Kimura 2011), *Yersinia pseudotuberculosis* (Garrity-Ryan 2010), *Chlamydia trachomatis* (Slepenkin et al. 2011) and *Salmonella enterica* (Hudson et al. 2007; Nesterenko et al. 2016) infections. More recently, the plant phenolic compound *p*-coumaric acid (PCA) was identified as an inhibitor of T3SS transcription in the phytopathogen *Dickeya dadantii* (Li et al. 2009). Recent reports show that some PCA derivatives can suppress T3SS functionality in *Xanthomonas oryzae* (Fan et al. 2017) and in *Erwinia amylovora* (Yang et al. 2014) in rice and apple flower infection, respectively. Other PCA derivatives have been shown to be efficient in

reducing blossom blight caused by *E. amylovora* on apple trees in the field (Sundin et al. 2016).

In this work, we have determined the effect of several plant extracts and some molecules already described as T3SS inhibitors of bacterial animal pathogens against plant pathogens. We have taken advantage of a luminescent reporter system developed for *R. solanacearum* (Monteiro et al. 2012b) to select those compounds/extracts that specifically inhibit transcription of *R. solanacearum hrpB* and *hrpY* genes. Positive candidates were tested for their ability to suppress T3SS functionality *in vitro* and *in vivo*. Finally, their efficiency in controlling bacterial wilt or bacterial speck in tomato plants was examined.

Results

In vitro screen for compounds that reduce *hrpY* transcription

We used *R. solanacearum* as a model bacterial plant pathogen to evaluate the potential T3SS inhibitory effect of a number of pure compounds and plant extracts. We tested molecules already described as T3SS inhibitors in human and animal pathogens, including ***p***-coumaric acid and analogues (PP1-6), cytosporone B (CB), salicylidene acylhydrazides (SA1-4), (–)-hopeaphenol (HA) as well as the plant-derived extracts (E1-9). All tested molecules as well as their source are summarized in Table 1. To detect and quantify their inhibitory effects we took advantage of a strain that bears a transcriptional fusion of the *hrpY* promoter (*PhrpY*), controlling expression of the T3SS pilus component, with the *luxCDABE* operon (Monteiro *et al.* 2012a).

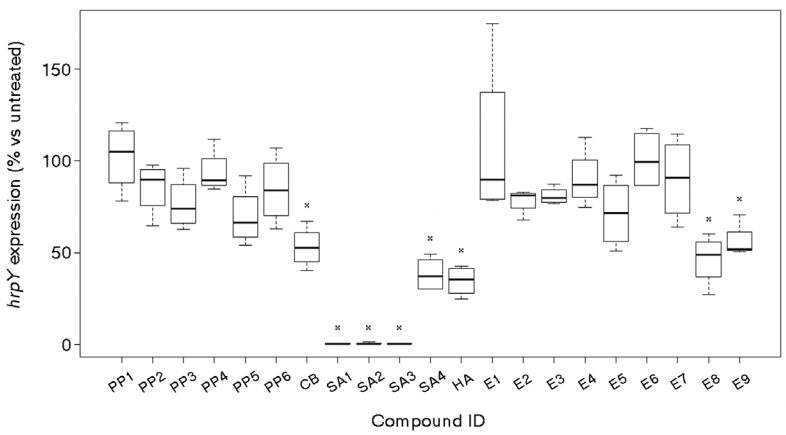

Figure 1. Expression of the T3SS pilus gene (*hrpY)* in the presence of different compounds.

Ralstonia solanacearum carrying the *PhrpY::luxCDABE* fusion was grown in minimal medium supplemented with each compound/extract (detailed in Table 1) at 100 µM final concentration or with DMSO (control). *hrpY* expression was quantified at 8 hpi by luminescence, normalised by cell density and represented with respect to the value obtained with DMSO (control). Compounds/extracts marked with an asterisk showed statistical reduction in *hrpY* expression compared to control conditions. Each measurement corresponds to the average of four replicates.

Table 1. List of compounds and plant extracts in evaluated this work.

ID	Compound or the most abundant compound in extract	Source of the material (Reference)
PP1	p-coumaric acid	Synthetic plant phenylpropanoid (Li et al. 2009)
PP2	2,4-dihydroxycinnamic acid (umbellic acic)	Synthetic plant phenylpropanoid (Li et al. 2009)
PP3	4-chlorocinnamic acid	Synthetic plant phenylpropanoid (Li et al. 2009)
PP4	3,4-dihydroxycinnamic acid (caffeic acid)	Synthetic plant phenylpropanoid (Li et al. 2009)
PP5	4-methoxycinnamic acid	Synthetic plant phenylpropanoid (Li et al. 2009)
PP6	4-methylcinnamic acid	Synthetic plant phenylpropanoid (Li et al. 2009)
CB	cytosporone B	Synthetic fungal compound (Li et al. 2013)
SA1	ME0054 (benzoic acid N´-(2,3,4-trihydoxy-benzylidene)-hydrazide)	Synthetic salicylidene acylhydrazide (Nordfelth et al. 2005)
SA2	ME0055 (4-nitrobenzoic acid N´-(2,4-dihydoxy-benzylidene)-hydrazide)	Synthetic salicylidene acylhydrazide (Nordfelth et al. 2005, Dahlgren et al. 2010)
SA3	ME0177 (2-nitro-benzoic acid N´-(3,5-dichloro-2-hydroxy-benzylidene)-hydrazide)	Synthetic salicylidene acylhydrazide (Dahlgren et al. 2010)
SA4	ME0192 (3,5-dichloro-benzoic acid N´-(4-diethylamino-2-hydroxy-benzylidene)-hydrazide	Synthetic salicylidene acylhydrazide (Dahlgren et al. 2010)
HA	(-)-hopeaphenol	Plant natural compound (Zetterstrom et al. 2013, Davis et al. 2014)
E1	4,11-dimethoxy-5-methyl-[1,3]dioxolo[4,5-b]acridin-10(5H)-one	Melicope elleryana leaf extract (Crow and Price 1949)
E2	4-methoxy-6-[(E)-2-(4-methoxyphenyl)ethenyl]pyran-2-one	Piper methysticum root extract (Bu'Lock and Smith 1960)
E3	3,7,8-trihydroxyserrulat-14-en-19-oic acid	Eremophila microtheca leaf extract (Barnes et al. 2013)
E4	7-[3-(5,5-dimethyl-4-oxofuran-2-yl)but-2-enoxy]chromen-2-one	Geijera parviflora leaf extract (Dreyer and Lee 1972)
E5	4,4'-((1R,2R,3S,4S)-3,4-dimethylcyclobutane-1,2-diyl)bis(2-methoxyphenol)	Endiandra anthropophagorum root extract (Davis et al. 2007, Davis et al. 2009)
E6	1a-acetoxy-4b,8a-dihydroxy-6b,9a-dibenzoyl-b-agarofuran	Denhamia celastroides leaf extract (Levrier et al. 2015)
E7	(E)-1,3-diphenylprop-2-en-1-one	Syzygium tierneyanum leaf extract (Kumar et al. 2016)
E8	5,6-dimethoxy-10-methyl-2H-pyrano[2,3-f]quinolin-2-one	Goniothalamus australis bark extract (Levrier et al. 2013)
E9	5-(4-methoxybenzyl)-6-methyl-[1,3]dioxolo[4,5-g]isoquinolin-6-ium	Doryphora sassafras leaf extract (Carroll et al. 2001)

This strain emits luminescence and does not require antibiotic selection as the promoter::reporter fusion is stably integrated in monocopy in the bacterial chromosome. Bacteria were grown in minimal medium – a condition ensuring maximal induction of *hrpY* expression – and luminescence was directly measured 8 hours after incubation with each of the compounds and normalized by cell density (OD_{600}). Figure 1 shows *hrpY* expression levels after incubation with each extract/ molecule normalized by expression levels in control conditions (DMSO addition). As shown in Figure 1, CB, SA1-4, HA, E8 and E9 showed a statistically significant repression of *hrpY* expression. The inhibitory effect was mild after addition of compounds CB, SA4, HA, E8 and E9 while SA1, SA2 and SA3 almost completely abolished *hrpY* expression. We thus selected these molecules as well as a molecule and an extract with intermediate effects (SA4 and E8) for further characterisation.

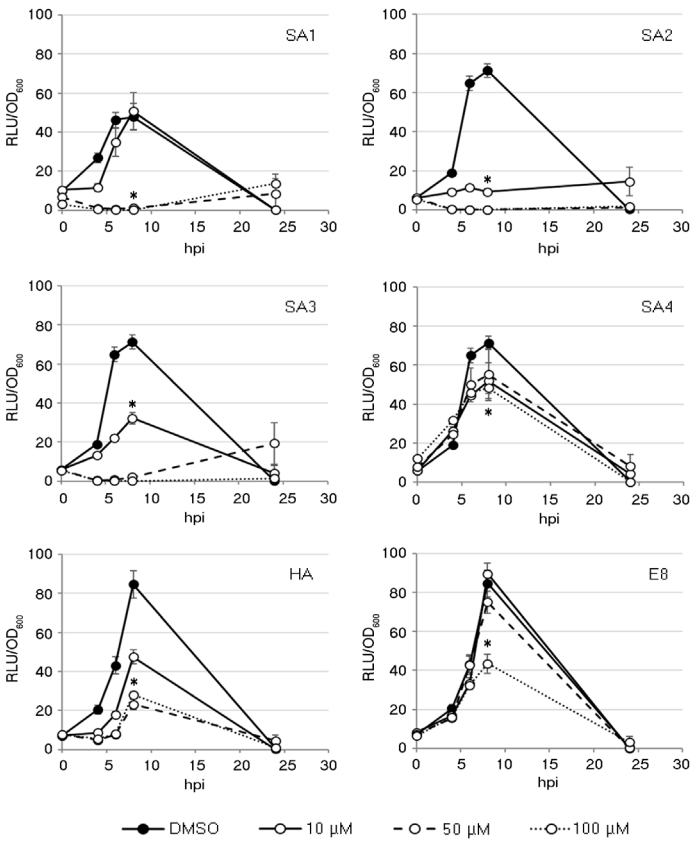

Figure 2. Time course expression of *hrpY* after addition of selected T3SS inhibitors.

hrpY expression was quantified at 4, 6, 8 and 24 hpi by direct luminescence quantification from bacteria growing in minimal medium supplemented with SA1 to 4, HA or E8 at different concentrations or with DMSO as control. Expression is represented as Relative Luminescent Units (RLU) normalized by bacterial density (OD_{600}) at each time point. Asterisks indicate the minimal effective concentration of each compound or extract at the most informative time point. Each measurement represents the average of four replicates.

Salicylidene acylhydrazides inhibit T3SS expression at the *hrpB* level

We performed a time-course analysis monitoring *hrpY* expression upon addition of varying amounts of the identified inhibitors to determine their minimal effective concentration (Figure 2). This experiment revealed that a minimal concentration of 10 µM for SA2, SA3 and HA, and 50 µM for SA1, was sufficient to cause full inhibition, while for SA4 and E8, 100 µM was needed for maximal effect. Next, to determine if the analysed substances caused a general inhibition of the T3SS, and not only on *hrpY*, we measured transcription of *hrpB* – the master regulator controlling expression of the T3SS genes – over time (Suppl Figure 1). As can be observed in figure 3, six of the eight substances inhibiting *PhrpY* caused a comparable reduction in ***hrpB*** transcription, implying a shutdown of all T3SS-encoding genes and the associated effectors controlled by this regulator (Occhialini et al. 2005).

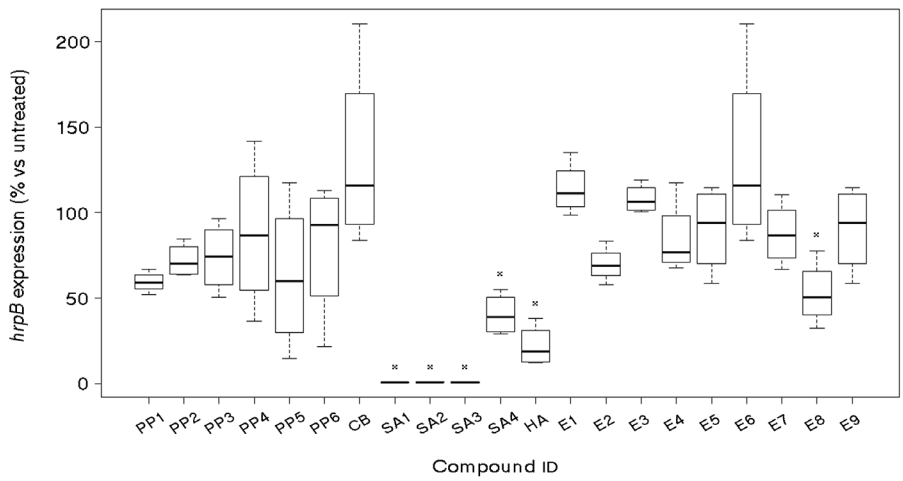

Figure 3. Expression of the main T3SS regulator (*hrpB*) in the presence of different compounds.

Ralstonia solanacearum bearing the *PhrpB::luxCDABE* fusion was grown in minimal medium supplemented with each compound/extract (detailed in Table 1) at 100 µM final concentration or with DMSO (control). *hrpB* expression was quantified at 8 hpi by luminescence, normalised by cell density and represented with respect to that in DMSO. Compounds/extracts marked with an asterisk showed statistical reduction in *hrpB* expression compared to control conditions. Each measurement corresponds to the average of four replicates.

To rule out that the observed effects were due to a general, unspecific inhibition of gene expression we made use of a *R. solanacearum* strain containing the luminescence reporter under the control of the heterologous promoter *PpsbA*. *PpsbA* is a chloroplastic promoter that shows strong, constitutive expression when introduced in Gram-negative bacteria (Wang et al. 2007). As shown in Figure 4A, at 8 hpi *PpsbA* was not affected by most compounds tested. A slight but significant induction of *PpsbA* expression was detected after bacterial incubation with SA2,

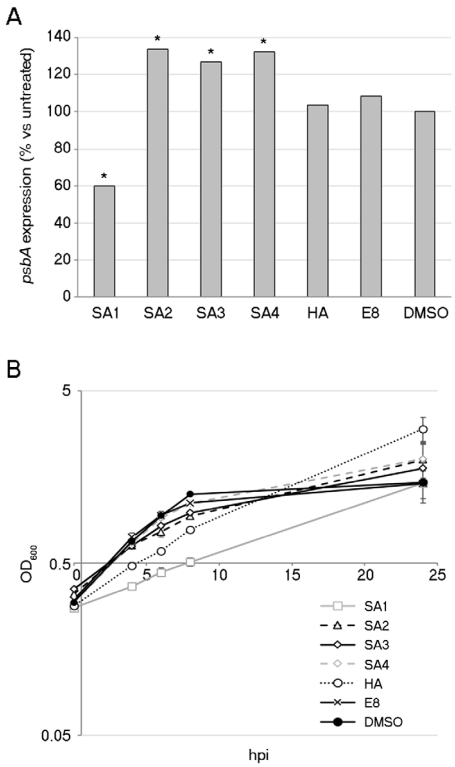

Figure 4. *PpsbA* transcription and *R. solanacearum* growth upon treatment with identified T3SS inhibitors.

(a) *R. solanacearum* bearing the *PpsbA::luxCDABE* fusion was grown for 8 h in liquid minimal medium supplemented with each compound/extract at their in vitro minimal effective concentration (50 µM for SA1, 10 µM for SA2 and SA3, 50 µM for SA4 and HA, and 100 µM for E8). Transcription was quantified by measuring luminescence divided by bacterial growth. Percentage of *psbA* expression in each treatment was normalized by basal expression after DMSO addition (control). Each measurement corresponds to an average of four replicates, and experiments were repeated with similar results. Standard errors never exceeded 25%. Compounds marked with an asterisk showed statistical reduction or increase in psbA expression compared to addition of DMSO (control). (b) Bacterial growth was measured at 4, 6, 8 and 24 h in the same conditions using *R. solanacearum* containing the *PhrpY::luxCDABE* construct. Cell densities were measured as absorbance at 600 nm and are represented in a logarithmic scale.

SA3 and HA (Figure 4A) showing that inhibition of the transcription of the T3SS was selective. In contrast, incubation with SA1 caused repression of *PpsbA* expression, an effect due to the slower bacterial growth caused by addition of this compound (see below and Figure 4B). Bacterial growth defects were not observed during our gene expression analyses using reporter strains. However, to accurately determine whether the used compounds affected bacterial viability, we measured the growth of *R. solanacearum PhrpY::Lux* in liquid culture after addition of the transcriptional inhibitors. Figure 4B shows that, at their minimal inhibitory concentrations, SA1 and HA are slightly bacteriostatic, as their effects can only be observed at short time points and are not apparent after 24 h.

Salicylidene acylhydrazides inhibit T3SS effector translocation

To determine if transcriptional inhibitors of the T3SS impaired its functionality, we tested their effect on the T3SS-dependent secretion of effector proteins *in vitro*. To this end, we used a *R. solanacearum* strain producing an HA-tagged version of the T3SS effector AvrA. To ensure AvrA-HA production in the presence of T3SS inhibitors, this tagged version was placed under the control of the constitutive *psbA* promoter, which is highly expressed under our experimental conditions (Cruz et al. 2014). As shown in Figure 5, incubation of bacteria with the strongest

T3SS inhibitors – the salicylidene acylhydrazide derivatives SA1, SA2 and SA3 – inhibited AvrA secretion, as this effector was detected only in the cytosolic bacterial fraction (C) and not in the secreted fraction (S). These results support the lack of a functional T3SS in bacteria incubated with these compounds, as AvrA could not be secreted to the medium through this apparatus. This effect was accentuated for the strongest T3SS inhibitors, as bacterial incubation with the mild inhibitor E8 allowed detection of secreted AvrA in the culture medium, although at lower levels than the control condition (DMSO).

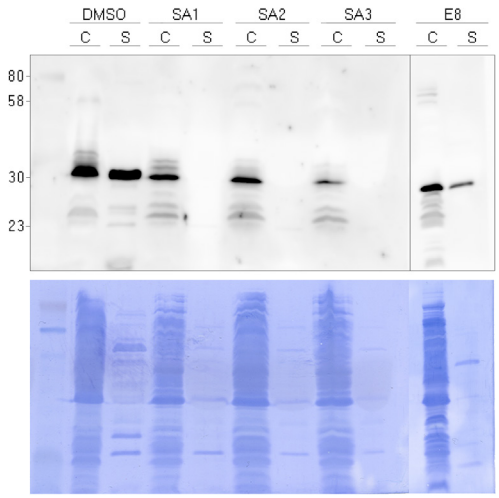

Figure 5. Effector secretion is inhibited by bacterial pre-incubation with salycidene acylhydrazides.

R. solanacearum bearing the *Pps-AvrA-HA* construct was grown for 8 hours in minimal medium supplemented with congo red to promote protein secretion and with each of the T3SS inhibitors (SA1-3 and E8) at 100 µM. Incubation with DMSO was used as a control to verify that protein secretion was not altered. The cytosolic (C) and secreted (S) protein fractions were separated by centrifugation followed by protein precipitation and AvrA was detected with an anti-HA antibody. Coomassie-stained SDS-PAGE membranes used in the Western Blotting are also shown.

The AvrA effector secreted by the *R. solanacearum* strain used in this work has been shown to trigger a Hypersensitive Response (HR) on tobacco plants (Poueymiro et al. 2009). To validate our *in vitro* results and determine whether inhibition of T3SS secretion was physiologically relevant *in planta*, we tested the influence of pre-incubating bacteria with salicylidene acylhydrazides on the plant HR. *N. tabacum* and *N. benthamiana* plants were leaf-infiltrated with 5-fold *R. solanacearum* dilutions obtained after 8-hour incubation with SA1-3 or DMSO (control). As shown in Figure 6, HR was inhibited when *N. tabacum* leaves were infiltrated with bacteria grown in the presence of some salicylidene acylhydrazides (SA1-3), showing that inhibition of effector secretion resulted in evasion of recognition by the plant immune system. Similar results were obtained when using *N. benthamiana* as host (Supplementary Figure 2).

Figure 6. Hypersensitive response inhibition by salicylidene acylhydrazides.

Bacteria grown for 8 hpi in liquid minimal medium after addition of SA1-3 at 100 µM or DMSO alone were serially diluted 5-fold in water (10^7, $5{\cdot}10^6$, 10^6 and $5{\cdot}10^5$ CFUs/ml top to bottom) and leaf-infiltrated in *Nicotiana tabacum*. HR responses were photographed at 2 dpi. Numbers indicate the proportion of positive leaves (showing HR inhibition due to T3SS suppressors) in relation to the total tested leaves.

Salicylidene acylhydrazides limit *R. solanacearum* growth *in planta* and protect tomato plants from bacterial speck

The *R. solanacearum* reporter strains proved to be very useful to identify small molecules that inhibit T3SS. As a first step to validate the ability of these compounds in limiting *R. solanacearum* infection, we measured multiplication of bacteria that were infiltrated on tomato leaves alone or in the presence of the inhibitors. As shown in Figure 7, a significant decrease in bacterial growth was observed when the most effective T3SS inhibitors (SA1-3) were present. This result demonstrates that salicylidene acylhydrazides are effective in limiting *R. solanacearum* growth *in planta,* although no differences in wilting symptoms could be observed after watering tomato plants with a *R. solanacearum* inoculum containing SA2 at 100 µM (Supplementary Figure 3). However, as *R. solanacearum* infects plants through the roots, high amounts of inhibitors would be needed to treat the soils and protect crops from bacterial wilt. Thus, we used the foliar pathogen *Pseudomonas syringae* pv. tomato DC3000, which requires effector translocation via T3SS to cause bacterial speck disease in tomato (Munkvold et al. 2009) to test the preventative effect of the potent T3SS inhibitors (SA1-3). Tomato plants were sprayed with a solution containing these compounds or with DMSO alone (control) and subsequently inoculated by spray with a bacterial suspension. Symptoms were quantified using a necrosis index, and a clear symptom reduction was observed at 3 dpi in plants that had been pre-treated with SA1-3 compared to control plants (Figure 8). This was in accord with their inhibitory effect on the transcription and functionality of the main bacterial virulence determinant: the T3SS. Taken together, our results indicate that some salicylidene acylhydrazides show a protective effect against bacterial speck, suggesting that they could be utilized as virulence inhibitors to control bacterial plant diseases in the field.

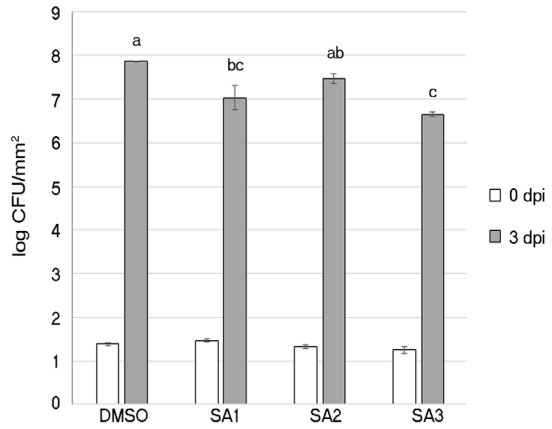

Figure 7. *Ralstonia solanacearum* growth in tomato is impaired by the addition of compounds SA1-3.

R. solanacearum was leaf-inoculated at 10^5 CFU/ml with SA1-3 at 100 µM. Leaf disks were taken at 0 and 3 days after inoculation to monitor bacterial multiplication. Bacterial growth is represented as colony forming units (CFU) per mm^2 in logarithmic scale at day 3 and day 0 (immediately after inoculation). Each point represents the mean of three biological replicates consisting on two different leaf disks. Experiments were repeated three times with similar results. Statistical groups were obtained following Tukey's HSD test using $p<0.05$.

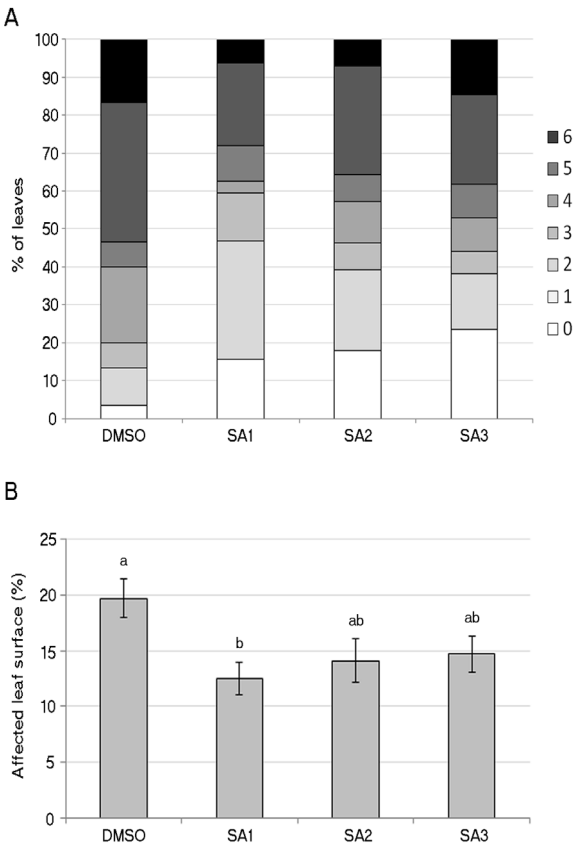

Figure 8. Symptom development in tomato plants pre-treated with T3SS inhibitors and inoculated with *Pseudomonas syringae*.

Effect of T3SS inhibitors on disease symptoms. Plants were pre-treated with SA1-3 at 100 µM or with DMSO 1 hour before bacterial inoculation with *P. syringae*. Symptoms were recorded three days post inoculation and are represented as A) percentage of leaves categorized in a disease scale from 0 (no visible symptoms) to 6 (extensive necrosis on >35% of the leaf), or as B) average on percentage of affected leaf surface with the corresponding standard error. Statistical groups were obtained with Tukey's HSD test using $p<0.05$. The experiment was performed three times with similar results.

Discussion

An effective screening methodology to identify T3SS inhibitors

Bacterial plant diseases represent a major limitation in crop production and contribute to significant economic losses yearly. Copper compounds and antibiotics have been successfully employed as management strategies in fields since the early 1900s (Zaumeyer, 1958). However, the use of chemical bactericides as crop protectants represents a threat to the environment, and may result in a risk for public health due to the rapid emergence of resistances that could eventually be acquired by clinical pathogens (Sundin et al. 2016). In this work, we screened 22 compounds and plant extracts in search for antimicrobial alternatives that downregulate gene expression of the T3SS, the main virulence determinant of most pathogenic bacteria. We used a luminescent reporter strain of the model phytopathogen *R. solanacearum* to directly monitor expression of *hrpY*, which has the highest transcriptional output amongst the *hrp* genes (our own unpublished data). We found eight compounds and extracts (CB, SA1-4, HA, E8 and E9) capable of specifically repressing *hrpY* transcription to various degrees (Figure 1). Six of these inhibitors also repressed *hrpB* expression (Figure 3 and Supplementary Figure 1) and thus seem to act upstream of the *hrp* regulatory cascade. The exceptions are cytosporone B and E9, which might interfere specifically with *hrpY* transcription. The effects on gene expression perfectly correlated with T3SS functional analyses, as the strongest inhibitors SA1-3 were also able to inhibit *in vitro* and *in vivo* effector production and secretion through the T3SS, whereas milder inhibitors such as E8 had a minor effect on secretion (Figures 5). Our screening methodology has proved to be very effective, probably due to the high sensitivity of the luminescent reporter used. This system could also be scaled to 96-well plates or even be used qualitatively by presence/absence of light emission (Kauppi et al. 2003).

R. solanacearum T3SS inhibitors are effective against several plant pathogenic bacteria

The *R. solanacearum* T3SS regulators targeted by the molecules identified here have orthologues in various *Xanthomonas ssp*. and *Burkholderia ssp.* strains (Zou et al., 2006; Li et al., 2011; Lipscomb and Schell, 2011), showing the potential of our screening method to isolate virulence inhibitors that can be effective against other pathogens. Interestingly, we found that the salicylidene acylhydrazide SA1, inhibited *R. solanacearum* T3SS expression and could also protect plants from *P. syringae* infection (Figure 8). In fact, cross-inhibition is not surprising in our case, as salicylidene acylhydrazides were selected for our screening because they had already been shown to inhibit the T3SS of *E. amylovora* (Yang et al. 2014), whose T3SS is closely related to *P. syringae* (Alfano and Collmer 1997, Tang et al. 2006). In any case, our findings suggest that salicylidene acylhydrazides act on proteins that affect T3SS expression, privileging this mode of action over the alternative hypotheses proposed: direct effects on the T3SS basal apparatus proteins or possible changes in iron availability (Wang et al. 2011).

In contrast, despite the conservation of the *hrp* genes, some molecules seem to act in a species-specific manner. This is the case of the plant phenolic compound *p*-coumaric acid (PCA) and its derivatives, which were recently found to act as T3SS inhibitors in *D. dadantii, E. amylovora* and *P. aeruginosa* (Li et al. 2009, Yamazaki et al. 2012, Khokhani et al. 2013). We showed that neither PCA nor some derivatives (PP1-3) were effective *R. solanacearum* T3SS inhibitors, similarly to what was described for the closely related rice pathogen *X. oryzae* (Fan et al. 2017).

Effectiveness of salicylidene acylhydrazides as crop protectants against bacterial pathogens

Salicylidene acylhydrazides SA1-3 proved to be powerful inhibitors of the *R. solanacearum* T3SS, our results demonstrated that SA1-3 inhibited its functionality *in vivo* and impaired bacterial multiplication *in planta* (Figure 7). However, no symptom reduction was visible in tomato wilting assays by soil-inoculating a *R. solanacearum* suspension containing one of these potent inhibitors (Supplementary Figure 3). *R. solanacearum* is a soil-borne pathogen, and direct soil treatments are usually challenging and cost-ineffective (Yadeta and BP 2013). On the other hand, aerial plant treatments are widely used to control diseases caused by pathogens that infect the aerial part of plants. Here we demonstrated the efficiency of such treatments under laboratory conditions, as tomato plants sprayed with the potent T3SS inhibitors SA1-3 before *P. syringae* inoculation displayed less disease symptoms compared to control plants (Figure 8). To assess the effectiveness of inhibitors, previous studies have pre-treated bacteria prior to pathogenicity assays (Fan et al. 2017, Yang et al. 2014). A recent report showed that bacterial pre-treatment with other T3SS inhibitors could impede their virulence in plants (Fan et al. 2017). To simulate a more realistic application in the field, in this study plants instead of bacteria were pre-treated with the T3SS inhibitor during the pathogenicity tests. This is the first report proving that T3SS inhibitors can be applied to plants for protection against pathogens and opens the way to the development of analogous molecules that are cost-effective crop protectants.

T3SS inhibitor analogues thus represent a potential and cost-effective source of antimicrobials that could successfully control wilt diseases in fields. Salicylidene acylhydrazides can be efficiently prepared in one step from commercially available starting materials. Finally, identification of such functional analogues would open the way to explore new treatment strategies for vascular wilts and other challenging bacterial plant diseases, for which no effective management strategy is currently available (Yadeta and BP 2013).

Materials and Methods

Bacterial strains and gene cloning

The *R. solanacearum* GMI1000 luminescent reporter strains for *hrpB* and *psbA* promoters used in this work were described elsewhere (Monteiro et al. 2012a, Cruz et al. 2014). Gene constructs were introduced in *R. solanacearum* GMI1000 through natural transformation of linearized plasmids and double-recombination events as described (Boucher et al. 1985). The hrpY

reporter strain was constructed after transformation of SfiI-digested vector pRCG-PhrpY-lux. For pRCG-PhrpY-lux construction, the *hrpY* promoter was PCR amplified from the genome of strain GMI1000 with primers that added 5'AvrII and 3'KpnI flanking sites and cloned into the pRCG-PhrpB-Lux backbone (Monteiro et al. 2012b) using the introduced sites. The *R. solanacearum* GMI1000 strain expressing an HA-tagged *avrA* gene under the *psbA* promoter was generated after transformation with linearized plasmid pRCK-Pps-AvrA. pRCK-Pps-AvrA was created by Gateway LR reaction (Invitrogen, USA) between plasmids pENTR/SD-AvrA and pRCG-Pps-GWY (Cruz MPMI 2014). *R. solanacearum* was routinely grown in rich B medium (10g/l bactopeptone, 1 g/l yeast extract, 1 g/l casaminoacids, 0.5% glucose) supplemented with gentamycin 10 µg/ml (solid media) or 5 µg/ml (liquid media) at 28ºC. For T3SS inhibition tests, the bacterial cultures were grown in Boucher's Minimal Medium (Boucher et al. 1985) supplemented with 20 mM glutamate and 5 µg/ml gentamycin. *Pseudomonas syringae* DC3000 was routinely grown at 28ºC on KB-agar plates supplemented with 25 µg/ml rifampicin and 50 µg/ml kanamycin or in liquid Luria Bertani broth. The sequence of oligonucleotides used as primers is available upon request.

Compound/extract supply

A list of the compounds and plant extracts used in this work can be found in Table 1. Synthetic plant phenylpropanoids (PP) 1–6 and cytosporone B (CB) were purchased from Sigma-Aldrich. Salicylidene acylhydrazides (SA) 1–4 were provided by Dr. M. Elofsson (Dahlgren et al. 2010, Nordfelth et al. 2005), and (–)-hopeaphenol (HA) (Zetterstrom et al. 2013, Davis et al. 2014) and the 9 plant extracts (E) 1–9 were provided by Dr. R. Davis (Bu'Lock and Smith 1960, Carroll et al. 2001, Crow and Price 1949, Davis et al. 2009, Davis et al. 2007, Dreyer and Lee 1972, Kumar et al. 2016, Levrier et al. 2013, Levrier et al. 2015, Barnes et al. 2013).

The NatureBank biota repository (www.griffith.edu.au/gridd) was the source of the plant material from which the extracts were derived. In order to generate the plant extracts, a portion of dry plant material (300 mg) was added to a solid phase extraction (SPE) cartridge (Phenomenex polypropylene SPE, 10 mm x 50 mm,) and dichloromethane (8 ml) followed by methanol (8 ml) were percolated through the material under gravity. Both organic extracts were combined and weighed in order to create the extract that was tested. (–)-Hopeaphenol (>99% purity) was obtained from the Davis Open Access Natural Product Library, which is currently housed at Compounds Australia (Griffith University; www.compoundsaustralia.com). All compounds were dissolved in DMSO at a final concentration of 100 mM and stored at-20 ºC. Plant extract concentrations were calculated according to their prevalent compound (specified in Table 1) molarity, dissolved in DMSO and stored at 100 mM at-20 ºC.

T3SS inhibition test

For the T3SS inhibition tests, *R. solanacearum* luminescent reporter strains were grown overnight in rich B medium and diluted to an OD_{600} of 0.3 in 1.5 ml of fresh Boucher's Minimal Medium supplemented with the test compounds. Compounds were normally evaluated at 100 µM (or 10 and 50 µM when testing the minimal effective concentration). Plant extracts were used at the equivalent molarity of their major compound (indicated in Table 1). 1.5 µl of DMSO was used as a control condition. Growth and luminescence measurements were taken at 0, 4, 6, 8 and 24 hpi. Luminescence was measured using a FB12 luminometer (Berthold detection systems) and is expressed as Relative Luminescence Units (luminometer values divided by 1000). Bacterial growth was measured at OD_{600} in a V-1200 spectrophotometer (VWR).

Effector secretion and immunodetection

To induce production and secretion of AvrA effector protein, $2x10^8$ cells/ml were inoculated in 10 ml of Minimal Medium supplemented with 5 µg/ml gentamycin, 10 mM glutamate, 10 mM sucrose, 100 µg/ml congo red and 100 µg/ml of the test compound (or 10 µl DMSO) and grown at 25 ºC for 14 h. Bacterial cultures were centrifuged at 4000 *x g* for 10 minutes and the culture medium supernatant was filter sterilized, mixed with 10 ml of cold 25% trichloroacetic acid and incubated overnight at 4ºC. Samples were then centrifuged at 6000 *x g* for 30 minutes at 4 ºC, the supernatant was discarded and the protein pellet was washed twice with cold 90% acetone. The bacterial pellet was dissolved in 50 µl phosphate buffered saline (PBS) 1X and 10 µl Laemmli buffer 5X, sonicated for 90 sec (30% amplification, 10 sec ON/OFF intervals) using a Digital Sonifier (Model 250/450, Branson) and boiled for 5 min. AvrA was detected by Western Blotting using a primary anti-HA rat monoclonal antibody already conjugated to HRP (clone 3F10, Roche), diluted 1:4000 in 40 ml Tris-buffered saline (TBS) buffer supplemented with 0.1% tween 20 and 1% skimmed milk. Immunodetected AvrA-HA was developed using Immobilon ECL (Millipore) and membranes were photographed using a LAS-4000 mini system (Fujifilm).

Plant material and hypersensitive response assays

Nicotiana benthamiana, Nicotiana tabacum and *Solanum lycopersicum* cv Marmande plants were grown for 3 weeks in pots containing peat soil in a greenhouse under long-day conditions (16 h light at 25 ºC, 8 h dark at 22 ºC).

For hypersensitive response assays, *R. solanacearum* GMI1000 bearing the *PhrpY::luxCDABE* fusion was grown for 8 hours in Boucher's Minimal Medium supplemented with glutamate and the test compound at 100 µM (or with DMSO for the non-treated condition). Bacteria were recovered by centrifugation, washed with sterile distilled water and adjusted to 10^7, $5x10^6$, 10^6 and 10^5 cells/ml in sterile distilled water. Bacterial solutions were leaf-infiltrated in *Nicotiana tabacum* and *Nicotiana benthamiana* plants. Hypersensitive response cell death was annotated at 2 days post infiltration in *N. tabacum* plants and 5 days post infiltration in *N. benthamiana* plants. For a better HR cell death visualization, *N. benthamiana* leaves were ethanol-bleached in 100% ethanol at 60 ºC for 20 minutes.

R. solanacearum growth *in planta*

For *in planta* growth assays, *R. solanacearum* recovered from overnight cultures as described above were hand-infiltrated in tomato leaves at a final concentration of 10^5 CFU/ml together with compounds SA 1-3 at 100 µM (or with DMSO alone in the non-treatment condition). Two 5 mm-diameter disks per biological replicate were taken from different infiltrated leaves, homogenized and 10 µl of serial ten-fold dilutions plated in selective rich medium plates. Plates were incubated at 28 ºC until colonies could be counted. Samples were taken at day 0 and at day 3 after-infiltration. Three biological replicates were used per treatment.

Virulence tests on tomato plants

R. solanacearum pathogenicity assays were performed as follows: 3-week old tomato plants were acclimated for three days at 28 ºC and 12/12 hour-photoperiod conditions. Roots were wounded by disturbing the soil with a 1 ml pipette tip. Twenty five ml of a suspension 10^8 bacterial cells/ml supplemented with 100 µM of the test compound (or DMSO alone for non-treated) was used to water each plant. Twelve plants were used in each condition and wilting symptoms were annotated per plant using an established semi-quantitative wilting scale ranging from 0 (no wilting) to 4 (death) (Vailleau et al. 2007).

P. syringae pathogenicity assays were performed as follows: 3-week old tomato plants were sprayed with a 100 µM dilution of the test compound (or DMSO alone for non-treated) and air dried for 1 hour. Each plant was then sprayed with 6 ml of a *P. syringae* suspension at a final OD_{600}= 0.2. To maintain high humidity, plants were placed in trays inside transparent boxes containing a layer of water. A total of 20 plants were used in each test and 3-4 leaves were evaluated per plant. Symptoms were annotated for each leaf 3 days post inoculation using a necrosis scale (0: healthy leaf, 1: chlorosis, 2: necrosis in one leaflet, 3: chlorosis and necrosis in one leaflet, 4: necrosis in several leaflets, 5: chlorosis and necrosis in several leaflets, 6: general necrosis).

Statistical analyses

The effect of the compounds on gene expression and *in planta* bacterial growth was determined by the Analysis of Variance (One-Way ANOVA) followed by the Tukey's HSD posthoc test using the agricolae package (version 1.2-4) in R (version 3.3.3). Differences were considered to be statistically significant at $p<0.05$.

Funding

This work was funded by projects AGL2013-46898-R, AGL2016-78002-R and RyC 2014-16158 from the Spanish Ministry of Economy and Competitiveness. We also acknowledge financial support from the "Severo Ochoa Program for Centres of Excellence in R&D" 2016-2019 (SEV-2015-0533) and the CERCA Program of the Catalan Government (Generalitat de Catalunya) and from COST Action SUSTAIN (FA1208) from the European Union. MP received a project collaboration grant (project 307624) from Fundació Bosch i Gimpera (Universitat de Barcelona) and holds an APIF doctoral fellowship from Universitat de Barcelona. RAD and KDB were supported by an Australian Research Council (ARC) Linkage Grant (LP120200339) and ARC Grants (LE0668477 and LE0237908).

Acknowledgements

We thank C. Popa and P. Zuluaga for their valuable advice and their technical assistance. F. Monteiro is acknowledged for cloning the *PhrpY::luxCDABE* construct. RAD and KDB also acknowledge the NatureBank biota repository that is housed at the Griffith Institute for Drug Discovery, Griffith University (www.griffith.edu.au/gridd) and from which the plant extracts were derived.

Supplementary Data

8

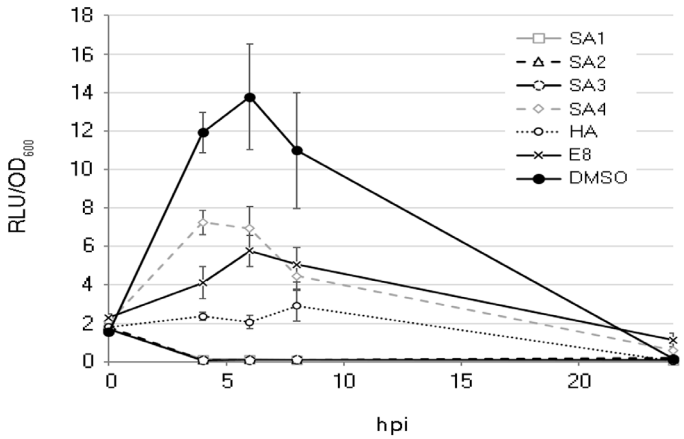

Supplementary Figure 1. Analysis of time course expression of *hrpB* in the presence of candidate T3SS inhibitors.

hrpB expression was quantified at 4, 6, 8 and 24 hpi by direct quantification of luminescence from bacteria growing in minimal medium supplemented with SA1 to 4, HA or E8 at 100 µM or with DMSO as control. Expression is represented as Relative Luminescent Units (RLU) normalized by bacterial density (OD_{600}) at each time point. Four replicates were used in each measurement and the experiment was repeated two times with similar results.

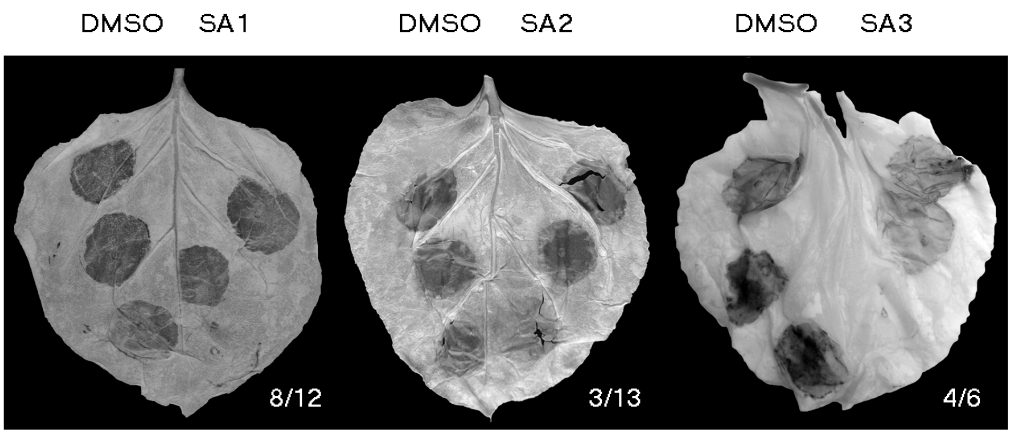

Supplementary Figure 2. Hypersensitive response inhibition by salicylidene acylhydrazides.

Bacteria grown for 8 hpi in liquid minimal medium after addition of SA1-3 at 100 µM or DMSO alone were serially diluted 5-fold in water ($5{\cdot}10^6$, 10^6 and $5{\cdot}10^5$ CFUs/ml top to bottom for left and central leaves, 10^7, $5{\cdot}10^6$ and 10^6 CFUs/ml top to bottom for right leaf) and leaf-infiltrated in Nicotiana benthamiana. HR responses were photographed at 5 dpi. Leaves were ethanol-bleached for better HR visualization. Numbers indicate the proportion of positive leaves (showing HR inhibition due to T3SS suppressors) in relation to the total tested leaves, with the rest of leaves showing no effect.

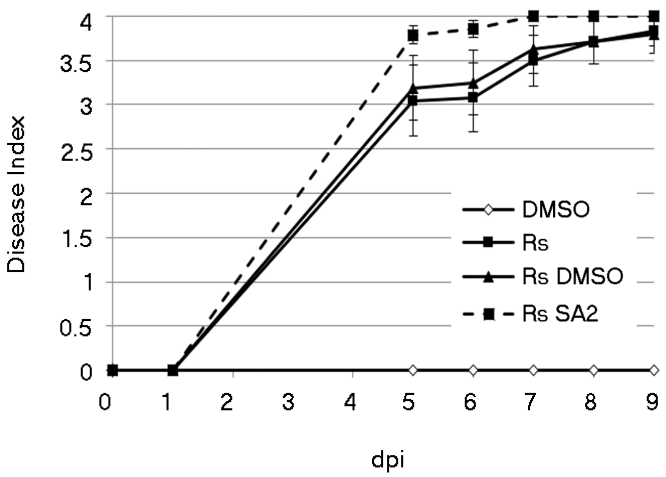

Supplementary Figure 3. Wilting symptoms are unaltered in tomato plants pre-treated with SA2 prior to *Ralstonia solanacearum* soil inoculation.

Symptoms were recorded over time on tomato plants inoculated with *R. solanacearum* by soil drenching after watering with a DMSO solution (black triangles) or a SA2 solution (dashed line). As a control, plants watered with DMSO (white diamonds) or inoculated with *R. solanacearum* (black squares) were also included in the experiment. Disease progression was annotated per plant according to a scale ranging from 0 to 4 (0- no wilting, 1- 25% wilted leaves, 2- 50%, 3- 75%, 4- dead plant). 12 plants were used per condition and each measurement corresponds to the mean and standard error.

chapter 9

Discussion

R. solanaceaeum is the causal agent of bacterial wilt, a lethal disease with worldwide distribution and associated to important economic losses (Hayward 1991). Strains belonging to phylotype IIB-1 are of special concern since they are acclimated to temperate climates and have already caused outbreaks in some European countries (Janse et al. 2004). In this work, we characterized a IIB-1 strain highly aggressive on potato called UY031 (Siri et al. 2011) from several perspectives: its genome (chapter 3), its methylome profile (chapter 4) and its transcriptome during plant colonization (chapters 5 and 7). We also discovered a new player involved in bacterial adaptation to plant intercellular spaces (chapter 6) and, finally, we performed a proof of concept study to identify antimicrobial compounds to control bacterial plant diseases (chapter 8).

A new layer on the regulation of virulence gene expression in *R. solanacearum*?

Although the genomes of many *R. solanacearum* strains have been completely sequenced in the last years, the first IIB-1 strain to have a closed genome was *R. solanacearum* strain UY031 (chapter 3). We used SMRT technology to completely sequence *R. solanacearum* UY031 genome (5.4 Mb). This opened the path for the identification of virulence related genes in this strain and revealed that it contains a repertoire of at least 60 T3Es. Genomic comparison with other *R. solanacearum* strains, let us conclude that approximately 60% of the genes belong to the core genome. This result indicates that there is a high percentage of variability between strains that may account for variations in host specificity or aggressiveness. In addition, SMRT sequencing (chapter 3) provided us for the first time with the DNA methylation profile of a *R. solanacearum* strain.

Epigenetic marks have been extensively studied during the last years in eukaryotes, and although they have diverged during evolution and across kingdoms, their origin is known to be prokaryotic (Willbanks et al. 2016). DNA methylation has been mostly associated to Restriction-Modification (RM) systems in prokaryotes, as a protective mechanisms against exogenous DNA (Tock and Dryden 2005). Beyond RM-systems, adenine methylation (m6A) is the main epigenetic modification controlling replication, DNA repair, transposition and gene expression in prokaryotes (Casadesus and Low 2006; Low and Casadesus 2008). Furthermore, loci of several regulators, such as OxyR or Fur, have been described to be controlled by adenine methylation, indicating their potential transcriptional regulation at the methylome level (Sanchez-Romero et al. 2015). Interestingly, loss of methylation has also been associated to increased virulence in *Salmonella enterica*, *Mycobacterium tuberculosis* and the enterohemorrhagic *Escherichia coli* O157:H7 (Sanchez-Romero et al. 2015).

In chapter 4, we compared the methylomes of *R. solanacearum* UY031 and GMI1000 strains. The analysis revealed a highly conserved methyl-transferase (MTase) responsible for the G<u>T</u>WW**A**C motif methylation, which appeared to be preferentially present in upstream regions of coding

genes. The upstream region of EpsR, the EPS biosynthesis regulator, contained two methylated GTWW**A**C sites close to the promoter region in both strains.

In an attempt to explore the possible role of this orphan MTase on *eps* expression, we created deletion mutants in both *R. solanacearum* strains and measured *eps* expression by using luminescent reporters. We show that in both strains, a slight reduction in *eps* expression can be detected when bacterial cultures were started with very diluted cell densities (10^6 CFU/ml). The same expression pattern was detected in both strains, which had the same methylation profile in the EpsR upstream region. These results point to the direction of a novel layer in the control of virulence gene expression mediated by DNA methylation. To test this hypothesis, it would be interesting to test whether genes with different methylation patterns between *R. solanacearum* GMI1000 and UY031 in GTWW**A**C sites of upstream regions also show different expression profiles. Finally, virulence tests using MTase deletion mutants will provide information about the final impact of DNA methylation on *R. solanacearum* virulence.

Setting the path towards the study of *R. solanacearum in planta* gene expression

To date, a large battery of virulence factors in *R. solanacearum* has been identified (Meng 2013) and much effort has been devoted to unveil the regulatory networks controlling their expression (Peyraud et al. 2016). Yet, the study of the pathogen's gene expression during disease raised some inconsistencies with previous *in vitro* analyses. For instance, the assumption of an early role of the T3SS appeared to be contradictory to *hrp* expression at advanced disease stages (Jacobs et al. 2012; Monteiro et al. 2012a). Since then, many other *in planta* transcriptomes became available all focusing at only one particular stage of the pathogen's life cycle: xylem colonization at the onset of the disease. (Meng et al. 2015; Ailloud et al. 2016; Khokhani et al. 2017). These analyses led to the identification of new bacterial traits involved in the colonization of xylem vessels (Jacobs et al. 2012; Dalsing and Allen 2014). The fact that *R. solanacearum* bears complex regulatory networks to control expression of virulence factors in a bacterial population or plant-cell contact dependent manner, suggests that there might be sets of early/late pathogenicity determinants (Álvarez et al. 2010). In this line, some functional studies suggested an early role in infection of some bacterial virulence factors, such as motility driven by flagella and chemotaxis (Tans-Kersten et al. 2001; Yao and Allen 2006), while a late role was mainly assigned to EPS (Schell 2000). However, the coordinate expression of these virulence factors during the development of the disease remained unknown.

In an attempt to better understand the interplay of different virulence factors that drive pathogenicity in *R. solanacearum*, we studied its transcriptome at different and unexplored stages of the infection process in potato plants. In our first approach, we analyzed the bacterial transcriptome during root colonization of wild potato plants (chapter 5). With our method we

were able to study bacterial gene expression in a realistic manner by bioinformatically selecting the pathogen's mRNAs from the total sample. Accuracy in our analysis was possible thanks to the completely sequenced genome of the *R. solanacearum* UY031 strain (chapter 3). We demonstrated that, compared to bacteria grown on rich medium, *R. solanacearum* induces the expression of virulence-associated genes and down-regulates the expression of most metabolic pathways. The notable exceptions were nitrogen (*narL, ptsN)*, phosphate (*pstS1*, *pstB*) and sulfate (*cysI1)* metabolism genes, which were induced at that stage. We were also able to identify several differentially expressed genes reported to play a role in virulence in other pathogens, such as the T3SS and T3Es, motility and stress-response related genes, and provided a list of candidate genes necessary for root colonization. The fact that more than 30% of the genes overlapped to previous reported *in planta* transcriptomes revealed two ideas. First, it validated our approach, demonstrating that we were able to identify genes with a conserved role in plant colonization. Second, the fact that many genes involved in xylem colonization also appeared at the root stage, suggested that our samples contained a mixture of populations colonizing both the apoplast and the xylem vessels.

Although this work contributed to the understanding of the pathogen behavior within the roots, the main constraints were: the under-representation of low expressed genes due to low bacterial RNA yields, and the fact that we only studied an isolated stage out of the context of bacterial plant colonization. To overcome these issues, we next studied the pathogen's gene expression during its transition across different infection stages by enriching our samples with bacterial cells (chapter 7). Prokaryotic cells or RNA enrichment is the preferred approach for bacterial *in planta* transcriptomes (Nobori et al. 2018) in order to have sufficient sequencing representation of the whole genome. Our new approach, however, could be associated to several limitations. In the first place, we used leaf instead of root apoplast to obtain a robust initial condition for our time-course transcriptome, since it has been reported that bacteria deploy the same mechanisms in both environments (Hikichi 2016). In any case, our results further validated the usefulness of leaf apoplast as a mimic root condition, since we were able to detect the expression of genes whose expression is upstream in plant cell contact-dependent regulatory cascades (eg. *prh* genes in the T3SS signaling cascade). The other associated limitation to our leaf apoplast condition was the artificial high bacterial yields that we infiltrated within leafs. Apoplast is the first environment colonized by bacterial plant pathogens (Du et al. 2016), and it is known that *R. solanacearum* does not multiply as extensively as in the xylem vessels (Vasse et al. 1995). Although we observed an unexpected strong induction of quorum sensing (QS) and EPS biosynthesis genes in the apoplast (reviewed in the next sections), the rest of virulence determinants followed an expected expression profile along the infection process. Even virulence traits controlled by QS such as the flagellum, which was reported to be repressed at high bacterial densities (Clough et al. 1997a), showed the expected induction at early infection stages. Members of the T3SS signaling cascade, also regulated by the cell-growth dependent regulator PhcA, also showed the expression profile

expected from previous studies (Valls et al. 2006). Finally, the fact that approximately 15% and 20% of genes differentially expressed in apoplast and early xylem, respectively, were previously found in our root transcriptome, further supports the notion that root samples contained bacterial populations in different environments, which we could better dissect in our second approach.

Deciphering the *R. solanacearum* genetic virulence program throughout infection

In this work, we focused on profiling the virulence gene expression of *R. solanacearum* at different potato infection stages (chapter 7). As mentioned before, studying the whole infection process rather than isolated stages strengthens its biological relevance. Our study shows that *R. solanacearum* expression of virulence factors is dynamic, and that within the apoplast, bacteria mostly expresses flagella and type IVa pili, Reactive Oxygen Species detoxification, T2SS and some T3SS regulatory proteins. Largely, these results correlate well with previous studies. For instance, type IVa pili are needed for bacterial adhesion to the host surfaces (Kang et al. 2002), and similarly, it was reported that the flagellum was needed during root invasion but lost during xylem colonization (Tans-Kersten et al. 2001). Likewise, previous results in the study of T2SS in *R. solanacearum* showed that a mutant lacking this system lost completely its virulence (Kang et al. 1994). In addition, ROS are known to be rapidly produced by plants in response to a pathogen attack (Bolwell et al. 2002). Therefore, it is not surprising that *R. solanacearum* antagonizes the ROS effect by expressing ROS detoxification enzymes early in the infection process. Finally, T3SS expression is also triggered by plant cell contact through the activation of the regulatory genes *Prh* and *HrpG* (Marenda et al. 1998; Brito et al. 1999).

Regarding gene expression in the xylem, our data shows that the downstream T3SS regulator HrpB, whose expression is known to be triggered both by HrpG via cell contact and by PrhG via minimal medium (Plener et al. 2010), is in fact induced at early xylem conditions together with downstream *hrp* genes encoding structural units of the T3SS pilus. These results reinforce the notion that the HrpB and HprG-pathways may play different roles at different colonization steps (Valls et al. 2006). We also observed an induction of the T6SS at this stage, in line with previous studies that demonstrate the existence of a negative correlation between flagella and T6SS (Zhang et al. 2012; Zhang et al. 2014). In early xylem conditions, *R. solanacearum* also appeared to induce nitrogen respiration genes (Dalsing et al. 2015) and HCA degradation enzymes (Lowe et al. 2015). In this same condition, we also noticed that bacteria synthesize arginine and degrade other amino acids such as histidine, tyrosine, leucine and isoleucine. These metabolic activities were previously validated by quantification of amino acid concentration before and after bacterial growth in exogenous xylem sap (see annex (Zuluaga et al. 2013)). Interestingly, we observed a general metabolic repression, including downregulation of transcription and translation, during colonization of wilted plants. However, there was a clear up-regulation of many transcription factors and T3Es in this late stage of the disease, contrasting to the previous scenario. Actually,

the function of most *R. solanacearum* T3Es has not yet been elucidated (Deslandes and Genin 2014). This fact makes it difficult to interpret whether the "late" group of effectors are necessary for nutrient uptake from plant cells or to adapt to the next environment in the pathogen life cycle. Considering that there were sets of T3E with contrasting expression profiles, it would be interesting to check their contribution at different stages of the disease. For instance, RipAD, RipAI, RipD, PopF1 and PopS seem to play a specific role during apoplast colonization. Furthermore, inactivation of RipD or PopS contributed to full disease development, while PopF1 rendered bacteria completely non virulent (Cunnac et al. 2004; Meyer et al. 2006; Jacobs et al. 2013) (Cunnac et al. 2004; Meyer et al. 2006; Jacobs et al. 2013). Considering the difficulty in observing a phenotype by the effect of a single T3Es, our data suggest that these T3E are actually involved at the early infection stages. Future research will be addressed at unraveling the translocation patterns of apoplastic (or early) and xylematic (or late) effectors by using the novel split-GFP *in vivo* tracking system (Henry et al. 2017; Park et al. 2017).

As mentioned before and contrary to what was expected, we observed a strong induction of QS networks and EPS biosynthesis genes in the apoplast. By using a different approach, we demonstrated that the actual *eps* expression tendency was to decrease in the xylem vessels at three different points of the infection, validating our transcriptomic results. An explanation to this could be the fact that high bacterial densities were infiltrated in leaves, triggering an artificial activation of QS mechanisms. As similar bacterial yields were present in the three *in planta* conditions, it seems plausible that bacterial confinement within intercellular spaces was higher than in the xylem vessels. It is thus tempting to speculate, that QS and EPS expression are high in apoplastic microcolonies to promote biofilm formation. Later on, as bacteria multiply within the xylem vessels, less expression levels per cell would be needed to induce a massive production of EPS.

These results, however, seem contradictory to the above findings that bacteria during apoplast colonization induce the expression of flagella. This observation raises the question whether EPS and flagella are transcriptionally controlled by another system besides QS, or whether there are microenvironments in the apoplast that lead to distinct bacterial populations: a motile community expressing flagella, and another expressing high amounts of EPS within microcolonies attached to host cells. In fact, the existence of phenotypically distinct bacterial subpopulations was already proved for *P. syringae* (Rufian et al. 2016). The development of dual reporters to target distinct bacterial populations followed by single cell RNAseq will be key to test this hypothesis.

Altogether, our results shed light on the metabolic preferences of the pathogen in each *in planta* condition, and suggests a spatiotemporal role of the different virulence factors along the infection process. However, *R. solanacearum* also thrives in soil, waterways and reservoir weeds. To complement this work, transcriptional changes of *R. solanacearum* at other stages of its life cycle beyond the disease could be explored.

New *R. solanacearum* virulence regulators

The transcriptome analysis of infected resistant roots compared to susceptible wild potato plants (chapter 5) only revealed two *R. solanacearum* differentially expressed genes: a MarR transcriptional regulator and a hypothetical protein. On one hand, this observation suggested that the fate of the disease outcome was greatly influenced by the host plant rather than the pathogen. In fact, major gene expression differences could be observed between the two plant accessions upon infection (Zuluaga et al. 2015). On the other hand, we assumed the two differentially expressed genes identified in the tolerant accession might be somehow involved in bacterial wilt development. Since no described orthologues for the hypothetical protein could be found across other species genomes, we focused on the characterization of the MarR transcriptional regulator (re-named RepR in this work, chapter 6). Furthermore, *repR* also appeared to be induced in all *in planta* conditions tested in our time-course transcriptome compared to bacteria grown in either rich or minimal medium. Bacterial colonization in tolerant plants is limited by the formation of chemical and structural barriers (Prior et al. 1994). Together with the facts that *repR* was up-regulated in resistant versus susceptible plants and specially induced in leaf apoplast compared to any other *in planta* condition in our time-course, we hypothesized that it would be involved in early stages of the infection process.

By contrasting previous gene expression data, we learnt that PhcA, a global regulator controlling the trade-off between growth and virulence in *R. solanacearum*, represses *repR* expression both *in vitro* and *in planta* (Khokhani et al. 2017; Perrier et al. 2018). Notwithstanding PhcA induction in the apoplast, this observation suggests that RepR is a member of the PhcA-regulon and might be involved in pathogenicity. In fact, *in planta* growth assays in potato leaf apoplast and soil-soaking virulence tests in potato and tomato further supported this hypothesis. On the contrary, RepR did not appear to be involved in HR elicitation in tobacco, suggesting that its role in virulence goes beyond the regulation of the T3SS, which is required for HR (Boucher et al. 1987). To understand the mechanisms underlying RepR virulence regulation, an RNAseq analysis of the *repR* deletion mutant was performed in potato leaf apoplast, revealing that it mainly acts as a metabolic repressor. The RNAseq analysis identified the following RepR-regulated metabolic pathways: lipopolysaccharide biosynthesis, benzoate, fatty acid and several amino acid degradation pathways and cofactor metabolism. Additional experiments testing the actual metabolic capabilities of RepR will illustrate the specific pathways that mediate bacterial adaptation to early infection stages.

In a similar fashion, the newly described catabolic repressor EfpR was reported to contribute to bacterial fitness in the plant as well as virulence (Perrier et al. 2016). EfpR regulates EPS production, motility and catabolism of many amino acids such as gamma-Amino-n-Butyric Acid (GABA), Glutamate, Alanine and Histidine. The authors describe that EfpR gains adaptive loss-of-function mutations during the infection process, in a way that the bacterium increases its

metabolic versatility at advanced disease stages. We found up-regulation of EfpR in leaf apoplast, which is line with the described process. The fact that loss-of-function mutations are a common event in bacteria to regulate their adaptability to new environments (Hottes et al. 2013), makes it tempting to speculate that RepR acts in a similar fashion as EfpR. In this case, it would be interesting to test whether the RepR mutant increases its virulence when directly inoculated into the xylem vessels.

Collectively, this data evidences the importance of regulatory switches controlling metabolism and virulence in *R. solanacearum,* allowing a fine-tuned virulence gene expression dependent on the infection stage.

Novel approaches to fight bacterial wilt disease

Plant vascular diseases are challenging to control due to the complexity of the pathogen lifestyle (Yadeta and BP 2013). Specially controversial is brown rot disease, caused by a type of *R. solanacearum* strains acclimated to temperate weathers (Fegan and Prior 2005). No treatment showed efficiency in curing bacterial wilt, thus, efforts are on limiting bacterial spread and preventing their entrance within the plant (Ellis et al. 2008). The most extended practices to manage the disease in affected areas is the use of resistant cultivars, soil amendment, crop rotation and surveillance of tools, seeds, and irrigation water (Yuliar et al. 2015).

In the last few years, several studies have focused on the development of specific bactericides against *R. solanacearum* (Chen et al. 2016; Su et al. 2016), or the use of biological agents such as *R. solancearum* specific bacteriophages and plant growth promoting rhizobacteria (Lemessa and Zeller 2007; Fujiwara et al. 2011). Actually, some field trials using BCAs showed relative successful results (reviewed in (Yuliar et al. 2015)). However, these alternatives have several disadvantages. Bactericides, on one hand, eliminate not only the pathogen but also the beneficial plant microbiome, and the high selective pressure drives the reappearance of resistances (Sundin et al. 2016). BCAs, on the other hand, are associated to inconsistent colonization resulting in a lower disease suppression than commercially acceptable. Problems involving production, storage and application in the field are also associated to non-sporulating BCAs (Yuliar et al. 2015).

An alternative to solve these problems could be the development of new compounds that target bacterial pathogenicity rather than viability (Clatworthy et al. 2007). To this end, we elaborated a screening method using *R. solanacearum* luminescent reporter strains of several members in the T3SS cascade, leading to the identification of some T3SS transcription inhibitors (chapter 8). Our pilot test demonstrates that these salicylidene acylhydrazides are potential protectors of bacterial diseases. However, the effectiveness of these compounds as crop protectants could only be tested on an aerial pathogen due to the complexity of soil-borne bacteria. Future research should be directed towards the identification of affordable analogues of T3SS inhibitors and development of

effective soil treatments. Moreover, the study of *R. solanacearum*'s gene expression at different infection stages will provide knowledge on traits that are crucial for the transition from one stage to the next. Therefore, defining signature genes of each stage and targeting these traits will limit disease development.

In summary, we have provided new insights on *R. solanacearum* virulence gene expression mediated by DNA methylation and we characterized RepR, a novel player controlling virulence in *R. solanacearum*. This work has also contributed to expanding the knowledge on *R. solanacearum* virulence gene expression during distinct *in planta* colonization steps and opens the path for future research in the pathogen physiology during its life cycle.

chapter 10

CONCLUSIONS

From the main goals in this work, we extract the following conclusions:

Genome and methylome profiling of *R. solanacearum* UY031

1. The genome of strain UY031 has a size of 5.4 Mb and contains at least 60 T3Es that were annotated. *R. solanacearum* bears a core genome that consists on more than 60% of its genes.
2. *R. solanacearum* UY031 harbors a non-conserved phage-borne type II Restriction-Modification system targeting a novel motif (CAACR**A**C).
3. The gene RSUY_RS11230 encodes a conserved orphan MTase that has two methylated motives (GTWW**A**C) located upstream of *epsR* and contributes to *eps* expression at low bacterial densities in *R. solanacearum* UY031 and GMI1000.

Characterization of *repR*, a new candidate virulence gene in *R. solanacearum*

4. *repR* encodes a MarR-transcriptional regulator conserved within the *R. solanacearum* species complex.
5. *repR* is specifically induced *in planta* and plays a key role in bacterial fitness during apoplast colonization.
6. *repR* contributes to *R. solanacearum* virulence in potato and tomato plants but does not affect HR elicitation in tobacco plants.
7. RepR potentially mediates *R. solanacearum* adaptation to plant apoplast by acting as a metabolic repressor.

Understanding the *R. solanacearum* UY031 transcriptomic changes during the infection process

8. Compared to growth in rich medium, *R. solanacearum* UY031 induces virulence-related genes and nitrogen, sulfate and phosphate metabolism, while represses most of its metabolic activities during root colonization.
9. Leaf apoplast is a robust mimic condition of root colonization that allows the identification of early virulence factors.
10. Expression of *R. solanacearum* virulence factors and metabolic pathways is dynamic across the different infection stages.
11. Exopolysaccharide biosynthesis can be induced at early infection stages, when the bacterium multiplies in the apoplast.
12. *R. solanacearum* expresses distinct sets of T3Es at different plant colonization stages. A large amount of T3Es is transcribed in the xylem at advanced disease stages.

Identification of T3SS inhibitors to combat bacterial plant diseases – Proof of Concept Study

13. The *R. solanacearum* luminescent reporters constitute a useful tool in the screening for T3SS inhibitors.

14. Salicylidene acylhydrazides are strong T3SS inhibitors in *R. solanacearum.*

15. Some salicylidene acylhydrazides prevent effector translocation *in vitro* and *in vivo* and limit *R. solanacearum* multiplication *in planta.*

16. Although the use of alicylidene acylhydrazides in preventing bacterial wilt was not proved, they showed potential in protecting tomato plants from *Pseudomonas syringae* infections.

SUMMARY IN ENGLISH

The plant pathogen *Ralstonia solanacearum* is the causal agent of bacterial wilt, a highly aggressive disease responsible for important worldwide economic losses. Many virulence factors in *R. solanacearum* have been already identified; however, their transcriptional regulation during disease development remained unknown.

In an effort to better characterize the gene expression changes driving bacterial virulence, we first provided the complete genome sequence of the potato *R. solanacearum* UY031 strain as a tool to perform robust transcriptomics *in planta*. By taking advantage of the novel sequencing technology called SMRT, we also supplied hints on the methylome profile and its contribution to virulence gene expression in UY031.

In this work, we performed two different *in planta* transcriptome approaches at different potato infection stages. On one hand, we analyzed the bacterial gene expression during root colonization and demonstrated that, although it is cost-ineffective, microbial transcriptomes *in planta* at low bacterial densities are possible without a prior enrichment of prokaryotic RNA. Furthermore, we identified a novel player controlling bacterial fitness during early infection stages that we named RepR for Repressor Regulator, since we discovered that it is a repressor of specific metabolic pathways. On the other hand, we performed a time-course transcriptome and show that expression of *R. solanacearum* virulence factors and metabolism is dynamic along the infection process. With our system, we validated the expression patterns of known virulence factors such as the Type III Secretion System (T3SS) or the flagellum, and unraveled the profiles of others like Type IVb pili or the T6SS. Contrary to the assumption that the T3SS might play only a role at early infection stages, we demonstrate that effector transcription is extremely high in advanced disease stages.

Finally, we performed a pilot test to identify T3SS inhibitors and demonstrate that some salicylidene acylhydrazides can potentially prevent bacterial plant diseases via T3SS transcription inhibition. This work adds growing knowledge on the pathogen behavior and its physiology at different points of the disease, which could eventually lead to the identification of new drugs targeting keys steps in disease development.

Resum en Català

Ralstonia solanacearum és l'agent causant del marciment bacterià en plantes, una malaltia altament agressiva i responsable de considerables pèrdues econòmiques d'impacte mundial. Molts factors de virulència de *R. solanacearum* han sigut identificats, però la seva regulació transcripcional al llarg del desenvolupament de la malaltia encara es desconeixia.

En un intent de caracteritzar els canvis en l'expressió genètica que modulen la virulència del bacteri, en primer lloc hem proporcionat la seqüència completa del genoma de la soca de patateres *R. solanacearum* UY031 com a eina per a dur a terme transcriptomes robustos dins de la planta. Gràcies a la nova tecnologia de seqüenciació anomenada SMRT, també proporcionem algunes pistes sobre el seu perfil de metilació i la contribució d'aquest en l'expressió de gens de virulència a UY031.

En aquest estudi hem realitzat dos transcriptomes del bacteri en patateres en diferents estadis d'infecció. Per una banda hem analitzat l'expressió genètica bacteriana durant la colonització de l'arrel i hem demostrat que, malgrat ser poc rentable, és possible analitzar el transcriptoma del bacteri dins de la planta sense enriquir prèviament les mostres amb ARN procariota. Així mateix, hem identificat un nou membre que regula l'eficàcia biològica del bacteri durant els estadis inicials de la infecció que hem anomenat RepR, de Repressor Regulador, ja que hem descobert que reprimeix rutes metabòliques concretes. Per altra banda, hem fet un transcriptoma a diferents estadis de la infecció i demostrem que l'expressió de factors de virulència i del metabolisme de *R. solanacearum* és dinàmica al llarg del procés infectiu. Amb el nostre sistema, hem validat els patrons d'expressió de factors de virulència ja coneguts, com el Sistema de Secreció de Tipus III (SST3) o el flagel, i hem desxifrat els perfils d'altres factors com el dels pilus de tipus IVb o el SST6. En contra de l'assumpció que el SST3 juga principalment un paper als estadis primerencs de la infecció, hem demostrat que la transcripció de molts efectors és extremadament alta en estadis avançats de la malaltia.

Finalment, hem dut a terme una prova pilot per a identificar inhibidors del SST3 i hem demostrat que algunes salicidèn-acilhidrazides tenen potencial per a prevenir malalties bacterianes de plantes mitjançant la inhibició de la transcripció del SST3. Aquest treball afegeix nou coneixement en el comportament i la fisiologia del patogen en diferents estadis de la malaltia, que amb el temps podria contribuir a la identificació de nous fàrmacs dirigits en passos claus en el desenvolupament de la malaltia.

References

Agrios, G. N. (2005). Plant pathology, Elsevier academic press San Diego.

Ahn, I.-P., S.-W. Lee, M. G. Kim, S.-R. Park, D.-J. Hwang and S.-C. Bae (2011). "Priming by rhizobacterium protects tomato plants from biotrophic and necrotrophic pathogen infections through multiple defense mechanisms." *Molecules and cells* 32(1): 7-14.

Ailloud, F., T. Lowe, G. Cellier, D. Roche, C. Allen and P. Prior (2015). "Comparative genomic analysis of Ralstonia solanacearum reveals candidate genes for host specificity." *BMC Genomics* 16: 270.

Ailloud, F., T. M. Lowe, I. Robene, S. Cruveiller, C. Allen and P. Prior (2016). "In planta comparative transcriptomics of host-adapted strains of Ralstonia solanacearum." *PeerJ* 4: e1549.

Akiyoshi, D. E., H. Klee, R. M. Amasino, E. W. Nester and M. P. Gordon (1984). "T-DNA of Agrobacterium tumefaciens encodes an enzyme of cytokinin biosynthesis." *Proc Natl Acad Sci U S A* 81(19): 5994-5998.

Aldon, D., B. Brito, C. Boucher and S. Genin (2000). "A bacterial sensor of plant cell contact controls the transcriptional induction of Ralstonia solanacearum pathogenicity genes." *EMBO J* 19(10): 2304-2314.

Alfano, J. R. and A. Collmer (1997). "The type III (Hrp) secretion pathway of plant pathogenic bacteria: trafficking harpins, Avr proteins, and death." *J. Bacteriol.* 179(18): 5655-5662.

Alfano, J. R. and A. Collmer (2004). "Type III secretion system effector proteins: double agents in bacterial disease and plant defense." *Annu Rev Phytopathol* 42: 385-414.

Álvarez, B., E. G. Biosca and M. M. López (2010). "On the life of Ralstonia solanacearum, a destructive bacterial plant pathogen." *Current research, technology and education topics in applied microbiology and microbial biotechnology* 1: 267-279.

Alvarez, B., M. M. Lopez and E. G. Biosca (2007). "Influence of native microbiota on survival of Ralstonia solanacearum phylotype II in river water microcosms." *Appl Environ Microbiol* 73(22): 7210-7217.

Alves, A. A. and T. L. Setter (2004). "Response of cassava leaf area expansion to water deficit: cell proliferation, cell expansion and delayed development." *Ann Bot* 94(4): 605-613.

Allen, C., J. Gay and L. Simon-Buela (1997). "A regulatory locus, pehSR, controls polygalacturonase production and other virulence functions in Ralstonia solanacearum." *Mol Plant Microbe Interact* 10(9): 1054-1064.

Anders, S., P. T. Pyl and W. Huber (2015). "HTSeq--a Python framework to work with high-throughput sequencing data." *Bioinformatics* 31(2): 166-169.

Angot, A., N. Peeters, E. Lechner, F. Vailleau, C. Baud, L. Gentzbittel, E. Sartorel, P. Genschik, C. Boucher and S. Genin (2006). "Ralstonia solanacearum requires F-box-like domain-containing type III effectors to promote disease on several host plants." *Proc Natl Acad Sci U S A* 103(39): 14620-14625.

Arlat, M., C. L. Gough, C. E. Barber, C. Boucher and M. J. Daniels (1991). "Xanthomonas campestris contains a cluster of hrp genes related to the larger hrp cluster of Pseudomonas solanacearum." *Mol Plant Microbe Interact* 4(6): 593-601.

Arlat, M., C. L. Gough, C. Zischek, P. A. Barberis, A. Trigalet and C. A. Boucher (1992). "Transcriptional organization and expression of the large hrp gene cluster of Pseudomonas solanacearum." *Mol Plant Microbe Interact* 5(2): 187-193.

Bahar, O., T. Goffer and S. Burdman (2009). "Type IV Pili are required for virulence, twitching motility, and biofilm formation of acidovorax avenae subsp. Citrulli." *Mol Plant Microbe Interact* 22(8): 909-920.

Barnes, E. C., A. M. Kavanagh, S. Ramu, M. A. Blaskovich, M. A. Cooper and R. A. Davis (2013). "Antibacterial serrulatane diterpenes from the Australian native plant Eremophila microtheca." *Phytochemistry* 93: 162-169.

Barny, M. A., M. H. Guinebretiere, B. Marcais, E. Coissac, J. P. Paulin and J. Laurent (1990). "Cloning of a large gene cluster involved in Erwinia amylovora CFBP1430 virulence." *Mol Microbiol* 4(5): 777-786.

Beckman, C. H. (2000). "Phenolic-storing cells: keys to programmed cell death and periderm formation in wilt disease resistance and in general defence responses in plants?" *Physiological and Molecular Plant Pathology* 57(3): 101-110.

Ben, C., F. Debelle, H. Berges, A. Bellec, M. F. Jardinaud, P. Anson, T. Huguet, L. Gentzbittel and F. Vailleau (2013). "MtQRRS1, an R-locus required for Medicago truncatula quantitative resistance to Ralstonia solanacearum." *New Phytol* 199(3): 758-772.

Bender, C. L., F. Alarcon-Chaidez and D. C. Gross (1999). "Pseudomonas syringae phytotoxins: mode of action, regulation, and biosynthesis by peptide and polyketide synthetases." *Microbiol Mol Biol Rev* 63(2): 266-292.

Bjarnsholt, T. (2013). "The role of bacterial biofilms in chronic infections." *APMIS Suppl*(136): 1-51.

Bocsanczy, A. M., U. C. Achenbach, A. Mangravita-Novo, J. M. Yuen and D. J. Norman (2012). "Comparative effect of low temperature on virulence and twitching motility of Ralstonia solanacearum strains present in Florida." *Phytopathology* 102(2): 185-194.

Bogdanove, A. J., S. V. Beer, U. Bonas, C. A. Boucher, A. Collmer, D. L. Coplin, G. R. Cornelis, H. C. Huang, S. W. Hutcheson, N. J. Panopoulos and F. Van Gijsegem (1996). "Unified nomenclature for broadly conserved hrp genes of phytopathogenic bacteria." *Mol Microbiol* 20(3): 681-683.

Bolwell, G. P., L. V. Bindschedler, K. A. Blee, V. S. Butt, D. R. Davies, S. L. Gardner, C. Gerrish and F. Minibayeva (2002). "The apoplastic oxidative burst in response to biotic stress in plants: a three-component system." *J Exp Bot* 53(372): 1367-1376.

Boller, T. and G. Felix (2009). "A renaissance of elicitors: perception of microbe-associated molecular patterns and danger signals by pattern-recognition receptors." *Annu Rev Plant Biol* 60: 379-406.

Bonas, U., R. Schulte, S. Fenselau, G. V. Minsavage, B. J. Staskawicz and R. E. Stall (1991). "Isolation of a gene cluster from Xanthomonas campestris pv. vesicatoria that determines pathogenicity and the hypersensitive response on pepper and tomato." *Mol. Plant-Microbe Interact* 4(1): 81-88.

Boucher, C. A., P. A. Barberis, A. P. Triglaet and D. A. Démery (1985). "Transposon mutagenesis of *Pseudomonas solanacearum*: Isolation of Tn5-induced avirulent mutants." *Microbiology* 131(9): 2449-2457.

Boucher, C. A., F. Van Gijsegem, P. A. Barberis, M. Arlat and C. Zischek (1987). "Pseudomonas solanacearum genes controlling both pathogenicity on tomato and hypersensitivity on tobacco are clustered." *J Bacteriol* 169(12): 5626-5632.

Bradshaw, R. E., Y. Guo, A. D. Sim, M. S. Kabir, P. Chettri, I. K. Ozturk, L. Hunziker, R. J. Ganley and M. P. Cox (2016). "Genome-wide gene expression dynamics of the fungal pathogen Dothistroma septosporum throughout its infection cycle of the gymnosperm host Pinus radiata." *Molecular plant pathology* 17(2): 210-224.

Brito, B., D. Aldon, P. Barberis, C. Boucher and S. Genin (2002). "A signal transfer system through three compartments transduces the plant cell contact-dependent signal controlling Ralstonia solanacearum hrp genes." *Mol Plant Microbe Interact* 15(2): 109-119.

Brito, B., M. Marenda, P. Barberis, C. Boucher and S. Genin (1999). "prhJ and hrpG, two new components of the plant signal-dependent regulatory cascade controlled by PrhA in Ralstonia solanacearum." *Mol Microbiol* 31(1): 237-251.

Brown, D. G. and C. Allen (2004). "Ralstonia solanacearum genes induced during growth in tomato: an inside view of bacterial wilt." *Mol Microbiol* 53(6): 1641-1660.

Brown, D. G., J. K. Swanson and C. Allen (2007). "Two host-induced Ralstonia solanacearum genes, acrA and dinF, encode multidrug efflux pumps and contribute to bacterial wilt virulence." *Appl Environ Microbiol* 73(9): 2777-2786.

Brumbley, S. M., B. F. Carney and T. P. Denny (1993). "Phenotype conversion in Pseudomonas solanacearum due to spontaneous inactivation of PhcA, a putative LysR transcriptional regulator." *J Bacteriol* 175(17): 5477-5487.

Brumbley, S. M. and T. P. Denny (1990). "Cloning of wild-type Pseudomonas solanacearum phcA, a gene that when mutated alters expression of multiple traits that contribute to virulence." *J Bacteriol* 172(10): 5677-5685.

Bu'Lock, J. D. and H. G. Smith (1960). "Pyrones. Part I. Methyl ethers of tautomeric hydroxy-pyrones and the structure of yangonin." *J. Chem. Soc.* 502: 502-506.

Buddenhagen, I. (1962). "Designation of races in Pseudomonas solanacearum." *Phytopathology* 52: 726.

Buddenhagen, I. and A. Kelman (1964). "Biological and physiological aspects of bacterial wilt caused by Pseudomonas solanacearum." *Annual Review of phytopathology* 2(1): 203-230.

Buttner, D. (2016). "Behind the lines-actions of bacterial type III effector proteins in plant cells." *FEMS Microbiol. Rev.*: 894-937.

Buttner, D. and U. Bonas (2010). "Regulation and secretion of Xanthomonas virulence factors." *FEMS Microbiol Rev* 34(2): 107-133.

Capy, P., G. Gasperi, C. Biémont and C. Bazin (2000). "Stress and transposable elements: co-evolution or useful parasites?" *Heredity* 85: 101-106.

Carmeille, A., C. Caranta, J. Dintinger, P. Prior, J. Luisetti and P. Besse (2006). "Identification of QTLs for Ralstonia solanacearum race 3-phylotype II resistance in tomato." *Theoretical and Applied Genetics* 113(1): 110-121.

Carputo, D., R. Aversano, A. Barone, A. Di Matteo, M. Iorizzo, L. Sigillo, A. Zoina and L. Frusciante (2009). "Resistance to Ralstonia solanacearum of sexual hybrids between Solanum commersonii and S. tuberosum." *American Journal of Potato Research* 86(3): 196-202.

Carroll, A. R., R. A. Davis, P. I. Forster, G. P. Guymer and R. J. Quinn (2001). "A benzylisoquinoline alkaloid from *Doryphora sassafras*." *J. Nat. Prod.* 64(12): 1572-1573.

Caruso, P., J. L. Palomo, E. Bertolini, B. Álvarez, M. M. López and E. G. Biosca (2005). "Seasonal variation of Ralstonia solanacearum biovar 2 populations in a Spanish river: recovery of stressed cells at low temperatures." *Appl Environ Microbiol* 71(1): 140-148.

Casacuberta, E. and J. Gonzalez (2013). "The impact of transposable elements in environmental adaptation." *Mol Ecol* 22(6): 1503-1517.

Casadesus, J. and D. Low (2006). "Epigenetic gene regulation in the bacterial world." *Microbiol Mol Biol Rev* 70(3): 830-856.

Caserta, R., M. A. Takita, M. L. Targon, L. K. Rosselli-Murai, A. P. de Souza, L. Peroni, D. R. Stach-Machado, A. Andrade, C. A. Labate, E. W. Kitajima, M. A. Machado and A. A. de Souza (2010). "Expression of Xylella fastidiosa fimbrial and afimbrial proteins during biofilm formation." *Appl Environ Microbiol* 76(13): 4250-4259.

Ciampi, L. and L. Sequeira (1980). "Influence of temperature on virulence of race 3 strains ofPseudomonas solanacearum." *American Potato Journal* 57(7): 307-317.

Clatworthy, A. E., E. Pierson and D. T. Hung (2007). "Targeting virulence: a new paradigm for antimicrobial therapy." *Nat. Chem. Biol.* 3: 541-548.

Clough, S., M. Schell and T. Denny (1994). "Evidence for involvement of a volatile extracellular factor in Pseudomonas solanacearum virulence gene expression." *Molecular plant-microbe interactions: MPMI (USA)*.

Clough, S. J., A. B. Flavier, M. A. Schell and T. P. Denny (1997a). "Differential Expression of Virulence Genes and Motility in Ralstonia (Pseudomonas) solanacearum during Exponential Growth." *Appl Environ Microbiol* 63(3): 844-850.

Clough, S. J., K. E. Lee, M. A. Schell and T. P. Denny (1997b). "A two-component system in Ralstonia (Pseudomonas) solanacearum modulates production of PhcA-regulated virulence factors in response to 3-hydroxypalmitic acid methyl ester." *J Bacteriol* 179(11): 3639-3648.

Cohen, S. P., L. M. McMurry, D. C. Hooper, J. S. Wolfson and S. B. Levy (1989). "Cross-resistance to fluoroquinolones in multiple-antibiotic-resistant (Mar) Escherichia coli selected by tetracycline or chloramphenicol: decreased drug accumulation associated with membrane changes in addition to OmpF reduction." *Antimicrob Agents Chemother* 33(8): 1318-1325.

Colburn-Clifford, J. M., J. M. Scherf and C. Allen (2010). "Ralstonia solanacearum Dps contributes to oxidative stress tolerance and to colonization of and virulence on tomato plants." *Appl Environ Microbiol* 76(22): 7392-7399.

Coll, N. S. and M. Valls (2013). "Current knowledge on the Ralstonia solanacearum type III secretion system." *Microb Biotechnol* 6(6): 614-620.

Collmer, A. and N. T. Keen (1986). "The role of pectic enzymes in plant pathogenesis." *Annual review of phytopathology* 24(1): 383-409.

Collonnier, C., K. Mulya, I. I. Fock, I. I. Mariska, A. Servaes, F. Vedel, S. Siljak-Yakovlev, V. V. Souvannavong, G. Ducreux and D. Sihachakr (2001). "Source of resistance against Ralstonia solanacearum in fertile somatic hybrids of eggplant (Solanum melongena L.) with Solanum aethiopicum L." *Plant Sci* 160(2): 301-313.

Cornelis, G. R. and F. Van Gijsegem (2000). "Assembly and function of type III secretory systems." *Annu Rev Microbiol* 54: 735-774.

Crow, W. D. and J. R. Price (1949). "Alkaloids of the Australian Rutaceae: *Melicope fareana*. II. Preliminary examination of melicopine, melicopidine, and melicopicine." *Aust. J. Sci. Res., Ser. A* 2(2): 255-263.

Cruz, A. P., V. Ferreira, M. J. Pianzzola, M. I. Siri, N. S. Coll and M. Valls (2014). "A novel, sensitive method to evaluate potato germplasm for bacterial wilt resistance using a luminescent *Ralstonia solanacearum* reporter strain." *Mol. Plant-Microbe Interact.* 27(3): 277-285.

Cui, H., T. Xiang and J. M. Zhou (2009). "Plant immunity: a lesson from pathogenic bacterial effector proteins." *Cell Microbiol* 11(10): 1453-1461.

Cunnac, S., C. Boucher and S. Genin (2004). "Characterization of the cis-acting regulatory element controlling HrpB-mediated activation of the type III secretion system and effector genes in Ralstonia solanacearum." *J Bacteriol* 186(8): 2309-2318.

Cunnac, S., A. Occhialini, P. Barberis, C. Boucher and S. Genin (2004). "Inventory and functional analysis of the large Hrp regulon in Ralstonia solanacearum: identification of novel effector proteins translocated to plant host cells through the type III secretion system." *Mol Microbiol* 53(1): 115-128.

Champoiseau, P. G., J. B. Jones and C. Allen (2009). "Ralstonia solanacearum race 3 biovar 2 causes tropical losses and temperate anxieties." *Plant Health Progress* 10: 1-10.

Chen, D., B. Liu, Y. Zhu, J. Wang, Z. Chen, J. Che, X. Zheng and X. Chen (2017). "Complete Genome Sequence of Ralstonia solanacearum FJAT-1458, a Potential Biocontrol Agent for Tomato Wilt." *Genome Announc* 5(14).

Chen, J., Y. Yu, S. Li and W. Ding (2016). "Resveratrol and Coumarin: Novel Agricultural Antibacterial Agent against Ralstonia solanacearum In Vitro and In Vivo." *Molecules* 21(11).

Christie, P. J., K. Atmakuri, V. Krishnamoorthy, S. Jakubowski and E. Cascales (2005). "Biogenesis, architecture, and function of bacterial type IV secretion systems." *Annu Rev Microbiol* 59: 451-485.

Dahlgren, M. K., C. E. Zetterstrom, S. Gylfe, A. Linusson and M. Elofsson (2010). "Statistical molecular design of a focused salicylidene acylhydrazide library and multivariate QSAR of inhibition of type III secretion in the Gram-negative bacterium *Yersinia*." *Bioorg. Med. Chem.* 18(7): 2686-2703.

Dalsing, B. L. and C. Allen (2014). "Nitrate assimilation contributes to Ralstonia solanacearum root attachment, stem colonization, and virulence." *J Bacteriol* 196(5): 949-960.

Dalsing, B. L., A. N. Truchon, E. T. Gonzalez-Orta, A. S. Milling and C. Allen (2015). "Ralstonia solanacearum uses inorganic nitrogen metabolism for virulence, ATP production, and detoxification in the oxygen-limited host xylem environment." *MBio* 6(2): e02471.

Danhorn, T. and C. Fuqua (2007). "Biofilm formation by plant-associated bacteria." *Annu Rev Microbiol* 61: 401-422.

Davis, R. A., E. C. Barnes, J. Longden, V. M. Avery and P. C. Healy (2009). "Isolation, structure elucidation and cytotoxic evaluation of endiandrin B from the Australian rainforest plant *Endiandra anthropophagorum*." *Bioorg. Med. Chem.* 17(3): 1387-1392.

Davis, R. A., K. D. Beattie, M. Xu, X. Yang, S. Yin, H. Holla, P. C. Healy, M. Sykes, T. Shelper, V. M. Avery, M. Elofsson, C. Sundin and R. J. Quinn (2014). "Solving the supply of resveratrol tetramers from Papua New Guinean rainforest *Anisoptera* species that inhibit bacterial type III secretion systems." *J. Nat. Prod.* 77(12): 2633-2640.

Davis, R. A., A. R. Carroll, S. Duffy, V. M. Avery, G. P. Guymer, P. I. Forster and R. J. Quinn (2007). "Endiandrin A, a potent glucocorticoid receptor binder isolated from the Australian plant *Endiandra anthropophagorum*." *J. Nat. Prod.* 70(7): 1118-1121.

Delaspre, F., C. G. Nieto Penalver, O. Saurel, P. Kiefer, E. Gras, A. Milon, C. Boucher, S. Genin and J. A. Vorholt (2007). "The Ralstonia solanacearum pathogenicity regulator HrpB induces 3-hydroxy-oxindole synthesis." *Proc Natl Acad Sci U S A* 104(40): 15870-15875.

Denny, T. (2006). Plant pathogenic Ralstonia species, p. 573–644In Gnanamanickam SS, editor.(ed.), Plant-associated bacteria, Springer Publishing, Dordrecht, The Netherlands.

Denny, T. P. and S.-R. Baek (1991). "Genetic Evidence that Extracellular Polysaccharide Is a Virulence Factor." *Molecular Plant-Microbe Interactions* 4(2): 198-206.

Denny, T. P., B. F. Carney and M. A. Schell (1990). "Inactivation of multiple virulence genes reduces the ability of Pseudomonas solanacearum to cause wilt symptoms." *Mol. Plant-Microbe Interact* 3(2.93).

Dereeper, A., S. Audic, J. M. Claverie and G. Blanc (2010). "BLAST-EXPLORER helps you building datasets for phylogenetic analysis." *BMC Evol Biol* 10: 8.

Dereeper, A., V. Guignon, G. Blanc, S. Audic, S. Buffet, F. Chevenet, J. F. Dufayard, S. Guindon, V. Lefort, M. Lescot, J. M. Claverie and O. Gascuel (2008). "Phylogeny.fr: robust phylogenetic analysis for the non-specialist." *Nucleic Acids Res* 36(Web Server issue): W465-469.

Deslandes, L. and S. Genin (2014). "Opening the Ralstonia solanacearum type III effector tool box: insights into host cell subversion mechanisms." *Curr Opin Plant Biol* 20: 110-117.

Deslandes, L., J. Olivier, N. Peeters, D. X. Feng, M. Khounlotham, C. Boucher, I. Somssich, S. Genin and Y. Marco (2003). "Physical interaction between RRS1-R, a protein conferring resistance to bacterial wilt, and PopP2, a type III effector targeted to the plant nucleus." *Proc Natl Acad Sci U S A* 100(13): 8024-8029.

Deslandes, L., F. Pileur, L. Liaubet, S. Camut, C. Can, K. Williams, E. Holub, J. Beynon, M. Arlat and Y. Marco (1998). "Genetic characterization of RRS1, a recessive locus in Arabidopsis thaliana that confers resistance to the bacterial soilborne pathogen Ralstonia solanacearum." *Mol Plant Microbe Interact* 11(7): 659-667.

Digonnet, C., Y. Martinez, N. Denance, M. Chasseray, P. Dabos, P. Ranocha, Y. Marco, A. Jauneau and D. Goffner (2012). "Deciphering the route of Ralstonia solanacearum colonization in Arabidopsis thaliana roots during a compatible interaction: focus at the plant cell wall." *Planta* 236(5): 1419-1431.

Dreyer, D. L. and A. Lee (1972). "Extractives of *Geijera paraviflora*." *Phytochemistry* 11(2): 763-767.

Du, Y., M. Stegmann and J. C. Misas Villamil (2016). "The apoplast as battleground for plant-microbe interactions." *New Phytol* 209(1): 34-38.

Duffy, B., H. J. Schärer, M. Bünter, A. Klay and E. Holliger (2005). "Regulatory measures against *Erwinia amylovora* in Switzerland." *EPPO Bulletin* 35: 239-244.

Duncan, M. C., R. G. Linington and V. Auerbuch (2012). "Chemical inhibitors of the type three secretion system: disarming bacterial pathogens." *Antimicrob. Agents Chemother.* 56(11): 5433-5441.

Elphinstone, J. (1996). "Survival and possibilities for extinction ofPseudomonas solanacearum (Smith) Smith in cool climates." *Potato Research* 39(3): 403-410.

Elphinstone, J., H. Stanford and D. Stead (1998). Detection of Ralstonia solanacearum in potato tubers, Solanum dulcamara and associated irrigation water. *Bacterial Wilt Disease*, Springer: 133-139.

Ellis, S. D., M. J. Boehm and D. Coplin (2008). "Bacterial diseases of plants." *Agriculture and Natural Resources*: 401-406.

Ellison, D. W. and V. L. Miller (2006). "Regulation of virulence by members of the MarR/SlyA family." *Curr Opin Microbiol* 9(2): 153-159.

Fan, S., F. Tian, J. Li, W. Hutchins, H. Chen, F. Yang, X. Yuan, Z. Cui, C. H. Yang and C. He (2017). "Identification of phenolic compounds that suppress the virulence of *Xanthomonas oryzae* on rice via the type III secretion system." *Mol. Plant Pathol.* 18(4): 555-568.

Fegan, M. and P. Prior (2005). How complex is the Ralstonia solanacearum species complex, APS press.

Ferreira, V., M. J. Pianzzola, F. L. Vilaro, G. A. Galvan, M. L. Tondo, M. V. Rodriguez, E. G. Orellano, M. Valls and M. I. Siri (2017). "Interspecific Potato Breeding Lines Display Differential Colonization Patterns and Induced Defense Responses after Ralstonia solanacearum Infection." *Front Plant Sci* 8: 1424.

Flavier, A. B., S. J. Clough, M. A. Schell and T. P. Denny (1997). "Identification of 3-hydroxypalmitic acid methyl ester as a novel autoregulator controlling virulence in Ralstonia solanacearum." *Mol Microbiol* 26(2): 251-259.

Flavier, A. B., L. M. Ganova-Raeva, M. A. Schell and T. P. Denny (1997). "Hierarchical Autoinduction in Ralstonia solanacearum: Control of Acyl-Homoserine Lactone Production by a Novel Autoregulatory System Responsive to 3-Hydroxypalmitic Acid Methyl Ester " *Journal of Bacteriology* 179(22): 7089-7097.

Flavier, A. B., M. A. Schell and T. P. Denny (1998). "An RpoS (sigmaS) homologue regulates acylhomoserine lactone-dependent autoinduction in Ralstonia solanacearum." *Mol Microbiol* 28(3): 475-486.

Flemming, H. C. and J. Wingender (2010). "The biofilm matrix." *Nat Rev Microbiol* 8(9): 623-633.

Flores-Cruz, Z. and C. Allen (2009). "Ralstonia solanacearum Encounters an Oxidative Environment During Tomato Infection." *Molecular Plant-Microbe Interactions* 22(7): 773-782.

Flores-Cruz, Z. and C. Allen (2011). "Necessity of OxyR for the hydrogen peroxide stress response and full virulence in Ralstonia solanacearum." *Appl Environ Microbiol* 77(18): 6426-6432.

Flusberg, B. A., D. R. Webster, J. H. Lee, K. J. Travers, E. C. Olivares, T. A. Clark, J. Korlach and S. W. Turner (2010). "Direct detection of DNA methylation during single-molecule, real-time sequencing." *Nat Methods* 7(6): 461-465.

French, E. (1982). "Evaluación de campo para clones del CIP mejorados por resistencia a la marchitez bacteriana [Solanum phureja, Pseudomonas solanacearum, Perú].;[Field evaluation of improved CIP clones for resistance to brown rot [Solanum phureja, Pseudomonas solanacearum, Peru]]." *Seminario de Investigación y de Trabajo sobre Avances en el Control de la Marchitez Bacteriana (Pseudomonas solanacearum) de la Papa en América Latina., Brasilia (Brasil)., 31 Ago-3 Set 1982..*

Fujiwara, A., M. Fujisawa, R. Hamasaki, T. Kawasaki, M. Fujie and T. Yamada (2011). "Biocontrol of Ralstonia solanacearum by treatment with lytic bacteriophages." *Appl Environ Microbiol* 77(12): 4155-4162.

Fuqua, C. and E. P. Greenberg (1998). "Self perception in bacteria: quorum sensing with acylated homoserine lactones." *Curr Opin Microbiol* 1(2): 183-189.

Futschik, M. E. and B. Carlisle (2005). "Noise-robust soft clustering of gene expression time-course data." *J Bioinform Comput Biol* 3(4): 965-988.

Galan, J. E. (2009). "Common themes in the design and function of bacterial effectors." *Cell Host Microbe* 5(6): 571-579.

Garrity-Ryan, L. K., Kim, O.K., Balada-Llasat, J.M., Bartlett, V.J., Verma, A.K., Fisher, M.L., Castillo, C., Songsungthong, W., Tanaka, S.K., Levy, S.B., Mecsas, J. and Alekshun, M.N. (2010). "Small molecule inhibitors of LcrF, a *Yersinia pseudotuberculosis* transcription factor, attenuate virulence and limit infection in a murine pneumonia model." *Infect. Immun.* 78(11): 4683-4690.

Genin, S. (2010). "Molecular traits controlling host range and adaptation to plants in Ralstonia solanacearum." *New Phytol* 187(4): 920-928.

Genin, S. and C. Boucher (2002). "Ralstonia solanacearum: secrets of a major pathogen unveiled by analysis of its genome." *Mol Plant Pathol* 3(3): 111-118.

Genin, S., B. Brito, T. P. Denny and C. Boucher (2005). "Control of the Ralstonia solanacearum Type III secretion system (Hrp) genes by the global virulence regulator PhcA." *FEBS Lett* 579(10): 2077-2081.

Genin, S. and T. P. Denny (2012). "Pathogenomics of the Ralstonia solanacearum species complex." *Annu Rev Phytopathol* 50: 67-89.

Genin, S., C. L. Gough, C. Zischek and C. A. Boucher (1992). "Evidence that the *hrpB* gene encodes a positive regulator of pathogenicity genes from *Pseudomonas solanacearum*." *Mol. Microbiol.* 6(20): 3065-3076.

Genin, S., C. L. Gough, C. Zischek and C. A. Boucher (1992). "Evidence that the hrpB gene encodes a positive regulator of pathogenicity genes from Pseudomonas solanacearum." *Mol Microbiol* 6(20): 3065-3076.

Göhre, V. and S. Robatzek (2008). "Breaking the barriers: microbial effector molecules subvert plant immunity." *Annu. Rev. Phytopathol.* 46: 189-215.

Gonzalez, E. T. and C. Allen (2003). "Characterization of a Ralstonia solanacearum operon required for polygalacturonate degradation and uptake of galacturonic acid." *Mol Plant Microbe Interact* 16(6): 536-544.

Gonzalez, E. T., D. G. Brown, J. K. Swanson and C. Allen (2007). "Using the Ralstonia solanacearum Tat secretome to identify bacterial wilt virulence factors." *Appl Environ Microbiol* 73(12): 3779-3786.

González, M., G. Galván, M. I. Siri, A. Borges and F. Vilaró (2013). "Resistencia a la marchitez bacteriana de la papa en Solanum commersonii Dun." *Agrociencia Uruguay* 17(1): 45-54.

Gough, C. L., S. Genin, C. Zischek and C. A. Boucher (1992). "hrp genes of Pseudomonas solanacearum are homologous to pathogenicity determinants of animal pathogenic bacteria and are conserved among plant pathogenic bacteria." *Mol Plant Microbe Interact* 5(5): 384-389.

Graham, J., D. Jones and A. Lloyd (1979). "Survival of Pseudomonas solanacearum race 3 in plant debris and in latently infected potato tubers." *Phytopathology* 69(10): 1100-1103.

Grey, B. E. and T. R. Steck (2001). "The viable but nonculturable state of Ralstonia solanacearum may be involved in long-term survival and plant infection." *Appl Environ Microbiol* 67(9): 3866-3872.

Grove, A. (2013). "MarR family transcription factors." *Curr Biol* 23(4): R142-143.

Grove, A. (2017). "Regulation of Metabolic Pathways by MarR Family Transcription Factors." *Comput Struct Biotechnol J* 15: 366-371.

Guarischi-Sousa, R., M. Puigvert, N. S. Coll, M. I. Siri, M. J. Pianzzola, M. Valls and J. C. Setubal (2016). "Complete genome sequence of the potato pathogen Ralstonia solanacearum UY031." *Stand Genomic Sci* 11: 7.

Haque, M. M., H. Hirata and S. Tsuyumu (2015). "SlyA regulates motA and motB, virulence and stress-related genes under conditions induced by the PhoP-PhoQ system in Dickeya dadantii 3937." *Res Microbiol* 166(6): 467-475.

Haque, M. M., M. S. Kabir, L. Q. Aini, H. Hirata and S. Tsuyumu (2009). "SlyA, a MarR family transcriptional regulator, is essential for virulence in Dickeya dadantii 3937." *J Bacteriol* 191(17): 5409-5418.

Hayes, M. M., A. M. MacIntyre and C. Allen (2017). "Complete Genome Sequences of the Plant Pathogens Ralstonia solanacearum Type Strain K60 and R. solanacearum Race 3 Biovar 2 Strain UW551." *Genome Announc* 5(40).

Hayward, A. (1964). "Characteristics of Pseudomonas solanacearum." *Journal of Applied Microbiology* 27(2): 265-277.

Hayward, A. (1994). "Systematics and phylogeny of Pseudonmonas solanacearum and related bacteria." *Bacterial wilt: the disease and its causative agent, Pseudomonas solanacearum*: 123-135.

Hayward, A. C. (1991). "Biology and epidemiology of bacterial wilt caused by pseudomonas solanacearum." *Annu Rev Phytopathol* 29: 65-87.

He, L., L. Sequeira and A. Kelman (1983). "Characteristics of strains of Pseudomonas sp. and other bacterial plant pathogens." *Phytopathology* 61: 1430.

Henry, E., T. Y. Toruno, A. Jauneau, L. Deslandes and G. Coaker (2017). "Direct and Indirect Visualization of Bacterial Effector Delivery into Diverse Plant Cell Types during Infection." *Plant Cell* 29(7): 1555-1570.

Hernández-Romero, D., F. Solano and A. Sanchez-Amat (2005). "Polyphenol oxidase activity expression in Ralstonia solanacearum." *Appl Environ Microbiol* 71(11): 6808-6815.

Hikichi, Y. (2016). "Interactions between plant pathogenic bacteria and host plants during the establishment of susceptibility." *Journal of General Plant Pathology* 82(6): 326-331.

Hikichi, Y., T. Yoshimochi, S. Tsujimoto, R. Shinohara, K. Nakaho, A. Kanda, A. Kiba and K. Ohnishi (2007). "Global regulation of pathogenicity mechanism of Ralstonia solanacearum." *Plant biotechnology* 24(1): 149-154.

Hirsch, J., L. Deslandes, D. X. Feng, C. Balague and Y. Marco (2002). "Delayed Symptom Development in ein2-1, an Arabidopsis Ethylene-Insensitive Mutant, in Response to Bacterial Wilt Caused by Ralstonia solanacearum." *Phytopathology* 92(10): 1142-1148.

Hong, J. C., M. T. Momol, J. B. Jones, P. Ji, S. M. Olson, C. Allen, A. Perez, P. Pradhanang and K. Guven (2008). "Detection of Ralstonia solanacearum in irrigation ponds and aquatic weeds associated with the ponds in North Florida." *Plant disease* 92(12): 1674-1682.

Hong, J. K., H. J. Kim, H. Jung, H. J. Yang, D. H. Kim, C. H. Sung, C.-J. Park and S. W. Chang (2016). "Differential Control Efficacies of Vitamin Treatments against Bacterial Wilt and Grey Mould Diseases in Tomato Plants." *The plant pathology journal* 32(5): 469.

Hossain, M. M., S. Shibata, S.-I. Aizawa and S. Tsuyumu (2005). "Motility is an important determinant for pathogenesis of Erwinia carotovora subsp. carotovora." *Physiological and molecular plant pathology* 66(4): 134-143.

Hottes, A. K., P. L. Freddolino, A. Khare, Z. N. Donnell, J. C. Liu and S. Tavazoie (2013). "Bacterial adaptation through loss of function." *PLoS Genet* 9(7): e1003617.

Huang, J., B. F. Carney, T. P. Denny, A. K. Weissinger and M. A. Schell (1995). "A complex network regulates expression of eps and other virulence genes of Pseudomonas solanacearum." *J Bacteriol* 177(5): 1259-1267.

Huang, J., T. P. Denny and M. A. Schell (1993). "vsrB, a regulator of virulence genes of Pseudomonas solanacearum, is homologous to sensors of the two-component regulator family." *J Bacteriol* 175(19): 6169-6178.

Huang, J. and M. Schell (1995). "Molecular characterization of the eps gene cluster of Pseudomonas solanacearum and its transcriptional regulation at a single promoter." *Mol Microbiol* 16(5): 977-989.

Huang, Q. and C. Allen (1997). "An exo-poly-alpha-D-galacturonosidase, PehB, is required for wild-type virulence of Ralstonia solanacearum." *J Bacteriol* 179(23): 7369-7378.

Huang, Q. and C. Allen (2000). "Polygalacturonases are required for rapid colonization and full virulence of Ralstonia solanacearum on tomato plants." *Physiological and molecular plant pathology* 57(2): 77-83.

Huang, W., Y. Lin, S. Yi, P. Liu, J. Shen, Z. Shao and Z. Liu (2012). "QsdH, a novel AHL lactonase in the RND-type inner membrane of marine Pseudoalteromonas byunsanensis strain 1A01261." *PLoS One* 7(10): e46587.

Hudson, D. L., A. N. Layton, T. R. Field, A. J. Bowen, H. Wolf-Watz, M. Elofsson, M. P. Stevens and E. E. Galyov (2007). "Inhibition of type III secretion in Salmonella enterica serovar Typhimurium by small-molecule inhibitors." *Antimicrob Agents Chemother* 51(7): 2631-2635.

Huet, G. (2014). "Breeding for resistances to Ralstonia solanacearum." *Front Plant Sci* 5: 715.

Huysmans, M., A. S. Lema, N. S. Coll and M. K. Nowack (2017). "Dying two deaths - programmed cell death regulation in development and disease." *Curr. Opin. Plant Biol.* 35: 37-44.

Jacobs, J. M., L. Babujee, F. Meng, A. Milling and C. Allen (2012). "The in planta transcriptome of Ralstonia solanacearum: conserved physiological and virulence strategies during bacterial wilt of tomato." *MBio* 3(4).

Jacobs, J. M., A. Milling, R. M. Mitra, C. S. Hogan, F. Ailloud, P. Prior and C. Allen (2013). "Ralstonia solanacearum requires PopS, an ancient AvrE-family effector, for virulence and To overcome salicylic acid-mediated defenses during tomato pathogenesis." *MBio* 4(6): e00875-00813.

Janse, J. (1996). "Potato brown rot in Western Europe–history, present occurrence and some remarks on possible origin, epidemiology and control strategies." *EPPO Bulletin* 26(3-4): 679-695.

Janse, J. (2012). "Review on brown rot (Ralstonia solanacearum race 3, biovar 2, phylotype IIB) epidemiology and control in the Netherlands since 1995: a success story of integrated pest management." *Journal of Plant Pathology* 94(2): 257-272.

Janse, J., H. Van den Beld, J. Elphinstone, S. Simpkins, N. Tjou-Tam-Sin and J. Van Vaerenbergh (2004). "Introduction to Europe of Ralstonia solanacearum biovar 2, race 3 in Pelargonium zonale cuttings." *Journal of Plant Pathology*: 147-155.

Jones, J. D. and J. L. Dangl (2006). "The plant immune system." *Nature* 444(7117): 323-329.

Kado, C. (2002). Crown gall. The Plant Health Instructor. doi: 10.1094, PHI-I-2002-1118-01.

Kai, K., H. Ohnishi, Y. Mori, A. Kiba, K. Ohnishi and Y. Hikichi (2014). "Involvement of ralfuranone production in the virulence of Ralstonia solanacearum OE1-1." *Chembiochem* 15(17): 2590-2597.

Kai, K., H. Ohnishi, M. Shimatani, S. Ishikawa, Y. Mori, A. Kiba, K. Ohnishi, M. Tabuchi and Y. Hikichi (2015). "Methyl 3-Hydroxymyristate, a Diffusible Signal Mediating phc Quorum Sensing in Ralstonia solanacearum." *Chembiochem* 16(16): 2309-2318.

Kang, Y., J. Huang, G. Mao, L. He and M. Schell (1994). "Dramatically reduced virulence of mutants of Pseudomonas solanacearum defective in export of extracellular proteins across the outer membrane." *Molecular plant-microbe interactions: MPMI (USA)*.

Kang, Y., H. Liu, S. Genin, M. A. Schell and T. P. Denny (2002). "Ralstonia solanacearum requires type 4 pili to adhere to multiple surfaces and for natural transformation and virulence." *Mol Microbiol* 46(2): 427-437.

Kao, C. C., E. Barlow and L. Sequeira (1992). "Extracellular polysaccharide is required for wild-type virulence of Pseudomonas solanacearum." *J Bacteriol* 174(3): 1068-1071.

Kauppi, A. M., R. Nordfelth, H. Uvell, H. Wolf-Watz and M. Elofsson (2003). "Targeting bacterial virulence: inhibitors of type III secretion in *Yersinia*." *Chem. Biol.* 10(3): 241-249.

Kelman, A. (1954). "The relationship of pathogenicity of Pseudomonas solanacearum to colony appearance in a tetrazolium medium." *Phytopathology* 44(12).

Kelman, A. and J. Hruschka (1973). "The role of motility and aerotaxis in the selective increase of avirulent bacteria in still broth cultures of Pseudomonas solanacearum." *J Gen Microbiol* 76(1): 177-188.

Khokhani, D., T. M. Lowe-Power, T. M. Tran and C. Allen (2017). "A Single Regulator Mediates Strategic Switching between Attachment/Spread and Growth/Virulence in the Plant Pathogen Ralstonia solanacearum." *MBio* 8(5).

Khokhani, D., C. Zhang, Y. Li, Q. Wang, Q. Zeng, A. Yamazaki, W. Hutchins, S. S. Zhou, X. Chen and C. H. Yang (2013). "Discovery of plant phenolic compounds that act as type III secretion system inhibitors or inducers of the fire blight pathogen, *Erwinia amylovora*." *Appl. Environ. Microbiol.* 79(18): 5424-5436.

Kim, M. G., L. da Cunha, A. J. McFall, Y. Belkhadir, S. DebRoy, J. L. Dangl and D. Mackey (2005). "Two Pseudomonas syringae type III effectors inhibit RIN4-regulated basal defense in Arabidopsis." *Cell* 121(5): 749-759.

Kim, O. K., L. K. Garrity-Ryan, V. J. Bartlett, M. C. Grier, A. K. Verma, G. Medjanis, J. E. Donatelli, A. B. Macone, S. K. Tanaka, S. B. Levy and M. N. Alekshun (2009). "N-hydroxybenzimidazole inhibitors of the transcription factor LcrF in *Yersinia*: novel antivirulence agents." *J. Med. Chem.* 52(18): 5626-5634.

Kim, S., Y. J. Cho, E. S. Song, S. H. Lee, J. G. Kim and L. W. Kang (2016). "Time-resolved pathogenic gene expression analysis of the plant pathogen Xanthomonas oryzae pv. oryzae." *BMC Genomics* 17: 345.

Kimura, K., Iwatsuki, M., Nagai, T., Matsumoto, A., Takahashi, Y., Shiomi, K., Omura, S. and Abe, A. (2011). "A small-molecule inhibitor of the bacterial type III secretion system protects against in vivo infection with *Citrobacter rodentium*." *J. Antiobiot. (Tokyo)* 64(2): 197-203.

Kraepiel, Y. and M. A. Barny (2016). "Gram-negative phytopathogenic bacteria, all hemibiotrophs after all?" *Mol Plant Pathol* 17(3): 313-316.

Kumar, L. and E. F. M (2007). "Mfuzz: a software package for soft clustering of microarray data." *Bioinformation* 2(1): 5-7.

Kumar, R., Y. Lu, A. G. Elliott, A. M. Kavanagh, M. A. Cooper and R. A. Davis (2016). "Semi-synthesis and NMR spectral assignments of flavonoid and chalcone derivatives." *Magn. Reson. Chem.* 54(11): 880-886.

Langmead, B. and S. L. Salzberg (2012). "Fast gapped-read alignment with Bowtie 2." *Nat Methods* 9(4): 357-359.

Lebeau, A., M. Gouy, M. C. Daunay, E. Wicker, F. Chiroleu, P. Prior, A. Frary and J. Dintinger (2013). "Genetic mapping of a major dominant gene for resistance to Ralstonia solanacearum in eggplant." *Theor Appl Genet* 126(1): 143-158.

Lemessa, F. and W. Zeller (2007). "Screening rhizobacteria for biological control of Ralstonia solanacearum in Ethiopia." *Biological control* 42(3): 336-344.

Leng, N., Y. Li, B. E. McIntosh, B. K. Nguyen, B. Duffin, S. Tian, J. A. Thomson, C. N. Dewey, R. Stewart and C. Kendziorski (2015). "EBSeq-HMM: a Bayesian approach for identifying gene-expression changes in ordered RNA-seq experiments." *Bioinformatics* 31(16): 2614-2622.

Levrier, C., M. Balastrier, K. D. Beattie, A. R. Carroll, F. Martin, V. Choomuenwai and R. A. Davis (2013). "Pyridocoumarin, aristolactam and aporphine alkaloids from the Australian rainforest plant *Goniothalamus australis*." *Phytochemistry* 86: 121-126.

Levrier, C., M. C. Sadowski, C. C. Nelson, P. C. Healy and R. A. Davis (2015). "Denhaminols A-H, dihydro-*beta*-agarofurans from the endemic Australian rainforest plant *Denhamia celastroides*." *J. Nat. Prod.* 78(1): 111-119.

Li, J., C. Lv, W. Sun, Z. Li, X. Han, Y. Li and Y. Shen (2013). "Cytosporone B, an inhibitor of the type III secretion system of *Salmonella enterica* serovar *Typhimurium*." *Antimicrob. Agents Chemother.* 57(5): 2191-2198.

Li, P., D. Wang, J. Yan, J. Zhou, Y. Deng, Z. Jiang, B. Cao, Z. He and L. Zhang (2016). "Genomic Analysis of Phylotype I Strain EP1 Reveals Substantial Divergence from Other Strains in the Ralstonia solanacearum Species Complex." *Front Microbiol* 7: 1719.

Li, S., Y. Yu, J. Chen, B. Guo, L. Yang and W. Ding (2016). "Evaluation of the antibacterial effects and mechanism of action of protocatechualdehyde against Ralstonia solanacearum." *Molecules* 21(6): 754.

Li, Y., Q. Peng, D. Selimi, Q. Wang, A. O. Charkowski, X. Chen and C. H. Yang (2009). "The plant phenolic compound *p*-coumaric acid represses gene expression in the *Dickeya dadantii* type III secretion system." *Appl. Environ. Microbiol.* 75(5): 1223-1228.

Li, Z., S. Wu, X. Bai, Y. Liu, J. Lu, B. Xiao, X. Lu and L. Fan (2011). "Genome sequence of the tobacco bacterial wilt pathogen Ralstonia solanacearum." *J Bacteriol* 193(21): 6088-6089.

Lindgren, P. B., R. C. Peet and N. J. Panopoulos (1986). "Gene cluster of Pseudomonas syringae pv. "phaseolicola" controls pathogenicity of bean plants and hypersensitivity of nonhost plants." *J Bacteriol* 168(2): 512-522.

Lipscomb, L. and M. A. Schell (2011). "Elucidation of the regulon and cis-acting regulatory element of HrpB, the AraC-type regulator of a plant pathogen-like type III secretion system in Burkholderia pseudomallei." *J Bacteriol* 193(8): 1991-2001.

Liu, H., S. J. Coulthurst, L. Pritchard, P. E. Hedley, M. Ravensdale, S. Humphris, T. Burr, G. Takle, M. B. Brurberg, P. R. Birch, G. P. Salmond and I. K. Toth (2008). "Quorum sensing coordinates brute force and stealth modes of infection in the plant pathogen Pectobacterium atrosepticum." *PLoS Pathog* 4(6): e1000093.

Liu, H., S. Zhang, M. A. Schell and T. P. Denny (2005). "Pyramiding unmarked deletions in Ralstonia solanacearum shows that secreted proteins in addition to plant cell-wall-degrading enzymes contribute to virulence." *Mol Plant Microbe Interact* 18(12): 1296-1305.

Lo Presti, L., D. Lanver, G. Schweizer, S. Tanaka, L. Liang, M. Tollot, A. Zuccaro, S. Reissmann and R. Kahmann (2015). "Fungal effectors and plant susceptibility." *Annu Rev Plant Biol* 66: 513-545.

Lohou, D., M. Turner, F. Lonjon, A. C. Cazale, N. Peeters, S. Genin and F. Vailleau (2014). "HpaP modulates type III effector secretion in Ralstonia solanacearum and harbours a substrate specificity switch domain essential for virulence." *Mol Plant Pathol* 15(6): 601-614.

Lonjon, F., D. Lohou, A. C. Cazale, D. Buttner, B. G. Ribeiro, C. Peanne, S. Genin and F. Vailleau (2017). "HpaB-Dependent Secretion of Type III Effectors in the Plant Pathogens Ralstonia solanacearum and Xanthomonas campestris pv. vesicatoria." *Sci Rep* 7(1): 4879.

Lonjon, F., M. Turner, C. Henry, D. Rengel, D. Lohou, Q. v. d. Kerkhove, A.-C. Cazalé, N. Peeters, S. Genin and F. Vailleau (2016). "Comparative Secretome Analysis of Ralstonia solanacearum Type 3 Secretion-Associated Mutants Reveals a Fine Control of Effector Delivery, Essential for Bacterial Pathogenicity." *Molecular & Cellular Proteomics*.

Love, M. I., W. Huber and S. Anders (2014). "Moderated estimation of fold change and dispersion for RNA-seq data with DESeq2." *Genome Biol* 15(12): 550.

Low, D. A. and J. Casadesus (2008). “Clocks and switches: bacterial gene regulation by DNA adenine methylation.” *Curr Opin Microbiol* 11(2): 106-112.

Low, D. A., N. J. Weyand and M. J. Mahan (2001). “Roles of DNA adenine methylation in regulating bacterial gene expression and virulence.” *Infect Immun* 69(12): 7197-7204.

Lowe-Power, T. M., C. G. Hendrich, E. von Roepenack-Lahaye, B. Li, D. Wu, R. Mitra, B. L. Dalsing, P. Ricca, J. Naidoo, D. Cook, A. Jancewicz, P. Masson, B. Thomma, T. Lahaye, A. J. Michael and C. Allen (2017). “Metabolomics of tomato xylem sap during bacterial wilt reveals Ralstonia solanacearum produces abundant putrescine, a metabolite that accelerates wilt disease.” *Environ Microbiol*.

Lowe, T. M., F. Ailloud and C. Allen (2015). “Hydroxycinnamic Acid Degradation, a Broadly Conserved Trait, Protects Ralstonia solanacearum from Chemical Plant Defenses and Contributes to Root Colonization and Virulence.” *Mol Plant Microbe Interact* 28(3): 286-297.

Lundgren, B. R., M. P. Connolly, P. Choudhary, T. S. Brookins-Little, S. Chatterjee, R. Raina and C. T. Nomura (2015). “Defining the Metabolic Functions and Roles in Virulence of the rpoN1 and rpoN2 Genes in Ralstonia solanacearum GMI1000.” *PLoS One* 10(12): e0144852.

Ma, K.-W. and W. Ma (2016). “Phytohormone pathways as targets of pathogens to facilitate infection.” *Plant Molecular Biology* 91(6): 713-725.

Macho, A. P. and C. Zipfel (2015). “Targeting of plant pattern recognition receptor-triggered immunity by bacterial type-III secretion system effectors.” *Curr Opin Microbiol* 23: 14-22.

Mansfield, J., S. Genin, S. Magori, V. Citovsky, M. Sriariyanum, P. Ronald, M. Dow, V. Verdier, S. V. Beer, M. A. Machado, I. Toth, G. Salmond and G. D. Foster (2012). “Top 10 plant pathogenic bacteria in molecular plant pathology.” *Mol Plant Pathol* 13(6): 614-629.

Marenda, M., B. Brito, D. Callard, S. Genin, P. Barberis, C. Boucher and M. Arlat (1998). “PrhA controls a novel regulatory pathway required for the specific induction of Ralstonia solanacearum hrp genes in the presence of plant cells.” *Mol Microbiol* 27(2): 437-453.

McGarvey, J., C. Bell, T. Denny and M. Schell (1998). Analysis of extracellular polysaccharide I in culture and in planta using immunological methods: new insights and implications. *Bacterial Wilt Disease*, Springer: 157-163.

McGarvey, J. A., T. P. Denny and M. A. Schell (1999). “Spatial-Temporal and Quantitative Analysis of Growth and EPS I Production by Ralstonia solanacearum in Resistant and Susceptible Tomato Cultivars.” *Phytopathology* 89(12): 1233-1239.

McWilliams, R., M. Chapman, K. M. Kowalczuk, D. Hersberger, J. Sun and C. C. Kao (1995). “Complementation analyses of Pseudomonas solanacearum extracellular polysaccharide mutants and identification of genes responsive to EpsR.” *Mol Plant Microbe Interact* 8(6): 837-844.

Melotto, M. and B. N. Kunkel (2013). Virulence strategies of plant pathogenic bacteria. *The Prokaryotes*, Springer: 61-82.

Melotto, M., W. Underwood, J. Koczan, K. Nomura and S. Y. He (2006). “Plant stomata function in innate immunity against bacterial invasion.” *Cell* 126(5): 969-980.

Meng, F. (2013). “The Virulence Factors of the Bacterial Wilt Pathogen *Ralstonia solanacearum* “ *Plant Pathology & Microbiology* 4(3).

Meng, F., L. Babujee, J. M. Jacobs and C. Allen (2015). “Comparative Transcriptome Analysis Reveals Cool Virulence Factors of Ralstonia solanacearum Race 3 Biovar 2.” *PLoS One* 10(10): e0139090.

Meng, F., J. Yao and C. Allen (2011). "A MotN mutant of Ralstonia solanacearum is hypermotile and has reduced virulence." *J Bacteriol* 193(10): 2477-2486.

Meyer, D., S. Cunnac, M. Gueneron, C. Declercq, F. Van Gijsegem, E. Lauber, C. Boucher and M. Arlat (2006). "PopF1 and PopF2, two proteins secreted by the type III protein secretion system of Ralstonia solanacearum, are translocators belonging to the HrpF/NopX family." *J Bacteriol* 188(13): 4903-4917.

Misas-Villamil, J. C., I. Kolodziejek, E. Crabill, F. Kaschani, S. Niessen, T. Shindo, M. Kaiser, J. R. Alfano and R. A. van der Hoorn (2013). "Pseudomonas syringae pv. syringae uses proteasome inhibitor syringolin A to colonize from wound infection sites." *PLoS Pathog* 9(3): e1003281.

Mole, B. M., D. A. Baltrus, J. L. Dangl and S. R. Grant (2007). "Global virulence regulation networks in phytopathogenic bacteria." *Trends Microbiol* 15(8): 363-371.

Monteiro, F., S. Genin, I. van Dijk and M. Valls (2012a). "A luminescent reporter evidences active expression of Ralstonia solanacearum type III secretion system genes throughout plant infection." *Microbiology* 158(Pt 8): 2107-2116.

Monteiro, F., M. Sole, I. van Dijk and M. Valls (2012b). "A chromosomal insertion toolbox for promoter probing, mutant complementation, and pathogenicity studies in Ralstonia solanacearum." *Mol Plant Microbe Interact* 25(4): 557-568.

Mori, Y., K. Inoue, K. Ikeda, H. Nakayashiki, C. Higashimoto, K. Ohnishi, A. Kiba and Y. Hikichi (2016). "The vascular plant-pathogenic bacterium Ralstonia solanacearum produces biofilms required for its virulence on the surfaces of tomato cells adjacent to intercellular spaces." *Mol Plant Pathol* 17(6): 890-902.

Mori, Y., S. Ishikawa, H. Ohnishi, M. Shimatani, Y. Morikawa, K. Hayashi, K. Ohnishi, A. Kiba, K. Kai and Y. Hikichi (2018). "Involvement of ralfuranones in the quorum sensing signalling pathway and virulence of Ralstonia solanacearum strain OE1-1." *Mol Plant Pathol* 19(2): 454-463.

Mougous, J. D., M. E. Cuff, S. Raunser, A. Shen, M. Zhou, C. A. Gifford, A. L. Goodman, G. Joachimiak, C. L. Ordonez, S. Lory, T. Walz, A. Joachimiak and J. J. Mekalanos (2006). "A virulence locus of Pseudomonas aeruginosa encodes a protein secretion apparatus." *Science* 312(5779): 1526-1530.

Munkvold, K. R., A. B. Russell, B. H. Kvitko and A. Collmer (2009). "*Pseudomonas syringae* pv. tomato DC3000 type III effector HopAA1-1 functions redundantly with chlorosis-promoting factor PSPTO4723 to produce bacterial speck lesions in host tomato." *Mol. Plant-Microbe Interact.* 22(11): 1341-1355.

Muschiol, S., L. Bailey, A. Gylfe, C. Sundin, K. Hultenby, S. Bergstrom, M. Elofsson, H. Wolf-Watz, S. Normark and B. Henriques-Normark (2006). "A small-molecule inhibitor of type III secretion inhibits different stages of the infectious cycle of *Chlamydia trachomatis*." *Proc. Natl. Acad. Sci. U. S. A.* 103(39): 14566-14571.

Naito, K., Y. Ishiga, K. Toyoda, T. Shiraishi and Y. Ichinose (2007). "N-terminal domain including conserved flg22 is required for flagellin-induced hypersensitive cell death in Arabidopsis thaliana." *Journal of General Plant Pathology* 73(4): 281-285.

Nesterenko, L. N., N. A. Zigangirova, E. S. Zayakin, S. I. Luyksaar, N. V. Kobets, D. V. Balunets, L. A. Shabalina, T. N. Bolshakova, O. Y. Dobrynina and A. L. Gintsburg (2016). "A small-molecule compound belonging to a class of 2,4-disubstituted 1,3,4-thiadiazine-5-ones suppresses *Salmonella* infection *in vivo*." *J. Antibiot. (Tokyo)* 69(6): 422-427.

Nguyen, L. C., F. Taguchi, Q. M. Tran, K. Naito, M. Yamamoto, M. Ohnishi-Kameyama, H. Ono, M. Yoshida, K. Chiku, T. Ishii, Y. Inagaki, K. Toyoda, T. Shiraishi and Y. Ichinose (2012). "Type IV pilin is glycosylated in Pseudomonas syringae pv. tabaci 6605 and is required for surface motility and virulence." *Mol Plant Pathol* 13(7): 764-774.

Nicaise, V., M. Roux and C. Zipfel (2009). "Recent advances in PAMP-triggered immunity against bacteria: pattern recognition receptors watch over and raise the alarm." *Plant Physiol* 150(4): 1638-1647.

Nobori, T., A. C. Velasquez, J. Wu, B. H. Kvitko, J. M. Kremer, Y. Wang, S. Y. He and K. Tsuda (2018). "Transcriptome landscape of a bacterial pathogen under plant immunity." *Proc Natl Acad Sci U S A*.

Nordfelth, R., A. M. Kauppi, H. A. Norberg, H. Wolf-Watz and M. Elofsson (2005). "Small-molecule inhibitors specifically targeting type III secretion." *Infect. Immun.* 73(5): 3104-3114.

Nurnberger, T., F. Brunner, B. Kemmerling and L. Piater (2004). "Innate immunity in plants and animals: striking similarities and obvious differences." *Immunol Rev* 198: 249-266.

O'Connell, R. J., M. R. Thon, S. Hacquard, S. G. Amyotte, J. Kleemann, M. F. Torres, U. Damm, E. A. Buiate, L. Epstein and N. Alkan (2012). "Lifestyle transitions in plant pathogenic Colletotrichum fungi deciphered by genome and transcriptome analyses." *Nature genetics* 44(9): 1060.

Occhialini, A., S. Cunnac, N. Reymond, S. Genin and C. Boucher (2005). "Genome-wide analysis of gene expression in Ralstonia solanacearum reveals that the hrpB gene acts as a regulatory switch controlling multiple virulence pathways." *Mol Plant Microbe Interact* 18(9): 938-949.

Oerke, E.-C. and H.-W. Dehne (2004). "Safeguarding production—losses in major crops and the role of crop protection." *Crop protection* 23(4): 275-285.

Orgambide, G., H. Montrozier, P. Servin, J. Roussel, D. Trigalet-Demery and A. Trigalet (1991). "High heterogeneity of the exopolysaccharides of Pseudomonas solanacearum strain GMI 1000 and the complete structure of the major polysaccharide." *J Biol Chem* 266(13): 8312-8321.

Pan, Y., F. Liang, R. J. Li and W. Qian (2018). "MarR-Family Transcription Factor HpaR Controls Expression of the vgrR-vgrS Operon of Xanthomonas campestris pv. campestris." *Mol Plant Microbe Interact* 31(3): 299-310.

Park, E., H. Y. Lee, J. Woo, D. Choi and S. P. Dinesh-Kumar (2017). "Spatiotemporal Monitoring of Pseudomonas syringae Effectors via Type III Secretion Using Split Fluorescent Protein Fragments." *Plant Cell* 29(7): 1571-1584.

Patil, V. U., V. Girimalla, V. Sagar, R. S. Chauhan and S. K. Chakrabarti (2017). "Genome sequencing of four strains of Phylotype I, II and IV of Ralstonia solanacearum that cause potato bacterial wilt in India." *Braz J Microbiol* 48(2): 193-195.

Peeters, N., S. Carrere, M. Anisimova, L. Plener, A. C. Cazale and S. Genin (2013). "Repertoire, unified nomenclature and evolution of the Type III effector gene set in the Ralstonia solanacearum species complex." *BMC Genomics* 14: 859.

Peeters, N., A. Guidot, F. Vailleau and M. Valls (2013). "Ralstonia solanacearum, a widespread bacterial plant pathogen in the post-genomic era." *Mol Plant Pathol* 14(7): 651-662.

Perrier, A., X. Barlet, R. Peyraud, D. Rengel, A. Guidot and S. Genin (2018). "Comparative transcriptomic studies identify specific expression patterns of virulence factors under the control of the master regulator PhcA in the Ralstonia solanacearum species complex." *Microb Pathog* 116: 273-278.

Perrier, A., R. Peyraud, D. Rengel, X. Barlet, E. Lucasson, J. Gouzy, N. Peeters, S. Genin and A. Guidot (2016). "Enhanced in planta Fitness through Adaptive Mutations in EfpR, a Dual Regulator of Virulence and Metabolic Functions in the Plant Pathogen Ralstonia solanacearum." *PLoS Pathog* 12(12): e1006044.

Petrocelli, S., M. R. Arana, M. N. Cabrini, A. C. Casabuono, L. Moyano, M. Beltramino, L. M. Moreira, A. S. Couto and E. G. Orellano (2016). "Deletion of pilA, a Minor Pilin-Like Gene, from Xanthomonas citri subsp. citri Influences Bacterial Physiology and Pathogenesis." *Curr Microbiol* 73(6): 904-914.

Peyraud, R., L. Cottret, L. Marmiesse and S. Genin (2018). "Control of primary metabolism by a virulence regulatory network promotes robustness in a plant pathogen." *Nat Commun* 9(1): 418.

Peyraud, R., L. Cottret, L. Marmiesse, J. Gouzy and S. Genin (2016). "A Resource Allocation Trade-Off between Virulence and Proliferation Drives Metabolic Versatility in the Plant Pathogen Ralstonia solanacearum." *PLoS Pathog* 12(10): e1005939.

Plener, L., P. Boistard, A. Gonzalez, C. Boucher and S. Genin (2012). "Metabolic adaptation of Ralstonia solanacearum during plant infection: a methionine biosynthesis case study." *PLoS One* 7(5): e36877.

Plener, L., P. Manfredi, M. Valls and S. Genin (2010). "PrhG, a transcriptional regulator responding to growth conditions, is involved in the control of the type III secretion system regulon in Ralstonia solanacearum." *J Bacteriol* 192(4): 1011-1019.

Poueymiro, M., S. Cunnac, P. Barberis, L. Deslandes, N. Peeters, A. C. Cazale-Noel, C. Boucher and S. Genin (2009). "Two type III secretion system effectors from Ralstonia solanacearum GMI1000 determine host-range specificity on tobacco." *Mol Plant Microbe Interact* 22(5): 538-550.

Pradhan, B. B., M. Ranjan and S. Chatterjee (2012). "XadM, a novel adhesin of Xanthomonas oryzae pv. oryzae, exhibits similarity to Rhs family proteins and is required for optimum attachment, biofilm formation, and virulence." *Mol Plant Microbe Interact* 25(9): 1157-1170.

Pradhanang, P., P. Ji, M. Momol, S. Olson, J. Mayfield and J. Jones (2005). "Application of acibenzolar-S-methyl enhances host resistance in tomato against Ralstonia solanacearum." *Plant Disease* 89(9): 989-993.

Prior, P., V. Grimault and J. Schmit (1994). "Resistance to bacterial wilt (Pseudomonas solanacearum) in tomato: present status and prospects."

Pritchard, L. and P. R. Birch (2014). "The zigzag model of plant-microbe interactions: is it time to move on?" *Mol Plant Pathol* 15(9): 865-870.

Puigvert, M., R. Guarischi-Sousa, P. Zuluaga, N. S. Coll, A. P. Macho, J. C. Setubal and M. Valls (2017). "Transcriptomes of Ralstonia solanacearum during Root Colonization of Solanum commersonii." *Front Plant Sci* 8: 370.

Pukatzki, S., A. T. Ma, A. T. Revel, D. Sturtevant and J. J. Mekalanos (2007). "Type VI secretion system translocates a phage tail spike-like protein into target cells where it cross-links actin." *Proc Natl Acad Sci U S A* 104(39): 15508-15513.

Puri, A. W. and M. Bogyo (2009). "Using small molecules to dissect mechanisms of microbial pathogenesis." *ACS Chem. Biol.* 4(8): 603-616.

Qian, W., Y. Jia, S. X. Ren, Y. Q. He, J. X. Feng, L. F. Lu, Q. Sun, G. Ying, D. J. Tang, H. Tang, W. Wu, P. Hao, L. Wang, B. L. Jiang, S. Zeng, W. Y. Gu, G. Lu, L. Rong, Y. Tian, Z. Yao, G. Fu, B. Chen, R. Fang, B. Qiang, Z. Chen, G. P. Zhao, J. L. Tang and C. He (2005). "Comparative and functional genomic analyses of the pathogenicity of phytopathogen Xanthomonas campestris pv. campestris." *Genome Res* 15(6): 757-767.

Qian, Y.-l., X.-s. Wang, D.-z. Wang, L.-n. Zhang, C.-l. Zu, Z.-l. Gao, H.-j. Zhang, Z.-y. Wang, X.-y. Sun and D.-n. Yao (2013). "The detection of QTLs controlling bacterial wilt resistance in tobacco (N. tabacum L.)." *Euphytica* 192(2): 259-266.

Ramesh, R. and G. S. Phadke (2012). "Rhizosphere and endophytic bacteria for the suppression of eggplant wilt caused by Ralstonia solanacearum." *Crop Protection* 37: 35-41.

Rasko, D. A. and V. Sperandio (2010). "Anti-virulence strategies to combat bacteria-mediated disease." *Nat. Rev. Drug Discovery* 9(2): 117-128.

Ray, S. K., R. Kumar, N. Peeters, C. Boucher and S. Genin (2015). "rpoN1, but not rpoN2, is required for twitching motility, natural competence, growth on nitrate, and virulence of Ralstonia solanacearum." *Front Microbiol* 6: 229.

Raza, W., N. Ling, D. Liu, Z. Wei, Q. Huang and Q. Shen (2016). "Volatile organic compounds produced by Pseudomonas fluorescens WR-1 restrict the growth and virulence traits of Ralstonia solanacearum." *Microbiological research* 192: 103-113.

Remenant, B., L. Babujee, A. Lajus, C. Medigue, P. Prior and C. Allen (2012). "Sequencing of K60, type strain of the major plant pathogen Ralstonia solanacearum." *J Bacteriol* 194(10): 2742-2743.

Remenant, B., B. Coupat-Goutaland, A. Guidot, G. Cellier, E. Wicker, C. Allen, M. Fegan, O. Pruvost, M. Elbaz, A. Calteau, G. Salvignol, D. Mornico, S. Mangenot, V. Barbe, C. Medigue and P. Prior (2010). "Genomes of three tomato pathogens within the Ralstonia solanacearum species complex reveal significant evolutionary divergence." *BMC Genomics* 11: 379.

Rivard, C. L. and F. J. Louws (2008). "Grafting to manage soilborne diseases in heirloom tomato production." *HortScience* 43(7): 2104-2111.

Roberts, D. P., T. P. Denny and M. A. Schell (1988). "Cloning of the egl gene of Pseudomonas solanacearum and analysis of its role in phytopathogenicity." *J Bacteriol* 170(4): 1445-1451.

Rojas, C. M., J. H. Ham, W.-L. Deng, J. J. Doyle and A. Collmer (2002). "HecA, a member of a class of adhesins produced by diverse pathogenic bacteria, contributes to the attachment, aggregation, epidermal cell killing, and virulence phenotypes of Erwinia chrysanthemi EC16 on Nicotiana clevelandii seedlings." *Proceedings of the National Academy of Sciences* 99(20): 13142-13147.

Romantschuk, M. (1992). "Attachment of plant pathogenic bacteria to plant surfaces." *Annu Rev Phytopathol* 30: 225-243.

Rufian, J. S., M. A. Sanchez-Romero, D. Lopez-Marquez, A. P. Macho, J. W. Mansfield, D. L. Arnold, J. Ruiz-Albert, J. Casadesus and C. R. Beuzon (2016). "Pseudomonas syringae Differentiates into Phenotypically Distinct Subpopulations During Colonization of a Plant Host." *Environ Microbiol* 18(10): 3593-3605.

Saile, E., J. A. McGarvey, M. A. Schell and T. P. Denny (1997). "Role of Extracellular Polysaccharide and Endoglucanase in Root Invasion and Colonization of Tomato Plants by Ralstonia solanacearum." *Phytopathology* 87(12): 1264-1271.

Salanoubat, M., S. Genin, F. Artiguenave, J. Gouzy, S. Mangenot, M. Arlat, A. Billault, P. Brottier, J. C. Camus, L. Cattolico, M. Chandler, N. Choisne, C. Claudel-Renard, S. Cunnac, N. Demange, C. Gaspin, M. Lavie, A. Moisan, C. Robert, W. Saurin, T. Schiex, P. Siguier, P. Thebault, M. Whalen, P. Wincker, M. Levy, J. Weissenbach and C. A. Boucher (2002). "Genome sequence of the plant pathogen Ralstonia solanacearum." *Nature* 415(6871): 497-502.

Sanchez-Romero, M. A., I. Cota and J. Casadesus (2015). "DNA methylation in bacteria: from the methyl group to the methylome." *Curr Opin Microbiol* 25: 9-16.

Schell, M. A. (2000). "Control of Virulence and Pathogenicity Genes of Ralstonia Solanacearum by an Elaborate Sensory Network." *Annu Rev Phytopathol* 38: 263-292.

Schell, M. A., D. P. Roberts and T. P. Denny (1988). "Analysis of the Pseudomonas solanacearum polygalacturonase encoded by pglA and its involvement in phytopathogenicity." *J Bacteriol* 170(10): 4501-4508.

Segonzac, C. and C. Zipfel (2011). "Activation of plant pattern-recognition receptors by bacteria." *Curr Opin Microbiol* 14(1): 54-61.

Sequeira, L. and P. Rowe (1969). "Selection and utilization of Solanum phureja clones with high resistance to different strains of Pseudomonas solanacearum." *American Potato Journal* 46(12): 451-462.

Shi, X. and H. Lin (2018). "The chemotaxis regulator pilG of Xylella fastidiosa is required for virulence in Vitis vinifera grapevines." *European Journal of Plant Pathology* 150(2): 351-362.

Shirasu, K. and C. I. Kado (1993). "Membrane location of the Ti plasmid VirB proteins involved in the biosynthesis of a pilin-like conjugative structure on Agrobacterium tumefaciens." *FEMS Microbiol Lett* 111(2-3): 287-294.

Shrivastava, S. and S. S. Mande (2008). "Identification and functional characterization of gene components of Type VI Secretion system in bacterial genomes." *PLoS One* 3(8): e2955.

Siri, M. I., A. Sanabria and M. J. Pianzzola (2011). "Genetic Diversity and Aggressiveness ofRalstonia solanacearumStrains Causing Bacterial Wilt of Potato in Uruguay." *Plant Disease* 95(10): 1292-1301.

Sjoblom, S., H. Harjunpaa, G. Brader and E. T. Palva (2008). "A novel plant ferredoxin-like protein and the regulator Hor are quorum-sensing targets in the plant pathogen Erwinia carotovora." *Mol Plant Microbe Interact* 21(7): 967-978.

Slepenkin, A., H. Chu, M. Elofsson, P. Keyser and E. M. Peterson (2011). "Protection of mice from a *Chlamydia trachomatis* vaginal infection using a *Salicylidene acylhydrazide*, a potential microbicide." *J. Infect. Dis.* 204(9): 1313-1320.

Smidt, M. and T. Kosuge (1978). "The role of indole-3-acetic acid accumulation by alpha methyl tryptophan-resistant mutants of Pseudomonas savastanoi in gall formation on oleanders." *Physiological Plant Pathology* 13(2): 203IN17211-210213.

Smith, E. F. (1896). "bacterial disease of the tomato, eggplant, and Irish potato (Bacillus solanacearum n. sp.)."

Smith, E. F. (1914). Bacteria in relation to plant diseases, Carnegie institution of Washington.

Souza, D. P., G. U. Oka, C. E. Alvarez-Martinez, A. W. Bisson-Filho, G. Dunger, L. Hobeika, N. S. Cavalcante, M. C. Alegria, L. R. Barbosa and R. K. Salinas (2015). "Bacterial killing via a type IV secretion system." *Nat Commun* 6: 6453.

Strange, R. N. and P. R. Scott (2005). "Plant disease: a threat to global food security." *Annu Rev Phytopathol* 43: 83-116.

Su, S., X. Zhou, G. Liao, P. Qi and L. Jin (2016). "Synthesis and Antibacterial Evaluation of New Sulfone Derivatives Containing 2-Aroxymethyl-1, 3, 4-Oxadiazole/Thiadiazole Moiety." *Molecules* 22(1): 64.

Sun, Y., K. Wang, C. Caceres-Moreno, W. Jia, A. Chen, H. Zhang, R. Liu and A. P. Macho (2017). "Genome sequencing and analysis of Ralstonia solanacearum phylotype I strains FJAT-91, FJAT-452 and FJAT-462 isolated from tomato, eggplant, and chili pepper in China." *Stand Genomic Sci* 12: 29.

Sun, Z., Z. Liu, W. Zhou, H. Jin, H. Liu, A. Zhou, A. Zhang and M. Q. Wang (2016). "Temporal interactions of plant - insect - predator after infection of bacterial pathogen on rice plants." *Sci Rep* 6: 26043.

Sundin, G. W., L. F. Castiblanco, X. Yuan, Q. Zeng and C. H. Yang (2016). "Bacterial disease management: challenges, experience, innovation and future prospects: Challenges in Bacterial Molecular Plant Pathology." *Mol Plant Pathol* 17(9): 1506-1518.

Tang, X., Y. Xiao and J. M. Zhou (2006). "Regulation of the type III secretion system in phytopathogenic bacteria." *Mol. Plant-Microbe Interact.* 19(11): 1159-1166.

Tans-Kersten, J., D. Brown and C. Allen (2004). "Swimming motility, a virulence trait of Ralstonia solanacearum, is regulated by FlhDC and the plant host environment." *Mol Plant Microbe Interact* 17(6): 686-695.

Tans-Kersten, J., Y. Guan and C. Allen (1998). "Ralstonia solanacearum pectin methylesterase is required for growth on methylated pectin but not for bacterial wilt virulence." *Appl Environ Microbiol* 64(12): 4918-4923.

Tans-Kersten, J., H. Huang and C. Allen (2001). "Ralstonia solanacearum needs motility for invasive virulence on tomato." *J Bacteriol* 183(12): 3597-3605.

Thomma, B. P., T. Nurnberger and M. H. Joosten (2011). "Of PAMPs and effectors: the blurred PTI-ETI dichotomy." *Plant Cell* 23(1): 4-15.

Thoquet, P., J. Olivier, C. Sperisen, P. Rogowsky, H. Laterrot and N. Grimsley (1996). "Quantitative trait loci determining resistance to bacterial wilt in tomato cultivar Hawaii7996." *Molecular plant-microbe interactions: MPMI (USA)*.

Tock, M. R. and D. T. Dryden (2005). "The biology of restriction and anti-restriction." *Curr Opin Microbiol* 8(4): 466-472.

Tseng, T. T., B. M. Tyler and J. C. Setubal (2009). "Protein secretion systems in bacterial-host associations, and their description in the Gene Ontology." *BMC Microbiol* 9 Suppl 1: S2.

Turner, M., A. Jauneau, S. Genin, M. J. Tavella, F. Vailleau, L. Gentzbittel and M. F. Jardinaud (2009). "Dissection of bacterial Wilt on Medicago truncatula revealed two type III secretion system effectors acting on root infection process and disease development." *Plant Physiol* 150(4): 1713-1722.

Vailleau, F., E. Sartorel, M. F. Jardinaud, F. Chardon, S. Genin, T. Huguet, L. Gentzbittel and M. Petitprez (2007). "Characterization of the interaction between the bacterial wilt pathogen *Ralstonia solanacearum* and the model legume plant *Medicago truncatula*." *Mol. Plant-Microbe Interact.* 20(2): 159-167.

Valls, M., S. Genin and C. Boucher (2006). "Integrated regulation of the type III secretion system and other virulence determinants in Ralstonia solanacearum." *PLoS Pathog* 2(8): e82.

van Elsas, J. D., P. Kastelein, P. van Bekkum, J. M. van der Wolf, P. M. de Vries and L. S. van Overbeek (2000). "Survival of Ralstonia solanacearum Biovar 2, the Causative Agent of Potato Brown Rot, in Field and Microcosm Soils in Temperate Climates." *Phytopathology* 90(12): 1358-1366.

Van Gijsegem, F., S. Genin and C. Boucher (1993). "Conservation of secretion pathways for pathogenicity determinants of plant and animal bacteria." *Trends Microbiol* 1(5): 175-180.

Van Gijsegem, F., C. Gough, C. Zischek, E. Niqueux, M. Arlat, S. Genin, P. Barberis, S. German, P. Castello and C. Boucher (1995). "The hrp gene locus of Pseudomonas solanacearum, which controls the production of a type III secretion system, encodes eight proteins related to components of the bacterial flagellar biogenesis complex." *Mol Microbiol* 15(6): 1095-1114.

Van Gijsegem, F., J. Vasse, J. C. Camus, M. Marenda and C. Boucher (2000). "*Ralstonia solanacearum* produces *hrp*-dependent pili that are required for PopA secretion but not for attachment of bacteria to plant cells." *Mol. Microbiol.* 36(2): 249-260.

Van Vliet, A. H. (2009). "Next generation sequencing of microbial transcriptomes: challenges and opportunities." *FEMS microbiology letters* 302(1): 1-7.

Vasse, J., P. Frey and A. Trigalet (1995). "Microscopic studies of intercellular infection and protoxylem invasion of tomato roots by Pseudomonas solanacearum." *Molecular plant-microbe interactions* 8.

Vasse, J., S. Genin, P. Frey, C. Boucher and B. Brito (2000). "The hrpB and hrpG regulatory genes of Ralstonia solanacearum are required for different stages of the tomato root infection process." *Mol Plant Microbe Interact* 13(3): 259-267.

Wairuri, C. K., J. E. van der Waals, A. van Schalkwyk and J. Theron (2012). "Ralstonia solanacearum needs Flp pili for virulence on potato." *Mol Plant Microbe Interact* 25(4): 546-556.

Wang, D., C. E. Zetterstrom, M. Gabrielsen, K. S. Beckham, J. J. Tree, S. E. Macdonald, O. Byron, T. J. Mitchell, D. L. Gally, P. Herzyk, A. Mahajan, H. Uvell, R. Burchmore, B. O. Smith, M. Elofsson and A. J. Roe (2011). "Identification of bacterial target proteins for the salicylidene acylhydrazide class of virulence-blocking compounds." *J. Biol. Chem.* 286(34): 29922-29931.

Wang, J. Y., L. Zhou, B. Chen, S. Sun, W. Zhang, M. Li, H. Tang, B. L. Jiang, J. L. Tang and Y. W. He (2015). "A functional 4-hydroxybenzoate degradation pathway in the phytopathogen Xanthomonas campestris is required for full pathogenicity." *Sci Rep* 5: 18456.

Wang, K., L. Kang, A. Anand, G. Lazarovits and K. S. Mysore (2007). "Monitoring in planta bacterial infection at both cellular and whole-plant levels using the green fluorescent protein variant GFPuv." *New Phytol.* 174(1): 212-223.

Wei, K., D. J. Tang, Y. Q. He, J. X. Feng, B. L. Jiang, G. T. Lu, B. Chen and J. L. Tang (2007). "hpaR, a putative marR family transcriptional regulator, is positively controlled by HrpG and HrpX and involved in the pathogenesis, hypersensitive response, and extracellular protease production of Xanthomonas campestris pathovar campestris." *J Bacteriol* 189(5): 2055-2062.

Weigel, W. and P. Dersch (2018). "Phenotypic heterogeneity: a bacterial virulence strategy." *Microbes and infection*.

Wengelnik, K. and U. Bonas (1996). "HrpXv, an AraC-type regulator, activates expression of five of the six loci in the hrp cluster of Xanthomonas campestris pv. vesicatoria." *J Bacteriol* 178(12): 3462-3469.

Wengelnik, K., G. Van den Ackerveken and U. Bonas (1996). "HrpG, a key hrp regulatory protein of Xanthomonas campestris pv. vesicatoria is homologous to two-component response regulators." *Mol Plant Microbe Interact* 9(8): 704-712.

Wenneker, M., M. Verdel, R. Groeneveld, C. Kempenaar, A. Van Beuningen and J. Janse (1999). "Ralstonia (Pseudomonas) solanacearum race 3 (biovar 2) in surface water and natural weed hosts: First report on stinging nettle (Urtica dioica)." *European Journal of Plant Pathology* 105(3): 307-315.

Whatley, M. H., N. Hunter, M. A. Cantrell, C. Hendrick, K. Keegstra and L. Sequeira (1980). "Lipopolysaccharide composition of the wilt pathogen, Pseudomonas solanacearum: correlation with the hypersensitive response in tobacco." *Plant physiology* 65(3): 557-559.

Wilson, G. G. and N. E. Murray (1991). "Restriction and modification systems." *Annu Rev Genet* 25: 585-627.

Willbanks, A., M. Leary, M. Greenshields, C. Tyminski, S. Heerboth, K. Lapinska, K. Haskins and S. Sarkar (2016). "The Evolution of Epigenetics: From Prokaryotes to Humans and Its Biological Consequences." *Genet Epigenet* 8: 25-36.

Wu, H. J., A. H. Wang and M. P. Jennings (2008). "Discovery of virulence factors of pathogenic bacteria." *Curr Opin Chem Biol* 12(1): 93-101.

Wu, H. Y., P. C. Chung, H. W. Shih, S. R. Wen and E. M. Lai (2008). "Secretome analysis uncovers an Hcp-family protein secreted via a type VI secretion system in Agrobacterium tumefaciens." *J Bacteriol* 190(8): 2841-2850.

Xu, J., H. J. Zheng, L. Liu, Z. C. Pan, P. Prior, B. Tang, J. S. Xu, H. Zhang, Q. Tian, L. Q. Zhang and J. Feng (2011). "Complete genome sequence of the plant pathogen Ralstonia solanacearum strain Po82." *J Bacteriol* 193(16): 4261-4262.

Yabuuchi, E., Y. Kosako, H. Oyaizu, I. Yano, H. Hotta, Y. Hashimoto, T. Ezaki and M. Arakawa (1992). "Proposal of Burkholderia gen. nov. and transfer of seven species of the genus Pseudomonas homology group II to the new genus, with the type species Burkholderia cepacia (Palleroni and Holmes 1981) comb. nov." *Microbiol Immunol* 36(12): 1251-1275.

Yabuuchi, E., Y. Kosako, I. Yano, H. Hotta and Y. Nishiuchi (1995). "Transfer of two Burkholderia and an Alcaligenes species to Ralstonia gen. Nov.: Proposal of Ralstonia pickettii (Ralston, Palleroni and Doudoroff 1973) comb. Nov., Ralstonia solanacearum (Smith 1896) comb. Nov. and Ralstonia eutropha (Davis 1969) comb. Nov." *Microbiol Immunol* 39(11): 897-904.

Yadeta, K. A. and J. T. BP (2013). "The xylem as battleground for plant hosts and vascular wilt pathogens." *Front Plant Sci* 4: 97.

Yamada, T., I. Letunic, S. Okuda, M. Kanehisa and P. Bork (2011). "iPath2. 0: interactive pathway explorer." *Nucleic acids research* 39(suppl_2): W412-W415.

Yamazaki, A., J. Li, Q. Zeng, D. Khokhani, W. C. Hutchins, A. C. Yost, E. Biddle, E. J. Toone, X. Chen and C. H. Yang (2012). "Derivatives of plant phenolic compound affect the type III secretion system of *Pseudomonas aeruginosa* via a GacS-GacA two-component signal transduction system." *Antimicrob. Agents Chemother.* 56(1): 36-43.

Yang, F., S. S. Korban, P. L. Pusey, M. Elofsson, G. W. Sundin and Y. Zhao (2014). "Small-molecule inhibitors suppress the expression of both type III secretion and amylovoran biosynthesis genes in *Erwinia amylovora*." *Mol. Plant Pathol.* 15(1): 44-57.

Yao, J. and C. Allen (2006). "Chemotaxis is required for virulence and competitive fitness of the bacterial wilt pathogen Ralstonia solanacearum." *J Bacteriol* 188(10): 3697-3708.

Yoshimochi, T., Y. Hikichi, A. Kiba and K. Ohnishi (2009). "The global virulence regulator PhcA negatively controls the Ralstonia solanacearum hrp regulatory cascade by repressing expression of the PrhIR signaling proteins." *J Bacteriol* 191(10): 3424-3428.

Yu, J. H., Z. Hamari, K. H. Han, J. A. Seo, Y. Reyes-Dominguez and C. Scazzocchio (2004). "Double-joint PCR: a PCR-based molecular tool for gene manipulations in filamentous fungi." *Fungal Genet Biol* 41(11): 973-981.

Yuliar, Y. A. Nion and K. Toyota (2015). "Recent trends in control methods for bacterial wilt diseases caused by Ralstonia solanacearum." *Microbes Environ* 30(1): 1-11.

Zaumeyer, W. J. (1958). "Antibiotics in the control of plant diseases." *Annu. Rev. Microbiol.* 12: 415-440.

Zetterstrom, C. E., J. Hasselgren, O. Salin, R. A. Davis, R. J. Quinn, C. Sundin and M. Elofsson (2013). "The resveratrol tetramer (-)-hopeaphenol inhibits type III secretion in the gram-negative pathogens Yersinia pseudotuberculosis and Pseudomonas aeruginosa." *PLoS One* 8(12): e81969.

Zhang, L., J. Xu, J. Xu, K. Chen, L. He and J. Feng (2012). "TssM is essential for virulence and required for type VI secretion in Ralstonia solanacearum." *Journal of Plant Diseases and Protection*: 125-134.

Zhang, L., J. Xu, H. Zhang, L. He and J. Feng (2014). "TssB is essential for virulence and required for type VI secretion system in Ralstonia solanacearum." *Microb Pathog* 74: 1-7.

Zhang, Y., A. Kiba, Y. Hikichi and K. Ohnishi (2011). "prhKLM genes of Ralstonia solanacearum encode novel activators of hrp regulon and are required for pathogenesis in tomato." *FEMS microbiology letters* 317(1): 75-82.

Zhang, Y., F. Luo, D. Wu, Y. Hikichi, A. Kiba, Y. Igarashi, W. Ding and K. Ohnishi (2015). "PrhN, a putative marR family transcriptional regulator, is involved in positive regulation of type III secretion system and full virulence of Ralstonia solanacearum." *Front Microbiol* 6: 357.

Zhu, Q. H., W. X. Shan, M. A. Ayliffe and M. B. Wang (2016). "Epigenetic Mechanisms: An Emerging Player in Plant-Microbe Interactions." *Mol Plant Microbe Interact* 29(3): 187-196.

Zou, L., Q. Zeng, H. Lin, P. Gyaneshwar, G. Chen and C. H. Yang (2012). "SlyA regulates type III secretion system (T3SS) genes in parallel with the T3SS master regulator HrpL in Dickeya dadantii 3937." *Appl Environ Microbiol* 78(8): 2888-2895.

Zuleta, M. C. (2007). Identification of Ralstonia solanacearum exoproteins secreted by the type two secretion system using proteomic techniques, uga.

Zuluaga, A. P., M. Puigvert and M. Valls (2013). "Novel plant inputs influencing Ralstonia solanacearum during infection." *Front Microbiol* 4: 349.

Zuluaga, A. P., M. Sole, H. Lu, E. Gongora-Castillo, B. Vaillancourt, N. Coll, C. R. Buell and M. Valls (2015). "Transcriptome responses to Ralstonia solanacearum infection in the roots of the wild potato Solanum commersonii." *BMC Genomics* 16: 246.

Zuluaga, A. P., J. C. Vega-Arreguin, Z. Fei, L. Ponnala, S. J. Lee, A. J. Matas, S. Patev, W. E. Fry and J. K. Rose (2016). "Transcriptional dynamics of Phytophthora infestans during sequential stages of hemibiotrophic infection of tomato." *Mol Plant Pathol* 17(1): 29-41.

ANNEX

frontiers in
MICROBIOLOGY

ORIGINAL RESEARCH ARTICLE
published: 20 November 2013
doi: 10.3389/fmicb.2013.00349

Novel plant inputs influencing *Ralstonia solanacearum* during infection

A. Paola Zuluaga[1,2], Marina Puigvert[1] and Marc Valls[1,2]*

[1] *Departament de Genètica, Universitat de Barcelona, Barcelona, Spain*
[2] *Centre for Research in Agricultural Genomics (CSIC-IRTA-UB-UAB), Bellaterra, Spain*

Edited by:
Carmen R. Beuzón, University of Málaga, Spain

Reviewed by:
Marta Marchetti, National Institute for Agricultural Research, France
Emilia López-Solanilla, Universidad Politécnica de Madrid, Spain

***Correspondence:**
Marc Valls, Departament de Genètica, Universitat de Barcelona, Av. Diagonal 643, Barcelona, Catalonia 08014, Spain
e-mail: marcvalls@ub.edu

Ralstonia solanacearum is a soil and water-borne pathogen that can infect a wide range of plants and cause the devastating bacterial wilt disease. To successfully colonize a host, *R. solanacearum* requires the type III secretion system (T3SS), which delivers bacterial effector proteins inside the plant cells. HrpG is a central transcriptional regulator that drives the expression of the T3SS and other virulence determinants. *hrpG* transcription is highly induced upon plant cell contact and its product is also post-transcriptionally activated by metabolic signals present when bacteria are grown in minimal medium (MM). Here, we describe a transcriptional induction of *hrpG* at early stages of bacterial co-culture with plant cells that caused overexpression of the downstream T3SS effector genes. This induction was maintained in a strain devoid of *prhA*, the outer membrane receptor that senses bacterial contact with plant cells, demonstrating that this is a response to an unknown signal. Induction was unaffected after disruption of the known *R. solanacearum* pathogenicity regulators, indicating that it is controlled by a non-described system. Moreover, plant contact-independent signals are also important *in planta*, as shown by the *hrpG* induction triggered by apoplastic and xylem extracts. We also found that none of the amino acids or sugars present in the apoplast and xylem saps studied correlated with *hrp*G induction. This suggests that a small molecule or an environmental condition is responsible for the T3SS gene expression inside the plants. Our results also highlight the abundance and diversity of possible carbon, nitrogen and energy sources likely used by *R. solanacearum* during growth *in planta*.

Keywords: *R. solanacearum in planta*, plant inputs in hrp regulon, apoplast and xylem contents, novel induction of HrpG, pathogenicity mutants, sugars and aminoacids tomato fluids

INTRODUCTION

The life cycle of most bacterial plant pathogens includes a long phase of survival or multiplication in the environment, entry and colonization of plants, and high multiplication in specific plant tissues that leads to symptom development in susceptible hosts. The bacterium successfully adapts to these disparate niches through differential gene expression in response to specific environmental signals (Mole et al., 2007; Saha and Lindeberg, 2013).

Ralstonia solanacearum is a soil-borne pathogen that infects more than 200 host species from over 50 botanical families (Peeters et al., 2013). Nonetheless, this pathogen can live as a saprophyte in the soil when there are no hosts available (Schell, 2000; Mansfield et al., 2012). In order to deal with the physiological demands of these contrasting situations, the bacterium possesses a complex regulatory network that responds to both environmental and internal cues (Schell, 2000; Genin and Denny, 2012). The main pathogenicity determinant in *R. solanacearum* is the type III secretion system (T3SS), which translocates effector proteins into the plant host cells (Coll and Valls, 2013). The T3SS is encoded by the *hrp* gene cluster and is regulated by plant and metabolic signals (Brito et al., 1999; Aldon et al., 2000). Plant signals are sensed by the outer membrane receptor PrhA, which responds to still-unknown cell wall components (Aldon et al., 2000) and transduces the signal through PrhR, PrhI, and PrhJ to induce the central *hrp*G regulator (Brito et al., 1999, 2002). HrpG controls the downstream HrpB activator that regulates transcription of the *hrp* genes and related T3SS effectors (Brito et al., 1999, 2002; Valls et al., 2006; Genin and Denny, 2012). Metabolic signals are also sensed in this complex regulatory network by PrhG, a close paralog of HrpG. PrhG is responsible for activating *hrpB* in response to plant cell contact (Plener et al., 2010). HrpG has been proposed to be a master regulator playing a role in the transition from saprophytic to parasitic life style by integrating the plant cell contact signal (Aldon et al., 2000), the metabolic inputs triggered in minimal medium (MM) (Brito et al., 1999), and a quorum sensing signal through the PhcA regulator (Genin et al., 2005). As a result, HrpG co-regulates the induction of the T3SS and other virulence determinants (Valls et al., 2006). PhcA is a global density-dependent regulator that indirectly suppresses *hrpB* expression by either lowering *prhIR* transcription (Genin et al., 2005; Yoshimochi et al., 2009a) or repressing *hrpG* (Yoshimochi et al., 2009b). It was recently reported that *prh*G is activated by PhcA, proposing that *R. solanacearum* switches from HrpG to PrhG to ensure *hrpB* activation in a cell density-dependent manner (Zhang et al., 2013). On the other hand, PhcA

controls exopolysaccharide production via XpsR, motility and cell wall-degrading activities via pehSR and quorum sensing through the transcriptional activator solR, responsible of sensing the acyl-homoserine-lactone (AHL) (Brito et al., 1999; Aldon et al., 2000; Genin et al., 2005).

Despite the wealth of knowledge gained in the last years, we remain quite naïve about the environmental inputs that elicit the *R. solanacearum hrp* regulon in natural conditions, as most gene regulation studies have been performed in *in vitro* culture. Discrepancies with recent gene expression analyses *in planta* (Monteiro et al., 2012) suggest that the bacterium may receive unknown signals during saprophytic life. In this work we aimed to further our understanding of the environmental inputs that control the *hrp* regulon and identified a novel regulatory signal triggering *hrpG* expression at early stages of the interaction with *Arabidopsis* cells. We demonstrate that this signal is not dependent on PrhA or PrhJ, and that, contrary to what was currently known, *hrpG* can be strongly activated by plant apoplast and xylem saps in the absence of cell-wall derived signals. We describe the most abundant carbon and nitrogen sources available *in planta* for pathogen growth and conclude that none of them seems to influence the newly described *hrpG* induction.

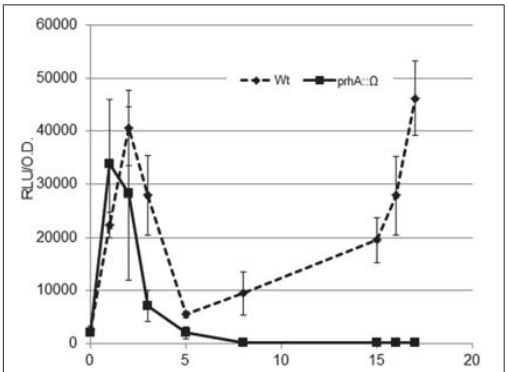

FIGURE 1 | Expression profile of the *hrpG* promoter during bacterial co-culture with *Arabidopsis* cells. The wild-type *R. solanacearum* strain GMI1000 (wt, solid line) or its *prhA*-defficient derivative (prhA::Ω, dashed line) carrying the *PhrpG::LuxCDABE* fusion were grown in Gamborg medium in the presence of plant cells and luminescence measured at different time points. A representative result using three biological replicates is shown. Promoter output is presented as relative luminescence units (R.L.U) produced by the *lux* reporter corrected by cell density estimated by OD_{600}. Error bars indicate standard deviations.

RESULTS AND DISCUSSION

THE HrpG REGULON IS INDUCED BY A CELL CONTACT-INDEPENDENT SIGNAL WHEN *R. solanacearum* GROWS IN THE PRESENCE OF PLANT CELLS

HrpG is a central transcriptional regulator that drives the expression of the T3SS and other virulence determinants in *R. solanacearum* (Genin and Denny, 2012; Zhang et al., 2013). Studies on *hrpG* expression have often been carried out measuring transcriptional output from cultures grown overnight in MM or in co-culture with plant cells (Marenda et al., 1998). In order to gain a better understanding of *hrp* regulation earlier in the plant-pathogen interaction, we performed a time course experiment in co-cultures of *R. solanacearum* with *Arabidopsis* cells by measuring transcription of *hrpG* every hour. To this end, we used a modified bacterial strain containing the *hrpG* promoter fused to the *luxCDABE* operon integrated in a permissive site of the chromosome (Monteiro et al., 2012). With this strain, real time information of *hrpG* transcription could be obtained by measuring luminescence. To our surprise, the wild type (wt) strain showed a bimodal induction of *hrpG*, with clear induction of the *HrpG* promoter during the first 2 h of co-culture with plant cells (**Figure 1**). This early induction was significant, although less strong than the one observed at later times (8–16 h). PrhA is the outer membrane receptor responsible for the well-described *hrp* gene induction upon contact with plant cells (Marenda et al., 1998). To check if the two *hrpG* induction peaks observed were mediated by PrhA, we introduced the *PhrpG::lux* construct in the *prhA* mutant background and evaluated luminescence. Interestingly, the strong induction at 2 h of co-culture with plant cells was maintained while the second peak was abolished (**Figure 1**). Thus, the outer membrane receptor PrhA mediated the second induction peak but was dispensable for *hrp* induction at early stages. This was confirmed by the fact that the early induction also remained unaltered in a strain deficient for PrhJ, the regulator that transduces the PrhA cell-contact induction to HrpG (data not shown). In these experiments, high variability in gene expression was observed at early times, likely due to the fact that cultures were still adapting to the new growth conditions in co-culture after dilution. However, a robust induction resulting in the early expression peak was always detected.

In order to test the relevance of the initial *hrpG* induction on downstream genes, we measured the expression profiles of the type III-secreted effector *avrA* and the gene coding for the *R. solanacearum* ethylene-forming enzyme (*efe*). These genes were selected because *avrA is* controlled by HrpG and HrpB while the *efe* gene is specifically regulated by HrpG in a HrpB-independent manner (Valls et al., 2006). The *R. solanacearum* PavrA-lux and Pefe-lux strains were created and luminescence was measured as shown in **Figure 2**. Absolute expression levels of the *avrA*, *efe*, and *hrpG* promoters differ due to different promoter strength, but remarkably, expression of both downstream genes showed the bimodal profile, maintaining an early induction at 2 h of co-culture with plant cells (**Figure 2**). Differences in the magnitude of the early induction in these genes might be explained by additional regulatory inputs that over impose to the HrpG action. We presume that this induction could have implications in plant-pathogen interactions, since pathogen effectors are being expressed and likely secreted to the host within few hours of contact with the host cells.

THE PrhA-INDEPENDENT INDUCTION OF *HrpG* IS NOT MEDIATED BY ANY OF THE KNOWN PATHOGENICITY REGULATORS

Next, we used a classical genetics approach to determine if any of the known regulatory pathways mediated the newly-identified signal. To this end, we tested *hrpG* induction in

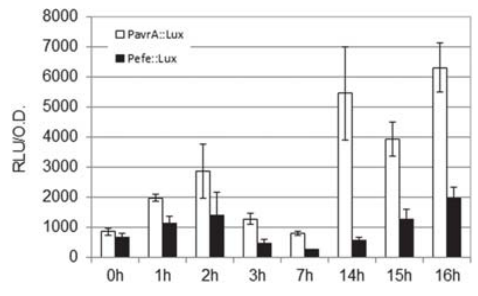

FIGURE 2 | Expression profile of *HrpG*-controlled genes in co-culture with *Arabidopsis* cells. Luminescence was measured from *R. solanacearum* GMI1000 carrying fusions of the *avrA* or *efe* promoters to the *luxCDABE* reporter (PavrA-lux or Pefe-lux, respectively). Growth conditions and units as in **Figure 1**.

R. solanacearum mutants defective in the main pathogenicity regulators (**Supplementary Table 1**). The analyzed mutants were: *solR*, a quorum sensing transcriptional activator responsible of sensing the AHL; *vsrA*, which activates *xpsR* and represses motility; *vsrC*, an activator of EPS and motility that represses pectinase activity; *xpsR*, which induces EPS synthesis; *phcA*, the master regulator that represses *hrpG* in culture, and *pehR*, which activates the pectinase-encoding gene *pehA* and motility (Genin and Denny, 2012). All these mutants were transformed with the *hrpG* promoter fused to the lux operon and luminescence measured in co-culture with plant cells. **Figure 3A** shows the expression profiles in the wt or the *phcA*, *pehR*, *vsrC*, *solR*, *xpsR*, and *vsrA* mutants. All mutants showed a similar expression profile, except for *phcA,* that showed a strongly enhanced *hrpG* expression, as expected due to the well-described PhcA inhibition on *hrp* gene expression (Genin et al., 2005). **Figure 3B** shows a zoom-in of the *hrpG* expression profile during the first 3 h of co-culture. All the regulatory mutants maintained the early cell-contact-independent induction of *hrpG*, indicating that none of them is directly mediating the inducing signal. This finding suggests that there are yet unknown triggers of *hrp* gene expression.

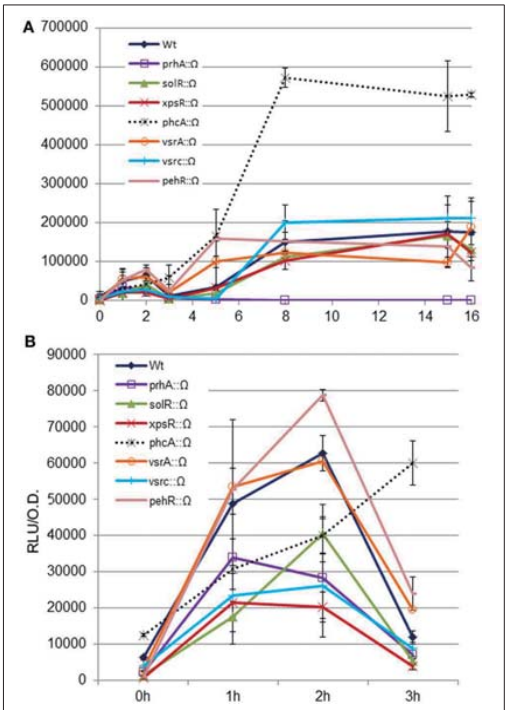

FIGURE 3 | Expression profiles of the *hrpG* promoter in wild type *R. solanacearum* or virulence regulatory mutants in co-culture with Arabidopsis cells. The wt or the prhA, solR, xpsR, phcA, vsrA, vsrC, and pehR disruption mutants carrying the *PhrpG::LuxCDABE* fusion were grown in Gamborg medium in the presence of plant cells and luminescence measured at different time points **(A)**. Zoom-in of *hrpG* expression during the first 3 h of co-culture with *Arabidopsis* cells to better appreciate that all mutants show comparable expression profiles as the wild type in the first induction peak during growth in the presence of plant cells **(B)**. A representative result using three biological replicates is shown. Promoter output is presented as relative luminescence units (R.L.U) produced by the *lux* reporter corrected by cell density estimated by OD_{600}. Error bars indicate standard deviations.

PLANT CELL CONTACT IS NOT ESSENTIAL FOR *HrpG* INDUCTION *in planta*

To test whether plant cell contact-independent induction also occurs *in planta*, we extracted apoplast and xylem fluids from tomato plants as described in (Coplin et al., 1974; Rico and Preston, 2008) and performed *hrpG* expression profiles from bacteria growing in both exudates (**Figure 4**). In agreement with our previous observations, we observed high expression of the *HrpG* promoter comparable to the induction we detected in co-cultures (**Figure 3**) when bacteria were grown in plant extracts in the absence of plant cells (**Figure 4**). However, differences in growth rate and bacterial physiology in plant extracts and co-cultures with plant cells make it difficult to compare the induction timings in both conditions. These results indicate that, contrary to what has been hypothesized until now, cell contact-independent induction of *R. solanacearum hrpG* is also triggered *in planta* in addition to the well-established cell wall contact response mediated by PrhA (Aldon et al., 2000; Brencic and Winans, 2005; Rico and Preston, 2008). The precise plant molecules or environmental cues responsible for the newly described *hrp* gene induction remained unknown.

NO AMINOACID OR SUGAR IN TOMATO EXTRACTS CORRELATES WITH *HrpG* EXPRESSION

To shed light on the nature of the signals involved in contact-independent *hrp* gene induction *in planta*, we performed an analysis of the sugars and amino acids present in both tomato xylem sap and apoplastic fluid before and after sustaining growth of *R. solanacearum*. These fluids were chosen

because they correspond to the two main compartments where *R. solanacearum* grows inside the plant (Vasse et al., 1995; Ward et al., 2010). Since the observed *hrpG* induction peaked at 7 h of growth in the apoplastic fluid but remained roughly unchanged in the xylem, we searched for an aminoacid or sugar whose abundance diminished after 7 h of *R. solanacearum* growth in apoplast sap and that showed a similar pattern or remained constant in xylem cultures. Molecule contents for both xylem and apoplast were measured by chromatography at time 0 and at 7 or 21 h after bacterial growth and are presented in **Tables 1**, **2**. Surprisingly, sugars and aminoacids concentrations were similar at either 7 or 21 h of bacterial growth; thus, only the latter time point is shown. However, none of the detected molecules showed the expected abundance profile, indicating that common aminoacids or sugars do not play a role in the induction of *hrpG* and the subsequent trigger of the main *R. solanacearum* virulence determinants *in planta*.

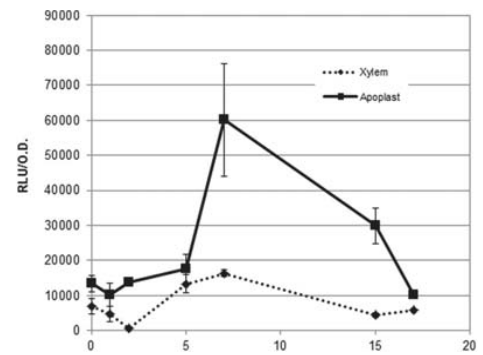

FIGURE 4 | Expression profile of the hrpG promoter in both apoplast and xylem exudates. Induction of the hrpG promoter in bacteria grown in cell-free plant exudates. A representative result using three biological replicates is shown. Promoter output is presented as relative luminescence units (R.L.U) produced by the *lux* reporter corrected by cell density estimated by OD_{600}. Error bars indicate standard deviations.

Table 1 | Sugar content in tomato exudates before and after growth of *R. solanacearum*.

	Apoplast		Xylem	
	− bacteria	+ bacteria	− bacteria	+ bacteria
Sucrose	193.43	21.22	ND	ND
Fructose	156.74	0	8.54	0
Glucose	110.93	10.04	4.08	0
Galactose	14.67	0.72	0	0
Mannose	11.54	10.94	0	0

Sugar concentrations in mg/l determined from tomato xylem sap or the apoplastic fluid before (− bacteria) or after (+ bacteria) sustaining growth of R. solanacearum for 21 h.

PLANT SUGARS ARE READILY CONSUMED BY *R. solanacearum* DURING GROWTH IN TOMATO

The possible carbon and energy sources used by *R. solanacearum* during saprophytic growth inside its plant hosts remain unknown. Thus, although we could not identify the *hrpG* inducing signal, the sugar content analyses provided interesting clues on the biology of the bacterium inside the plant. From the results presented in **Table 1**, it is apparent that the tomato apoplast is rich in sugar contents, in agreement to what has been reported (Rico and Preston, 2008). In addition, we were able to determine that, despite the general assumption that it mainly contains water and minerals, xylem sap was rich in sugars as well. The tomato apoplast showed a high concentration of sucrose, glucose, galactose, mannose and fructose, while the xylem contained glucose and fructose, although at lower concentrations (**Table 1**). Growth of *R. solanacearum* in these extracts indicated that the bacterium likely catabolizes all abundant apoplast or xylem sugars, which

Table 2 | Aminoacid content in tomato exudates before and after growth of *R. solanacearum*.

	Apoplast		Xylem	
	− bacteria	+ bacteria	− bacteria	+ bacteria
Gaba	599.4	0	62.2	0
Asp	281.1	0	13.2	0.7
Glu	274.3	0	11.3	2
Ala	156.7	13.7	1.7	1.7
Gln	146.9	0	195.5	0
Urea	133.6	0	0	0
Leu	85.6	8.4	24.7	0
Val	83.5	7.8	51.7	23.8
Pro	76.3	0	4.1	0
Asn	64.2	0	94	1.2
Lys	53.9	12.1	49.4	96
Phe	48.9	2.9	5	0
Ile	46.5	10.6	24.8	0
Phser	34	20.2	2.9	12.6
Arg	27	9	28.2	102.6
Tyr	21	1.4	6.8	0
Ser	19.4	0	5.5	2.7
His	19	1.6	25	0.45
Orn	14.6	0	1.2	4.7
Taur	0	4	0	4
Hylys	0	5.3	0	5.3
1-Mhis	4	11.2	16.3	20.1

Aminoacid concentrations in micromolar units determined from tomato xylem sap or the apoplastic fluid before (− bacteria) or after (+ bacteria) sustaining growth of R. solanacearum for 21 h. Red shading indicates the most abundant aminoacids in each compartment that seem to be metabolized by the pathogen. Blue shading denotes aminoacids whose concentrations increased after bacterial growth. Abbreviations are as follows: Ala, alanine; Arg, arginine; Asn, asparagine; Asp, aspartic acid; Gaba, gamma aminobutyric acid; Glu, glutamic acid; Gln, glutamine; His, histidine; Hylys, hydroxylysine; Ile, isoleucine; Leu, leucine; Lys, lysine; Orn, Ornithine; Phe, phenylalanine; Phser, phosphoserine; Pro, proline; Ser, serine; Taur, taurine; Tyr, tyrosine;Val, valine.

were undetectable after bacterial inoculation. The only exception was the less abundant mannose, which did not seem to be metabolized by bacteria growing in the apoplast and was undetected in the xylem sap (**Table 1**). Interestingly, studies of two different *R. solanacearum* lectins (RSL) showed contrasting affinity to sugars. RSL was found to bind fucose and arabinose in a higher degree than mannose (Sudakevitz et al., 2002) while RSIIL recognizes fucose, but displays a higher affinity to fructose and mannose (Sudakevitz et al., 2004). A variable pattern of carbon source utilization correlating with genomic variability has been reported among *Pseudomonas spp* (Rico and Preston, 2008). It would be interesting to test if such metabolic diversity is present also in the *R. solanacearum* species complex and if it correlates with sugar abundance in different plant hosts.

AMINOACID CONTENTS *in planta* VARY IN DIFFERENT TOMATO COMPARTMENTS AND AFTER BACTERIAL INFECTION

Interesting conclusions could also be extracted from the analyses of the amino acid content and concentrations measured in apoplast and xylem fluids before and after bacterial growth. **Table 2** shows all aminoacids and related compounds detected in both apoplast and xylem, ordered from the most to the less abundant in the apoplast. Similar to what had been reported previously (Rico and Preston, 2008), the most abundant amino acid in this tomato intercellular compartment was gamma aminobutyric acid (GABA), followed by aspartic and glutamic acids (**Table 2**, 1st column). It was also apparent that the xylem presented a very different amino acid composition from the apoplast, with glutamine as the most abundant aminoacid, followed by asparagine and GABA (**Table 2**, 3rd column). Marked differences in abundance were detected for urea, which was undetectable in xylem but highly abundant in the apoplast and aspartic acid, glutamic acid and alanine, major components of the apoplast that were much less abundant in the xylem (**Table 2**). These results demonstrated the variability of resources present in plant compartments and suggest that *R. solanacearum* has to cope with these contrasting environments and switch its metabolism along the plant colonization process.

Bacterial growth also impacted the amino acid composition of plant fluids *in vitro*. The amino acid profiles could be divided into those whose concentrations increased after bacterial growth (**Table 2**, blue shading) and the rest, which often decreased after bacterial growth. Interestingly, the most abundant amino acids were depleted in both compartments after bacterial growth (**Table 2**, red shading), suggesting bacterial adaptation to preferentially use the most abundant carbon sources. Arginine and lysine are the major exceptions to this rule, since their concentrations were high but almost always increased after bacterial growth in our *in vitro* experiments. Other amino acids whose abundance increased by bacterial metabolism were the least abundant in plant extracts, in agreement with the idea that they do not play a role in pathogen growth (**Table 2**, blue shading). Interestingly, higher amounts of aminoacids seemed to be released by bacteria in the xylem than in the apoplast. In particular, lysine, arginine and ornithine, which were abundantly produced by the bacteria in the xylem but naturally present in the apoplast and rather consumed by the pathogen growing in this fluid (**Table 2**). It was previously reported that tryptophan, phenylalanine, tyrosine, leucine, valine, and GABA concentrations increased when *R. solanacearum* grew on tobacco and tomato xylem 3–5 days after inoculation (Coplin et al., 1974). Likewise, Ward et al. (2010) recently described that the levels of tryptophan, tyrosine and phenylalanine increased in abundance in Arabidopsis plants after *Pseudomonas syringae* infection, while sucrose levels decreased. All these aminoacids where found abundantly in our study and rapidly consumed by *R. solanacearum*. We hypothesize that the pathogen might be able to reconfigure the host metabolism to induce the production of the aminoacids required for its growth. Experiments are under way to validate this hypothesis.

CONCLUSIONS

In this work we identified a novel regulatory signal triggering *hrpG* expression at early stages of the interaction with *Arabidopsis* cells. Challenging current knowledge (Aldon et al., 2000; Brencic and Winans, 2005; Rico and Preston, 2008), we show that the transcriptional induction of *hrpG* at early stages of bacterial co-culture with plant cells, which caused overexpression of the downstream T3SS effector genes is independent of bacterial contact with plant cells as demonstrated by the *hrpG* induction in the outer membrane receptor mutant strain *prhA*. The precise plant molecules or environmental cues responsible for the newly described *hrp* gene induction remained unknown. This induction was unaffected after disruption of the known *R. solanacearum* pathogenicity regulators, indicating that it is controlled by a non-described system. Moreover, our work suggests that plant contact-independent signals might also be important *in planta*, as shown by the *hrpG* induction triggered by apoplastic and xylem extracts. However, it must be taken into account that bacterial cultures with either plant cells or plant extracts do not perfectly mimic the spatial and environmental conditions encountered during growth *in planta*. New inputs when bacteria grow parasitically inside the plant host and the real contribution of the signals already described in these natural conditions remain to be determined.

Finally, we gained insight into the plant metabolic resources available for pathogen growth and concluded that invading bacteria not only have to cope with plant defenses but also with contrasting niches inside the host. An example of this adaptation is the specific response of the HrpG virulence regulon to the unknown metabolic or environmental plant signals described here.

MATERIALS AND METHODS

BACTERIAL STRAINS, CULTURE MEDIA, AND GROWTH CONDITIONS

Bacterial strains and plasmids used in this study are listed in **Supplementary Table 1**. *R. solanacearum* was routinely grown in rich B medium (10 g/l bactopeptone, 1 g/l yeast extract and 1 g/l casamino acids) or Boucher's MM (200 g/l KH_2PO_4, 50 g/l (NH4)2SO4, 10 g/l MgSO4-7H2O, KOH 10 N, 1.26 g/l FeSO4,-7H2O) at 30°C. For bacterial growth in plant extracts, 10 ml aliquots of xylem sap or apoplastic fluid in 50 ml erlenmeyers were inoculated with the *R. solanacearum* strain GMI1000 transformed the PhG-lux reporter fusion. The hrpG promoter was PCR-amplified from a cDNA library using primers that

added *Avr*II and *Kpn*I restriction sites upstream and downstream of the sequence, respectively. This PCR fragment was cloned into pGEM-T-EASY (Life Technologies, Paisley, UK), giving rise to pG-PhG. The *PhG* promoter was then excised from pG-PhG using *Avr*II-*Kpn*I and cloned into the same sites of pRCG-GWY (Monteiro et al., 2012), creating the plasmid pRCG-PhG-GWY. Finally, to generate pRCG-PhG-lux a *Sfi*I-*Kpn*I fragment containing the entire *LuxCDABE* operon, excised from plasmid pRCGent-Pep-lux (Monteiro et al., 2012), was cloned into the same sites of pRCG-PhG-GWY. This plasmid bears the *PhG::LuxCDABE* reporter fusion and a gentamycin-resistance gene, all flanked by two homology regions for recombination into the bacterial chromosome. Similarly, pRCG-PavrA-lux and pRCG-Pefe-lux were generated by cloning a *Kpn*I/*Bgl*II fragment from plasmid PavrA and pG-Pefe into the same sites of pRCG-GWY, respecively. PCR amplifications were performed with the proofreading Pfx DNA polymerase (Life Technologies, Paisley, UK) following the manufacturer's conditions and other general molecular biology techniques were performed as described in (Ausubel et al., 1994).

ARABIDOPSIS CO-CULTURE ASSAYS AND LUMINESCENCE MEASUREMENTS

Co-culture expression assays were carried out using *Arabidopsis* cells LT87 grown in Gamborg B5 (GB5). For co-culture assays, bacteria were diluted from overnight cultures grown in B medium to an $O.D._{600v} = 0.1$ in 20 ml-cultures of seven day-old *Arabidopsis* culture cells. Samples were taken every hour to measure cell density and luminescence. To carry out 24 h time course experiments, two cultures were started with 10 h of delay and the results of the two cultures superimposed. To recover only bacterial cells grown in the presence of *Arabidopsis* cells, 1 ml aliquots of the co-cultures were filtrated through a 20 μm-pore nylon membrane as described before (Monteiro et al., 2012). Luminescence measurements of filtered bacteria were done with a Berthold FB-12 luminometer and promoter output of the reporter was expressed as relative luminescence units (RLU) referred to cell density estimated as the $O.D._{600}$ in a Shimadzu UV-1603 spectrophotometer.

APOPLAST AND XYLEM EXTRACTIONS

Apoplast extraction was carried out as described in (Rico and Preston, 2008). Briefly, tomato leaves were cut, washed with distilled water and dried with a paper towel. Then, one to three leaves were introduced into a 50 ml syringe with 20 ml of distilled water and pressure—vacuum cycles applied until the leaves were completely infiltrated. After infiltration, leaves were carefully removed from the syringe and blotted with a paper towel. Each leaf was then introduced into a 5 ml tip placed inside a 50 ml conical tube containing a 1.5 ml collection tube. Apoplast extract was collected by spinning the tubes at 0.6 g for 5 min at 4°C. The fraction collected in the 1.5 ml tube was centrifuged again for 10 min at 0.8 g at 4°C. The supernatant was collected and stored in at −20°C until used.

Xylem sap extraction was performed as described by (Kehr and Rep, 2007). Briefly, 5 week-old tomato plants were cut at the stems ∼10 cm above ground with a razor blade. The cut stem was rinsed with 2 ml of distilled water and dried with a paper towel to remove the content from cut cells and the first exuded sap. Xylem sap spontaneously oozing from the stem was recovered after discarding the first two drops. Collection tubes were placed on ice and the sap collected for up to 6 h. Xylem sap was filtered through a 0.2 μm pore filter and kept frozen at −20°C until used.

ANALYSIS OF AMINOACID AND SUGAR CONTENTS

Apoplastic and xylem samples (10 ml each) both before and after bacterial growth, were analyzed for their amino acid content by cation exchange chromatography at the Scientific and Technologic Centers from the University of Barcelona (CCITUB). The internal control (norleucine) was added to apoplast and xylem samples and then dried. Samples were resuspended in lithium citrate buffer at pH2.2 and then filtered and injected into the chromatography system (50–100 μl). An automated aminoacid autoanalyzer (Biochrom 30) was used. For sugar quantification, samples (100 μl) were filtered and injected into Aminex HPX-87P (300 × 7.8 mm) + Aminex HPX-87C (300 × 7.8 mm) (BioRad) serial columns in a Waters 717 plus autosampler chromatograph: refractive index Water 2414 at 37°C and $S = 256$. Bacterial content from apoplast and xylem was filtered using a Whatman FP 30/0.45 CA-S pore size 0.45 μm.

AUTHOR CONTRIBUTIONS

A. Paola Zuluaga performed the experiments, contributed to the experimental design, data analysis, data interpretation, manuscript writing and critical revision. Marina Puigvert performed the experiments and contributed with data analysis and interpretation. Marc Valls contributed to the experimental design, data analysis, data interpretation, drafting of the article and manuscript writing and critical revision.

ACKNOWLEDGMENTS

We thank Dr. S. Genin for kindly providing the mutant strains used in this work and N.S. Coll and C. Popa for interesting suggestions and critical reading of the manuscript. We also thank the Centres Científics i Tecnològics from the University of Barcelona (CCITUB) for technical support with sugar and aminoacid measurements. This work was supported by grants from Comissionat per Universitats i Recerca of the Generalitat de Catalunya (SGR0052 and CONES2010-0030) and from the Ministerio de Ciencia, Tecnología e Innovación of the Spanish Government (HF2008-0021 and AGL2010-21870).

SUPPLEMENTARY MATERIAL

The Supplementary Material for this article can be found online at: http://www.frontiersin.org/Journal/10.3389/fmicb.2013.00349/abstract

Table S1 | Description of mutant strains used in this work. All strains were kindly provided by Dr. S.Genin and transformed with the hrpG-lux in this work. Sp stands for streptomycin/spectinomycin resistance.

REFERENCES

Aldon, D., Brito, B., Boucher, C., and Genin, S. (2000). A bacterial sensor of plant cell contact controls the transcriptional induction of *Ralstonia solanacearum* pathogenicity genes. *EMBO J.* 19, 2304–2314. doi: 10.1093/emboj/19.10.2304

Ausubel, F. M., Brent, R., Kingston, R. E., Moore, D. D., Seidman, J. G., Smith, J. A., et al. (1994). *Current Protocols in Molecular Biology.* New York, NY: John Wiley and Sons.

Brencic, A., and Winans, S. C. (2005). Detection of and response to signals involved in host-microbe interactions by plant-associated bacteria. *Microbiol. Mol. Biol. Rev.* 69, 155–194. doi: 10.1128/MMBR.69.1.155-194.2005

Brito, B., Aldon, D., Barberis, P., Boucher, C., and Genin, S. (2002). A signal transfer system through three compartments transduces the plant cell contact-dependent signal controlling *Ralstonia solanacearum* hrp genes. *Mol. Plant Microbe Interact.* 15, 109–119. doi: 10.1094/MPMI.2002.15.2.109

Brito, B., Marenda, M., Barberis, P., Boucher, C., and Genin, S. (1999). prhJ and hrpG, two new components of the plant signal-dependent regulatory cascade controlled by PrhA in *Ralstonia solanacearum*. *Mol. Microbiol.* 31, 237–251. doi: 10.1046/j.1365-2958.1999.01165.x

Coll, N. S., and Valls, M. (2013). Current knowledge on the *Ralstonia solanacearum* type III secretion system. *Microb. Biotechnol.* 6, 614–620. doi: 10.1111/1751-7915.12056

Coplin, D. L., Sequeira, L., and Hanson, R. S. (1974). Pseudomonas solanacearum: virulence of biochemical mutants. *Can. J. Microbiol.* 20, 519–529. doi: 10.1139/m74-080

Genin, S., Brito, B., Denny, T. P., and Boucher, C. (2005). Control of the *Ralstonia solanacearum* Type III secretion system (Hrp) genes by the global virulence regulator PhcA. *FEBS Lett.* 579, 2077–2081. doi: 10.1016/j.febslet.2005.02.058

Genin, S., and Denny, T. P. (2012). Pathogenomics of the *Ralstonia solanacearum* species complex. *Ann. Rev. Phytopathol.* 50, 67–89. doi: 10.1146/annurev-phyto-081211-173000

Kehr, J., and Rep, M. (2007). "Protein extraction from xylem and phloem sap," in *Methods in Molecular Biology*, eds M. Z. H. Thiellement, C. Damerval, and V. Mechin (Totowa, NJ: Humana Press, Inc), 27–35.

Mansfield, J., Genin, S., Magori, S., Citovsky, V., Sriariyanum, M., Ronald, P., et al. (2012). Top 10 plant pathogenic bacteria in molecular plant pathology. *Mol. Plant Pathol.* 13, 614–629. doi: 10.1111/j.1364-3703.2012.00804.x

Marenda, M., Brito, B., Callard, D., Genin, S., Barberis, P., Boucher, C., et al. (1998). PrhA controls a novel regulatory pathway required for the specific induction of *Ralstonia solanacearum* hrp genes in the presence of plant cells. *Mol. Microbiol.* 27, 437–453. doi: 10.1046/j.1365-2958.1998.00692.x

Mole, B. M., Baltrus, D. A., Dangl, J. L., and Grant, S. R. (2007). Global virulence regulation networks in phytopathogenic bacteria. *Trends Microbiol.* 15, 363–371. doi: 10.1016/j.tim.2007.06.005

Monteiro, F., Genin, S., van Dijk, I., and Valls, M. (2012). A luminescent reporter evidences active expression of *Ralstonia solanacearum* type III secretion system genes throughout plant infection. *Microbiology* 158, 2107–2116. doi: 10.1099/mic.0.058610-0

Peeters, N., Guidot, A., Vailleau, F., and Valls, M. (2013). *Ralstonia solanacearum*, a widespread bacterial plant pathogen in the post-genomic era. *Mol. Plant Pathol.* 14, 651–662. doi: 10.1111/mpp.12038

Plener, L., Manfredi, P., Valls, M., and Genin, S. (2010). PrhG, a transcriptional regulator responding to growth conditions, is involved in the control of the type III secretion system regulon in *Ralstonia solanacearum*. *J. Bacteriol.* 192, 1011–1019. doi: 10.1128/JB.01189-09

Rico, A., and Preston, G. (2008). Pseudomonas syringae pv. tomato DC3000 uses constitutive and apoplast-induced nutrient assimilation pathways to catabolize nutrients that are abundant in the tomato apoplast. *Mol. Plant Microbe Interact.* 21, 269–282. doi: 10.1094/MPMI-21-2-0269

Saha, S., and Lindeberg, M. (2013). Bound to succeed: transcription factor binding site prediction and its contribution to understanding virulence and environmental adaptation in bacterial plant pathogens. *Mol. Plant Microbe Interact.* 26, 1123–1130. doi: 10.1094/MPMI-04-13-0090-CR

Schell, M. A. (2000). Control of virulence and pathogenicity genes of *Ralstonia Solanacearum* by an Elaborate Sensory Network. *Ann. Rev. Phytopathol.* 38, 263–292. doi: 10.1146/annurev.phyto.38.1.263

Sudakevitz, D., Imberty, A., and Gilboa-Gerber, N. (2002). Production, properties and specificity of a new bacterial L-fucose and D-arabinose-binding lectin of the plant aggressive pathogen *Ralstonia solanacearum*, and its comparison to related plant and microbial lectins. *J. Biochem.* 132, 353–358. doi: 10.1093/oxfordjournals.jbchem.a003230

Sudakevitz, D., Kostlanova, N., Blatman-Jan, G., Mitchell, E. P., Lerrer, B., Wimmerova, M., et al. (2004). A new *Ralstonia solanacearum* high-affinity mannose-binding lectin RS-IIL structurally resembling the *Pseudomonas aeruginosa* fucose-specific lectin PA-IIL. *Mol. Microbiol.* 52, 691–700. doi: 10.1111/j.1365-2958.2004.04020.x

Valls, M., Genin, S., and Boucher, C. (2006). Integrated regulation of the type III secretion system and other virulence determinants in *Ralstonia solanacearum*. *PLoS Pathog.* 2:e82. doi: 10.1371/journal.ppat.0020082

Vasse, J., Frey, P., and Trigalet, A. (1995). Microscopic studies of intercellular infection and protoxylem invasion of tomato roots by *Pseudomonas solanacearum*. *Mol. Plant Microbe Interact.* 8, 241–251. doi: 10.1094/MPMI-8-0241

Ward, J. L., Forcat, S., Beckmann, M., Bennett, M., Miller, S. J., Baker, J. M., et al. (2010). The metabolic transition during disease following infection of Arabidopsis thaliana by *Pseudomonas syringae* pv. tomato. *Plant J.* 63, 443–457. doi: 10.1111/j.1365-313X.2010.04254.x

Yoshimochi, T., Hikichi, Y., Kiba, A., and Ohnishi, K. (2009a). The global virulence regulator PhcA negatively controls the *Ralstonia solanacearum* hrp regulatory cascade by repressing expression of the PrhIR signalling proteins. *J. Bacteriol.* 191, 3424. doi: 10.1128/JB.01113-08

Yoshimochi, T., Zhang, Y., Kiba, A., Hikichi, Y., and Ohnishi, K. (2009b). Expression of hrpG and activation of response regulator HrpG are controlled by distinct signal cascades in *Ralstonia solanacearum*. *J. Gen. Plant Pathol.* 75, 196–204. doi: 10.1007/s10327-009-0157-1

Zhang, Y., Chen, L., Yoshimochi, T., Kiba, A., Hikichi, Y., and Ohnishi, K. (2013). Functional analysis of *Ralstonia solanacearum* PrhG regulating the hrp regulon in host plants. *Microbiology* 159(Pt 8), 1695–1704. doi: 10.1099/mic.0.067819-0

Conflict of Interest Statement: The authors declare that the research was conducted in the absence of any commercial or financial relationships that could be construed as a potential conflict of interest.

Received: 26 August 2013; accepted: 04 November 2013; published online: 20 November 2013.

*Citation: Zuluaga AP, Puigvert M and Valls M (2013) Novel plant inputs influencing Ralstonia solanacearum during infection. Front. Microbiol. **4**:349. doi: 10.3389/fmicb.2013.00349*

This article was submitted to Plant-Microbe Interaction, a section of the journal Frontiers in Microbiology.

Cell Death and Differentiation (2014) 21, 1399–1408

www.nature.com/cdd

The plant metacaspase AtMC1 in pathogen-triggered programmed cell death and aging: functional linkage with autophagy

NS Coll*[,1,2], A Smidler[1,8], M Puigvert[2], C Popa[2], M Valls[2,3] and JL Dangl[1,4,5,6,7]

Autophagy is a major nutrient recycling mechanism in plants. However, its functional connection with programmed cell death (PCD) is a topic of active debate and remains not well understood. Our previous studies established the plant metacaspase AtMC1 as a positive regulator of pathogen-triggered PCD. Here, we explored the linkage between plant autophagy and AtMC1 function in the context of pathogen-triggered PCD and aging. We observed that autophagy acts as a positive regulator of pathogen-triggered PCD in a parallel pathway to AtMC1. In addition, we unveiled an additional, pro-survival homeostatic function of AtMC1 in aging plants that acts in parallel to a similar pro-survival function of autophagy. This novel pro-survival role of AtMC1 may be functionally related to its prodomain-mediated aggregate localization and potential clearance, in agreement with recent findings using the single budding yeast metacaspase YCA1. We propose a unifying model whereby autophagy and AtMC1 are part of parallel pathways, both positively regulating HR cell death in young plants, when these functions are not masked by the cumulative stresses of aging, and negatively regulating senescence in older plants.
Cell Death and Differentiation (2014) **21,** 1399–1408; doi:10.1038/cdd.2014.50; published online 2 May 2014

An emerging theme in cell death research is that cellular processes thought to be regulated by linear signaling pathways are, in fact, complex. Autophagy, initially considered merely a nutrient recycling mechanism necessary for cellular homeostasis, was recently shown to regulate cell death, mechanistically interacting with components that control apoptosis. Deficient autophagy can result in apoptosis[1–3] and autophagy hyper-activation can also lead to programmed cell death (PCD).[4] In addition, the pro-survival function of autophagy is mediated by apoptosis inhibition and apoptosis mediates autophagy, although this cross-regulation is not fully understood.[5]

In plants, autophagy can also have both pro-survival and pro-death functions. Autophagy-deficient plants exhibit accelerated senescence,[6–8] starvation-induced chlorosis,[6,7,9] hypersensitivity to oxidative stress[10] and endoplasmic reticulum stress.[11] Further, autophagy-deficient plants cannot limit the spread of cell death after infection with tissue-destructive microbial infections.[12,13] The plant phytohormone salicylic acid (SA) mediates most of these phenotypes.[8] Autophagy has an essential, pro-survival role in situations where there is an increasing load of damaged proteins and organelles that need to be eliminated, that is, during aging or stress. Autophagy has an opposing, pro-death role during developmentally regulated cell death[14,15] or during the pathogen-triggered hypersensitive response PCD (hereafter, HR) that occurs locally at the site of attempted pathogen attack.[16,17] The dual pro-death/pro-survival functions of plant autophagy remain a topic of active debate.

Also under scrutiny are possible novel functions of caspases and caspase-like proteins as central regulators of pro-survival processes. Caspases were originally defined as executioners of PCD in animals, but increasing evidence indicates that several caspases have non-apoptotic regulatory roles in cellular differentiation, motility and in the mammalian immune system.[18–20]

Yeast, protozoa and plants do not have canonical caspases, despite the occurrence of morphologically heterogeneous PCDs.[21] More than a decade ago, distant caspase homologs termed metacaspases were identified in these organisms using structural homology searches.[22] Metacaspases were classified into type I or type II metacaspases based on the presence or absence of an N-terminal prodomain, reminiscent of the classification in animals into initiator/inflammatory or executioner caspases, respectively. Despite the architectural analogy between caspases and metacaspases, differences in their structure, function, activation and mode of action exist.[23–25]

Metacaspases mediate PCD in yeast,[26–31] leishmania,[32,33] trypanosoma[34] and plants.[24] We demonstrated that two type I metacaspases, AtMC1 and AtMC2, antagonistically regulate HR in *Arabidopsis thaliana*.[35] Our work showed that AtMC1 is

[1]Department of Biology, University of North Carolina, Chapel Hill, NC 27599, USA; [2]Centre for Research in Agricultural Genomics, Barcelona, Spain; [3]Department of Genetics, Universitat de Barcelona, Barcelona, Spain; [4]Howard Hughes Medical Institute, University of North Carolina, Chapel Hill, NC 27599, USA; [5]Curriculum in Genetics and Molecular Biology, University of North Carolina, Chapel Hill, NC 27599, USA; [6]Department of Microbiology and Immunology, University of North Carolina, Chapel Hill, NC 27599, USA and [7]Carolina Center for Genome Sciences University of North Carolina, Chapel Hill, NC, USA
*Corresponding author: NS Coll, Centre for Research in Agricultural Genomics, Campus UAB, Edifici CRAG, Bellaterra 08193, Barcelona, Spain. Tel: +34 93 5636600; Fax: +34 93 5636601; E-mail: nuria.sanchez-coll@cragenomica.es
[8]Current address: Department of Immunology and Infectious Diseases, Harvard School of Public Health, Boston, MA 02115, USA.
Abbreviations: PCD, programmed cell death; HR, hypersensitive response cell death; SA, salicylic acid; ROS, reactive oxygen species; FB1, fumonisin B1; NLR, nucleotide-binding domain and leucine-rich repeat containing; BTH, benzo(1,2,3)thiadiazole-7-carbothioic acid *S*-methyl ester
Received 06.2.14; revised 11.3.14; accepted 13.3.14; Edited by G Salvesen; published online 02.5.14

a positive regulator of HR and that this function is mediated by its catalytic activity and negatively regulated by the AtMC1 N-terminal prodomain. AtMC2 antagonizes AtMC1-mediated HR.

Besides AtMC2, new examples of metacaspases with a pro-life/non-PCD role are emerging. Protozoan metacaspases are involved in cell cycle dynamics[34,36–38] and cell proliferation.[39] The yeast metacaspase Yca1 alters cell cycle dynamics[40] and interestingly, is required for clearance of insoluble protein aggregates, thus contributing to yeast fitness.[41]

Here, we explore the linkage between plant autophagy and AtMC1 function in the context of pathogen-triggered HR and aging. Our data support a model wherein autophagy and AtMC1 are part of parallel pathways, both positively regulating HR cell death in young plants and negatively regulating senescence in older plants.

Results

Autophagy components and AtMC1 act additively to positively regulate HR. Autophagy is induced by activation of plant intracellular NLR (nucleotide-binding domain and leucine-rich repeat containing) immune receptors upon pathogen recognition, and thus can be a positive regulator of HR in Arabidopsis young leaves.[16,17] To ascertain whether AtMC1- and autophagy-mediated HR are part of the same pathway, we crossed Arabidopsis *atmc1* knockout plants[35] to two different autophagy-deficient knockout mutants: *atg5*[42] and *atg18a*.[13] ATG5 and ATG18a are each required for autophagosome formation at different points of the autophagic pathway.[7,43] We infected 2-week-old wild-type Col-0, *atmc1*, *atg5*, *atg18a*, *atmc1 atg5* and *atmc1 atg18a* plants with *Pseudomonas syringae* pathovar tomato strain (*Pto* DC3000 expressing the type III effector *avrRpm1 Pto* DC3000(*avrRpm1*)). Recognition of AvrRpm1 triggers HR mediated by the intracellular NLR receptor RPM1.[44] We quantified HR using a single-cell death assay,[35] and we observed suppression of RPM1-mediated HR both in *atmc1*[35] and in autophagy-deficient mutant plants. When combined, autophagy and *atmc1* deficiencies had an additive effect on HR suppression (Figure 1a). Thus, autophagy and AtMC1 mediate independent pathways triggered by NLR activation that contribute to HR.

Using the same assay, we observed that the lack of AtMC2, a negative regulator of AtMC1-mediated HR cell death,[35] has no effect on autophagy-mediated HR cell death (Supplementary Figure 1). In *atmc1* and autophagy-deficient mutants, HR suppression does not result in increased susceptibility to *Pto* DC3000(*avrRpm1*), uncoupling HR and pathogen growth restriction.[35] Thus, the additive HR suppression in *atmc1 atg18a* double mutants did not result in enhanced pathogen proliferation (Figure 1b).

We also investigated whether *atmc1* mutants were defective in autophagy. Figure 1c and Supplementary Figure 2 show Col-0 and *atmc1* transgenic plants expressing the autophagosome marker GFP-ATG8a with or without concanamycin A treatment.[43] Plants lacking *atg18a* (or *atg5*) are defective in autophagosome formation.[10,17,43] *Atmc1* mutants displayed normal autophagosome formation (Figure 1c).

Recently, the plant cargo receptor NBR1 was demonstrated to be a selective autophagy marker that constitutively over-accumulates in autophagy-deficient plants.[45] We performed immunoblot analysis of mock- or *Pto* DC3000 (*avrRpm1*)-treated plants using anti-NBR1 antisera to address whether selective autophagy was induced during HR. We observed slightly increased NBR1 accumulation 12-h post-inoculation in all lines tested (Figures 1d and e), indicating that selective autophagy is not induced after RPM1 activation at a time point when the HR cell death is complete (Figure 1). *Atmc1* plants expressed wild-type NBR1 levels in either uninfected controls or following RPM1 activation, indicating that AtMC1 deficiency alone did not result in NBR1-mediated selective autophagy defects. As expected, *atg18a* and *atmc1 atg18a* mutants express higher NBR1 levels than wild-type plants because of defective selective autophagy.[45] This NBR1 over-accumulation is more pronounced in *atmc1 atg18* double mutants, indicating that AtMC1 may have a role in selective autophagy when bulk autophagy is defective.

SA accumulation negatively regulates the contribution of autophagy, but not of AtMC1, to RPM1-mediated HR. SID2 encodes the chloroplastic isochorismate synthase 1, the rate-limiting SA biosynthetic enzyme required for the increased accumulation of this phytohormone observed following pathogen recognition.[46] To investigate if the HR suppression phenotypes observed in young autophagy- and *atmc1*-deficient plants were SA dependent, we quantified HR in wild-type, *atmc1*, *atg18a, sid2*, *atmc1 atg18a*, *atmc1 sid2* and *atg18a sid2* and *atmc1 atg18a sid2* plants (Figure 2). *Sid2* plants supported wild-type HR cell death levels, indicating that SA accumulation is dispensable for RPM1-mediated HR.[47] Interestingly, we observed that the loss of SA accumulation restores nearly wild-type levels of HR in *atg18a*, but not in *atmc1* plants (Figure 2). This suggests that SA accumulation negatively regulates the contribution of autophagy to RPM1-mediated HR in *atg18a sid2*, but does not significantly regulate the AtMC1 contribution in *atmc1 sid2*. This observation also reinforces our hypothesis that autophagy and AtMC1 participate in separate HR signaling pathways. In *atmc1 atg18a sid2* plants, the lack of SA accumulation reverts only partially HR suppression, indicating that the additive effects on HR observed in *atmc1 atg18a* cannot be solely explained by the sum of both deficiencies. It is worth noting that at the developmental stage used for the single-cell HR assay, *atmc1*, *atg18a* and *atmc1 atg18a* expressed essentially equivalent basal SA levels (Supplementary Figure 3).

The plant respiratory burst NADPH oxidase encoded by AtrbohD is required for the reactive oxygen species (ROS) burst downstream of RPM1 activation, but contributes only modestly to regulation of RPM1-mediated HR (Supplementary Figure 4).[48] Consistent with these data, the lack of an NADPH-dependent ROS burst did not alter HR suppression in *atmc1*, *atg18a* or *atmc1 atg18a* mutants (Supplementary Figure 4), indicating that this ROS burst acts independently or upstream of AtMC1 and autophagy.

Autophagy components and AtMC1 act additively to negatively regulate senescence. Autophagy-deficient plants exhibit an early senescence phenotype, evidenced by premature leaf chlorosis.[6–9] Interestingly, *atmc1* mutants

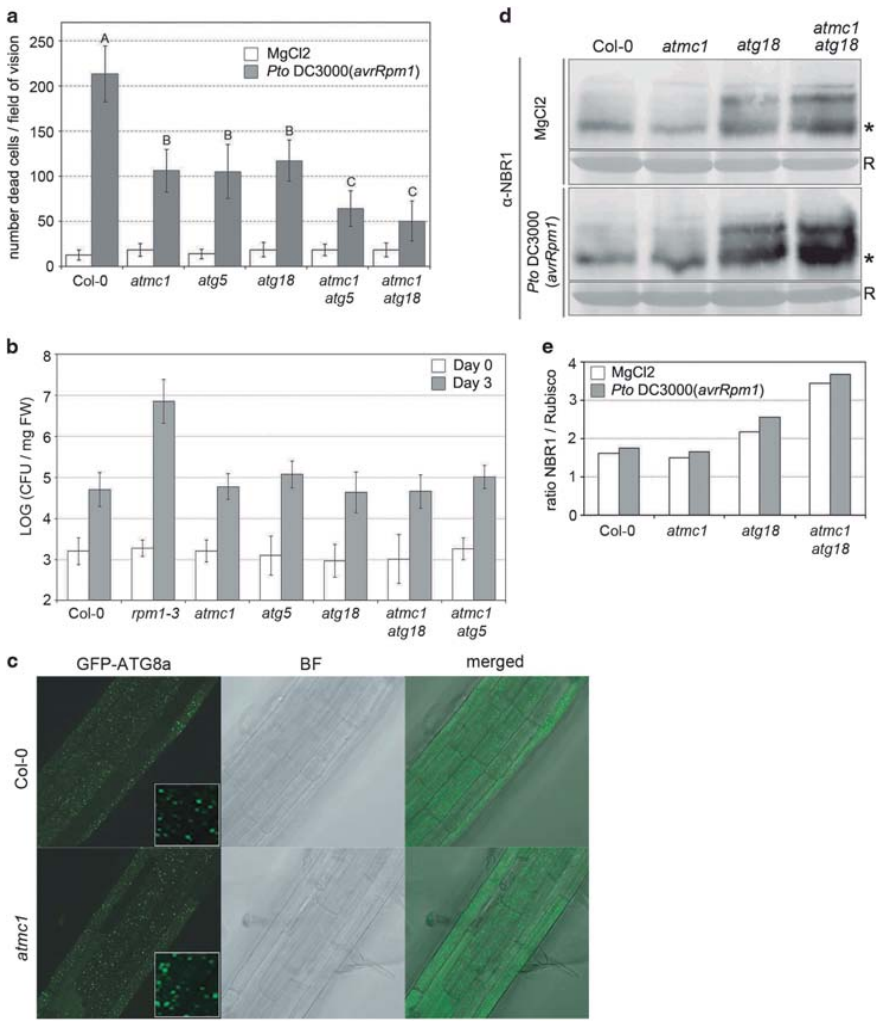

Figure 1 Autophagy components and AtMC1 act additively to positively regulate HR. (**a**) Two-week-old plants of the indicated phenotypes were vacuum infiltrated with 500 000 colony-forming units (CFU)/ml of *Pto* DC3000(*avrRpm1*) or $MgCl_2$. After 12 h, plants were stained with the cell death dye Trypan blue. To quantify cell death, all dead cells per field of vision ($\times$ 10 magnification) were counted. Values correspond to the average of 20 leaves per genotype and treatment $\pm$ 2 $\times$ S.E. Letters indicate a significant difference following post-ANOVA Student's *t*-test ($\alpha = 0.05$). The experiment is representative of three independent replicates. (**b**) Two-week-old plants of the indicated phenotypes were dip inoculated with 2.5×10^7 CFU/ml of *Pto* DC3000(*avrRpm1*). Bacterial growth was monitored at days 0 and 3 after infection. Values indicate the average of four samples per genotype $\pm$ 2 $\times$ S.E. The experiment was repeated three times. (**c**) One-week-old transgenic Col-0 and *atmc1* plants constitutively expressing GFP-ATG8 were treated with 1 μM concanamycin A to allow autophagosome visualization in the vacuole of root cells using confocal microscopy. BF, bright field. Inlets show $\times$ 16 magnifications of the central part of each root shown. (**d**) Western blot analysis of the NBR1 cargo receptor protein using plants of the noted genotypes treated as in (**a**). The band corresponding to NBR1 is marked with an asterisk. Coomassie-stained Rubisco (R) was used as a loading control. (**e**) Densitometry analysis of the samples in (**d**) using Multi Gauge (Fujifilm, ScienceLab 2005, version 3.0, Minato, Tokyo, Japan)

also senesce prematurely (Figure 3a). In *atmc1 atg18a*, this early senescence phenotype is enhanced and progresses faster than in either Col-0, *atmc1* or *atg18a* plants (Supplementary Figure 5). These observations indicate that similar to autophagy, AtMC1 is also required for correctly timed leaf senescence and that autophagy and AtMC1 act additively on these processes.

Quantitative PCR analysis using the senescence marker *SAG12*[49] confirmed the early senescence phenotype in 5-week-old *atmc1*, *atg18a* and *atmc1 atg18a* plants at the

transcriptional level (Figure 3b). We did not detect any differences in *SAG12* expression in 2-week-old plants. This indicates that the HR suppression phenotypes observed in *atmc1*, *atg18a* and *atmc1 atg18a* mutants cannot be explained by the early senescence onset, which occurs later.

Early senescence in autophagy-deficient plants, but not in *atmc1* plants, requires SA accumulation. It was previously shown that the onset of early senescence and growth retardation in autophagy-deficient plants is correlated with SA hyper-accumulation.[8] We confirmed and extended this result, showing that the lack of SA accumulation in *sid2 atg18a* largely reverts the early senescence phenotype of *atg18* (Figure 3a). In contrast, AtMC1-regulated senescence processes occur independently of SA accumulation, as evidenced by the *sid2 atmc1* early senescence phenotype. In addition, the fact that the lack of SA cannot fully revert the extreme early senescence phenotype of *atmc1 atg18a* indicates that the additive effects on this phenotype cannot be solely explained by the sum of both deficiencies and that other – yet unknown – factors likely mediate this additivity.

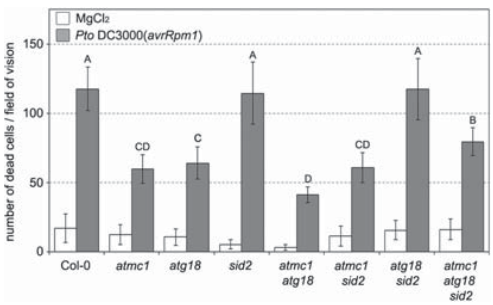

Figure 2 SA accumulation negatively regulates the autophagy contribution to RPM1-mediated HR, but does not significantly regulate the AtMC1 contribution. Two-week-old plants of the indicated phenotypes were vacuum infiltrated with 500 000 colony-forming units (CFU)/ml of *Pto* DC3000(*avrRpm1*) or $MgCl_2$. After 12 h, plants were stained with the cell death dye Trypan blue. To quantify cell death, all dead cells per field of vision ($\times$ 10 magnification) were counted. Values indicate the average of 20 samples per genotype and treatment $\pm 2 \times$ S.E. Letters indicate a significant difference following post-ANOVA Student's *t*-test ($\alpha = 0.05$). The experiment is representative of three independent replicates

***atmc1* and *atg18a* mutants are hypersensitive to the SA agonist BTH and to externally generated ROS.** We next treated *atmc1*, *atg18a* and *atmc1 atg18a* with either the SA agonist benzo(1,2,3)thiadiazole-7-carbothioic acid *S*-methyl ester (BTH) or different ROS-generating agents. BTH treatment resulted in leaf chlorosis in both *atmc1* and *atg18a*, and this phenotype was enhanced in *atmc1 atg18a* but not in wild-type plants (Figure 4a). Leaf chlorosis was accompanied by increased ROS production and cell death (Figures 4b and c). The phenotype caused by BTH on these plants, grown under short-day conditions, is reminiscent of untreated plants grown 4 weeks under short-day conditions and then transferred to long-day conditions (Figure 3a). This suggests that light-dependent increases in SA accumulation trigger autophagy and AtMC1-mediated processes important for the proper remobilization of resources to reach a timely senescence.

To study the effect of ROS on autophagy or *AtMC1*-regulated processes, plants were treated with rose bengal, methyl viologen or the fungal toxin fumonisin B1 (FB1) and cell death progression was visualized using Trypan blue (Figures 4d and e). Methyl viologen treatment resulted in confined cell death in wild-type plants, modestly enhanced cell death in *atmc1* and *atg18a*, and runaway cell death in *atmc1 atg18a*. These results suggest that both AtMC1 and autophagy have a function in downregulating the toxicity of ROS. Similar results were observed using rose bengal and FB1 as ROS accumulation triggers (Figure 4b). Together, these results indicate that the primary roles of autophagy and AtMC1 in older plants may be to protect the cells against the consequences of increasing ROS and SA levels during aging. Furthermore, aging autophagy- and *atmc1*-deficient plants cannot restrict cell death caused by the necrotrophic fungus *Botrytis cinerea* (Supplementary Figure 6).[50] We infer from these results that autophagy and AtMC1 also act additively to limit cell death following necrotroph infection.

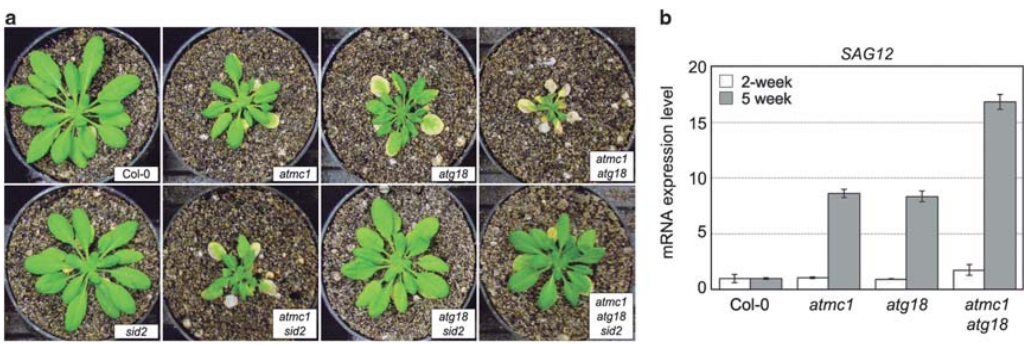

Figure 3 Autophagy components and AtMC1 act additively to negatively regulate senescence. (**a**) Early senescence was SA-dependent in autophagy-deficient plants but SA-independent in *atmc1* mutants. Pictures show plants grown for 3 weeks under short-day conditions and then transferred to long-day conditions for 4 additional weeks. (**b**) Quantitative real-time PCR analysis of the senescence marker gene SAG12 in 2- and 5-week-old plants of the indicated genotypes, normalized to EF-1α. The S.E. was calculated from three samples per genotype and the experiment was performed three times

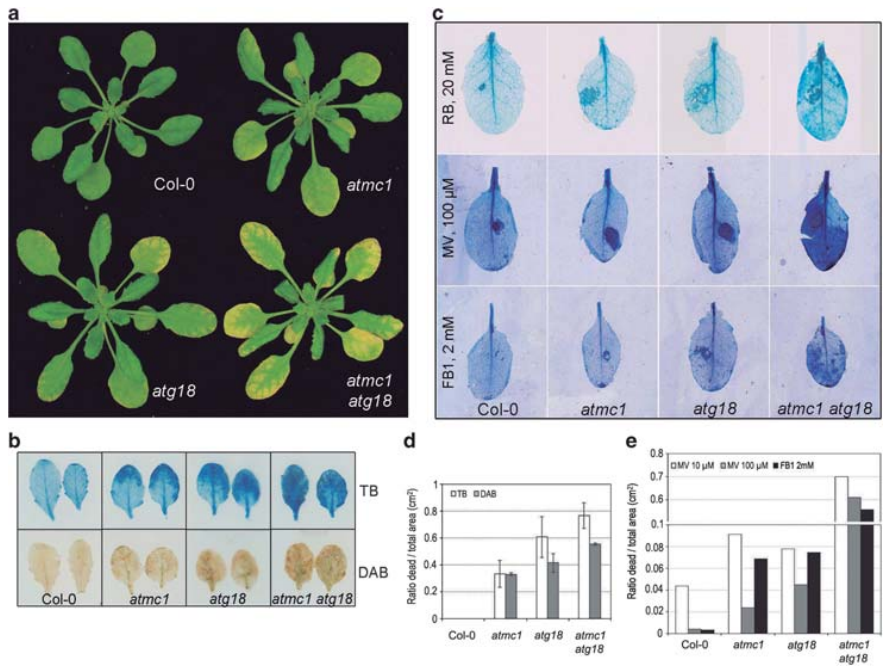

Figure 4 *Atmc1* and *atg18a* mutants are hypersensitive to the SA agonist BTH and to externally generated ROS. (**a**) Pictures of representative 4-week-old plants grown under short-day conditions, 4 days after 300 μM BTH treatment. (**b**) Representative leaves of plants treated as in (**a**) were stained with Trypan blue (TB, upper panel) or with 3,3-diamino-benzidine (DAB, lower panel) to visualize cell death and H_2O_2 accumulation, respectively. (**c**) Quantification of cell death and H_2O_2 accumulation in (**b**) by measuring the stained area (excluding the central vein) relative to the whole area of the leaf. (**d**) Pictures of representative 4-week-old plants 24 h after treatment with the ROS donors rose bengal (RB), methyl viologen (MV), the fungal toxin FB1, stained with Trypan blue to visualize cell death. (**d** and **e**) Quantification of cell death in (**d**) performed as in (**c**)

A fraction of full-length AtMC1 localizes to insoluble aggregates. The budding yeast *Saccharomyces cerevisiae* expresses a single type I metacaspase (Yca1), which mediates catalytic site-dependent PCD in this organism.[26–31] However, Yca1 also can be localized to insoluble protein aggregates where it promotes aggregate clearance independent of the Yca1 catalytic site.[41] Yca1 localization in protein aggregates is mediated by its N-terminal putative prodomain. We hypothesized that AtMC1 may also target protein aggregates and mediate its clearance, independent of its pro-death role during HR. Such a function could explain the early senescence and ROS/SA hypersensitivity of *atmc1* plants. Furthermore, it could account for the observed enhancement of the SA and ROS sensitivity phenotypes of *atmc1 atg18a*, since those plants would lack two complementary pro-life processes required to cope with the strains of aging.

We studied AtMC1 subcellular localization in plants conditionally overexpressing AtMC1-HA (Figure 5a).[35] Total protein extract (T) contained equal amounts of full-length and cleaved, presumably active AtMC1 (Figure 5a, left). Most of the cleaved AtMC1 localized in the soluble fraction (S), whereas full-length AtMC1 was also present in the microsomal/insoluble fraction (M + A). Subsequent solubilization of the microsomal/insoluble fraction revealed that AtMC1, in particular the full-length form, was insoluble (A). This indicates that a fraction of full-length AtMC1 likely localizes to insoluble protein aggregates. We performed the same fractionation using plants expressing the catalytic dead version of AtMC1 (AtMC1-C99A-C220A-HA).[35] The catalytic dead AtMC1 protein remained mostly insoluble. Taken together, these data indicate that at least part of the full-length AtMC1 localizes to insoluble aggregates independently of its catalytic activity, similar to yeast Yca1.

We also tested AtMC1 localization when expressed under the control of its native promoter (*atmc1 pAtMC1::AtMC1-HA*) using untreated or pathogen-treated young plants and older plants. Figure 5b shows that natively expressed AtMC1 protein accumulation is induced by pathogen-triggered HR cell death and aging. As expected, AtMC1 aggregate localization reaches its maximum in aging plants.

Subsequently, we analyzed aggregate content in Col-0, *atmc1*, *atg18a* and *atmc1 atg18a* under basal (Figure 5d), pathogen-induced cell death and aging conditions using the total and soluble fractions as a loading control (Figure 5c). Early senescing *atmc1* and *atg18a* mutants showed a higher aggregate content than wild-type plants. In *atmc1 atg18a* plants, aggregate over-accumulation was even more marked as expected from their additive phenotypes (Figure 5d). We hypothesize that localization mediates clearance of insoluble

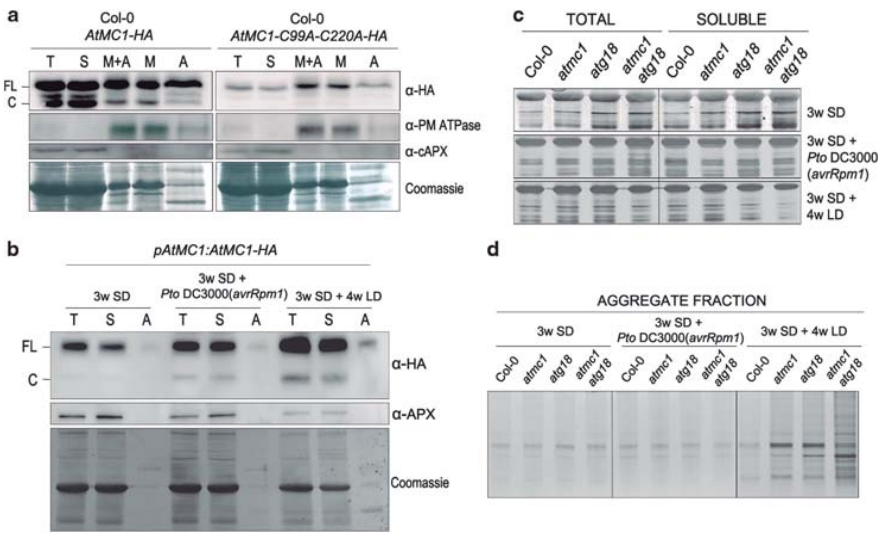

Figure 5 A fraction of full-length AtMC1 localizes to insoluble aggregates independent of its catalytic activity, contributing to aggregate clearance. (**a**) Protein extracts of 4-week-old Col-0 plants conditionally overexpressing AtMC1-HA (left) and AtMC1-C99AC220A-HA (right) were subjected to cellular fractionation. Total protein extract (T) was fractionated into a supernatant containing the soluble proteins (S) and a pellet, containing microsomal proteins and aggregates (S + A). This pellet was further fractionated into a supernatant, containing most of the microsomal proteins (M), and a pellet, containing insoluble protein aggregates (A). After separation on an SDS-PAGE gel, the fractions were either Coomassie-stained or analyzed by immunoblot using anti-HA, anti-cytosolic ascorbate peroxidase (cAPX) and anti-plasma membrane (PM) H^+ ATPase. The HA antibody recognized full-length AtMC1 (FL) and cleaved, putatively active AtMC1 (C). (**b**) *atmc1 pAtMC1::AtMC1-HA* plants were grown for 3 weeks under short-day conditions (3w SD), treated with 500 000 CFU/ml of *Pto* DC3000(*avrRpm1*) (3w SD + *Pto* DC3000(*avrRpm1*)) or transferred to long-day conditions (3w SD + 4w LD) and western blot analysis using anti-HA antibody or anti-cAPX was performed after fractionation into total (T), soluble (S) and insoluble aggregate (A) fractions. (**c** and **d**) Silver stains of total, soluble (**c**) and insoluble aggregate fractions (**d**) of plants of the indicated genotypes treated as in (**b**)

aggregates and thus contributes to cellular homeostasis and stress responses in a process that acts genetically in parallel to autophagy. This function is independent of, and does not preclude, the pro-death catalytic activity-dependent function of AtMC1 during HR cell death, which is most evident in young, non-stressed tissues.

Discussion

Autophagy and AtMC1 act in separate pathways as positive regulators of pathogen-triggered HR cell death. We previously demonstrated that AtMC1 is a positive regulator of HR cell death triggered by activation of different plant intracellular NLR innate immune receptors.[35] A similar pro-death function was reported for autophagy.[16,17] These findings were in sharp contrast to other studies, where autophagy was proposed as a pro-survival mechanism during HR cell death in plants.[8,51,52] These apparent discrepancies can be reconciled in a model where autophagy has a pro-death role locally in the HR site, whereas in the surrounding uninfected tissue, autophagy promotes survival, protecting cells beyond the HR site from unnecessary damage.[53,54] Signaling gradients that establish cell death control borders at sites of pathogen recognition have been demonstrated in plants.[48,55–58] Importantly, the studies that reported a pro-survival role of autophagy during pathogen-triggered HR cell death used relatively old plants.[8,51,52] With age, autophagy mutants become prematurely senescent and accumulate high levels of ROS that can drive accumulation of SA, potentially increasing their vulnerability to ER stress. Activation of defense responses upon infection may further destabilize the already altered homeostasis in autophagy mutants, rendering them unable to restrict cell death. Consistent with this proposal, prevention of SA accumulation suppresses premature senescence and runaway cell death after pathogen infection in *atg5*.[8]

We therefore assayed young autophagy mutant plants treated with low-dose bacterial inocula more closely mimicking natural infections to avoid the unwanted effects of combinatorial stresses. Our data confirm previous findings defining autophagy as a positive regulator of HR.[16,17] Autophagy and AtMC1 act separately to contribute to HR, as evidenced by the further suppression of cell death in *atmc1 atg18a*. However, the independent pathways thus defined cannot account for full HR, as cell death suppression in the double mutant is incomplete. Hence, there must exist (an)other pathway(s), which account for the remaining HR.

The idea that AtMC1 and autophagy function in separate pathways during HR is supported by the fact that they are differentially regulated. The metacaspase AtMC2 negatively regulates AtMC1[35] but not autophagy. SA mediates the pro-death function of autophagy, but not of AtMC1. In fact, SA is a negative regulator of the combined contributions to HR regulated by AtMC1 and undefined contributors to HR, as

illustrated by the nearly complete recovery of HR in *atg18a sid2* and the partial recovery of HR in *atmc1 atg18a sid2.* The recovery of HR in *atg18a sid2* is not due to altered basal SA levels in these mutants. Our data are in agreement with previous findings establishing that SA can act as a negative regulator of HR.[59] Furthermore, our results are consistent with the idea that autophagy can be both a positive and a negative regulator of HR depending on the spatio-temporal context (HR site *versus* adjacent tissues or young *versus* old tissue).[17,54] Finally, our data also show that HR suppression phenotypes in *atmc1*, *atg18a* and *atmc1 atg18a* is not accompanied by altered bacterial growth in any of these lines, further decoupling HR from pathogen growth restriction.[35]

The suppressed cell death phenotype in plants lacking AtMC1 is not due to defective autophagy. In order to explore the role of selective autophagy in pathogen-triggered HR and the possible linkage of AtMC1 to this process, we used the recently identified NBR1 autophagosome cargo protein marker.[45] Autophagy-deficient mutants accumulate higher NBR1 basal levels than wild-type,[45] which are further increased during the HR onset after RPM1 activation. This indicates that NBR1-mediated degradation of target proteins by autophagy may have an important role in HR cell death, perhaps contributing to vacuolar collapse.

Autophagy and AtMC1 independently control timely senescence in aging plants. Considering that autophagy has a main role in nutrient recycling,[6,7,9] it is not surprising that autophagy-deficient plants are prematurely senescent.[6–8] Furthermore, SA levels increase during senescence; this increase has been proposed to accelerate senescence once initiated.[60] Autophagy mutants start accumulating SA at an earlier developmental stage than the wild-type[8,13] and this over-accumulation underlies their premature senescent phenotype, as SA removal in these mutants results in normal timing of senescence.[8]

Besides its role in senescence, SA, in conjunction with ROS, is a potent defense regulator during infection.[61,62] Treatment with the SA analog BTH causes chlorosis, ROS hyper-accumulation and cell death in autophagy-deficient plants, but not in wild-type plants. This hypersensitivity could result from accumulation of damaged proteins and organelles in these plants because of impaired autophagy-dependent recycling, which renders them less able to cope with further stress. Like autophagy-deficient plants, *atmc1* plants are prematurely senescent and hypersensitive to BTH, ROS and necrotrophic fungi. In *atmc1 atg18a* plants, this phenotype is enhanced, indicating that the proteins act independently to downregulate these responses. Thus, AtMC1 has an additional, pro-survival homeostatic function in aging plants that acts in parallel to a similar pro-survival function of autophagy in aging.

A possible role of AtMC1 in protein aggregate clearance. Our data show that a fraction of the total full-length AtMC1 localizes to insoluble protein aggregates and this accumulation increases with age. Similar to yeast, aggregate localization of AtMC1 is also mediated by its N-terminal prodomain, and AtMC1 localization to protein aggregates does not require its catalytic activity. Furthermore, *atmc1* and *atg18a* plants, and to a further extent *atmc1 atg18a*, over-accumulate insoluble protein aggregates with age, which may be the cause of their premature senescence. The observed additive effects corroborate our notion that both pathways act independently to restrict insoluble protein aggregate accumulation.

Our hypothesis that AtMC1 functions in aggregate clearance is supported by the autophagy-like phenotypes of aging *atmc1* null mutants: premature senescence and ROS hypersensitivity AtMC1-mediated aggregate clearance and autophagy could constitute two complementary processes controlling cellular homeostasis during stress responses and aging by virtue of their ability to eliminate accumulated cellular debris.

A proposed model integrating the dual pro-death/pro-survival functions of AtMC1 and autophagy at different developmental stages. In young plants, we defined pro-death functions for autophagy and AtMC1 in HR control, as these functions were not masked by the cumulative stresses of aging. Figure 6a schematically shows a young plant cell undergoing HR after pathogen recognition. Under basal conditions, AtMC1 activation is prevented by the action of several negative regulators (AtMC2, LSD1[35] and probably other, unknown). Pathogen recognition leads to activation of intracellular NLR innate immune receptors, which results in local HR. In these circumstances, AtMC1 contributes to HR. Alternatively, enhanced auto-processing or processing by other metacaspases may contribute to accumulation of active AtMC1 in the cell. We speculate that the pro-death function of autophagy could be mediated by an active overload of the vacuole because of autophagy induction during HR, ultimately leading to vacuolar lysis. Interestingly, it has been recently reported that in Norway spruce the programmed vacuolar cell death that normally occurs in the

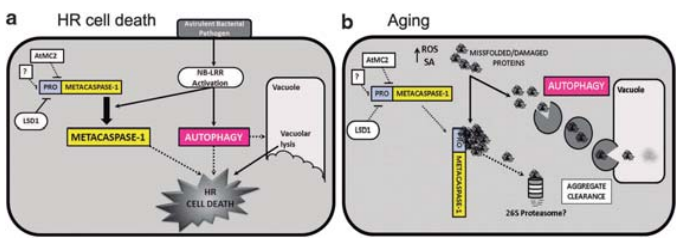

Figure 6 Proposed model integrating the dual pro-death/pro-survival functions of AtMC1 and autophagy at different developmental stages. (**a**) Pro-death functions of autophagy and AtMC1 in HR control in young plants. (**b**) Pro-survival role of autophagy and AtMC1 in aging cells

embryo suspensor requires autophagy, which lies downstream of a type II metacaspase,[15] indicating that the interactions between the various cell death regulators may vary depending on the cellular scenario.

In aging cells, the pro-survival functions of AtMC1 and autophagy are revealed by the constant increase of damaged proteins and organelles that accumulate in the cell and require clearance (Figure 6b). In this developmental scenario, autophagy is induced to clear aggregates via their autophagosome-mediated delivery to the vacuole. We hypothesize that AtMC1 also contributes to this process by independently targeting aggregates and facilitating their degradation. Our genetic framework sets the stage for the elucidation of these mechanisms.

Materials and Methods

Plant materials and growth. All experiments were performed using *Arabidopsis thaliana* accession Col-0. Single mutant lines have been previously described elsewhere: *atmc1* and *atmc2*,[35] *atg5* (SALK_020601),[42] *atg18a* (GABI651D08),[13] *atrbohD*,[59] *rpm1-3*[63] and *sid2/eds16*.[46] Transgenic Col-0 *35S::GFP-ATG8a* plants are described in Thompson *et al*.[43] and *atmc1 35S::GFP-ATG8a* plants were obtained by transformation using the floral dip method.[64]

Plants were grown under short-day conditions (9-h light, 21 °C; 15-h dark, 18 °C) for most experiments. To study senescence, plants were transferred to long-day conditions (15-h light, 21 °C; 8-h dark, 18 °C) 3 or 4 weeks after germination.

Cell death assay and bacterial growth. Single HR cell death events after infection with *Pto* DC3000(*avrRpm1*) were quantified according to Coll *et al*.[35]

Growth of *Pto* DC3000(*avrRpm1*) was tested using dip inoculations as previously described.[65]

Chemical treatments. Plants were grown 4 weeks under short-day conditions before treatment. For BTH treatment, plants were sprayed 300 μM BTH supplemented with 0.005% Silwett.

To monitor oxidative stress, a 2 μl drop of 100 μM Methyl viologen, a 10 μl drop of 2 mM rose bengal or a 5 μl drop of the necrotrophic fungal toxin FB1 were applied onto the abaxial surface of the leaf.

Stains. In order to visualize dead cells after chemical treatments, leaves were stained with Trypan blue as described.[66,67] H_2O_2 accumulation in leaves treated with BTH was visualized using 3,3′-diaminobenzidine staining as previously described.[59] To quantify cell death and H_2O_2 accumulation from the pictures, total leaf area and cell death or stained area was measured using ImageJ (Bethesda, MD, USA), and the ratio (area of cell death/ total leaf area) was calculated.

Infection with the necrotroph *Botrytis cinerea*. Five-week-old plants were sprayed with 1×10^6 spores/ml of *Botrytis cinerea*. Symptoms were visually followed for 1 week.

Total SA measurement. Total SA (free SA + glucose-conjugated SA, SAG) was measured as previously described,[68] using as starting material 100 mg of leaves from 2-week-old plants grown under short-day conditions (untreated).

RT-qPCR. Plant RNA was obtained from 2-week-old plants grown under short-day conditions or 5-week-old plants grown for 3 weeks under short-day and then transferred to long-day conditions. RNA was extracted using TRIzol (Life Technologies, Carlsbad, CA, USA) according to the manufacturer's instructions. RNA was treated 30 min with Ambion TURBO DNase (Life Technologies) to eliminate DNA contamination. Two microgram RNA was reverse transcribed using the Ambion RETROscript kit random decamers (Life Technologies).

RT-qPCR was performed using the Life Technologies SYBR Green PCR Master Mix in a total volume of 25 μl: 12.5 μl SYBR Green PCR Master Mix, 1 μl cDNA, 1 μl forward primer (10 μM), 1 μl reverse primer 2 (10 μM) and 9.5 μl H_2O. The reaction was run at 95 °C for 5 min, followed by 40 cycles at 95 °C for 15 s, 55 °C for 30 s and 72 °C for 30 s. Relative expression of SAG12 was calculated using the $\Delta\Delta$Ct method.[69] SAG12 (At5g45890) expression was first normalized to expression of the housekeeping gene elongation factor1α (At5g60390).

Confocal laser scanning microscopy. Seeds from transgenic lines expressing 35S::GFP-ATG8a in the Col-0 wild-type or *atmc1* mutant backgrounds were surface sterilized in a 50% bleach and 0.2% Triton X-100 solution for 10 min. Sterile seeds were plated onto solid MS medium plates (Murashige-Skoog Vitamin and Salt Mixture (Life Technologies), 2.4 mM MES (pH 5.7) and 0.9% Phyto Agar (Duchefa Biochemie, Haarlem, The Netherlands)). After 3 days vernalization at 4 °C in the dark, seedlings were grown for 1 week under short-day conditions. Seedlings were subsequently transferred to MS liquid medium (Murashige-Skoog Vitamin and Salt Mixture (Life Technologies), 2.4 mM MES (pH 5.7)) with or without 1 μM concanamycin A and incubated for 15 h in the dark.

Roots were imaged using a Zeiss LSM 710 confocal laser scanning microscope (Zeiss, Oberkochen, Germany). All images were collected using a 40x/1.2NA C-Apochromat water immersion objective. Imaging of cells expressing GFP was performed using 480 nm excitation Scan parameters including pinhole, gain and offset were identical for each experiment to ensure image accuracy. Images were analyzed using the ZEN 2009 software (Zeiss).

Protein analysis. For the analysis of NBR1 protein accumulation, 2-week-old plants were vacuum infiltrated with ~250 000 colony-forming units/ml of *Pto* DC3000(*avrRpm1*). Leaf samples were snap frozen in liquid nitrogen 12 h after infection and mechanically ground in 250 μl of plant extraction buffer (20 mM Tris (pH 7.5), 150 mM NaCl, 1 mM EDTA, 1% Triton X-100 and 0.1% SDS, 5 mM DTT and 1 : 100 dilution of Protease Inhibitor Cocktail (Sigma, St. Louis, MO, USA)). Protein extract was centrifuged 15 min at 10 000 $\times$ *g* at 4 °C. The supernatants were collected, boiled on SDS-loading buffer (120 mM Tris, pH 6.8, 50% glycerol, 6% SDS, 3 mM DTT and 1% Bromophenol blue) and separated on 7.5% SDS-PAGE gels. Immunoblot analysis was performed using a 1 : 1000 dilution of anti-NBR1 polyclonal antibody.

Cell fractionation. Plants were grown 4 weeks under short-day conditions. In all, 200 mg of leaf tissue was ground in 4 ml sucrose buffer (20 mM Tris (pH 8), 0.33 M sucrose, 1 mM EDTA (pH 8) and 1 : 100 dilution of Protease Inhibitor Cocktail (Sigma)) and filtered through Miracloth (Millipore, Billerica, MA, USA). Samples were centrifuged 5 min at 4 °C at 2000 $\times$ *g* to remove large particles. The supernatants were subsequently centrifuged 10 min at 4 °C at 6000 $\times$ *g*. An aliquot of the supernatant was collected representing the total protein fraction (T) and the rest was centrifuged at 100 000 $\times$ *g* at 4 °C for 90 min. The supernatant (S) of this centrifugation was the soluble fraction. To separate microsomal proteins from protein aggregates in the pellet (M + A), sucrose buffer containing 0.3% Triton X-100 was added. The pellet was redissolved by pipetting and incubation at 4 °C for 1 h. Triton X-100-treated M + A was then centrifuged 50 000 $\times$ *g* at 4 °C for 90 min. The supernatant (M) of this centrifugation represented the microsomal fraction, whereas the pellet (A) corresponded to insoluble protein aggregates. Protein extracts were boiled on SDS-loading buffer and separated on 12% SDS-PAGE gels. Gels were either Coomassie-stained or subjected to immunoblot analyisis using a 1 : 5000 dilution of anti-HA monoclonal antibody (3F10, Roche, Basel, Switzerland), 1 : 10 000 anti-cAPX (Agrisera, Vännäs, Sweden) and anti-plasma membrane H^+ ATPase (Agrisera).

Alternatively, we used a modified version of the protocol described in Lee *et al*.[41] obtaining similar results. Essentially, 1 g of plant tissue was ground in liquid nitrogen and 2 ml of buffer B was added (Buffer B: 50 mM Tris, pH 7.5, 1 mM EDTA, 1% glycerol, 0.1% Nonidet P-40 and protease inhibitor cocktail (Roche)). Cell debris was eliminated by passing the protein extract through a Miracloth filter (Millipore) and two sequential spins of 2000 and 3000 $\times$ *g* at 4 °C. Equal amounts of supernatant were collected (total) and centrifuged at 100 000 $\times$ *g* at 4 °C for 90 min. The supernatant of this centrifugation corresponded to the soluble (S) fraction. The pellet was washed three times by adding buffer B supplemented with 2% Nonidet P-40 and centrifugation at 15 000 $\times$ *g* for 30 min. The resulting insoluble protein aggregate fractions were resuspended in an equal volume of buffer B (10 $\times$ concentrated relative to the total and soluble fractions) and sonicated using a Bioruptor (Diagenode, Seraing, Belgium). In all, 6 $\times$ loading buffer was then added and after boiling the samples for 10 min they were loaded on SDS-PAGE gels.

Silver staining. For silver staining, 40 μl of cell equivalents of the total, soluble and aggregate fractions (10 $\times$ concentrated) were loaded on 12% SDS-PAGE gels. Gels were fixed for 1 h in a 50% methanol, 37% formaldehyde and 12% acetic acid

solution. After three washes with 50% ethanol, gels were pre-treated 1 min with a 0.02% sodium thiosulfate solution, washed three times with water and stained 20 min in the dark with a 0.2% silver nitrate, 0.03% formaldehyde solution. Gels were then washed three times with water and treated with a 6% sodium carbonate, 0.02% formaldehyde, 0.0005% sodium thiosulfate solution until the bands became visible. Gels were then washed for 5 s with water and a stop solution (50% methanol and 12% acetic acid) was added for 10 min. Once the reaction was stopped, gels were transferred to water for short-term storage.

Conflict of Interest

The authors declare no conflict of interest.

Acknowledgements. We thank S Svenning (University of Tromsø, Norway) for the NBR1 antisera, T Nürnberger (University Tübingen, Tübingen, Germany) for the *atg18a* mutant seeds and S Dinesh-Kumar (University California-Davis, CA, USA) for the *atg5* mutant. We kindly thank R Vierstra (University Wisconsin-Madison, WI, USA) for critical reading of the manuscript and for sharing the Col-0 35S::GFP-ATG8a seeds with us. We also thank JL Crespo (Instituto de Bioquímica Vegetal y Fotosíntesis, Spain) for sharing the ATG8 antisera and for valuable advices. This research was supported by NIH grant RO1GM057171 JLD and PCDMC-321738 from EU-Marie Curie Actions and BP_B 00030 from the Catalan Government and to NSC. JLD is an HHMI investigator and this work was funded in part by the Howard Hughes Medical Institute and the Gordon and Betty Moore Foundation (GBMF3030).

1. Hara T, Nakamura K, Matsui M, Yamamoto A, Nakahara Y, Suzuki-Migishima R *et al.* Suppression of basal autophagy in neural cells causes neurodegenerative disease in mice. *Nature* 2006; **441**: 885–889.
2. Komatsu M, Waguri S, Chiba T, Murata S, Iwata J, Tanida I *et al.* Loss of autophagy in the central nervous system causes neurodegeneration in mice. *Nature* 2006; **441**: 880–884.
3. Takacs-Vellai K, Vellai T, Puoti A, Passannante M, Wicky C, Streit A *et al.* Inactivation of the autophagy gene bec-1 triggers apoptotic cell death in *C. elegans*. *Curr Biol* 2005; **15**: 1513–1517.
4. Gonzalez-Polo RA, Boya P, Pauleau AL, Jalil A, Larochette N, Souquere S *et al.* The apoptosis/autophagy paradox: autophagic vacuolization before apoptotic death. *J Cell Sci* 2005; **118**(Pt 14): 3091–3102.
5. Gordy C, He YW. The crosstalk between autophagy and apoptosis: where does this lead? *Protein Cell* 2012; **3**: 17–27.
6. Doelling JH, Walker JM, Friedman EM, Thompson AR, Vierstra RD. The APG8/12-activating enzyme APG7 is required for proper nutrient recycling and senescence in *Arabidopsis thaliana*. *J Biol Chem* 2002; **277**: 33105–33114.
7. Xiong Y, Contento AL, Bassham DC. AtATG18a is required for the formation of autophagosomes during nutrient stress and senescence in *Arabidopsis thaliana*. *Plant J* 2005; **42**: 535–546.
8. Yoshimoto K, Jikumaru Y, Kamiya Y, Kusano M, Consonni C, Panstruga R *et al.* Autophagy negatively regulates cell death by controlling NPR1-dependent salicylic acid signaling during senescence and the innate immune response in Arabidopsis. *Plant Cell* 2009; **21**: 2914–2927.
9. Hanaoka H, Noda T, Shirano Y, Kato T, Hayashi H, Shibata D *et al.* Leaf senescence and starvation-induced chlorosis are accelerated by the disruption of an Arabidopsis autophagy gene. *Plant Physiol* 2002; **129**: 1181–1193.
10. Xiong Y, Contento AL, Nguyen PQ, Bassham DC. Degradation of oxidized proteins by autophagy during oxidative stress in Arabidopsis. *Plant Physiol* 2007; **143**: 291–299.
11. Liu Y, Burgos JS, Deng Y, Srivastava R, Howell SH, Bassham DC. Degradation of the endoplasmic reticulum by autophagy during endoplasmic reticulum stress in Arabidopsis. *Plant Cell* 2012; **24**: 4635–4651.
12. Lai Z, Wang F, Zheng Z, Fan B, Chen Z. A critical role of autophagy in plant resistance to necrotrophic fungal pathogens. *Plant J* 2011; **66**: 953–968.
13. Lenz HD, Haller E, Melzer E, Kober K, Wurster K, Stahl M *et al.* Autophagy differentially controls plant basal immunity to biotrophic and necrotrophic pathogens. *Plant J* 2011; **66**: 818–830.
14. Kwon SI, Cho HJ, Jung JH, Yoshimoto K, Shirasu K, Park OK. The Rab GTPase RabG3b functions in autophagy and contributes to tracheary element differentiation in Arabidopsis. *Plant J* 2010; **64**: 151–164.
15. Minina EA, Filonova LH, Fukada K, Savenkov EI, Gogvadze V, Clapham D *et al.* Autophagy and metacaspase determine the mode of cell death in plants. *J Cell Biol* 2013; **203**: 917–927.
16. Hofius D, Schultz-Larsen T, Joensen J, Tsitsigiannis DI, Petersen NH, Mattsson O *et al.* Autophagic components contribute to hypersensitive cell death in Arabidopsis. *Cell* 2009; **137**: 773–783.
17. Kwon SI, Cho HJ, Kim SR, Park OK. The Rab GTPase RabG3b positively regulates autophagy and immunity-associated hypersensitive cell death in Arabidopsis. *Plant Physiol* 2013; **161**: 1722–1736.
18. Feinstein-Rotkopf Y, Arama E. Can't live without them, can live with them: roles of caspases during vital cellular processes. *Apoptosis* 2009; **14**: 980–995.
19. Portela M, Richardson HE. Death takes a holiday—non-apoptotic role for caspases in cell migration and invasion. *EMBO Rep* 2013; **14**: 107–108.
20. Rodrigue-Gervais IG, Saleh M. Caspases and immunity in a deadly grip. *Trends Immunol* 2013; **34**: 41–49.
21. van Doorn WG, Beers EP, Dangl JL, Franklin-Tong VE, Gallois P, Hara-Nishimura I *et al.* Morphological classification of plant cell deaths. *Cell Death Differ* 2011; **18**: 1241–1246.
22. Uren AG, O'Rourke K, Aravind LA, Pisabarro MT, Seshagiri S, Koonin EV *et al.* Identification of paracaspases and metacaspases: two ancient families of caspase-like proteins, one of which plays a key role in MALT lymphoma. *Mol Cell* 2000; **6**: 961–967.
23. McLuskey K, Rudolf J, Proto WR, Isaacs NW, Coombs GH, Moss CX *et al.* Crystal structure of a Trypanosoma brucei metacaspase. *Proc Natl Acad Sci USA* 2012; **109**: 7469–7474.
24. Tsiatsiani L, Van Breusegem F, Gallois P, Zavialov A, Lam E, Bozhkov PV. Metacaspases. *Cell Death Differ* 2011; **18**: 1279–1288.
25. Wong AH, Yan C, Shi Y. Crystal structure of the yeast metacaspase Yca1. *J Biol Chem* 2012; **287**: 29251–29259.
26. Gonzalez IJ, Desponds C, Schaff C, Mottram JC, Fasel N. Leishmania major metacaspase can replace yeast metacaspase in programmed cell death and has arginine-specific cysteine peptidase activity. *Int J Parasitol* 2007; **37**: 161–172.
27. Ivanovska I, Hardwick JM. Viruses activate a genetically conserved cell death pathway in a unicellular organism. *J Cell Biol* 2005; **170**: 391–399.
28. Khan MA, Chock PB, Stadtman ER. Knockout of caspase-like gene, YCA1, abrogates apoptosis and elevates oxidized proteins in *Saccharomyces cerevisiae*. *Proc Natl Acad Sci USA* 2005; **102**: 17326–17331.
29. Madeo F, Herker E, Maldener C, Wissing S, Lachelt S, Herlan M *et al.* A caspase-related protease regulates apoptosis in yeast. *Mol Cell* 2002; **9**: 911–917.
30. Mazzoni C, Herker E, Palermo V, Jungwirth H, Eisenberg T, Madeo F *et al.* Yeast caspase 1 links messenger RNA stability to apoptosis in yeast. *EMBO Rep* 2005; **6**: 1076–1081.
31. Silva RD, Sotoca R, Johansson B, Ludovico P, Sansonetty F, Silva MT *et al.* Hyperosmotic stress induces metacaspase- and mitochondria-dependent apoptosis in *Saccharomyces cerevisiae*. *Mol Microbiol* 2005; **58**: 824–834.
32. Lee N, Gannavaram S, Selvapandiyan A, Debrabant A. Characterization of metacaspases with trypsin-like activity and their putative role in programmed cell death in the protozoan parasite Leishmania. *Eukaryot Cell* 2007; **6**: 1745–1757.
33. Zalila H, Gonzalez IJ, El-Fadili AK, Delgado MB, Desponds C, Schaff C *et al.* Processing of metacaspase into a cytoplasmic catalytic domain mediating cell death in Leishmania major. *Mol Microbiol* 2011; **79**: 222–239.
34. Laverriere M, Cazzulo JJ, Alvarez VE. Antagonic activities of Trypanosoma cruzi metacaspases affect the balance between cell proliferation, death and differentiation. *Cell Death Differ* 2012; **19**: 1358–1369.
35. Coll NS, Vercammen D, Smidler A, Clover C, Van Breusegem F, Dangl JL *et al.* Arabidopsis type I metacaspases control cell death. *Science* 2010; **330**: 1393–1397.
36. Ambit A, Fasel N, Coombs GH, Mottram JC. An essential role for the Leishmania major metacaspase in cell cycle progression. *Cell Death Differ* 2008; **15**: 113–122.
37. Helms MJ, Ambit A, Appleton P, Tetley L, Coombs GH, Mottram JC. Bloodstream form Trypanosoma brucei depend upon multiple metacaspases associated with RAB11-positive endosomes. *J Cell Sci* 2006; **119**(Pt 6): 1105–1117.
38. Proto WR, Castanys-Munoz E, Black A, Tetley L, Moss CX, Juliano L *et al.* Trypanosoma brucei metacaspase 4 is a pseudopeptidase and a virulence factor. *J Biol Chem* 2011; **286**: 39914–39925.
39. Szallies A, Kubata BK, Duszenko M. A metacaspase of Trypanosoma brucei causes loss of respiration competence and clonal death in the yeast *Saccharomyces cerevisiae*. *FEBS Lett* 2002; **517**: 144–150.
40. Lee RE, Puente LG, Kaern M, Megeney LA. A non-death role of the yeast metacaspase: Yca1p alters cell cycle dynamics. *PLoS One* 2008; **3**: e2956.
41. Lee RE, Brunette S, Puente LG, Megeney LA. Metacaspase Yca1 is required for clearance of insoluble protein aggregates. *Proc Natl Acad Sci USA* 2010; **107**: 13348–13353.
42. Wang Y, Nishimura MT, Zhao T, Tang D. ATG2, an autophagy-related protein, negatively affects powdery mildew resistance and mildew-induced cell death in Arabidopsis. *Plant J* 2011; **68**: 74–87.
43. Thompson AR, Doelling JH, Suttangkakul A, Vierstra RD. Autophagic nutrient recycling in Arabidopsis directed by the ATG8 and ATG12 conjugation pathways. *Plant Physiol* 2005; **138**: 2097–2110.
44. Debener T, Lehnackers H, Arnold M, Dangl JL. Identification and molecular mapping of a single *Arabidopsis thaliana* locus determining resistance to a phytopathogenic Pseudomonas syringae isolate. *Plant J* 1991; **1**: 289–302.
45. Svenning S, Lamark T, Krause K, Johansen T. Plant NBR1 is a selective autophagy substrate and a functional hybrid of the mammalian autophagic adapters NBR1 and p62/SQSTM1. *Autophagy* 2011; **7**: 993–1010.
46. Wildermuth MC, Dewdney J, Wu G, Ausubel FM. Isochorismate synthase is required to synthesize salicylic acid for plant defence. *Nature* 2001; **414**: 562–565.
47. Tsuda K, Sato M, Glazebrook J, Cohen JD, Katagiri F. Interplay between MAMP-triggered and SA-mediated defense responses. *Plant J* 2008; **53**: 763–775.
48. Torres MA, Jones JD, Dangl JL. Pathogen-induced, NADPH oxidase-derived reactive oxygen intermediates suppress spread of cell death in *Arabidopsis thaliana*. *Nat Genet* 2005; **37**: 1130–1134.

49. Noh YS, Amasino RM. Identification of a promoter region responsible for the senescence-specific expression of SAG12. *Plant Mol Biol* 1999; **41**: 181–194.
50. Govrin EM, Levine A. The hypersensitive response facilitates plant infection by the necrotrophic pathogen Botrytis cinerea. *Curr Biol* 2000; **10**: 751–757.
51. Liu Y, Schiff M, Czymmek K, Talloczy Z, Levine B, Dinesh-Kumar SP. Autophagy regulates programmed cell death during the plant innate immune response. *Cell* 2005; **121**: 567–577.
52. Patel S, Dinesh-Kumar SP. Arabidopsis ATG6 is required to limit the pathogen-associated cell death response. *Autophagy* 2008; **4**: 20–27.
53. Hayward AP, Dinesh-Kumar SP. What can plant autophagy do for an innate immune response? *Annu Rev Phytopathol* 2011; **49**: 557–576.
54. Hofius D, Munch D, Bressendorff S, Mundy J, Petersen M. Role of autophagy in disease resistance and hypersensitive response-associated cell death. *Cell Death Differ* 2011; **18**: 1257–1262.
55. Costet L, Cordelier S, Dorey S, Baillieul F, Fritig B, Kauffmann S. Relationship between localized acquired resistance (LAR) and the hypersensitive response (HR): HR is necessary for LAR to occur and salicylic acid is not sufficient to trigger LAR. *Mol Plant Microbe Interact* 1999; **12**: 655–662.
56. Dorey S, Baillieul F, Pierrel MA, Saindrenan P, Fritig B, Kauffmann S. Spatial and temporal induction of cell death, defense genes, and accumulation of salicylic acid in tobacco leaves reacting hypersensitively to a fungal glycoprotein elicitor. *Mol Plant Microbe Interact* 1997; **10**: 646–655.
57. Roberts M, Tang S, Stallmann A, Dangl JL, Bonardi V. Genetic requirements for signaling from an autoactive plant NB-LRR intracellular innate immune receptor. *PLoS Genet* 2013; **9**: e1003465.
58. Shirasu K, Nakajima H, Rajasekhar VK, Dixon RA, Lamb C. Salicylic acid potentiates an agonist-dependent gain control that amplifies pathogen signals in the activation of defense mechanisms. *Plant Cell* 1997; **9**: 261–270.
59. Torres MA, Dangl JL, Jones JD. Arabidopsis gp91phox homologues AtrbohD and AtrbohF are required for accumulation of reactive oxygen intermediates in the plant defense response. *Proc Natl Acad Sci USA* 2002; **99**: 517–522.
60. Abreu ME, Munne-Bosch S. Photo- and antioxidant protection and salicylic acid accumulation during post-anthesis leaf senescence in Salvia lanigera grown under Mediterranean climate. *Physiol Plant* 2007; **131**: 590–598.
61. Lawton KA, Friedrich L, Hunt M, Weymann K, Delaney T, Kessmann H *et al.* Benzothiadiazole induces disease resistance in Arabidopsis by activation of the systemic acquired resistance signal transduction pathway. *Plant J* 1996; **10**: 71–82.
62. Yang Y, Shah J, Klessig DF. Signal perception and transduction in plant defense responses. *Genes Dev* 1997; **11**: 1621–1639.
63. Grant MR, Godiard L, Straube E, Ashfield T, Lewald J, Sattler A *et al.* Structure of the Arabidopsis RPM1 gene enabling dual specificity disease resistance. *Science* 1995; **269**: 843–846.
64. Clough SJ, Bent AF. Floral dip: a simplified method for Agrobacterium-mediated transformation of *Arabidopsis thaliana*. *Plant J* 1998; **16**: 735–743.
65. Tornero P, Dangl JL. A high-throughput method for quantifying growth of phytopathogenic bacteria in *Arabidopsis thaliana*. *Plant J* 2001; **28**: 475–481.
66. Keogh RC, Deverall BJ, McLeod S. Comparison of histological and physiological responses to Phakopsora pachyrhizi in resistant and susceptible soybean. *Trans Br Mycol Soc* 1980; **74**: 329–333.
67. Koch E, Slusarenko A. Arabidopsis is susceptible to infection by a downy mildew fungus. *Plant Cell* 1990; **2**: 437–445.
68. Bonardi V, Tang S, Stallmann A, Roberts M, Cherkis K, Dangl JL. Expanded functions for a family of plant intracellular immune receptors beyond specific recognition of pathogen effectors. *Proc Natl Acad Sci USA* 2011; **108**: 16463–16468.
69. Livak KJ, Schmittgen TD. Analysis of relative gene expression data using real-time quantitative PCR and the 2(-delta delta C(T)) method. *Methods* 2001; **25**: 402–408.

Supplementary Information accompanies this paper on Cell Death and Differentiation website (http://www.nature.com/cdd)